Studies into the immune response in lung disease of cohorts in rural Papua New Guinea and urban Australia

Tyler J. Gilstrom

Thesis submitted for the degree of

Doctor of Philosophy

College of Public Health, Medical and Veterinary Sciences

James Cook University

11th April 2024

Supervisors:

Associate Professor Jeffrey Warner

Associate Professor Catherine Rush

Associate Professor Ulf Schmitz

Dr. Jerry Minei

Acknowledgments

My sincere gratitude is extended to Associate Professor Melissa Crowe, Dr. Diana Mendez, and the Doctoral Studies Cohort Program. You both supported me through the expected and unexpected challenges in my doctoral studies. I would not have been able to finish my studies without both of you. Melissa, your commitment to excellence, willingness to go above and beyond, and integrity are exemplary. Your depth of knowledge and sunny disposition made meetings and 'Cohort Block Weeks' something I looked forward to. Diana, your can-do attitude and cheerful personality were refreshing when things looked bleak. Thank you both for your contributions to the Cohort program, which have truly exemplified how to foster a productive and harmonious work environment.

Kimberly Thornley, your expertise and confident presence were game-changing. Your empathy and wisdom are invaluable, and your commitment to student success was uplifting and strengthening. Thank you for all your help over the years. Nola Kuilboer, I genuinely appreciate your willingness to listen, thank you. Your kindness, eloquence, and desire to do what is right in the professional sector are qualities I hope to embody in my professional life.

Dr. Champa Ratnatunga, you trained me and showed me the ropes in my early days. Champa, you are brilliant and a powerhouse; I was fortunate to learn from you. Thank you for getting my project off the ground and going above and beyond and mentoring me. Thank you, Jessica, for helping me get situated in the lab and assisting me with some of my lab work. I appreciated having a reliable team member and a friendly face while at your campus.

Thank you, Associate Professor Jeffrey Warner taking the risk on my candidature as my primary advisor. Thanks for being a sturdy, no-dramas mentor who cleared the way for me to finish my studies. Thank you for your leadership and for managing the complex and political academic environment. Associate Professor Catherine Rush, I appreciate your expertise and thoroughness in my project. Thank you for your patience in teaching me in the lab and for your exceptional feedback on my writing. Thank you, Jeff, and Cathy, for allowing me to take part in your ongoing research in Papua New Guinea. Thank you, Associate Professor Ulf Schmitz, for helping me get started on my new project and for encouraging and mentoring me along the way. Thank you for your excellent advice on my transcriptomics work. Dr. Jerry Minei, your wisdom and kind demeanour were greatly admired. Thank you for imparting your knowledge to me.

I am deeply grateful to my parents, sister, and grandma, who never stopped believing in me for all their phone calls and support you gave me throughout my time in graduate school. Mom and Dad, your steadfast support has been the cornerstone of my confidence and peace; thank you.

Melissa Piontek, my partner in crime, thank you for staying by my side, mourning in my sorrows and celebrating my triumphs. You put aside my flaws and supported me when I needed it. ‘A three-stranded cord is not easily broken.’ Better days are on the horizon.

Finally, thank you Heavenly Father for sustaining me when I was unable.

“When I applied myself to gain wisdom and to observe how people occupy themselves on earth, that people’s eyes don’t see sleep either by day or by night, then, on looking over all of God’s work, I realized that it is impossible to grasp all the activity taking place under the sun; because even if a person works hard at searching it out, he won’t grasp it; and even if a wise person thinks he knows it, he still won’t be able to grasp it.”

Ecclesiastes 8:16-17 (CJB)

Statement of Contribution of Others

This thesis contains my original research and contains no material previously published or written by another person unless it has been stated in the text. I have stated the contribution of others, where appropriate, including statistical support and materials provided by other collaborators to facilitate my research that has contributed to this thesis. The results obtained for my higher degree research (HDR) candidature is the content of my thesis and has not been submitted to qualify for the award or any other degree at any university or institution. I acknowledge that an electronic copy of my thesis will be lodged with the University Library and, subject to the policy and procedures of James Cook University, the thesis be made available for research and study in accordance with the Copyright Act 1968 unless a period of embargo has been approved by the Dean of the Graduate School. I acknowledge that the copyright of all material contained in my thesis resides with the copyright holder(s) of that material. Where appropriate, I have obtained copyright permission from the copyright holder to reproduce material in this thesis.

Nature of assistance	Contributions
Supervision and Mentorship	This PhD project was supervised by A/Prof Jeffrey Warner (Primary Advisor), A/Prof Catherine Rush (Secondary Advisor), A/Prof Ulf Schmitz (Secondary Advisor), and Dr. Jerry Minei, MBBS (External Advisor). Prof. Champa Ratnatunga provided advice, support, and mentorship.
Intellectual Support	Prof. Champa Ratnatunga provided me with initial statistics training as well as training in the use of nSolver, GraphPad Prism, and Cytobank software. Dr. Katie Tungatt provided basic instruction on the analysis of flow cytometry data. A/Prof Catherine Rush trained me to perform multiparametric cytokine assays and data analysis. Additionally, she provided training on RNA handling and extractions. A/Prof Jeffrey Warner, A/Prof Catherine Rush, and A/Prof Ulf Schmitz assisted with conceptualization.
Chapter 2	I wrote the Chapter after an initial consultation with Prof. John Miles. Prof. Champa Ratnatunga, Dr. Katie Tungatt, and Dr. Yide Wong provided feedback.
Chapter 3	Initial sample and data collection was conducted by Prof. Champa Ratnatunga (previously AITHM, currently the University of Peradeniya), and Abella Murray under the supervision of Prof John Miles, Dr. David Reid, and Dr. Daniel Smith at the Queensland Institute of Medical Research. Prof. Champa Ratnatunga also performed some initial data analysis. Prof. Champa Ratnatunga provided initial training for the data analysis of this chapter. I further performed data analysis on the transcriptomic data using new R-based tools that were developed by another Ph.D. student (Dr. Martha Cooper). I then interpreted the findings and wrote the associated manuscript and Chapter 3 with the help of Prof. Champa Ratnatunga and A/Prof Ulf Schmitz.

Chapters 4 and 5	Sample collection in Papua New Guinea was led by A/Prof Jeffrey Warner and blood and sputum sample processing for flow cytometry assays and plasma cytokine assays was done by A/Prof Catherine Rush. I performed analysis on the gated datasets and completed multiparametric cytokine staining using the preserved plasma samples. Critical feedback was provided by A/Prof Jeffrey Warner, A/Prof Catherine Rush, and A/Prof Ulf Schmitz.
Chapter 6	Dr Yomani Sarathkumara (previously AITHM) performed RNA extraction on a subset of samples and submitted them for sequencing under the supervision of Prof. Denise Doolan (previously AITHM) as part of her PhD project. I performed the extraction on additional samples and submitted them for sequencing. I then developed an analysis pipeline and began analysis using the raw sequencing files from the combined dataset with guidance from A/Prof Ulf Schmitz. A/Prof Jeffrey Warner, A/Prof Catherine Rush, and A/Prof Ulf Schmitz provided feedback.
Financial Support	I was offered an Australian Institute of Tropical Health and Medicine scholarship which included a stipend and tuition waiver for the duration of my project. Funding for the initial project in Papua New Guinea was funded by a Hot North grant awarded to A/Prof Catherine Rush, and A/Prof. Jeffrey Warner. Additional funding for research activities specific to my Ph.D. project was provided by James Cook University. This included funds to determine the cytokine concentrations in blood plasma, RNA extractions, and RNA sequencing. Additional funds were awarded as a Higher Degree by Research Enhancement Scheme grant by the College of Public Health, Medical and Veterinary Sciences at James Cook University.

Declaration of Ethics

The study documented in this thesis adhered to the guidelines set forth by the National Statement on Ethical Conduct in Human Research, 2007, as established by the National Health and Medical Research Council (NHMRC).

Ethics approval was provided by the Human Ethics Review Board at Prince Charles Hospital (Brisbane, Australia) for the work conducted with the Australian patient cohort (HREC/14/QPCH/251).

For the work conducted on the cohort from Papua New Guinea, ethics was approved by the PNG Medical Research Advisory Council (MRAC 19.21) and by the James Cook University Human Research Ethics Committee (H8015).

Abstract

Chronic obstructive pulmonary disease (COPD) is a non-communicable inflammatory lung disease that is caused by chronic inhalation of irritants, most commonly smoke. COPD sufferers experience airflow obstruction and an abnormal inflammatory response in the lungs leading to a progressive decline in lung function. The therapies currently used can only reduce the rate of disease progression but are unable to fully stop or reverse lung damage. Tobacco smoking is a major environmental risk factor for COPD, particularly in high-income countries, however, in developing regions and in low- and middle-income countries (LMIC), household air pollution where biomass is used as a fuel source for cooking and heating, is a major risk factor. COPD is the third leading cause of death worldwide, with > 3 million deaths annually, with 90% of those occurring in individuals less than 70 years of age in LMIC.

Airway inflammation is an immunological response to smoke exposure and involves the recruitment of immune cells including neutrophils, macrophages, eosinophils and T-cells into the airways that contribute to tissue damage and airway and airspace remodelling. The primary features of COPD are inflammation of the small airways, airway remodelling and destruction of lung parenchyma (emphysema). In early stages of the disease, correlation of airway remodelling and lung functional measurements are care found. In advanced stages of COPD, airflow limitation is reflected by airway narrowing, and degree of emphysema. Most investigators have focused on tobacco smoke exposure to study the mechanisms of COPD; however, it is a heterogeneous disease and multiple endotypes and phenotypes have been described, characterised by the presence of different ratios of underlying conditions: emphysema, small airways disease, and chronic bronchitis. It has been proposed that COPD induced by chronic exposure to biomass smoke (BS-COPD), is a distinct phenotype of the disease and appears to be primarily characterised by chronic bronchitis with comparatively low rates of emphysema. While there are observable clinical differences between BS-COPD-affected individuals and patients with tobacco smoke-induced COPD (TS-COPD), the inflammatory and immunological drivers of this heterogenicity are poorly understood. Furthermore, it is unclear why only a portion of smoke-exposed individuals develop significant signs of disease.

Previous research suggests that COPD patients have been shown to exhibit dysregulated immune states. Specifically, an imbalanced ratio of pro-inflammatory to anti-inflammatory T-cells has been identified, leading to prolonged immune activation and inflammation. T-cells, which are highly adaptable immune cells, play a pivotal role in orchestrating subsequent immune responses. While many changes in T-cell phenotypes are linked to COPD, the specific variations in immune dysregulation across different COPD phenotypes remain unclear. The research presented in this

thesis explored the hypothesis that dysregulated immune responses to chronic smoke exposure show distinct characteristics in individuals with clinical symptoms and vary between those exposed to biomass smoke and those exposed to tobacco smoke. In essence, unique immune states underly the heterogenicity of COPD. It is crucial to understand the mechanisms underlying the phenotypes as they could have substantial implications for treatment.

To test this hypothesis two cohorts of participants were investigated. The first group of participants consisted of well-clinically characterised Australians with a history of tobacco smoking who were admitted to the hospital with an acute exacerbation of COPD. The second cohort of participants were poorly clinically characterised individuals from a rural community in Papua New Guinea (PNG) who were chronically exposed to biomass smoke from cooking fires. These contrasting cohorts enabled the examination of distinct phenotypes of COPD. The immune profiles of both cohorts were investigated using flow cytometry and transcriptomics techniques to better understand the dynamics of the disease and to identify potential markers or drivers.

Flow cytometric and transcriptomic analyses of peripheral blood T-cells from the urban Australian TS-COPD cohort revealed phenotypic differences in T-cells compared to healthy controls. Both $CD4^+$ helper and $CD8^+$ cytotoxic T-cells in TS-COPD had an activated and exhausted phenotype which provides evidence for T-cell impairment and dysregulation in these patients. Concurrently, there was a downregulation of many transcription factors associated with T-cell differentiation. Additionally, there was a reduction in the proportion of mucosal-associated invariant T-cells (MAITs) in COPD patients. A phenotypically distinct population of MAITs was identified in the exacerbating COPD patients that expressed high levels of the T-cell exhaustion markers CTLA4, PD1, and TIM3. These results indicated that T-cell exhaustion is involved in TS-COPD.

The biomass smoke-exposed cohort from PNG was the next focus of investigation. Initially, a baseline of peripheral blood leukocyte profiles was established from non-health-seeking biomass-smoke exposed (i.e., healthy) participants. Examination of peripheral blood from these participants revealed a trend toward lower concentrations of T-cells including T-helper and cytotoxic T-cells yet, increased concentrations of natural killer T-cells compared to Australian reference ranges. Furthermore, the concentrations of T-helper cell type-1 (Th1), type-2 (Th2), and Th17-related plasma cytokines were greatly increased compared to the reference ranges established in Australia and the United States of America.

These newly established baselines were then used to identify peripheral blood cellular and cytokine markers associated with symptoms of biomass-smoke-induced lung disease (i.e., unhealthy individuals). Participants in this group had elevated levels of plasma Th-17-related cytokines.

Furthermore, mitogen stimulation of whole blood samples from this cohort revealed that T-cells from the unhealthy participants were less able to respond to subsequent stimulation; they produced significantly lower concentrations of cytokines primarily related to Th-1 and Th-17-driven inflammation. This indicates that in this remote community from PNG, lung disease induced by chronic inhalation of biomass smoke results in increased inflammatory cytokines and functional impairment of peripheral immune cells, including T-cells. These changes may increase susceptibility to infectious disease, cancer, and other co-morbid conditions.

Transcriptomic profiling was subsequently used to gain a deeper understanding of the immune differences underlying disease in the biomass-smoke-exposed cohort. RNA sequencing of peripheral blood revealed altered transcriptomes relating to different T-cell states. This included reduced expression of *LY9* (Lymphocyte Antigen 9), *ITK* (Interleukin-2-inducible T-cell Kinase), *IL7R* (Interleukin 7 Receptor), and *CD96* (Cluster of Differentiation 96) in the unhealthy participants. Additionally, the expression of *HSPA1A* (Heat Shock Protein Family A Member 1A), and *NR1H1* (Nuclear Receptor Subfamily 1 Group H Member 2) was increased in these participants. Gene set enrichment analysis identified increased expression of gene sets relating to innate immune cells and concurrent reduced expression of gene sets relating to multiple T-cell subtypes. Notably, there was increased expression of gene sets related to neutrophil and monocyte activity and hypoxia. However, the results also provided evidence that unique immune mechanisms may underly biomass-smoke-induced versus tobacco-smoke-induced disease. The expression of *CD96* and *IL7R*, which exhibited heightened levels in the T-cells of TS-COPD patients, showed reduced expression in the peripheral blood of the unhealthy biomass-smoke-exposed participants compared to their healthy counterparts. Furthermore, whereas the expression of *NFKB1* (nuclear factor kappa B subunit 1), *TGFB1* (transforming growth factor beta 1), *IFNG* (Interferon Gamma), and *STAT3* (Signal Transducer and Activator Of Transcription 3) was diminished in the T-cells of TS-COPD patients, gene sets associated with these markers demonstrated increased expression in unhealthy participants from the PNG cohort.

Together, these studies show evidence of dysregulated immune responses associated with tobacco smoke and biomass smoke-induced lung disease. There was also evidence of functional impairment of immune cells in both cohorts of patients. TS-COPD patients expressed exhausted MAITs as well as T-helper and cytotoxic T-cells that displayed an activated and exhausted phenotype. Participants with biomass smoke-induced lung disease had immune profiles associated with increased and impaired Th-17-driven inflammation as well as impaired type-1 responses. These studies provide a better understanding of these unique aetiologies and begin to carve a path toward therapies that account for the heterogeneity of COPD.

Table of Contents

List of Figures

List of Tables

List of Abbreviations

AECOPD - Acute Exacerbations of Chronic Obstructive Pulmonary Disease

AGRF - Australian Genomics Research Facility

BAL - Bronchoalveolar Lavage

BAMBI – Bone Morphogenic Protein and Activin Membrane-bound Inhibitor

BCTs - Blood Collection Tubes

BMI - Body Mass Index

BS-COPD - Biomass Smoke-Induced Chronic Obstructive Pulmonary Disease

CCL4 - C-C Motif Chemokine Ligand 4

CCR3/CD193 - C-C chemokine receptor type 3

CCR6 - C-C Motif Chemokine Receptor 6

CD - Cluster of Differentiation (with specific numbers like CD4, CD8, etc.)

COPD - Chronic Obstructive Pulmonary Disease

CPM - Counts Per Million

CSE - Cigarette Smoke Extract

CTLA4 - Cytotoxic T-Lymphocyte-Associated protein 4

CXCL10 - C-X-C Motif Chemokine Ligand 10

CXCL8 - C-X-C Motif Chemokine Ligand 8

CXCR3 - C-X-C Motif Chemokine Receptor 3

CXCR6 - C-X-C Motif Chemokine Receptor 6

DNA - Deoxyribonucleic Acid

DNAM - DNAX Accessory Molecule-1

EDTA - Ethylenediaminetetraacetic Acid

FACS - Fluorescence-Activated Cell Sorting

FBS - Fetal Bovine Serum

FEV1% - Forced Expiratory Volume in 1 Second (percentage of predicted)

FEV1/FVC - Forced Expiratory Volume in One Second/Forced Vital Capacity

FITC - Fluorescein Isothiocyanate

FMO - Fluorescence Minus One

FOXP3 - Forkhead Box P3

FVC - Forced Vital Capacity

G-CSF - Granulocyte Colony-Stimulating Factor

GIMAP5 - GTPase IMAP Family Member 5

GM-CSF - Granulocyte-Macrophage Colony-Stimulating Factor

GOLD - Global Initiative for Chronic Obstructive Lung Disease

GSEA - Gene Set Enrichment Analysis

GZM - Granzyme (various types, e.g., GZMA, GZMB, etc.)

hg38 - Human Genome version 38

HIF-1α - Hypoxia-Inducible Factor 1 Alpha

HNRNPDL - Heterogeneous Nuclear Ribonucleoprotein D-like

HREC - Human Ethics Review Committee

HSPA1A - Heat Shock Protein Family A (Hsp70) Member 1A

ICOS - Inducible T-cell Costimulator

IDO - Indoleamine 2,3-Dioxygenase

IFNGR1 - Interferon Gamma Receptor 1

IFN-γ - Interferon Gamma

IgE - Immunoglobulin E

IL - Interleukin (with various numbers like IL-2, IL-6, etc.)

IL1-ra - Interleukin 1 receptor antagonist

IL21R - Interleukin 21 Receptor

IL4R - Interleukin 4 Receptor

ILC2s - Type 2 Innate Lymphoid Cells

ILK - Integrin Linked Kinase

iNKTs - Invariant Natural Killer T

ITGA4 - Integrin Alpha 4

ITK - Interleukin-2-inducible T-cell Kinase

JAK - Janus Kinase

JCU - James Cook University

KIR - Killer-cell Immunoglobulin-like Receptor

KLRG1 - Killer Cell Lectin Like Receptor G1

LMICs - Low to Middle-Income Countries

LOD - Limit of Detection

LXRβ - Liver X Receptor Beta

LY9 - Lymphocyte Antigen 9

MAITs - Mucosal Associated Invariant T-cells

MHC II - Major Histocompatibility Complex Class II

MIP-2 - Macrophage Inflammatory Protein 2

MR1 - MHC Class I-related Molecule

MRAC - Medical Research Advisory Council

MSigDB - Molecular Signatures Database

NATD1 - N-Acetyltransferase Domain Containing 1

Nf-κB - Nuclear factor kappa-light-chain-enhancer of activated B cells

NHANES III - National Health and Nutrition Examination Survey III

NK - Natural Killer

NKT - Natural Killer T

NR1H2 - Nuclear Receptor Subfamily 1 Group H Member 2

NTHi - Nontypeable Haemophilus influenzae

OS9 - Osteosarcoma Amplified 9, Endoplasmic Reticulum Lectin

PBMCs - Peripheral Blood Mononuclear Cells

PBS - Phosphate Buffered Saline

PCA - Principal Component Analysis

PD1 - Programmed Cell Death Protein 1

PNG - Papua New Guinea

PRF1 - Perforin 1

PTGER2 - Prostaglandin E Receptor 2

QFTs - Quantiferon TB GOLD Plus Tests

QIMRB - Queensland Institute of Medical Research Berghofer

qPCR - Quantitative Polymerase Chain Reaction

RANTES - Regulated on Activation, Normal T Cell Expressed and Secreted

RAS - Respiratory Airway Secretory

RNA - Ribonucleic Acid

RORα - Retinoic acid receptor-related Orphan Receptor Alpha

RORγ - Retinoic acid receptor-related Orphan Receptor Gamma

RUNX - Runt-Related Transcription Factor

S1PR1 - Sphingosine-1-Phosphate Receptor 1

SELL - Selectin L

SMAD - Mothers against decapentaplegic homolog

STAT - Signal Transducer and Activator of Transcription

STIM2 - Stromal Interaction Molecule 2

TC2N - Tandem C2 Domains, Nuclear

TCR - T-cell Receptor

TFG-β1 - Transforming Growth Factor Beta 1

TGF-βRI - TGF-beta Receptor Type I

TIM3 - T-cell Immunoglobulin and Mucin-domain containing-3

TIMP-1 - Tissue Inhibitor of Metalloproteinases 1

TLM1 - Talin 1

TLR - Toll-Like Receptor

TMM - Trimmed Mean of M-values

TNF-α - Tumor Necrosis Factor Alpha

TS-COPD - Tobacco Smoke-Induced Chronic Obstructive Pulmonary Disease

UBAP1 - Ubiquitin Associated Protein 1

Vα7.2 TCR - Variable alpha 7.2 T cell receptor

ZBTB16 - Zinc Finger and BTB Domain Containing 16

α-GalCer - Alpha-Galactosylceramide

Chapter 1: Introduction

The motivation for this study stems from the inadequate understanding and management of chronic obstructive pulmonary disease (COPD), especially in developing countries. COPD ranks as a foremost cause of mortality globally, characterized as a progressive condition impacting all regions of the lungs, which results in diminished respiratory function. This condition also has broader implications as it substantially contributes to co-morbidity within the impacted communities. COPD sufferers are unable to efficiently oxygenate their blood leading to dyspnea, lack of energy, and in severe cases reduced cognitive abilities causing confusion, and memory lapses. Currently, there are no therapies that can stop or reverse the disease. Treatment is rather aimed at suppressing the disease's progression.

COPD is caused by chronic inhalation of irritants. In Western countries, tobacco smoke is the primary aetiology. However, chronic biomass smoke exposure is a major cause in low-to-middle-income countries (LMICs). In these at-risk LMIC communities, the disease is particularly not well characterised due in part to poor access to health care and therefore the clinical management of these patients is even more challenging. Indeed, even though PNG has the second highest death rate due to COPD in the world, the clinical impact and pathology are not well described (1).

The ongoing impact of biomass smoke exposure can be severe. In many COPD patients, lung function continues to decline even after irritant exposure has been halted (2). This long-term lung damage is due in large part to an aberrant immune response initiated by inhaled irritants rather than solely by direct damage from the irritants. The immunopathology is complex and not fully understood and therefore treatment and management can be difficult. Even in countries with well-resourced health systems, clinical presentation is heterogeneous, and the immune response is complex leading to challenges in disease management. Recent literature has suggested that T-cell dysregulation might be particularly important in this COPD-driven immunopathology (See Chapter 2) and therefore our study focused on this aspect of the immune system and T-cell dysregulation. Therefore, this PhD project intended to further investigate the heterogenicity of immune and transcriptomic landscapes in COPD patients, particularly that of the cell-mediated immune responses, and compare and contrast urban (development world) vs rural (developing world) at-risk cohorts from these communities. The underlying hypothesis of this work was the following:

Dysregulated cellular immune responses to chronic smoke exposure have distinctive characteristics among individuals exhibiting clinical symptoms of disease, as well as variations between individuals

exposed to biomass smoke and cigarette smoke. Therefore, an understanding of these mechanisms is required for directed and evidence-based treatment and may prove useful as diagnostic biomarkers.

To test this hypothesis this project was established across two cohorts: a clinically well-characterized group of patients from urban Australia with tobacco smoke-induced COPD and a clinically poorly characterized group of biomass smoke-exposed participants from a rural area in Papua New Guinea (PNG). These cohorts allowed this project to capture and analyse much of the heterogenicity that is associated with COPD sufferers and to broadly identify the unique and common pathways involved in biomass-smoke-induced lung disease.

To establish a baseline understanding of COPD in a well-characterized population, a cohort from Australia was studied as a preliminary step towards investigating the condition in participants from a rural community in Papua New Guinea. Patients were recruited upon admission to the Prince Charles Hospital (Brisbane) with an acute exacerbation of COPD (AECOPD). These patients were clinically very well characterized and diagnosed using Global Initiative for Chronic Obstructive Lung Disease (GOLD) guidelines. Blood samples were acquired on admission, during recovery, and after recovery. The major T-cell subsets were isolated from the blood samples and used in downstream analyses to identify immune phenotypes and transcriptional changes associated with COPD in this cohort compared to healthy controls.

The next portion of the study shifted to focus on the participants from rural PNG. Characterization, treatment, and research in this region are limited due, in part, to the remoteness and lack of infrastructure and resources. There is often no diagnostic facility in this area or trained respiratory clinicians to accurately diagnose these patients. Participants in this study were recruited when they presented to Balimo District Hospital for investigation of respiratory symptoms. Additional participants who were not seeking medical attention were recruited from the general population to help determine a non-disease baseline. In all of these participants, biomass smoke exposure from cooking was ubiquitous. Participants were excluded from the study if they were found to have a pulmonary tuberculosis infection, which is endemic in this region. A portable spirometer supplied by the research team for the study was used to measure lung function. Additionally, blood and spontaneous sputum samples were acquired from participants. These samples and data were transported back to James Cook University (Townsville) for analysis.

Since lung function testing presents immense challenges in remote communities, this study attempted to characterise lung disease by focussing on immune parameters. The blood samples were analysed to determine the concentrations of immune cells and cytokines present. This data was initially analysed to determine how biomass smoke exposure affects immune responses. This

was accomplished by comparing the values to the range of what is expected in healthy individuals who have not been chronically exposed to smoke. Next, the participants were segregated into two groups: one with symptoms of respiratory disease and one without. This made it possible to distinguish immune profiles that were specific to lung disease from profiles that were solely artifacts of biomass smoke exposure.

To further elucidate markers of lung disease in this cohort transcriptomics was used. While the previous studies used flow cytometry to identify the major cell types and cytokines expressed in the participants, this allowed thousands of genes to be analysed that were differentially expressed in the entire cell population. This allows much deeper insights into the immune dysregulation that underlies biomass smoke-induced lung disease. These studies allowed for the identification of transcription factors that are associated with the development of specific immune cell lineages and phenotypes. Further, pathway and gene ontology analyses allowed for multi-gene signatures to reveal the biological processes that are active in biomass smoke-induced lung disease.

The combination of these cohorts provides a comprehensive analysis of immune and T-cell dysregulation, broadly comparing urban Australian populations with rural communities in Papua New Guinea (PNG). This dual-cohort approach is instrumental in identifying unique patterns of immune response associated with different aetiologies. Specifically, the inclusion of the cohort from rural PNG, where biomass smoke-induced lung disease is prevalent, addresses a significant gap in current research. By contrasting this with urban Australian cohorts, where lung disease aetiologies differ markedly, the study facilitates a deeper understanding of how biomass-smoke exposure contributes to immune dysregulation. These studies may advance our understanding of why biomass smoke-induced lung disease has a very different clinical presentation compared to tobacco smoke-induced disease and begin to provide insights into why only a portion of people chronically exposed to biomass smoke develop chronic lung disease. These studies may advance therapeutics and diagnostics, particularly in these underserved communities.

Chapter 2: Review of the Literature

2.1 Introduction

Chronic obstructive pulmonary disease (COPD) is a common lung disease caused by inhalation of noxious particles or gasses, most commonly from tobacco smoke. Biomass smoke, air pollution, and other factors also significantly contribute to its prevalence as about 30% of COPD patients have never smoked (3). Lung pathology of COPD is characterised by progressive narrowing of the airways due to small airways disease chronic bronchitis, and emphysema. These underlying conditions are present in varying ratios among patients and represent separate phenotypes of the disease. Currently, there is no cure for COPD as the airway and lung damage incurred is irreversible. COPD management is limited to the treatment of ongoing and acute symptoms, prevention and management of exacerbations, and management of co-morbidities. In 2019, COPD caused 3.23 million deaths making it the third leading cause globally (4). In Australia, approximately 638,000 people suffer from COPD and the direct costs totalled $831.6 million in 2020-2021 (5). Papua New Guinea has the highest rate of COPD in people under 50 years old and it has one of the highest age-standardized disability-adjusted life years (DALY) rates from COPD in the world (6).

While tobacco smoke exposure is the primary aetiology of COPD in industrialized countries, the increasing use of electronic cigarettes is associated with a 75% higher incidence of chronic bronchitis, emphysema, or COPD however, more evidence is needed to establish this link (7). However, biomass smoke-induced COPD is a major concern in low to middle-income countries where inefficient fuel sources (i.e., wood and crop waste) are used for cooking and heating and has distinct characteristics compared to tobacco smoke-induced disease (8, 9). The immune drivers underlying these unique clinical characteristics are not understood (10). Other clinical phenotypes based on the frequency of exacerbations and pattern of comorbidities have been described but no correlation to underlying inflammatory signatures has been identified thus far (11).

Current treatments for COPD are aimed at managing the symptoms. This includes a combination of short and long-acting bronchodilators (beta-agonists and muscarinic antagonists) however effectiveness reduces with prolonged use. Inhaled corticosteroids (ICS) and phosphodiesterase-4 (PDE-4) inhibitors are often used in combination with bronchodilators to reduce airway inflammation. Both ICS and PDE-4 inhibitors suppress immune function and increase susceptibility to infections which can lead to increased damage in the lungs. Additionally, ICS treatment is only effective in a subset of patient. None of these treatments target the root causes of COPD and reduce bronchoconstriction or inflammation. Better treatments are needed to target the underlying pathological mechanisms that cause COPD. However, this is challenging due to the clinical and

cellular heterogeneity of COPD. Understanding how immune drivers relate to clinical phenotypes and aetiologies will parallel the identification of biomarkers. These developments are necessary to pave the way for the personalized treatment of patients that consider the unique phenotypes of expressed across patients. Future treatments will be guided by biomarkers that inform clinicians of the specific pathophysiological characteristics of individual patients and will involve treatments targeted to the underlying causes of these unique disease mechanisms. In this review, we discuss the role of immune cells in COPD pathogenesis with an emphasis on T-cell phenotypes and dynamics.

T-cells are a diverse group of adaptive immune cells characterised by their expression of T-cell receptors. They recognize a vast array of antigens presented to them by other cells. In general, T-cells are split into two major subtypes: $CD4^+$ and $CD8^+$ cells, each with multiple subtypes. The subtype that a particular T-cell becomes is determined by the immune context (i.e., cytokines present) during their priming (12, 13). $CD4^+$ cells (or T-helper cells) recognize antigens presented on major histocompatibility complex (MHC) class-II molecules by antigen-presenting cells. When activated, these cells trigger an immune response through the release of cytokines and chemokines that induce the recruitment and activation of other immune cells. There are numerous subtypes of $CD4^+$ T-cells that are suited to fighting different types of threats by the recruitment of other immune cells. They are generally characterised by the cytokines they produce and the master transcription regulator they express (13). Of the $CD4^+$ subtypes, Th1, Th2, Th17, and Treg cells have been implicated in COPD and are the focus of this review. Th1 cells are inflammatory cells that produce Il-2, IFN-γ, and TNF-α. They are associated with macrophage infiltration during infections (14). Th2 cells mediate immune responses to allergies and parasites. They secrete Il-4, Il-5, and Il-13, which recruit mast cells and eosinophils and stimulate the production of antibodies from plasma cells (15). Th17 cells are associated with neutrophilic inflammation through their secretion of Il-17 and are generally involved in the clearance of extracellular bacteria. They are also capable of secreting Il-22, the action of which depends on the immune context (discussed later) (16). Regulatory T-cells (Tregs) are anti-inflammatory cells that suppress immune responses through the release of Il-10 and TGF- β. Tregs create a homeostatic balance with other immune cells and their activity is of particular importance in the prevention of autoimmune diseases (17).

$CD8^+$ cells recognize antigens presented on MHC class-I molecules. MHC class-I is present on all nucleated cells and is typically used to present digested intracellular antigens, such as viruses and intracellular bacteria, and cancer-related proteins. Upon recognition of an antigen, they release cytotoxic molecules which cause apoptosis of the infected cell (12). Of the $CD8^+$ subtypes, Tc1, Tc2, Tc17, and Tc10 cells play the largest roles in COPD (18). These cytotoxic T-cells also have similar

cytokine production functions to their equivalently named $CD4^+$ T-helper cells. That is, Tc1, Tc2, and Tc17 cells have similar capabilities to Th1, Th2, and Th17 cells respectively (12). Tc10s are $CD8^+$ cells named for their ability to secrete Il-10 similar to $CD4^+$ Tregs (18, 19).

2.2 Inflammatory pathogenesis of COPD

Many cell types play a role in the pathophysiology of COPD including innate and adaptive lymphocytes as well as epithelial cells. Inhaled irritants induce airway mucus hypersecretion, epithelial cell hyperplasia, and the release of inflammatory cytokines and chemokines from the airway epithelium that induce the migration of immune cells (20-22). Recruited macrophages and neutrophils cause inflammation and release proteases that destroy lung tissues (Figure 2.1A) (23, 24). Repair mechanisms result in excess collagen deposition leading to fibrosis and the permanent and progressive loss of elastic recoil (25). This results in the clinical symptoms of emphysema which is observed in some COPD patients and is typically preceded by small airway disease. In contrast to the neutrophilic inflammation seen in the majority of COPD patients, a subset (37%) of COPD patients also has eosinophilic inflammation which represents a distinct phenotype of the disease (26). The presence of eosinophilic inflammation may indicate pre-existing asthma and allergy underlying COPD (Figure 2.1B). These patients respond better to corticosteroid treatment which is less effective in non-eosinophilic driven COPD (27).

The cell types and cytokines driving inflammation vary across patients, the severity of the disease as well as stable and acute stages (28-32). T-cells display a high level of plasticity and can exert control over many other immune-cell types and likely play a role in the heterogeneous nature of COPD. Understanding the roles of these cells may lead to a better understanding of COPD pathophysiology and targeted treatment options.

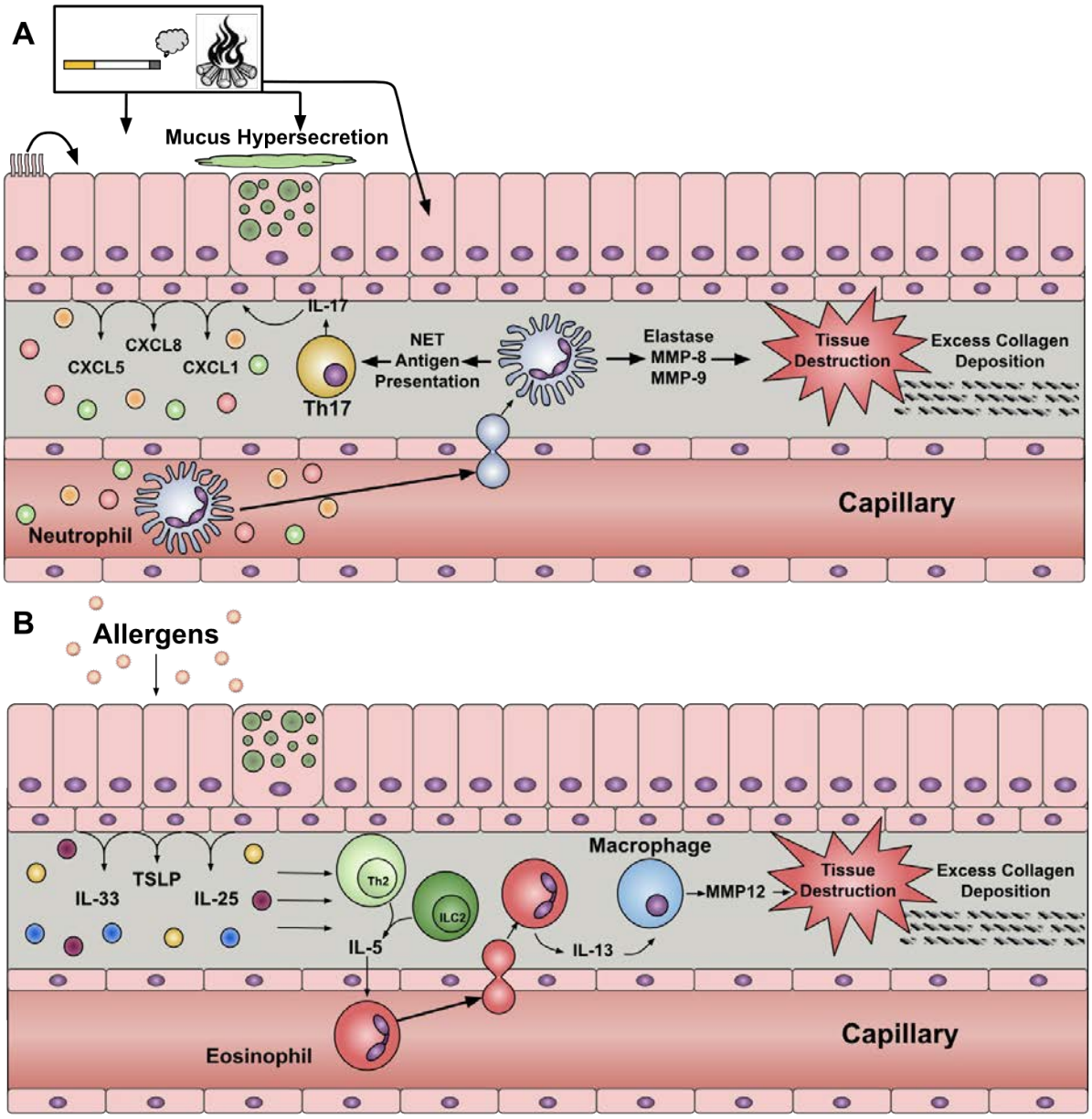

Figure 2.1. Neutrophilic and eosinophilic mechanisms in COPD.
(A) Neutrophilic inflammation in COPD lung. Excess biomass particles induce goblet cells to produce mucus hyper-secretion in the lung alveolar epithelium. Th17 cells are recruited that induce inflammatory chemokines that recruit neutrophils from the peripheral blood. This results in tissue destruction and excess collagen deposition in the alveolar epithelium via neutrophils releasing neutrophil extracellular traps (NETs), metalloproteinases (MMPs), and the further recruitment of Th17 cells. **(B)** Eosinophilic inflammation in COPD lung. Inhaled allergens stimulate alveolar epithelial cells to release cytokines that activate Th2 and ILC2 cells. Activated Th2 and ILC2 cells produce IL-5 which leads to eosinophil recruitment in the lungs. Lung eosinophils recruit macrophages which release MMP12 leading to tissue damage and collagen deposition. Figure created in Google Drawings.

2.3 Role of Th17 and regulatory T-cells in COPD pathology

Airway inflammation characterised by an infiltrate of neutrophils is present in the majority of COPD cases, especially those with chronic bronchitis. While the mechanisms underlying the pathophysiology of COPD are not fully understood, Th17 cells that produce cytokines associated with

neutrophilic inflammation, appear to play a significant role. There is evidence that COPD patients have dysregulated lung microbiomes with chronic colonization of pathogenic bacteria (33). This may, in part, drive the sustained Th17 cell activation in patients' lungs. However, it is not clear whether microbial dysbiosis in COPD is the cause of the dysregulated immune environment or the result of it. Th17 cells are characterised by their expression of the transcription factor retinoic acid-related orphan receptor gamma (RORγt) which regulates the production of Th17-related cytokines (34). Activated Th17 cells secrete several immune molecules, most characteristically the pro-inflammatory cytokine IL-17 however, this cytokine is also produced by epithelial cells, neutrophils, and macrophages (35, 36). IL-17 is a heterodimeric cytokine with six variants. However, IL-17A and IL-17F appear to be the only variants that play a role in COPD (36). The IL-17 receptor (IL-17R) is highly expressed on epithelial cells. Upon activation of IL-17R epithelial cells secrete the chemokine CXCL8 (IL-8) which recruits neutrophils and macrophages from the circulation (37). IL-17R activation can be induced by multiple factors in COPD patients. Cigarette smoke is a key contributor, with in vitro studies showing that cigarette smoke extract (CSE) can enhance IL-17A and IL-17F expression in lung epithelial cells, leading to increased IL-17R signalling (36-38). Additionally, bacterial infections, such as those caused by *Haemophilus influenzae*, may activate IL-17R through pathogen-associated molecular patterns (PAMPs), further exacerbating neutrophilic inflammation (39). Excess or chronic neutrophil recruitment to the lungs leads to tissue damage via the secretion of neutrophil proteases (40, 41).

In patients with COPD, there is an increase in Th17 cells and their related cytokines in the blood sputum and lung tissue over healthy smokers (HS) and healthy nonsmokers (HNS) with an even larger increase in patients suffering from acute exacerbations of COPD (AECOPD) (36, 42-45). *In vitro* studies have demonstrated that cigarette smoke extract (CSE) can elicit increased IL-17F and IL-17R expression in lung epithelial cell lines as well as both IL-17A and IL-17F expression in isolated peripheral blood mononuclear cells (PBMCs) (36). Further, in murine models, cigarette smoke exposure increased circulating Th17 cell counts and RORγt mRNA in lung tissue concurrently with IL-17 expression (46). IL-17A and IL-17 receptor A deficiency following the use of depleting antibodies or gene knockdown inhibited the secretion of the neutrophil chemo-attractants CXCL1 and CXCL5 and attenuated neutrophilia in cigarette smoke-exposed mice infected with non-typeable *Haemophilus influenzae* (NTHi) (47). Furthermore, airway fibrosis and pathogenic remodelling were attenuated in *IL17a* $^{-/-}$ mice exposed to cigarette smoke (48).

Several pathways appear to be involved in the aberrant IL-17 signalling seen in COPD, yet no definitive underlying mechanism has been elucidated. Most notably an imbalance of regulatory T-cells (Tregs) and Th17 cells is observed in the blood and sputum of COPD patients (42, 44, 49, 50).

Treg cytokines, particularly IL-10, can inhibit the differentiation of naïve $CD4^+$ T cells into Th17 cells. In COPD patients there is an increased ratio of Th17:Treg cells which may indicate a malfunction of Treg's ability to suppress Th17-driven inflammation. The peripheral blood Th17:Treg ratio negatively correlates with lung function indicated by forced vital capacity (FVC), forced expiratory volume in the first second (FEV_1), and FEV_1/FVC, which are indicators of both restrictive and obstructive airway disease (50).

Recent research has highlighted the role of Bone Morphogenic Protein and Activin Membrane-bound Inhibitor (BAMBI) in the Th17:Treg imbalance (45, 51). BAMBI is a pseudoreceptor for TGF-β that competes with TGF-β type 1 receptors (TGF-βRI) thereby negatively regulating TGF-β family signaling and the downstream Suppressor of Mothers Against Decapentaplegic (SMAD) signaling pathway (51). BAMBI is most notably expressed in macrophages and its expression is increased in the blood and bronchial mucosa COPD patients over healthy controls (45, 52). Increased TGF-β abundance appears to increase BAMBI expression (45). In COPD, both TGF-β1, TGF-βRI, and BAMBI are increased in peripheral blood and BAMBI expression is negatively correlated with FEV_1 (51). BAMBI expression appears to be linked to the upregulation of Th17 cells concurrent with the downregulation of Tregs (45). This observation is interesting as TGF- β is involved in the differentiation of both Th17s and Tregs (53, 54).

Evidence identifies an important role for macrophages as being responsible for inducing these changes. *In vitro* studies have demonstrated cigarette smoke extract can induce M0 macrophages to secret anti-inflammatory cytokines including IL-10 and TGF-β, appearing M2-like, while also increasing BAMBI expression. M2 macrophages are capable of inducing Tregs leading to an anti-inflammatory microenvironment in the lungs. This mechanism likely underlies homeostasis seen in healthy smokers. However, overexpression of BAMBI *in vitro* causes the conversion of M2 macrophages to M1 macrophages which secret pro-inflammatory cytokines such as IL-6 and TNF-α. M1 macrophages lose their ability to induce Treg differentiation (Figure 2.2). IL-6 secreted from these macrophages contributes to the differentiation of Th17 cells (51). Studies on lung tissue of COPD patients have shown that M1 macrophages are increased in the small airways compared to non-COPD patients. However, this increase is observed in healthy smokers as well indicating that it is likely not the sole mechanism underlying the Th17:Treg imbalance (55). The role of TGF-β in COPD is contentious as recent research has identified that increased microRNA miR-21 expression seen in COPD lungs induces Th17 differentiation via SMAD7/ TGF-β signalling (56). However, the true roles of TGF-β within COPD patients are likely dependent on the broader immune context.

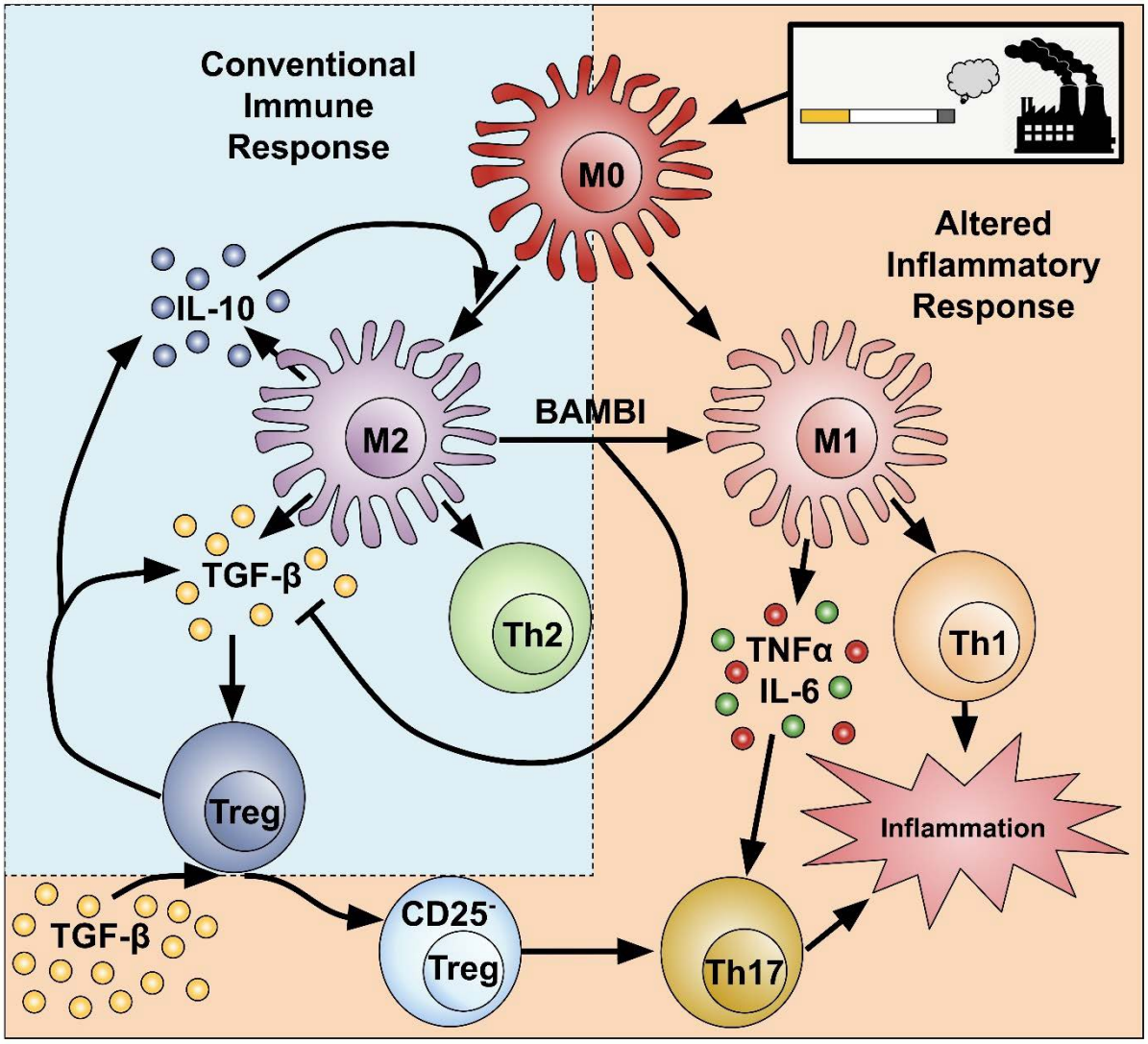

Figure 2.2. Macrophages and T-cells in COPD.
M0 macrophages are directed into hemostatic or inflammation phenotypes via biomass inhalation. Normal immunity comprises hemostatic M2 macrophages, Th2 $CD4^+$ T-cells, and $CD4^+$ Tregs (blue). Excessive biomass inhalation and overexpression of BAMBI result in inflammatory M1 macrophage formation, effector Th1 CD4+ T-cell recruitment, and tissue destruction from $CD4^+$ Th17 cells (orange). This cumulative results in chronic immune activation in the blood and lungs causing the thickening of the lung bronchial walls.

Recent research has highlighted the potential role of IL-36 in the induction of the Th17 responses observed in COPD. IL-36 is a pro-inflammatory cytokine that can be expressed in many cell types including macrophages, dendritic cells, neutrophils, and bronchial epithelium (57). Studies have shown that the expression of the isoforms IL-36a and IL-36y are increased in COPD patients compared to healthy controls. This effect is particularly pronounced in patients with a neutrophilic phenotype of COPD (58). The source of IL-36 has not been identified in COPD, however, macrophages and dendritic cells are likely candidates and are implicated as sources of IL-36 in the context of other inflammatory diseases (57). Further, *in vitro* studies and rat models have shown that biomass smoke exposure is capable of activating Toll-like receptor 2 (TLR2) on dendritic cells

and inducing naïve $CD4^+$ cells to produce IL-17 (59). IL-36 expression is dependent on Toll-like receptor activation. TLR2 activation by cigarette smoke may lead to IL-36 secretion in the lungs. Dendritic cells can become activated by IL-36 and subsequently mediate Th17 cell induction by the secretion of IL-23 (60, 61). However, these links have not been established in COPD and should be the subject of future research as they may reveal therapeutic targets for the treatment of neutrophilic COPD.

Previous research has shown that COPD patients have increased numbers of Tregs that lack the activation marker CD25 ($CD4^+$ $CD25^-$ $FOXP3^+$) compared to healthy smokers and non-smokers (62, 63). Additional studies found that the proportion of these cells in BAL negatively correlated with the rate of lung function decline in COPD patients (64). This altered Treg phenotype appears to have a role in COPD pathogenesis. Although the role of these cells is not fully understood, they resemble memory T-cells with increased expression of the IL-7 receptor. $CD4^+$ $CD25^-$ FOXP3 cells have a lower expression of FOXP3, inhibitory ligands CTLA-4, HELIOS, and TIGIT indicating reduced suppressive capacity while the proliferation marker Ki-67 expression is increased. Interestingly, these cells can aid the differentiation of naïve $CD4^+$ cells into Th17 cells and under certain conditions, can convert into Th17 cells. TGF-β1 decreased the expression of CD25 *in vitro* and appears to be responsible for this altered phenotype (62). Further, Th17 cells can express functionally distinct phenotypes depending on the greater immune context (65, 66). In-depth phenotypic analysis of Th17 cells across COPD phenotypes has not been performed, yet it may provide insights into its pathological mechanism.

2.4 Altered Th1/Th2 responses in COPD patients

Th1 and Th2 cells are also key players in the pathogenesis of COPD. Th1 cells are orchestrators of the cellular immune responses, primarily through the release of IL-2 and IFN-γ which are upregulated in COPD patients (67). Conversely, Th2 cells mediate eosinophil trafficking to the lungs as well as IgE-type humoral immunity by secreting IL-4, IL-5, IL-10, and IL-13 (67, 68). Both lineages counter regulate each other. However, in COPD patients the cytokine profiles of both cell types are elevated compared to healthy controls. Interestingly, during an exacerbation, there is a greater increase in Th2 cytokines than in Th1 cytokines. During stable COPD, Th1-driven inflammation dominates as indicated by relatively high ratios of Th1:Th2 cytokines in the blood. However, this study did not account for neutrophilic or eosinophilic phenotypes in the study participants (67). It has been demonstrated that the sustained inflammation in COPD may be due in part to Th1 cell recognition of elastin as an autoantigen. Th1 cells isolated from COPD patients released more IFN-γ when stimulated with elastin than with collagen (69). Elastin has been used as a Th1 autoantigen in mouse

models leading to signs of bronchitis (70). The proteolytic destruction of the extracellular matrix by macrophage and neutrophil proteases is followed by phagocytic uptake of extracellular matrix material containing elastin and subsequent presentation to naive $CD4^+$ T-cells by antigen-presenting cells. Upon recognition of elastin autoantigens, naïve $CD4^+$ cells differentiate into Th1 cells in the presence of IFN-γ and express CXCR3. The binding of chemotactic factors to CXCR3 induces the migration of Th1 cells to the lung tissue where they release their inflammatory cytokines and activate more macrophages. COPD patients have a higher expression of CXCR3 (69). $CD4^+$ Th1 cells isolated from AECOPD patients secrete more IFN-γ in the presence of elastin than they do when exposed to collagen (69). Studies in mouse models and *in vitro* found that erythromycin treatment reduced elastin-induced release of IFN-γ, IL-17A, and IL-6 and differentiation of Th1 (71). Interestingly, both Th1 and Th17 cells produce inflammatory cytokines in response to elastin stimulation. However, the autoimmune mechanisms behind elastin autoantigens may not be limited to Th1 responses as elastin-induced Th17 inflammation has been demonstrated in cigarette smoke-exposed mice (70, 71). This may create a cycle of auto-immune inflammation in stable COPD patients.

Stable COPD patients have reduced IL-4-producing Th2 compared to healthy controls, however, during an exacerbation event there is an increase in the Th2 cytokines IL-4 and IL-10 with a concomitant increase in IgE in peripheral blood (67, 72). Although the mechanism creating the shift in cytokine profiles is not fully understood, there is evidence that Type 2 innate lymphoid cells (ILC2s) are responsible for inducing Th2 cell skewing (73). ILC2s are the primary effector cells of early Th2 immune responses through their production of IL-4 (74). ILC2s are increased in the peripheral blood of AECOPD patients, and they express increased levels of major histocompatibility complex class II (MHCII) and CD80 which are involved in the differentiation of T cells. Co-culture of $CD4^+$ T-cells from healthy controls and ILC2s from AECOPD patients resulted in an increased proportion of Th2 cells as well as the Th2-related cytokines IL-4, IL-5, and IL-13. This effect was reduced in the presence of an MHC II blocking antibody indicating that antigen presentation by ILC2s primed Th2 differentiation (73). This does not rule out the participation of other innate immune cells in the activation of Th2 cells during exacerbations, but it highlights an area for future research.

2.5 The roles of $CD8^+$ cells in COPD

$CD8^+$ cytotoxic T-cells are primarily responsible for the adaptive response to intracellular bacteria, and viruses and play a role in autoimmune diseases and anti-tumour defence. Both inflammatory cytokines and cytotoxic molecules released from $CD8^+$ T-cells take part in the pathogenesis of COPD (75). $CD8^+$ T-cell numbers are increased and express more cytotoxic proteins in the lungs of COPD

patients compared to controls (18). Despite the increase in $CD8^+$ cell types, COPD patients have an increased susceptibility to viral infections, possibly due to the breakdown of innate defences of the respiratory tract. COPD patients have a disturbed balance of pro-inflammatory and anti-inflammatory subsets $CD8^+$ subsets similar to that observed in $CD4^+$ subsets although there is a larger overall increase in $CD8^+$ T-cells than in $CD4^+$ T-cells (18, 76). $CD8^+$ T-cell numbers negatively correlate with FEV_1% in COPD patients (77, 78). Stable COPD patients primarily have an increased proportion of Tc1 cells and a decreased proportion of Tc2 and Tc10 cells. During exacerbations, patients also display an increase in Tc17 cells along with the upregulation of Tc2 cells to baseline (18). Healthy smokers have an increased proportion of $CD8^+$ Tregs over COPD patients. *In vitro* studies have shown that cigarette smoke extract is involved in both the proliferation and apoptosis of $CD8^+$ Tregs and the fate of these cells is likely dependent on the cytokine microenvironment. The deficiency of $CD8^+$ Tregs undoubtedly has consequences on the inflammatory environment of the lungs in COPD patients (77). This is consistent with the studies on $CD4^+$ and T-regs and similar interactions are likely involved, but little research has been performed on $CD8^+$ T-regs in COPD.

Multiple altered $CD8^+$ phenotypes have been identified in COPD patients. It has been shown that $CD8^+$ $CD28^{null}$ T-cells are increased in COPD patients. CD28 is a costimulatory receptor that is involved in the activation and survival of T-cells. A murine model has demonstrated that cigarette smoke exposure can increase the proportion of $CD8^+CD28^{null}$ cells yet, ex-smokers COPD patients still exhibit increased $CD8^+CD28^{null}$ cell numbers. $CD8^+CD28^{null}$ cells express more pro-inflammatory cytokines and cytotoxic molecules upon stimulation than $CD8^+CD28^+$ cells and may be implicated in the inflammatory response of COPD (79). These cells were further shown to have lost expression of glucocorticoid receptors. This may further explain the resistance to steroid treatment observed in COPD patients (75). A classification of $CD8^+$ T cells based on one or two additional markers may not provide a great deal of functional insight into pathology. For example, CD28 is an activation marker, and $CD28^+$ T cells may be already committed to a particular cytokine profile, while $CD28^{null}$ cells are simply more receptive to stimulation. How these cells are implicated in the pathology of COPD is uncertain.

COPD patients have an increased susceptibility to lung viral infections. The PD-1/PD-L1 pathway plays an important role in viral immunity in the lungs yet it appears to be disrupted in COPD patients. The binding of the PD-1 ligand, PD-L1, inhibits proliferation and cytokine secretion. PBMCs from COPD patients had higher PD-1 expression than those from controls indicating an exhausted cell phenotype (80). PD-1 expression on $CD8^+$ cells was positively correlated to disease severity in COPD patients (81). Similarly, lung tissue from COPD patients displayed higher expression of PD1 on $CD8^+$ T-cells than lung tissue from controls. Further, upon *in vitro* H3N2 virus infection COPD tissues

released more IFN-y than controls. Expression of the cytotoxic degranulation marker CD107-A was increased in control tissues following infection, but this was not observed in COPD lung tissues (82). In mouse models, anti-PD-1 antibodies reduced lung damage and neutrophilic inflammation in response to chronic cigarette smoke exposure or *Haemophilus influenzae* infection (83). However, other studies have found that anti-PD-1L antibody therapy response is dependent on CD28 activation in the clearance of chronic viral infections (84). These findings show that $CD8^+$ T-cells in COPD lungs exhibit an aberrant response to viral infections and may explain, at least in part, why patients have a reduced ability to clear viral infections.

Dendritic cells appear to take part in the imbalance of pro-inflammatory and anti-inflammatory $CD8^+$ T cell subsets. *In vitro* exposure to cigarette smoke extract induced plasmacytoid dendritic cell maturation. These cells express high levels of the co-stimulatory molecules CD40 or CD86. Concurrently, they release IFN-α, IL-6, and IL-12 capable of preferentially causing the differentiation of Tc1 and Tc12 cells with a likely concurrent increase in Th1 cells (85, 86). *In vivo* studies have demonstrated that $CD8^+$ cells from COPD patients can express IL-17, not solely $CD4^+$ cells (87). Dendritic cells may be a mechanism that contributes to the activation of $CD8^+$ cells and increased IFN-y and IL-17 measured in COPD patients.

2.6 The roles of non-conventional immune cells in COPD pathology

NK, NKT, and NKT-like cells may also participate in the progression of COPD. All three cell types have cytotoxic properties and are important components of viral immunity. The role of these cell types in COPD is not fully understood. NK and NKT-like cells are increased in peripheral blood and BAL fluid of COPD patients over healthy controls, but their levels are correlated with pack-years, a measure of lifetime cigarette smoke exposure, not disease status (88-90). Conversely, induced sputum and BAL samples show elevated NK cells in COPD patients which was related to disease status (89). Lower total numbers of invariant NKT cells (iNKTs) were detected in the blood and sputum of COPD patients compared to healthy controls. However, $CD4^+$ iNKT cell numbers were increased in the peripheral blood (91). Further, repeated administration of the iNKT ligand α-GalCer in mice led to the development of COPD-like symptoms including emphysema, increased mucus production, and pulmonary fibrosis. The symptoms were accompanied by an increase in pro-inflammatory molecules IL-6 and TNF-α. The development of emphysema in this model was reduced following the neutralization of IL-4 (92). In a Sendai virus-induced mouse model of chronic lung disease, COPD-like symptoms developed after clearance of infection independent of an adaptive immune response. Instead, the symptoms were driven by IL-13 release from macrophages activated by iNKT cells (93). NKT cells are phenotypically diverse and can be categorized into three distinct subtypes determined

by the expression of different transcription factors and the cytokines they release (94). In-depth phenotypic analysis of NKT cells in COPD is lacking yet it may provide new insights into the mechanisms of COPD pathogenesis.

A few studies have investigated the activity of mucosal-associated invariant T-cells (MAITs) in COPD. MAITs also express a unique TCR that recognizes riboflavin pathway-related antigens presented on MR1 molecules. MAITs are implicated in the defence against bacterial pathogens in mucosal membranes. COPD patients have reduced numbers of MAIT cells in their peripheral blood (91, 95, 96). Concurrently, COPD patients have increased expression of CXCR2 and CXCL1 in the lungs which facilitates the migration of MAIT cells (96). The reduced MAIT cell counts in the blood may be an artifact of recruitment into lung tissues. MAIT cell counts are positively correlated with lung function measured by FEV_1/FVC ratio (95). However, other studies have shown that in peripheral blood and bronchial samples, MAITs are only reduced in patients who have received steroid treatments (97).

2.7 Experimental Model Limitations

The use of animals to model COPD is common despite their limitations. Mouse models of COPD have been able to replicate many of the features of the disease in a short timeframe (98). However, mouse lungs have important anatomical differences compared to humans including different branching patterns in the airways and the lack of respiratory bronchioles (99, 100). The respiratory bronchioles in humans contain respiratory airway secretory cells that are transcriptionally distinct from any cells found in the mouse lung (100). Additionally, mice have reduced numbers of goblet cells in their bronchi and bronchioles compared to humans (101). Large studies in humans have suggested that it takes years of chronic smoke exposure to induce sustained inflammation and structural changes in the lungs whereas mouse models can be established in weeks to months of intense cigarette smoke exposure (102). The differences bring into question the validity of mouse models in producing meaningful results. To circumvent many of the differences between mouse models and human COPD, a non-human primate model of COPD was proposed. Macaques were exposed to cigarette smoke five days per week for 12 weeks. The animals developed many of the features of COPD, yet they failed to develop emphysema (103). This may have been due to the short timeframe of the model. However, none of these models consider the multiple phenotypes seen in COPD. Animal models may provide insights into specific features of lung disease but are not useful in wholistically replicating human disease.

2.8 Conclusion

The immune mechanisms involved in COPD are complex. There is evidence for the role of T-cell autoimmunity as well as autoinflammatory responses from neutrophils and macrophages. The degree to which each of these mechanisms plays a role in COPD is unclear. Cell counts are altered and out of balance as are cell phenotypes. Type 1 and type 2 adaptive responses are misaligned along with Th17 and Treg activity. Multiple potential causes for these imbalances have been investigated but no singular mechanism has been identified that can account for all these changes. Much of the research that has been performed has focused on changes in cell counts and ratios. Yet, these studies are limited in their ability to decipher the complex interactions that are occurring in COPD patients. Future research should be focused on in-depth analysis of clinical and cellular phenotypes as some cell types with known phenotypic subsets, such as $CD4^+$ Th22 cells, have not been studied in COPD. The observed phenotypic differences in patients exposed to biomass smoke compared to tobacco smoke have been understudied. It is unknown whether the phenotypic differences seen in patients with these distinct induction triggers have unique immune drivers or if they are related to the vastly different demographics that are typical in these groups. Increased understanding of the immune drivers of COPD may provide clinically translational advances in the form of new treatments as well as diagnostic biomarkers that can allow clinicians to provide personalized treatment to patients. Some molecular signatures have already been identified that relate to disease phenotypes and lung function in patients but these need to be expanded to enable diagnostics that are of sufficient precision and accuracy to diagnose treatable characteristics of COPD patients. This will come through an improved understanding of the mechanics underpinning disease phenotypes. The mechanisms underlying both infective and non-infective exacerbation patients also warrant investigation. Exacerbations greatly accelerate lung damage and functional decline. Treatments that can prevent or halt exacerbations could substantially increase patients' lifespans and quality of life.

Adding to the complexity of COPD, the disease presents differently from one patient to the next. For example, some patients colloquially termed 'pink puffers', primarily suffer from emphysema whereas the 'blue bloaters' are plagued with chronic bronchitis. Additionally, these conditions are often preceded by small airway disease. It is not clear why patients experience these conditions in varying degrees and ratios which creates challenges for clinicians. Only about half of patients diagnosed with COPD have an accelerated decline in their lung function trajectory (104). There is also a significant overlap between other chronic lung pathologies like asthma and bronchiectasis. COPD-Asthma overlap syndrome yields different responses to treatments (105). All of this points to the need for awareness of the heterogeneity of COPD. It appears to be a disease with many subtypes

that have yet to be fully elucidated. It is unlikely that a singular mechanism will be deduced from all the immunological changes that have been and will be revealed. Future studies should attempt to find mechanistic differences and biomarkers in patients with different phenotypes of the disease. This may allow for more effective, individualized treatments for COPD patients.

Chapter 3: Pattern of early T-cell activation and exhaustion in patients with acute exacerbations of chronic obstructive pulmonary disease

3.1 Introduction

Chronic obstructive pulmonary disease (COPD) is an inflammatory condition of the small airways with emphysematous destruction of lung tissue that leads to irreversible airway obstruction (106). COPD is the 3rd leading cause of death worldwide with age-adjusted mortality that has doubled in the past 30 years (107). COPD is strongly associated with smoking however 25-45% of COPD patients have never smoked (108), suggesting that exposure to biomass smoke may be another leading risk factor.

The clinical course of COPD is characterised by recurrent exacerbations of symptoms including cough and shortness of breath associated with impaired respiratory functions. These acute exacerbations of COPD (AECOPD) events are often triggered by viral or bacterial infection of the airways to which these patients are highly susceptible. COPD is therefore qualified by the level of airway obstruction, as defined by the forced vital capacity (FEV1%) into mild, moderate, or severe disease, and by the frequency of exacerbations requiring hospitalization in the GOLD classification (109).

Previous research has shown that lymphocyte numbers are increased in the airways and blood of COPD patients with a further increase during exacerbations (18, 42, 44, 67). Both $CD4^+$ and $CD8^+$ T-cell subsets have been shown to play a role in the pathology of COPD. In addition, MAITs cells are reduced in the blood of stable COPD patients (91) (95, 96). Previous studies revealed that the ratios of T-cell subsets are skewed and favor an inflammatory environment. (42, 44, 67, 110). Importantly, altered phenotypes of these T-cell subsets also appear to contribute to COPD pathology. In particular, Tregs have lower expression of inhibitory ligands and have reduced immune suppressive abilities in COPD patients compared to controls (62). Further, $CD8^+$ T-cells in COPD patients express altered phenotypes and release increased levels of inflammatory cytokines (79).

Flow cytometry and qPCR analysis on lung-specific $CD4^+$ T-cells have demonstrated impaired function and unique phenotypes in COPD patients (111). T-cells are known to freely circulate between the blood and the lung (112), suggesting that there is likely bidirectional movement between the diseased lung and the circulation. Indeed, using microarray gene profiling on whole blood, COPD gene modules were identified and could be linked to disease severity. Some of the strongest signals came from $CD4^+$ and $CD8^+$ T-cell-specific gene signatures (113). MAITs cells were also shown to have altered phenotypes in COPD patients. MAITs from COPD patients had increased

expression of CD38 indicating that they were more active (114). *Ex vivo* studies discovered that MAITs from COPD patients were less responsive to microbial infections than those from heathy donors indicating that MAITs activation may be dysregulated (115). However, it is unknown if dysfunctional T-cells in the peripheral blood are involved in the cause or the effect of the disease.

AECOPD results in increased $CD8^+$ T-cells in the lung (116) and peripheral blood (18)and increased $CD8^+$/IL-17^+ T-cells (18) and Treg cells (117)in the peripheral blood. PD1 and CTLA4 are differentially expressed in T-cells from AECOPD patients indicating T-cell exhaustion (82, 117), while exacerbation-defining T-cell gene modules have been described in both blood and sputum (118, 119). The pathophysiological significance of these remains unclear.

The aim of this chapter was:

- To characterise peripheral blood T-cell phenotypes and gene expression in relation to clinical parameters in a cohort of patients from urban Australia with a clinical diagnosis of COPD.

In this study, we enumerated and phenotyped human T-cell subsets in patients with AECOPD and matched healthy controls (HC) using high-dimensional NanoString transcriptomic profiling and multiparametric flow cytometry. T-cell phenotypes and transcriptomics data were analysed in relation to exacerbation status and spirometry. We also tracked the T-cell kinetics from AECOPD presentation through to convalescence. Collectively, the data revealed new insight into the pathology of COPD and AECOPD, including the identification of a new cell phenotype that may have a functional role in COPD.

3.2 Methods

3.2.1 Sample Collection

Ethics was approved by the Human Ethics Review Board at Prince Charles Hospital, Brisbane, Australia (HREC/14/QPCH/251). Patients, who were predominantly from Brisbane, a rural area in Australia, were recruited for the study on admission to the Hospital with an acute exacerbation of COPD. Written informed consent was acquired from all participants. Patient's clinical data including age, sex, smoking history, spirometry at stability, number of admissions in the 12 prior months, and duration of the current admission was obtained. Patients with malignancy, current intravenous illicit drug use, or undergoing long-term domiciliary oxygen therapy were excluded from the study. Patient severity was assigned based on the Global Initiative for Obstructive Lung Disease (GOLD) guidelines (2011).

3.2.2 PBMC Isolation

Blood samples were collected at four time points for each patient where possible: on admission to the hospital with an AECOPD (day 0), between days 3-5 post-admission, days 12-18 post-admission, and at stability (ST-COPD) (day 30+ post-admission). Age and sex-matched healthy controls (HCs) were recruited. Samples were immediately processed to separate the peripheral blood mononuclear cells (PBMCs) using density gradient centrifugation media (Lymphoprep, STEMCELL Technologies). Separated PBMCs were cryopreserved until used.

Prior to use cells were thawed, DNase treated, and counted for viability.

3.2.3 Fluorescence-activated sorting of $CD4^+$ and $CD8^+$ T-cells

PBMCs collected from patients during an AECOPD and at stability as well as from healthy controls were used for T-cell sorting. Approximately $1x10^6$ PBMCs were thawed and stained using a five-colour T-cell sorting panel (Appendix 1A). Sorting was performed on a BD-FACS ARIA cell sorter (BD Biosciences). $CD3^+CD4^+$ and $CD3^+CD8^+$ lymphocytes were sorted into separate populations and collected into 2% FBS in PBS. 50,000 or more $CD4^+$ and $CD8^+$ cells were collected and re-sorted to ensure purity (cell populations were >98% pure).

3.2.4 Flow Cytometry

Flow cytometric analysis was performed on PBMCs from each of the four time points and HCs. Each sample was stained with one of the three panels. Panel 1 included T-cell lineage markers (Appendix 1B). Panel 2 included surface markers and FoxP3 intracellular staining (Appendix 1C). Panel 3 investigated the activation and exhaustion states of mucosal-associated invariant T-cells (MAITs) (Appendix 1D). Data were acquired using an LSRFortessa-II flow cytometer (BD Biosciences) running FACSDiva software.

3.2.5 RNA Extraction and NanoString Transcriptomics

Sorted $CD4^+$ and $CD8^+$ cells were thawed, and RNA was extracted using RNAzol (Sigma-Aldrich). The resulting RNA was quantified on a NanoDrop ND-1000 spectrophotometer (Thermo Fisher Scientific) and frozen at -80^{o}C until further analysis. Gene expression was quantified using the NanoString nCounter system at the maximum resolution according to the manufacturer's instructions (NanoString Technologies, USA). A custom set of 135 T-cell genes that was optimized from other

experiments was used for this study. This included genes with established roles in T-cell functions (i.e. activation, exhaustion, etc.)

3.2.6 Data Analysis

Gene expression data were imported into R (V3.5.3) and normalized using the NanostringClustR package (V0.1.1) using the quantile normalization technique. Principal Component Analysis (PCA) and volcano plots were generated using the ggplot2 R package. Mann-Whitney U-tests were performed between two experimental groups using a false discovery rate of 5% in Prism (V9.4, GraphPad) and p values < 0.05 were considered to be significant. Additionally, Pearson's correlations were conducted on parametric gene expression data and clinical parameters using Prism.

Flow cytometry data was manually gated using fluorescence-minus-one controls in FlowJo (V10, Tree Star Inc.) (Appendix 2). Comparisons between AECOPD and HC groups were calculated by unpaired t-tests with a significance cut-off at $p<0.05$. Box plots were created in R using ggplot2.

Ungated raw flow cytometry data was also imported into Cytobank (Cytobank.org) for CITRUS (Cluster Identification, Characterization, and Regression) analysis. Samples were categorized and analysed within lymphocyte or MAIT cell populations. The CITRUS algorithm is a supervised learning method used to identify statistically significant differences in cell populations from high-dimensional cytometry data. The algorithm clusters cells based on similarities in marker expression and then correlates these clusters with a biological outcome (e.g., disease status). In this study, CITRUS was used to identify cell phenotypes that significantly differ between AECOPD patients and healthy controls (HCs). The nodes in the CITRUS plots represent clusters of cells with similar expression profiles for the markers tested. Nodes are linked by edges that represent hierarchical relationships between clusters, with parent nodes encompassing broader cell types and child nodes representing more specific cell subsets (120).

3.3 Results

3.3.1 Patient Demographics

In total, 32 AECOPD patients were recruited for the study with six providing follow-up samples at stability (Table 3.1). $CD4^+$ cells were isolated for gene expression from all AECOPD patients at all time points. $CD8^+$ cells were isolated for gene expression analysis from 25 of the AECOPD patients during admission but were not isolated from follow-up samples due to limited samples. In total, 20 age-matched HCs were recruited. $CD4^+$ cells were isolated for gene expression analysis from 14 HCs

while $CD8^+$ cells were isolated from six due to limited samples. The mean age was similar between groups.

Table 3.1. Rural Australia study participant characteristics across time point

	AECOPD (D1)	AECOPD (D3)	AECOPD (D14)	Stable COPD	Healthy Controls
n (total)	32	7	7	6	20
n (CD4)	32	7	7	6	14
n (CD8)	25	0	0	0	6
Age (SD)	70.6 (8.4)	69.7 (8.3)	66.9 (6.4)	69.0 (6.0)	64.6 (8.3)
Male:Female	17:15	6:1	5:2	6:0	13:7

3.3.2 AECOPD is associated with early-activated $CD4^+$ T-cells

Flow cytometry analysis enabled the dissection of $CD4^+$ T-cell phenotypes in AECOPD compared to healthy controls (Figure 3.1A). A significantly higher fraction of $CD4^+$ $CD25^+$ T-cells was seen in AECOPD compared to HCs. Further analysis revealed these cells to include $CD4^+$ $CD25^+$ $CD69^+$, $CD4^+$ $CD25^+$ $CTLA4^-$, and $CD4^+$ $CD25^+$ $PD1^-$ cells which may represent early activated cells or tissue-resident cells that have returned to circulation (121). Conversely, $CD4^+$ $CD25^-$ $CD69^+$ T-cells and $CD4^+$ $CD25^-$ $CTLA4^+$ cells were significantly lower in AECOPD compared to HCs. There was no significant difference in the percentage of Tregs or expression of PD1, CTLA4 or CD69 on Tregs between AECOPD and HCs. Similarly, no difference in $CD8^+$ T-cell expression of PD1, CTLA4, or CD69 was seen between groups.

3.3.3 MAIT cell numbers are reduced in AECOPD and overexpress inhibitory receptors

The percentage of MAIT cells of $CD3^+$ cells was significantly lower in AECOPD compared to HCs (Figure 3.1B). Median MAIT proportion of $CD3^+$ cells was 0.61% (IQR 0.24-0.96) compared to 3.52 (IQR 0.81-8.32%) in the HCs. The MAIT cells that were present in the circulation of AECOPD patients expressed significantly higher levels of CTLA4 and PD1 compared to HCs however there was no significant difference in CD69 expression between groups. The median proportion of total MAITs that were positive for CTLA4 was 21.40% (IQR 5.88-41.41%) in AECOPD patients and 4.35% (IQR 0.89-10.85%) in HCs. The median proportion of total MAITs that were positive for PD1 was 31.0% (IQR 20.8-50.0%) in AECOPD patients compared to 14.0 (IQR 4.56-28.7%) in HCs. Taken together, this indicates a higher occurrence of exhausted MAIT cells in AECOPD compared to HCs.

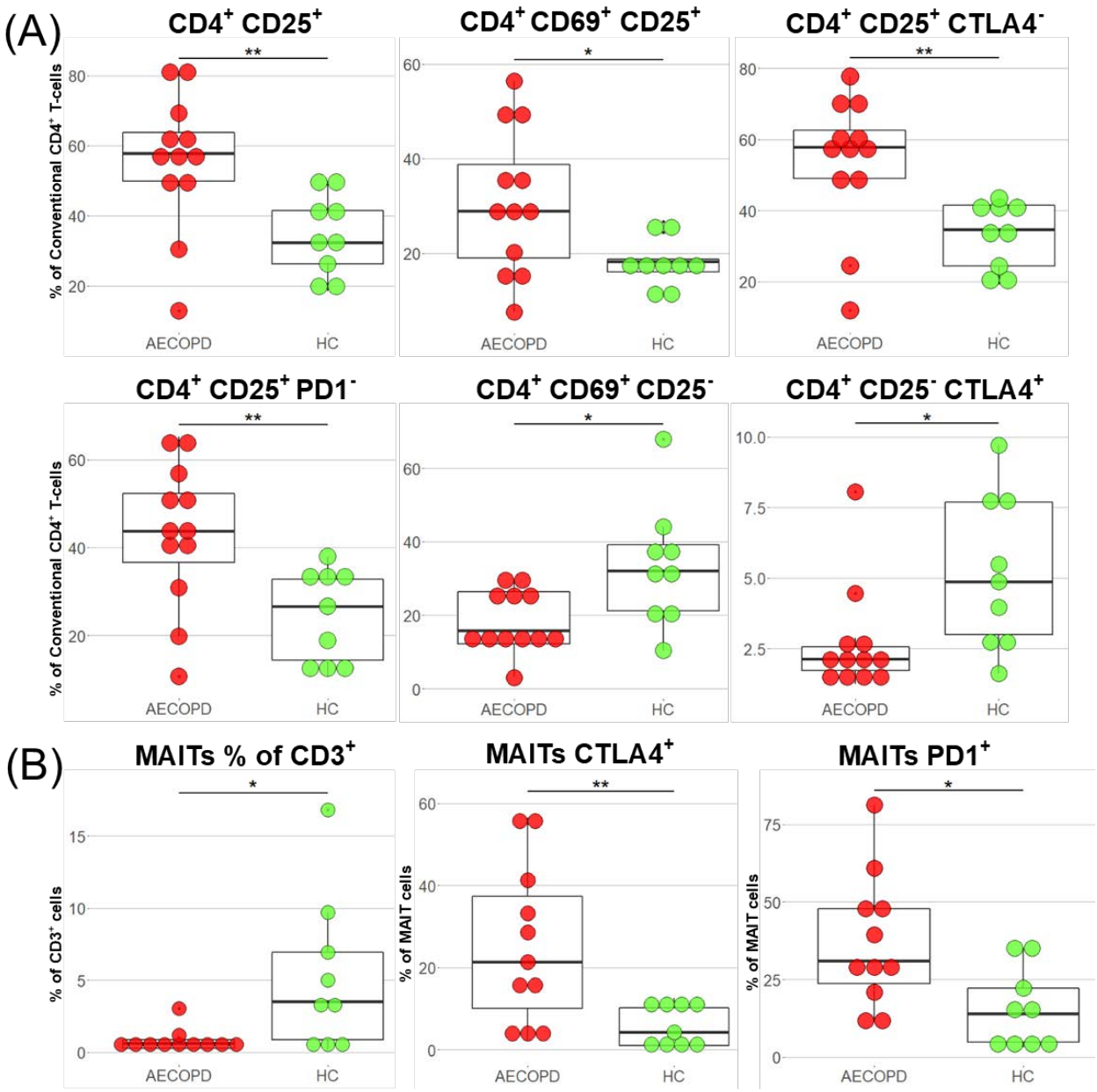

Figure 3.1. Activation and exhaustion marker expression on CD4 T-cells and MAIT cells in AECOPD compared to HCs.

A. Comparison of activation and exhaustion marker expression on $CD4^+$ T-cells. Significantly higher $CD4^+$ $CD25^+$ T-cells, $CD4^+$ $CD69^+$ $CD25^+$ T cells and CD4 $CD25^+$ $CTLA4^-$ or $PD1^-$ T-cells were seen in AECOPD. Significantly lower $CD4^+$ $CD69^+$ $CD25^-$ and $CD4^+$ $CD25^-$ $CTLA4^+$ cells were seen. **B.** MAIT cells were significantly lower in AECOPD compared to HCs. The MAIT cells present in AECOPD had significantly higher levels of CTLA4 and PD1 compared to HC MAIT cells. Mann-Whitney U-tests were performed between groups. Significance is indicated as * p<0.05, ** p<0.01, *** p<0.001.

3.3.4 T-cell subset compositions are altered during the transition from exacerbation to stable COPD

Serial blood samples obtained at admission, day 3, between days 12-18, and at clinical stability (day 30+) were analysed for patterns of change in the cell subsets of interest. $CD4^+$ $CD25^+$ $CD69^+$ and $CD4^+$

$CD25^+$ $CTLA4^-$ cells gradually reduce over time reaching similar levels to HCs by clinical stability of COPD (Figure 3.2A). In contrast, $CD4^+$ $CD69^+$ $CTLA4^-$ cells and $CD4^+$ $CD69^+$ $PD1^-$ cells gradually declined over time and were significantly lower in stable COPD compared to HCs (Figure 3.2B). MAIT cells remained constantly lower in COPD throughout the disease while MAIT cells that are $CTLA4^+$ remain constantly higher compared to HCs (Figure 3.2C)

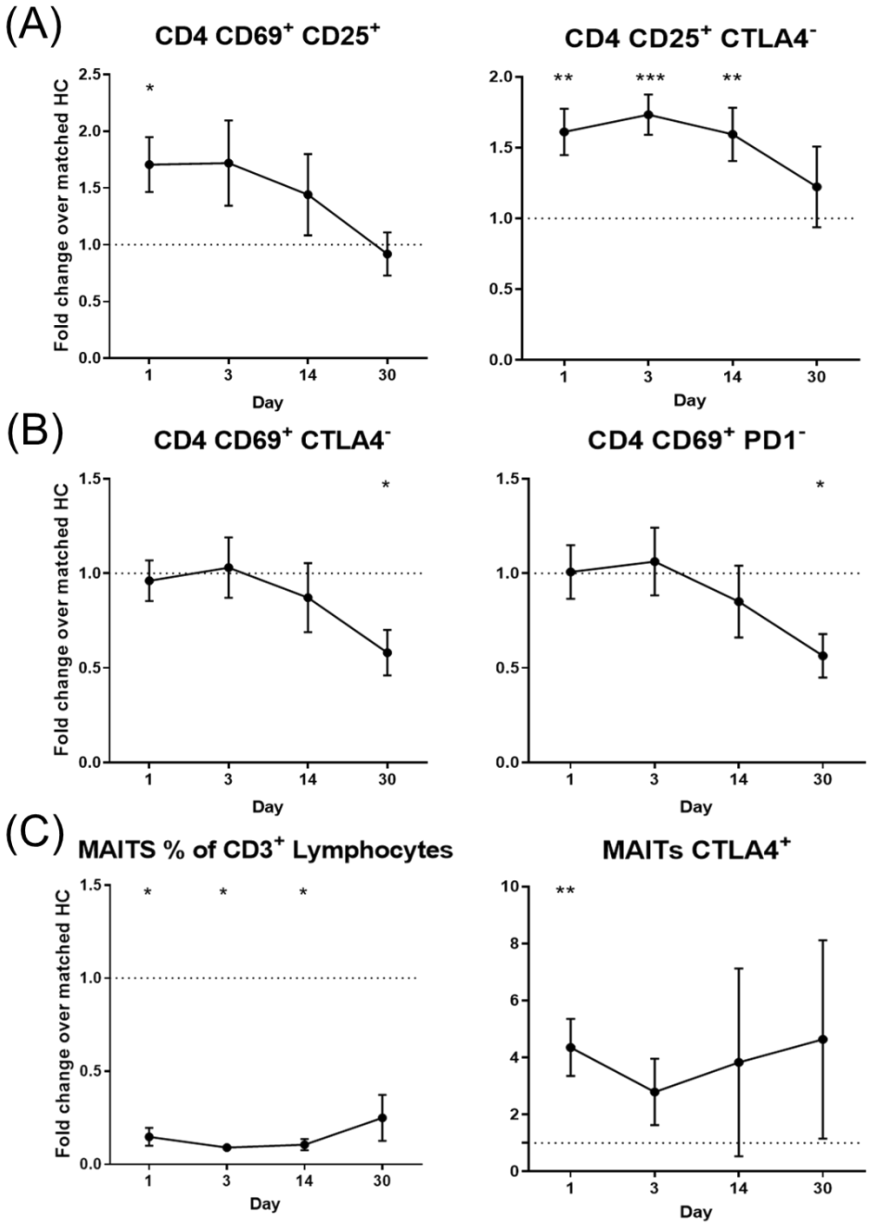

Figure 3.2 Changes in cell subsets over time in AECOPD.
Shown are the fold changes of cell subsets at admission, day 1, day 3, day 12-18 (denoted as day 14), and at clinical stability day 30+ compared to mean percentage values for healthy controls. Error bars represent the SEM around the mean (dots). A value of 1 indicates no change in cell percentage compared to HCs, whereas values <1 indicate a reduction in cells in COPD. **A.** Progressive reduction in $CD4^+$ $CD69^+$ $CD25^+$ early activated cells as well as $CD4^+$ CD25+ $CTLA4^+$ cells is seen until reaching HC levels at clinical stability. **B.** The $CD4^+$ $CD69^+$ cells ($CTLA4^-$ or $PD1^-$) progressively reduced over time until levels were significantly lower than HCs by clinical stability. **C.** MAIT cells remain low compared to HCs throughout while CTLA4 expression on MAIT cells remains

high. Percent cells at each time point were compared to HC levels (unpaired t-test). Significance is indicated as * p<0.05, ** p<0.01, *** p<0.001.

3.3.5 CITRUS analysis reveals clustering of distinct cell phenotypes in AECOPD

CITRUS (Cytobank.org) analysis was performed on cytometry data of AECOPD patients to identify clustering based on multiple expression markers. Analysis of lymphocytes revealed significant differences in the cell abundance at multiple T-cell nodes and in multiple nodes that were negative for lineage markers included in this panel (Figure 3.3). Distinct clusters of conventional CD4+ T-cells, CD8+ T-cells, and FOXP3+ CD25+ Tregs were identified. Nodes such as 87387, 87413, and 87402 in red, green, and blue respectively, are highlighted to indicate statistically significant differences in cell abundance compared to HCs, where maroon signifies a significant difference in abundance in AECOPD patients. The size of each node correlates with the cell count within that cluster.

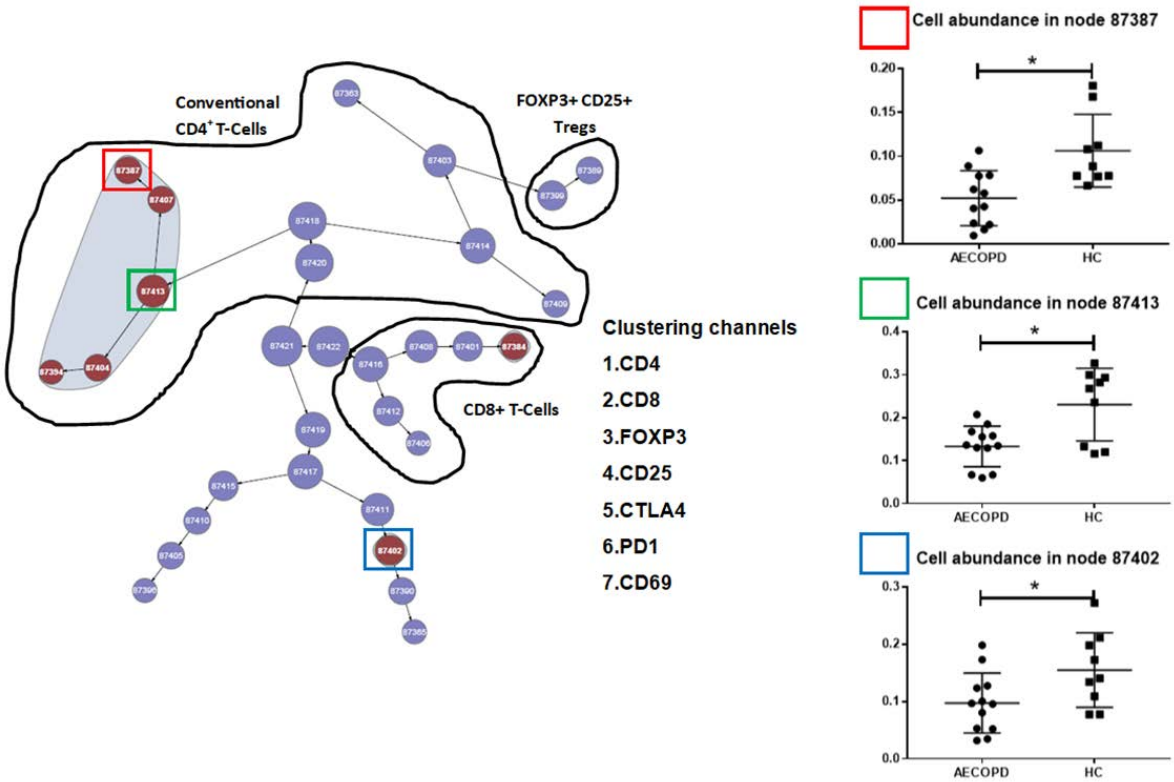

Figure 3.3 CITRUS analysis on lymphocytes from AECOPD patients vs HCs
CITRUS (Cytobank.org) analysis was performed on flow cytometric data from peripheral blood mononuclear cells isolated from ACEOPD (n=12) patients and HCs (n=9). Lymphocyte-gated samples showed clustering of conventional CD4+, CD8+, as well as FOXP3+ CD25+ Tregs; t-tests were calculated on the cell abundance between AECOPD and HCs for significant nodes. Significance is indicated as * p<0.05, ** p<0.01, *** p<0.001.

Similarly, the CITRUS analysis performed on MAIT cells ($CD3^+$ $V\alpha7.2^+$ $CD161^+$) and clustered on the exhaustion and activation markers showed that two subpopulations of MAIT cells existed. These

included an activation/ exhaustion high-expressing population and a comparatively low-expression population (Figure 3.4A). Within the expression plots (Figure 3.4B) nodes show specific marker combinations that characterize subpopulations within the MAIT cells, with colours depicting the relative expression levels: red indicates higher expression, and blue lower expression. These plots provide a detailed view of how expression profiles are distributed across the cell populations. Within the high-expression population, CTLA4, PD1 and TIM3 were often co-expressed while TIM3 and CD69 were often co-expressed on a different subset. Analysis of the abundance nodes showed that while healthy controls had higher numbers of cells that were negative for all markers, AECOPD patients had higher numbers of cells that had high expression of CTLA4, PD1 and TIM3 (Figure 3.4C).

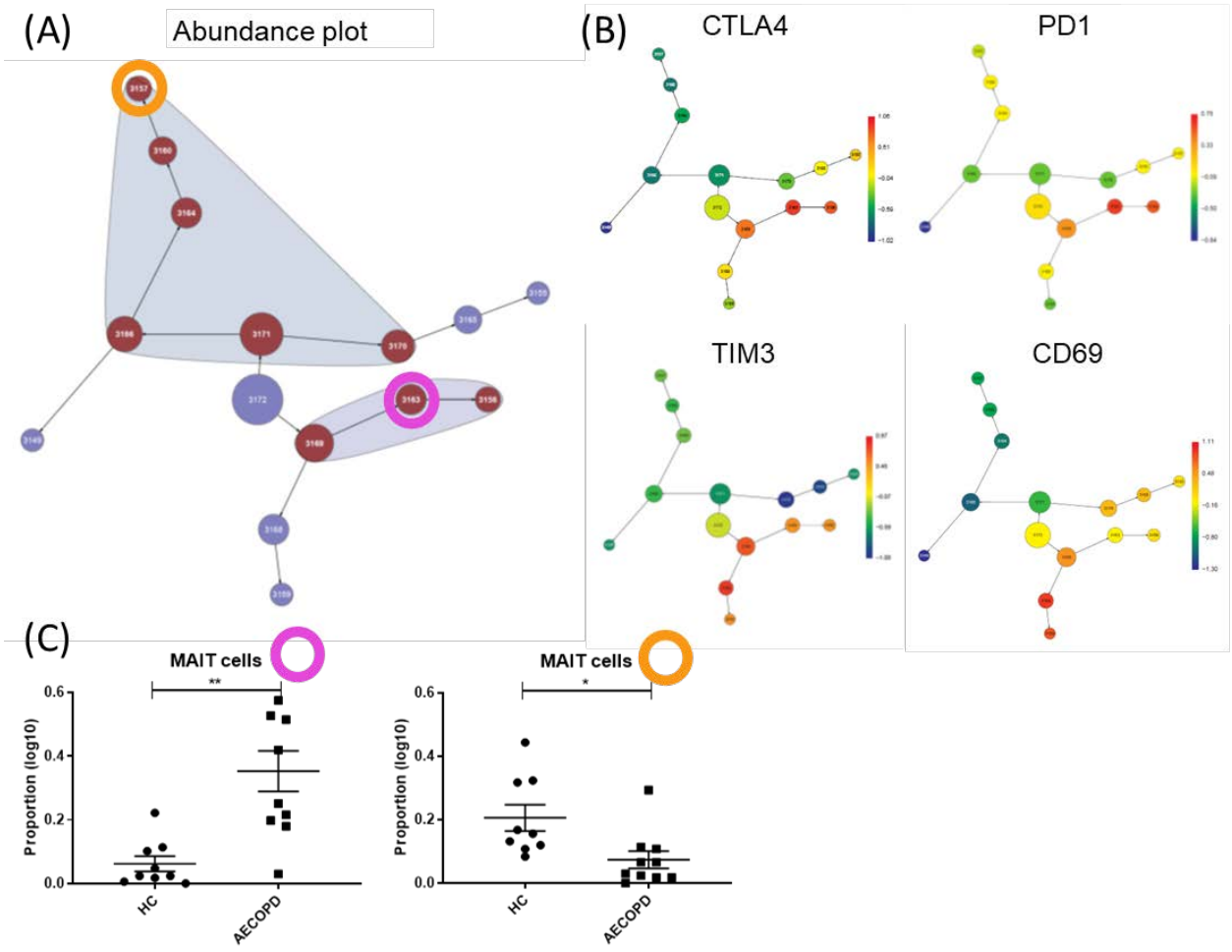

Figure 3.4 CITRUS analysis on MAIT cells.

CITRUS (Cytobank.org) analysis of MAIT cells isolated from PBMCs of ACEOPD (n=12) patients and HCs (n=9). MAIT cells were gated, and clustering was performed on CTLA4, PD1, TIM3, and CD69 markers. **(A)** Abundance plot shows a grouping of distinct phenotypes of MAIT cells based on their relative expression of clustering markers. Maroon clusters indicate phenotypic clusters that had significantly different proportions between AECOPD patients and HCs. Node size is proportional to the number of cells. **(B)** Marker expression plots show the relative expression of each marker for each node. Red clusters indicate high relative expression. Unique combinatorial relative expression levels define the cell population at each node. **(C)** Statistical analysis comparing the proportion of MAIT cells exhibiting the expression profile represented in each node between AECOPD patients and HCs. Mann Whitney tests were employed to assess differences in the proportion of total

MAIT cells with specific expression profiles between the two groups. Significance is indicated as * p<0.05, ** p<0.01, *** p<0.001.

3.3.6 Expression of activation, exhaustion, cell surface markers and transcription factors are altered in AECOPD patient T-cells

Multivariate principal component analysis (PCA) was used to reveal underlying patterns or latent (factor) variables between the gene expression of AECOPD and healthy control groups. Both the $CD4^+$ and $CD8^+$ T-cell data showed separation between AECOPD and HC groups (Figure 3.5A and B). However, stable COPD patients failed to separate from AECOPD patients (Appendix 4). To identify the differences in gene expression, between patient groups (AECOPD and Stable COPD) and HCs, t-tests were performed on the NanoString datasets. The results revealed many unique and overlapping genes between the groups (Figure 3.6 and Appendix 5).

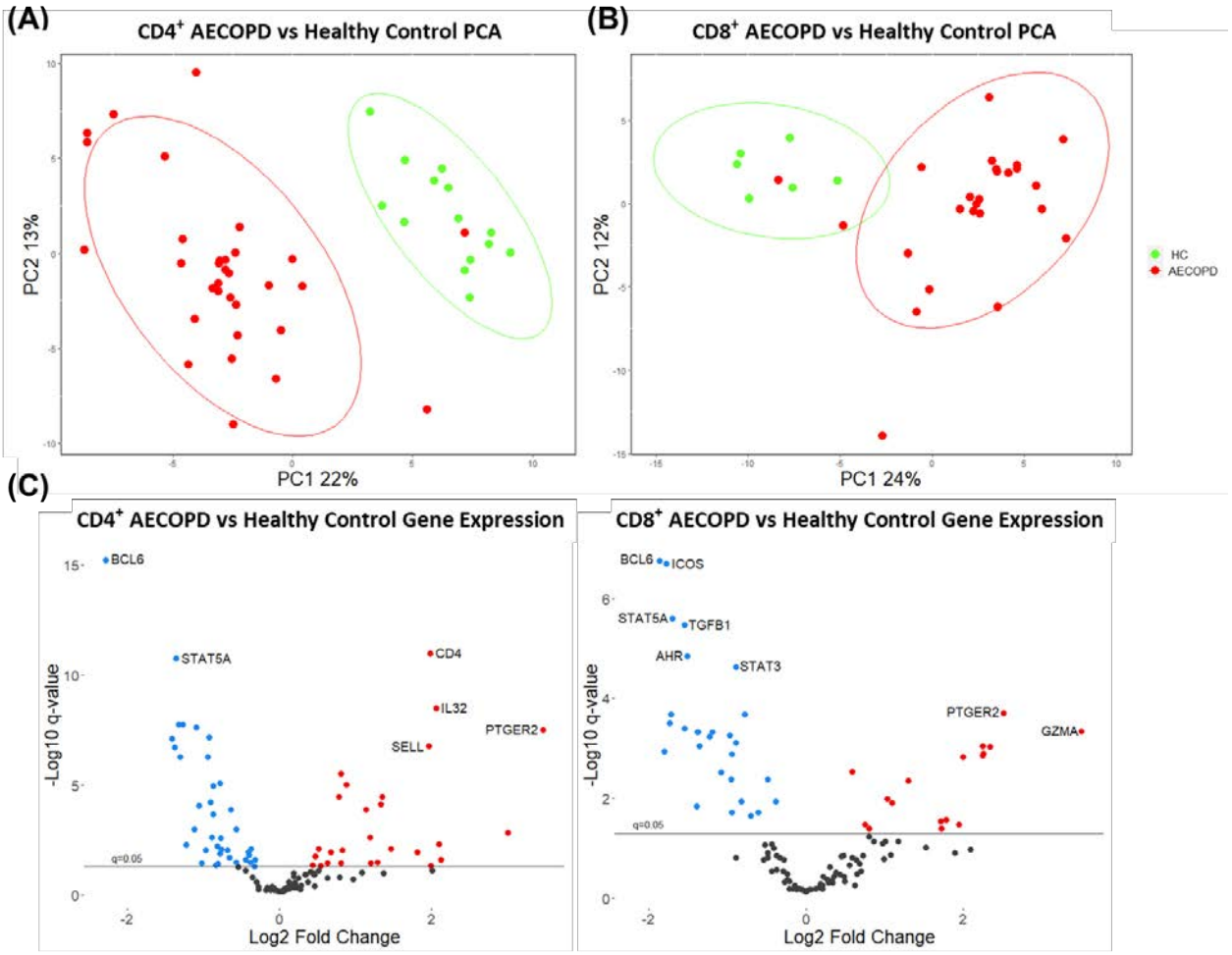

Figure 3.5 Principal Component Analysis and volcano plots for gene expression data.
(A) PCA on $CD4^+$ NanoString datasets displays clustering of AECOPD patients (n=32) and HCs (n=14). **(B)** PCA on $CD8^+$ datasets shows clusters of AECOPD patients (n=25) and HCs (n=14). **(C)** $CD4^+$ and $CD8^+$ gene expression volcano plots. Red dots represent genes that were significantly upregulated in AECOPD patients compared to HCs while blue dots are genes that were significantly downregulated. Grey dots represent genes that did not reach significance (adjusted p-value >0.05).

Upregulation of some immune checkpoint and exhaustion markers was seen in both $CD4^+$ and $CD8^+$ T-cells in AECOPD patients compared to HCs including *CD226* (DNAM), *KLRG1* and *CD244*. Expression of *CD226* in $CD4^+$ cells significantly correlated with FEV1% during exacerbation ($r(15)=0.64$, $p=0.006$) (Appendix 6). The immune checkpoints *CD96* and *CD300A* were increased in $CD4^+$ T-cells. *CTLA4* was decreased in $CD4^+$ T-cells from AECOPD patients which aligns with the expression of CTLA4 described above (Figure 3.1A). Genes for the pro-inflammatory cytokine IL-32 as well as the cytotoxic molecules granzyme and perforin (GZMA, GZMH, GZMK, GZMM and PRF1) were upregulated in both $CD4^+$ and $CD8^+$ T-cells indicating chronic stimulation of activated cells with lytic capabilities. The genes *SELL* (CD62L) and *ITGA4* (CD49d) which are involved in lymphocyte trafficking were both increased in $CD4^+$ T-cells from AECOPD patients while only *SELL* was increased in $CD8^+$ T-cells. The surface receptor *PTGER2* was increased in both T-cell subsets from AECOPD patients.

The activation markers *CD28* and *ICOS* were reduced on both $CD4^+$ and $CD8^+$ T-cells from AECOPD patients, as was *KLRB1* (CD161); expressed on MAIT cells, activated Th17 cells, NK cells and NKT cells. In addition, *CD69* gene expression was reduced in $CD4^+$ T-cells. Cell surface receptor genes *IFNGR1, IL21R, IL4R*, *CCR6, CXCR3, CXCR6* and *S1PR1* were reduced in both cell types. *CCR4* and *CXCR5* expression was reduced in $CD4^+$ T-cells from AECOPD patients while CCR5 was upregulated. *S1PR1* was downregulated in both subtypes and is involved in the SIP1 signalling pathway. Cytokine gene expression was also reduced, particularly in $CD4^+$ T cells, with *IL2, IFNG* and *TGFB1* expression significantly lower in AECOPD patients compared to HCs. *TGFB1* and *IL23A* were also reduced in $CD8^+$ T-cells. Further, *TGFB1* expression in $CD8^+$ cells from AECOPD patients was inversely correlated to FEV1% after the patient had recovered ($r(15)=-0.74$, $p=0.0007$ (Appendix 6)). *IL2RA* (CD25) expression was increased in $CD4^+$ T-cells which corresponds with the increased expression seen in the flow cytometric analysis.

Transcription factor genes *ZBTB16* (PLZF) and STAT5B were increased in $CD4^+$ T-cells from AECOPD patients. The signalling molecule *JAK2* was increased in both cell types while *JAK1* was increased only in $CD8^+$ cells. Transcription factors downregulated in both $CD4^+$ and $CD8^+$ T-cells included *STAT3, STAT5A*, *BACH2, GATA3, BCL6, NFKB1, RUNX3* and *AHR*.

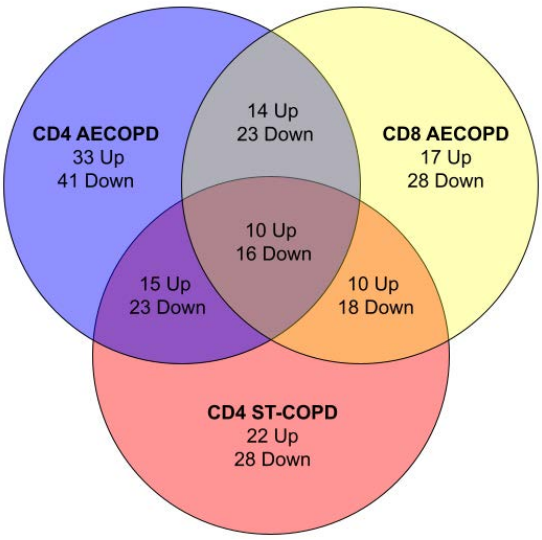

Figure 3.6 Venn diagram of gene expression by cell type and COPD status.
Gene expression data from $CD4^+$ and $CD8^+$ cells from AECOPD patients and $CD4^+$ cells from ST-COPD patients showed overlapping expression patterns when compared to $CD8^+$ or $CD4^+$ cells from HCs.

3.4 Discussion

Flow cytometric and gene expression analysis of peripheral blood T-cell subsets in COPD patients admitted to the hospital with acute exacerbations of the disease was performed. MAITs were significantly reduced in the peripheral blood of AECOPD and stable COPD patients. This is likely due to the homing of MAIT cells out of circulation and into lung tissues. Previous studies have found similar results (95, 96). Two phenotypically distinct populations of MAITs were identified in this study; one with high expression of the activation/checkpoint markers CTLA4, PD1 and TIM3, which may indicate exhaustion, and another with relatively low expression. The high-expressing subset was significantly increased in AECOPD patients while the low-expressing subset was significantly decreased. This MAIT cell phenotype may be implicated in the pathology of COPD. Studies involving MAITs isolated from Irritable Bowel Syndrome patients found that increased PD1 expression was associated with the reduced functional capacity of MAITs (122). It is probable that MAITs are also functionally restrained in COPD patients owing to the increased PD1 and CTLA4 expression observed in the present study. However, the role of this phenotype and its implications for new COPD therapies have not been elucidated.

$CD4^+$ and $CD8^+$ T-cells from AECOPD patients showed heterogeneous expression of activation and exhaustion markers compared to matched healthy control cells. However, the downregulation of genes was the predominant pattern observed (Figures 3.5C and 3.6). Multiple transcription factor genes, chemokine and cytokine receptor genes as well as cytokine genes were expressed at significantly lower levels compared to healthy controls. Transcription factors involved in the

differentiation of Th1, Th2, Th9, Th17 and Tfh cells were expressed at significantly lower levels in both $CD4^+$ and $CD8^+$ T-cell subsets from COPD patients. These included *STAT3, STAT5A*, *BACH2, GATA3, BCL6, NFKB1, RUNX3,* and *AHR* (123-130). This is an interesting finding as it has been demonstrated that the numbers of specific $CD4^+$ and $CD8^+$ subtypes are increased in COPD patients (18, 42, 43, 67, 68). However, expression of transcription factor *ZBTB16* (PLZF), which is found in terminally differentiated $CD4^+$ cells (131), was increased in $CD4^+$ cells from AECOPD patients. Additionally, *RUNX1* expression was upregulated in both $CD4^+$ and $CD8^+$ cells and is involved in T-cell maturation and quiescence (132, 133). *PTGER2* expression was increased in both cell subsets and during stability. PTGER2 was shown to be involved in T-cell priming, T-cell activation and Th1/Treg differentiation (134) and is an important part of the signalling pathway in IL-23-driven Th17 inflammation (135). S1PR1 expression was significantly downregulated in AECOPD and is involved in the SIP1 signalling pathway. SIP1 is implicated in COPD via alveolar macrophages and chronic inflammation (136) and has been shown that interference of S1PR1 by CD69 expression is involved in T-cell retention and establishment of memory cells (137). Gene expression of IL-32 was increased in both T-cell subsets during exacerbation and in $CD4^+$ cells at stability. IL-32 is a proinflammatory cytokine that has been shown to orchestrate the release of proinflammatory cytokines IL-1, IL-6, IL-8, TNF-α and MIP-2 (138, 139). Seminal studies involving IL-32 in COPD patients showed that macrophages were a source of IL-32 in the lungs (140). More recent studies have shown increased IL-32 concentration in the serum of COPD patients that correlated with disease severity (141). Here we showed that T-cells may be an important source of IL-32 in COPD patients.

Interestingly, gene expression of cytotoxic molecules classically associated with $CD8^+$ T-cells was increased in both cell subsets. Increased expression of cytotoxic molecules in $CD4^+$ cells was not only limited to patients with exacerbations but was also seen during stability. This may implicate the involvement of cytotoxic $CD4^+$ cells in COPD pathology. A previous study has noted the potential role of cytotoxic $CD4^+$ cells in COPD but this has never been fully investigated (142).

Specific subsets of $CD4^+$ T-cells increased during acute exacerbations were $CD25^+$ T-cells which co-expressed CD69. Whether these cells represent an early activation phenotype or tissue-resident phenotype that has returned to circulation is unclear. These cells also had lower expression of the immune checkpoints CTLA4 and PD1. This finding was supported by the observed decrease in *CTLA4* gene expression in $CD4^+$ cells. Concurrently, $CD4^+$ T-cells had higher gene expression of the immune checkpoints *CD226* (DNAM), *CD244*, *CD300A* and *CD96*. Both $CD4^+$ and $CD8^+$ cells had reduced expression of *ICOS* (CD278) which is expressed on activated T-cells however, they also had reduced expression of *CD28* which is expressed on naïve and memory cells. Taken together, these findings

suggest there may be reduced functional capacity in effector T-cells. However, functional studies may provide insight into the capabilities of these cells and their roles in AECOPD pathology.

We tracked marker expression patterns through admission up to clinical stability and found a dynamic shift in T-cell phenotype during the transition from an AECOPD to stability. MAIT cells remained low throughout. Activated $CD4^+$ $CD25^+$ T cells gradually reduced to normal healthy control levels over time but $CD4^+$ $CD69^+$ cells that were negative for CTLA4/PD1 gradually reduced over time and at clinical stability were below the level of healthy controls. We also found that *SOCS1* gene expression was associated with exacerbation status as it was upregulated in T-cells during an exacerbation compared to HCs and decreased at stability in $CD4^+$ cells. SOCS1 is involved in the maintenance of FOXP3 expression in Treg cells. Loss of SOCS1 expression in inflammatory environments can lead to Treg plasticity and conversion into Th1 or Th17 cells (143, 144). Our finding coincides with decreased expression of *FOXP3* in $CD4^+$ cells during an exacerbation and provides further evidence that the inflammation seen during an AECOPD is not merely an increase of the inflammation that is present in stable patients but is a dynamic shift of the entire immune profile. This shift is likely nuanced by the exacerbation trigger and studies involving larger cohorts of patients may succeed in identifying such biomarkers.

The role of immune checkpoints in AECOPD is still unclear. In COPD patients, elevated PD1 has been reported in lung $CD8^+$ T-cells (82) and elevated CTLA4 has been reported in peripheral blood $CD4^+$ T-cells (117). *Ex vivo* trials of anti-PD1 and anti-CTLA4 antibodies, which are currently in use in cancer immune therapeutics, have shown increased IFN-γ production by cells (80). However, the optimum balance of immune activation versus immune regulation in COPD remains to be established. Is the chronic activation of T-cells in the COPD lung what drives disease progression and when does immunity become ineffective, resulting in increased susceptibility to viral and bacterial infections? We hypothesize that both $CD4^+$ and $CD8^+$ T-cells which are highly exhausted, have increased expression of multiple immune checkpoints and could be returning to circulation in COPD patients.

Chapter 4: Peripheral blood immune profiling in a biomass smoke-exposed rural, remote community from PNG: establishing a baseline

4.1 Introduction

Tobacco smoke exposure is the predominant cause of COPD in Western countries. The studies in the previous chapter elucidated the T-cell immune response in the blood of patients suffering from exacerbations of the disease and during stability. These insights move us closer to developing new treatments for COPD and personalized precision medicine for patients in Western countries with tobacco smoke-induced COPD. However, knowledge of similar lung diseases caused by biomass smoke exposure in low to middle-income countries (LMICs) is severely lacking due to underdeveloped health system infrastructure including diagnostic capacity and patient management (145). Biomass, including wood, dung and crop waste, are commonly used as cooking and heating sources in areas where more efficient technologies are not easily obtainable. Studies on the effects of chronic biomass smoke exposure and resulting lung disease are of particular importance due to the frequent use of biomass fuels for cooking and heating in LMICs (146). According to the World Health Organization, 2.4 billion people use inefficient fuel sources, such as biomass, for cooking. Additionally, 3.2 million people die each year from illnesses associated with the use of these fuel sources (9). Despite this, the effects of biomass smoke on the body and immune system are poorly understood. To better understand how biomass smoke leads to COPD, we must first examine its impact on healthy individuals, as this will enable us to distinguish the specific immune differences that may be associated with disease states.

Tobacco smoke and biomass smoke have many similarities in their effects on the lung and systemic immune responses yet also many differences that prevent the extrapolation of immune effects from one to the other. This is evidenced by the different clinical effects that manifest in individuals exposed to these different types of smoke (see Chapter 5 Introduction). Hundreds of compounds have been identified in biomass smoke and thousands in tobacco smoke, many of which have been found to cause adverse health effects when inhaled (147-149). These include metals, oxidizing chemicals, volatile organic compounds, and others that damage lung tissues and may invoke an immune response (150). However, the composition and size of particulate matter in these two types of smoke vary significantly, which plays a critical role in their deposition within the respiratory tract. Tobacco smoke predominantly contains ultra-fine particulate matter ($PM_{2.5}$, particles ≤ 2.5 μm) that can reach distal areas of the lung including the alveoli (151, 152). These particles lead to the breakdown of alveolar connections and resulting emphysema (153). Biomass smoke, on the other

hand, tends to contain larger particles, predominantly in the PM_{10} range, which are deposited primarily in the upper respiratory tract, such as the trachea and bronchi(151, 154, 155). The larger size of particles in biomass smoke do not penetrate into the alveoli as easily but contribute to the development of chronic bronchitis and mucus hypersecretion(156-158). The route of exposure between biomass smoke and tobacco smoke also differs significantly. Biomass smoke exposure typically occurs for long periods (i.e. multiple hours) and begins early in life whereas tobacco smoking occurs in shorter intervals and begins at an older age. These differences may yield distinct immune responses however, it is poorly understood.

A limited amount of research has investigated the immune response to chronic biomass smoke exposure. Studies found higher neutrophil, eosinophil, alveolar macrophage, and lymphocyte counts in the sputum of biomass smoke-exposed women compared to non-exposed women. Further investigation found increased levels of inflammatory markers such as IL-6, IL-8, and TNF-α in the sputum of the exposed women (159). *In vitro* studies demonstrated that biomass smoke increased the release of the proinflammatory cytokines IL-8 and GM-CSF in primary human small airway epithelial cells which are capable of inducing innate immune cell migration (160). It has also been reported that biomass exposure lowered the expression of TIMP-1 (TIMP metallopeptidase inhibitor 1) compared to cigarette smoke in human airway epithelial cells. This molecule is important for maintaining the homeostasis of the extracellular matrix by inhibiting destructive metalloprotease activity. Mouse models exposed to biomass smoke had higher levels of G-CSF and GM-CSF in lavage fluid compared to tobacco smoke-exposed mice suggesting higher recruitment of granulocytes and monocytes in the respiratory tract (161). Further observational studies focused solely on female participants as they are the primary demographic exposed to biomass smoke in some countries. The research found that there were increased serum concentrations of IL1-ra, IL-6, CXCL8, CXCL10, eotaxin, and RANTES in biomass smoke-exposed women compared to healthy controls (162). Further analysis showed that, compared to tobacco smoke-exposed individuals, biomass smoke-exposed participants had higher serum CXCL8 and CXCL10 concentrations (162). These chemokines are largely responsible for the recruitment of neutrophils, macrophages, and T-cells into tissues (163-165). Biomass smoke participants also had lower IL-2 and CCL4 levels (162). IL-2 functions to activate T-cells while CCL4 (MIP-1β) is a chemoattractant for numerous immune cell types including monocytes/macrophages, T-lymphocytes, natural killer cells and dendritic cells (166, 167). These findings suggest that there may be unique inflammatory responses to biomass smoke compared to tobacco smoke, but this remains poorly understood.

Impaired immune responses are a hallmark feature of chronic tobacco smoking (see Chapter 2). This impairment is partially responsible for the increased susceptibility to respiratory infections that are

well-documented in cigarette smokers (168, 169). The dysfunctional immune response to tobacco smoke involves multiple cell types and has been described by numerous studies (see Chapter 2). It is unclear if the same mechanisms are involved with biomass smoke exposure. Susceptibility to respiratory infections is a significant concern in biomass-exposed individuals. In particular, multiple studies have found increased odds of contracting tuberculosis in people chronically exposed to biomass smoke (170-172). It has been speculated that biomass exposure also increases susceptibility to COVID-19 infection (173).

Increased risk of respiratory infections highlights the need to better understand the effects of chronic biomass smoke exposure on the body, particularly the immune system. People living in LMICs use biomass as a fuel source due to cultural reasons and because they do not have efficient access to cleaner technologies for cooking, so cessation is not an option (174, 175). Increased knowledge of the immune response to biomass smoke exposure may reveal drug targets that can reduce the negative effects of exposure. Further, it is important to understand the immune response across a multitude of settings. Biomass smoke is generated from burning an array of different materials. There is evidence to suggest that different sources of biomass smoke may induce different responses in the body (149, 176, 177). Additionally, it is unknown if biomass smoke tends to induce unique effects in people with different genetic backgrounds. Together, these underscore the need to research the effects of biomass smoke in multiple settings across the world.

Papua New Guinea reports the highest global prevalence of COPD (178) and, as is the case in other LMICs, rural communities rely heavily on the burning of biomass (typically plants/wood) to provide fuel for cooking. Our study site in PNG is Balimo in the Western Province and is representative of many other rural communities in PNG. Before commencing analysis of immune profiles in individuals from Balimo with respiratory disease, it was essential to describe the immune profiles of individuals who are chronically exposed to smoke from wood-fuelled cooking fires yet are not seeking healthcare.

Therefore, the Aim of the current Chapter is:

- To describe the peripheral blood immune profiles of participants from rural PNG who were chronically exposed to biomass smoke yet did not have signs of lung disease.

This is a novel context for research into the effects of biomass smoke and also expands knowledge of the immune cell types and inflammatory markers associated with exposure types and contrasts it with what is typically expected in Western countries. The baseline immune parameters established in this study lay the foundation for future studies into disease states in this community.

4.2 Methods

4.2.1 Participant recruitment and ethics

Ethics was approved by the PNG Medical Research Advisory Council (MRAC 19.21) and by the James Cook University Human Research Ethics Committee (H8015). This ethics approval entitled "*Tuberculosis co-morbidities: Implications for tuberculosis susceptibility in Balimo District, Papua New Guinea*" covered a broad study of tuberculosis co-morbid diseases including the effect of cooking smoke on participant parameters. These ethics approvals relate to Chapters 4-6. The questionnaire that was used for data collection from all study participants is provided in Appendix 7. Participants were recruited from the community in the Balimo district of the Western Province, Papua New Guinea. Balimo is a rural community in PNG and is home to about 4300 people. It is considered the urban centre of the Middle Fly District of the Western Province. There are few roads through the region and most transportation is on foot or by boat. Facilities at the Balimo District hospital are very limited and there is no resident physician. Demographic and clinical data including age, sex, height, weight, presence of cough, shortness of breath, and smoke exposure was recorded from each participant.

Participants of either sex were included in this initial baseline study if: (1) they were not currently seeking health care for any illness; (2) did not have a cough and; (3) were unable to produce a spontaneous sputum sample or produced a sputum sample lacking immune cells (see section 4.2.2). Community participants were excluded from this part of the study if they reported a current cough, shortness of breath or were able to produce a spontaneous sputum sample containing immune cells.

Figure 4.1. Photo of cooking fire in Balimo Community.
Cooking fires are typically underneath or within houses in this community leading to chronic exposure to wood smoke. Photo credit: Jeffrey Warner.

4.2.2 Sample collection

Facilities for sample processing and immunological assays were limited in Balimo, therefore collected blood samples were transported to James Cook University, Townsville, Australia within seven days of collection for processing, flow cytometry and plasma storage. For flow cytometric analysis of leukocyte subsets, peripheral blood was collected from participants into Cyto-Chex Blood Collection Tubes (BCTs containing EDTA as an anticoagulant, Streck). Following collection, samples were stored at 4°C before being transported to laboratory facilities at James Cook University for further processing. We have previously established a sample pipeline determined to ensure blood

and sputum sample quality suitable for flow cytometry analysis and plasma cytokine analysis (data not shown). We have confirmed previously that the Cyto-Chex leukocyte stabilisation solution preserved peripheral blood leukocyte integrity and absolute counts for at least seven days when transported from the collection site (Balimo, PNG) to the assay site (Townsville, Australia). Additionally, previously published studies have found that Cyto-Chex tubes are highly effective at preserving T-cells for seven days prior to flow cytometric analysis (179). Plasma used in the current study was collected as part of the broader tuberculosis study where Quantiferon TB GOLD Plus BCTs containing heparin were used for the collection of peripheral blood; the current study only used plasma collected from the Quantiferon "Nil" tubes i.e. BCTs without *Mycobacterium tuberculosis* antigens. See Section 4.2.4 for further information about plasma processing for cytokine analysis.

4.2.3 Whole blood flow cytometry

Flow cytometry differentials and determination of absolute counts were performed on whole blood samples collected in Balimo into Cyto-Chex BCTs and based on the procedures and gating strategies described by Faucher et al. (180) and Roussel et al. (181) with some modifications. Whole blood (100μl) from Cyto-Chex BCTs was aliquoted into 5ml Falcon flow cytometry tubes, washed in 2ml flow cytometry buffer (PBS/0.05% Tween 20) by centrifugation at 450xg for 5min and then resuspended in the residual volume. Two different antibody panels were prepared by diluting fluorochrome-conjugated antibodies (Table 4.1) to previously optimised concentrations in BD Brilliant Stain Plus buffer. 50μl of diluted antibody was added per test and tubes were incubated for 30-40min at 4°C. Following erythrocyte lysis in 1x BD FACS Lysing Solution for 10min at room temperature (25°C), tubes were centrifuged, and cells were then fixed in eBioscience Intracellular (IC) Fixation Buffer Fixation Buffer for 20min at RT. Cells were then washed twice in flow cytometry buffer before resuspension in 300μl cold BD Sheath Fluid. Fluorescence minus one (FMO) control tubes were prepared for each marker and BD CompBeads Anti-Mouse/Anti-Rat Ig, κ/Negative Control Compensation Bead Sets were used for compensation as appropriate. Before sample acquisition, 10μl of Invitrogen 123count eBeads Counting Beads (1,009,000 beads/ml) were added per tube to calculate absolute cell counts (cells/L). Sample acquisition was performed on a BD Biosciences FACSCanto II flow cytometer with BD FACS DIVA acquisition software and analysis was done using FlowJo V10.7.2 software (BD). Major leukocyte types were defined based on the markers shown in Table 4.2. The concentrations of major leukocytes were calculated as described by the manufacturers (i.e. Absolute count (cells/uL) = (cell count x eBead volume)/(eBead count x cell volume) x eBead concentration) with median counts determined as cells/L and plotted as boxplots

with 25th to 75th percentiles and outliers along with the reference ranges from the Royal College of Pathologists of Australasia or American College of Physicians (182, 183).

Table 4.1 Fluorochrome-conjugated antibodies and panels used for flow cytometry differentials and absolute counts from whole blood.

Marker	**Fluorochrome**	**Clone**	**Supplier, Cat No.**
Innate panel			
CD45	BD Horizon™ BV510	HI30	BD 563204
CD14	AF488	M5E2	BD 557700
CCR3/CD193	PE	5E8	BD 558165
CD16	APC-H7	3G8	BD 560195
CD56	BV421	NCAM16.2	BD 562751
CD3	BUV395	SK7	BD 564001
Lymphocyte panel			
CD3	BV711	SK7	BD 740832
CD8	BB515	RPA-T8	BD 564526
CD19	PerCP-Cy5.5	HIB19	BD 561295
CD161	PE	191B8	Miltenyi Biotec 130-092-677
CD4	PE-Cy7	SK3	BD 557852
CD294	AF647	BM16	BD 558042
Vα7.2 TCR	APC-Cy7	3C10	Biolegend 351714

Table 4.2 Marker combinations used to identify major leukocytes in peripheral blood.

Cell	**Markers**
Innate panel	
Monocytes	$CD45^{+}SSC^{lo}CD16^{lo/int}CD14^{+}$
Neutrophils	$CD45^{+}CD16^{+}$
Eosinophils	$CD45^{+}SSC^{hi}CD16^{lo}CCR3^{+}$
NK cells	$CD45^{+}SSC^{lo}CD16^{lo/int}FSC^{lo}CD3^{-}CD56^{+}CD16^{+/-}$
NKT cells	$CD45^{+}SSC^{lo}CD16^{lo/int}FSC^{lo}CD3^{+}CD56^{+}$
Lymphocyte panel	
T-cells	$FSC^{lo}SSC^{lo}CD3^{+}$
CD4 T-cells	$FSC^{lo}SSC^{lo}CD3^{+}CD4^{+}$
CD8 T-cells	$FSC^{lo}SSC^{lo}CD3^{+}CD8^{+}$
B-cells	$FSC^{lo}SSC^{lo}CD19^{+}$
MAIT	$FSC^{lo}SSC^{lo}CD3^{+}CD161^{++}$

4.2.4 Plasma cytokine profiling

Participant blood was collected into "Nil" blood collection tubes containing heparin from Quantiferon TB GOLD Plus tests (QFTs). QFT tube supernatants, processed in this way are routinely used for measuring Interferon-gamma (IFN-γ) via capture ELISA and other investigators have measured other cytokines in similar samples using capture ELISAs and/or multiplex bead assays (e.g Suzukawa et al. 2020 (184); Wergeland et al. 2016 (185), Lighter-Fisher et al. 2010 (186), and Ruhwald et al. 2007 (187)). After 16 hours of incubation at 37°C, "Nil" BCTs were centrifuged for 15min at 2500 x g. The gel plug in the BCT physically separated the plasma from cells and tubes were stored at 4°C until transported to James Cook University, within seven days of collection. Upon arrival in the laboratory, plasma was retrieved from BCTs and stored at -80°C until used for cytokine analysis. The sample pipeline, in terms of assessing sample quality for flow cytometry markers such as cells and cytokines, was validated through two approaches. First, a pilot study was established that mimicked the known (data tracked from a previous trip) temperature fluctuation and time variables encountered n PNG, was undertaken in Townsville. It was determined that the flow markers were not significantly affected compared to fresh controls at the temperature fluctuations expected up to 14 days storage prior to analysis. Also, internal controls comprising blood collected from a field trip participant was collected in-field and results of analysis was compared to fresh collected upon return. No significant differences in cell markers between infield control and fresh were revealed.

Plasma cytokine concentrations were measured using Biolegend LEGENDplex™ Human Th Cytokine Panel 12-plex assays in filter plates. Cytokine analytes included IL-2, IL-4, IL-5, IL-6, IL-9, IL-10, IL-13, IL-17A, IL-17F, IL-22, IFN-γ, and TNF-α. These cytokines are related to T-cell activity. Measurement of these allowed for the analysis of Type-1, Type-2, and Th17-driven inflammatory profiles. The role of type-1 and Th17-driven inflammation has been described in tobacco smoke-induced COPD (see Chapter 2) and aligns with our findings (see Chapter 3) while some studies on biomass smoke-induced COPD have identified a possible role of type-2 responses (28, 188). Measurement of these cytokines in healthy biomass smoke-exposed individuals establishes a broad baseline of T-cell-related inflammatory profiles which will allow for further research on biomass smoke-induced COPD. The manufacturer's instructions were followed except that the volume of each kit reagent (capture beads, standards and detector antibodies) was reduced by 30% as previous results from our laboratory indicated that reduced volumes did not impact results. Plasma samples were thawed and diluted 1:1 in Assay Buffer before use.

Data was acquired on a BD Biosciences FACSCanto™ II flow cytometer. Data was exported as FCS 3.0 files. Raw data files were uploaded into the BioLegend LEGENDplex™ cloud-based data analysis software. Standard concentrations were based on Certificates of Analysis for each kit lot number and to account for the two-fold dilution, all sample concentrations were multiplied by the dilution factor (x2). Standard curves were fitted with 5PL curve fitting and sample values for each analyte were determined by interpolation and extrapolation of these standard curves. Cytokine concentration values were exported from the LEGENDplex™ software using an option that includes values outside the limit of detection (LOD). This feature allows the software to estimate concentrations that fall below the minimum or exceed the maximum used for the standard curve. This approach was chosen to prevent the statistical biases that can arise from other methods such as substituting extreme values with the top standard concentration, exclusion of extreme values, or replacing low values with half the lower LOD.

As there are no generally accepted plasma/serum cytokine reference ranges for healthy individuals, the current study used ranges previously reported for healthy individuals (189-191). This data set was created by analysing the peripheral cytokine profiles of 126 carefully screened individuals from North Carolina, USA. Participants were between 18 and 64 years old, included an even age and sex distribution and at least 30% non-Caucasians. Extrapolated data was plotted against previously reported healthy ranges. This dataset was chosen as the comparative data as it used the cohort (n=126) among the datasets considered and contained the most overlap with the analytes measured in the present study. Descriptive statistics of cytokine concentrations were calculated and reported as medians and 95% confidence intervals. Processed data was downloaded and plotted in R Studio using the ggplot2 and ComplexHeatmap packages.

4.2.5 Other statistical analysis

All other statistical analyses were performed Graphpad Prism (V 9.0.0). The impact of age on cellular and cytokine profiles was determined by first using the Shapiro-Wilk test to determine the distribution of the data followed by Spearman's correlation or Pearson's correlations for non-normally distributed data or normally distributed data respectively. Additionally, age and sex data were overlayed on the heatmaps that were created from the cellular and cytokine data.

4.3 Results

4.3.1 Participant description and demographics

In total, 46 participants were included in this study with 11 males and 35 females. Balimo has a population of 4274 indicating that this study captured 1.1% of the population (192). Participant characteristics are presented in Table 4.3. The mean age was 45 years (range: 17-86). All (100%) participants reported that wood fuels were utilized for cooking in their homes. 61% of participants stated that the cooking fires were inside their house and 33% stated that the fire was underneath their house. 83% of participants reported that they regularly participated in cooking activities in their households. Therefore, chronic exposure to biomass smoke was a feature of this population.

Table 4.3 Participant characteristics of participants without evidence of biomass-smoke-induced lung disease

Variable	**Healthy (46)**
Females	76% (35)
Age (years)	45 (Range 17-86)
Cooking fire exposure	100%
Location of fire	
Inside house	61% (28)
Outside/Underneath house	33% (15)
Away from House	7% (3)
Current Tobacco Smoke (smoker)	11% (5)
Participate in Cooking	83% (38)

4.3.2 Immune cell counts in the peripheral blood of biomass smoke-exposed participants show evidence of dysregulation compared to Western reference ranges

Innate and lymphocyte cell counts in the peripheral blood of healthy, biomass-exposed, non-healthcare-seeking participants were determined by flow cytometry (Figure 4.2 A and B). The peripheral blood counts (cells/L) and frequencies of each of the major leukocyte types are shown in Table 4.4.

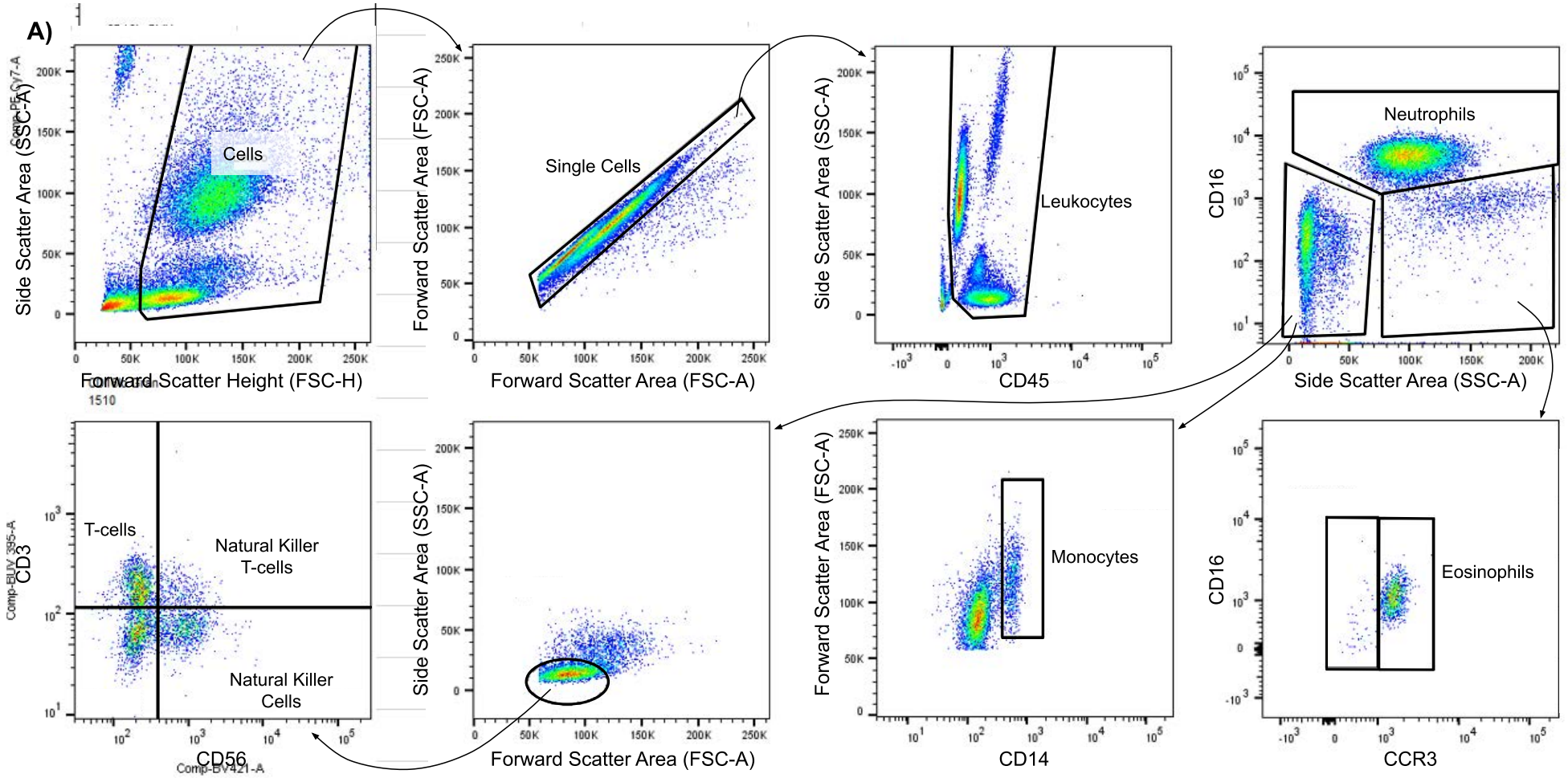
A)
Side Scatter Area (SSC-A)
Forward Scatter Height (FSC-H)
Cells
Forward Scatter Area (FSC-A)
Single Cells
Side Scatter Area (SSC-A)
CD45
Leukocytes
CD16
Side Scatter Area (SSC-A)
Neutrophils
CD3
CD56
T-cells
Natural Killer T-cells
Natural Killer Cells
Side Scatter Area (SSC-A)
Forward Scatter Area (FSC-A)
Forward Scatter Area (FSC-A)
CD14
Monocytes
CD16
CCR3
Eosinophils

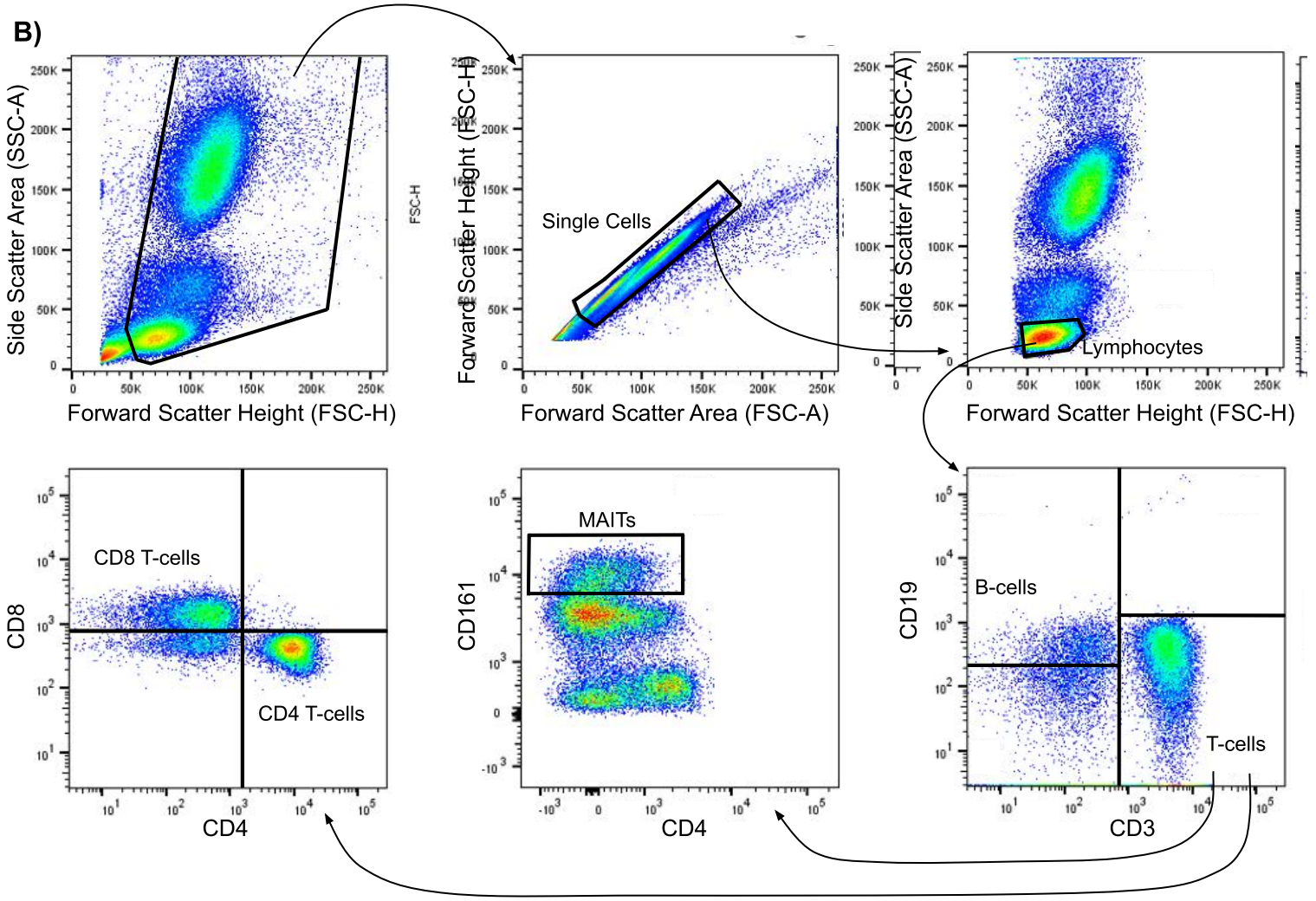

Figure 4.2 Gating strategies used to identify major immune cell types.
(A) Innate leukocyte panel used to identify neutrophils, eosinophils, monocytes, natural killer cells, and natural killer T-cells. **(B)** Lymphocyte panel used to identify B-cells, MAIT cells, CD4 T-cells, and CD8 T-cells.

Table 4.4 Peripheral blood immune cell concentrations and frequencies in a biomass smoke-exposed non-health-seeking community.

The median concentration as well as the upper and lower bounds of the 95% confidence interval were calculated. The median frequency of parent is the proportion of total leukocytes for innate cells and the proportion of total T-cells for helper and cytotoxic T-cells. No reference range is established for MAIT cells. Reference ranges were established by the Royal College of Pathologists of Australasia or American College of Physicians (182, 183)

Cell type	Median (10^9 Cells/L)	95% Confidence Interval (10^9 Cells/L)	Median Frequency of parent (%)	95% Confidence Interval (% of parent)	Reference Range (182, 183) (10^9 Cells/L)
Leukocytes	4.18	3.75-4.74	-	-	4.0-10
Neutrophils	2.27	1.89-2.79	55.0	52.1-57.8	2.0-7.5
Eosinophils	0.273	0.211-0.405	6.52	5.17-8.42	0.04-0.4
Monocytes	0.177	0.144-0.199	4.15	3.74-4.49	0.2-0.8
NK cells	0.187	0.157-0.220	4.57	3.41-5.47	0.05-0.35
NKT	0.0334	0.0252-0.0399	0.855	0.590-1.06	0-0.03
T-cells	0.607	0.528-0.761	-	-	0.6-2.4
B-cells	0.288	0.250-0.340	-	-	0.04-0.5
Helper T-cells	0.309	0.267-0.380	53.4	50.8-57.0	0.5-1.4
Cytotoxic T-cells	0.181	0.159-0.231	30.8	27.7-36.1	0.2-0.7
MAIT cells	0.0501	0.0398-0.0698	8.42	6.61-9.70	-

In the current study, Vα7.2 TCR staining, which, in combination with $CD161^{hi}$ staining within the CD3 T-cell gate, is typically used to identify MAIT cells, appeared downregulated. CD161 is most highly expressed on MAIT cells ($CD3^{+}CD161^{++}$), although both CD8 and CD4 T cells also express this marker. In the current study, the population showing the highest CD161 staining (i.e. $CD161^{++}$) within the CD3+ gate was defined as MAIT cells.

The results show that the median monocyte count was below the established reference range while total leukocyte and neutrophil counts trended low with 43% and 40% of participants respectively falling below the reference ranges. The mean natural killer T-cell count was above the reference range. The mean eosinophil count was on the upper end of the reference range with 35% of participants above the reference range. Natural killer cell counts were generally within the expected reference range (see Figure 4.3). Peripheral blood total lymphocyte, T-helper, and cytotoxic T-cell counts were lower on average compared to the reference range while B-cell counts were normal (see Figure 4.4). 95% confidence intervals were computed for the innate and lymphocyte cell counts with the aim of establishing normative ranges for this community Table 4.4).

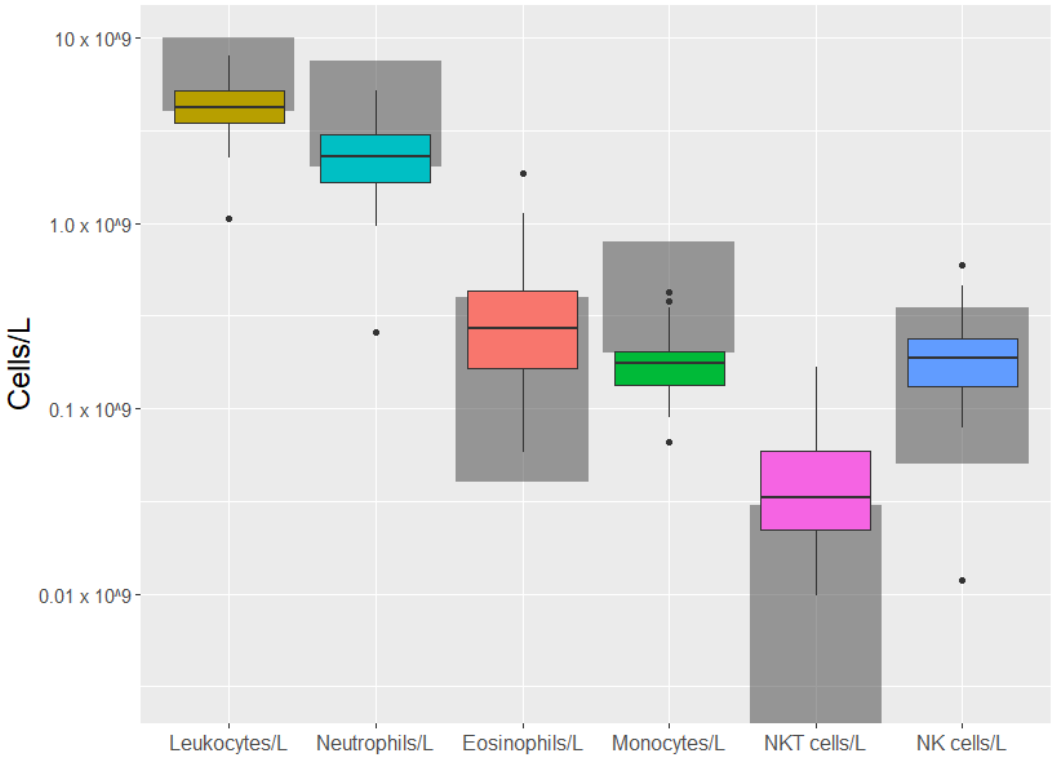

Figure 4.3 Peripheral blood innate cell concentrations.
Median and interquartile ranges (25th to 75th percentiles – boxes) and Tukey whiskers with outliers indicated of innate cell counts per litre were plotted on top of reference ranges established by the Royal College of Pathologists of Australasia or American College of Physicians (182, 183).

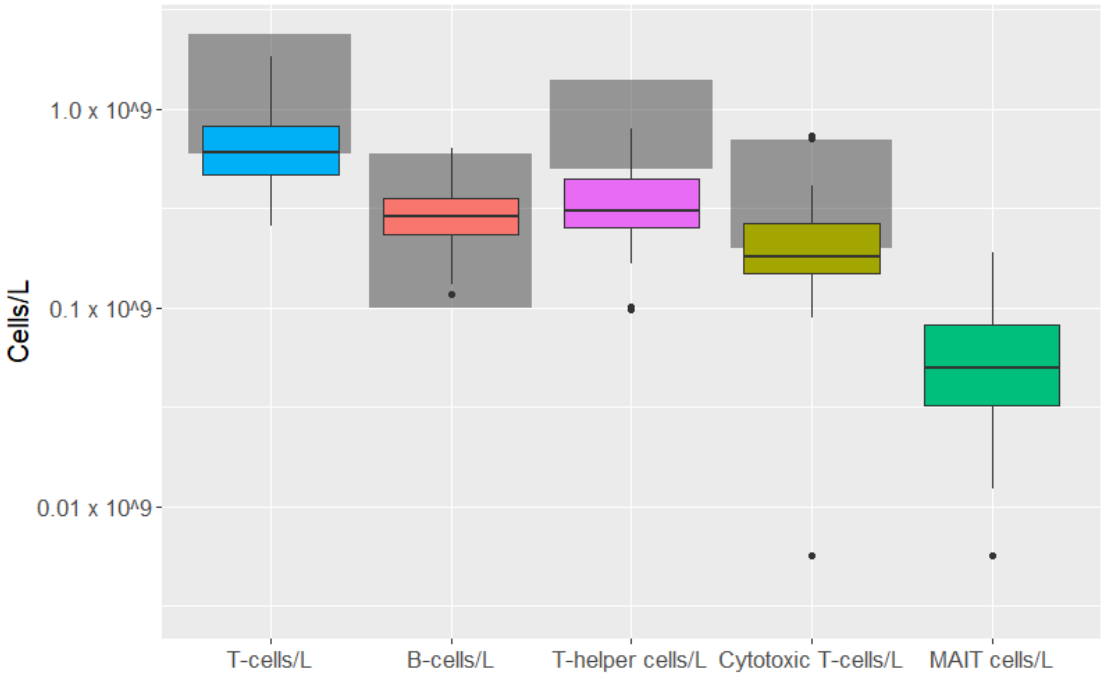

Figure 4.4 Peripheral blood lymphocyte concentrations.
Median and interquartile ranges of lymphocyte counts per litre were plotted on top of reference ranges established by the Royal College of Pathologists of Australasia (182, 183). There is no established reference range of MAIT cells in healthy individuals.

4.3.3 Peripheral blood immune cell populations do not have clear associations with participant age or sex

Heatmaps were constructed using peripheral blood cell count, and demographic data from each participant to identify trends in the data (see Figure 4.5). Overall, there were no clear associations between the cell count data and the demographic data. K-means clustering was applied to separate participants into three groups based on cell counts. This revealed a group of participants with relatively high counts of leukocytes, monocytes, and neutrophils and concurrent low counts of T-cell subsets. Additionally, there was a group with the opposite cellular profile and a third group with relatively low counts of all cell types.

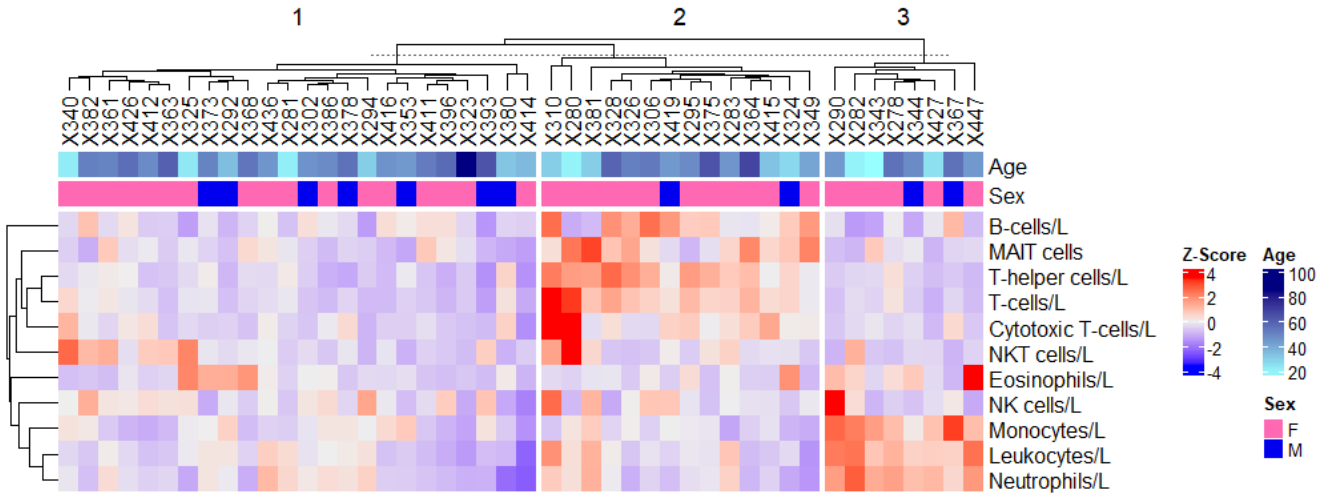

Figure 4.5 Heatmap of leukocyte concentration by participant.
Z-scores of peripheral blood immune cell concentrations were plotted for each participant; one per column. The hierarchical clustering of participants and immune cell types shows the relatedness of each variable. K-means clustering grouped the most similar participants into three groups based on immune cell concentration. Additional demographic and clinical data allow for the visualization of associations with cellular data.

Correlations were calculated with age as the independent variable and peripheral blood cell count for each cell type as the dependent variable. Leukocytes and neutrophils were significantly anti-correlated with age while B-cells were positively correlated (see Table 4.5).

Table 4.5 Significant correlations of variables to peripheral blood immune cell concentrations.

Independent Variable	Dependent Variable	r	p-value	Method

Age	Leukocytes/L	-0.37	0.0103	Spearman
Age	Neutrophils/L	-0.31	0.0414	Pearson
Age	B-Cells/L	0.34	0.0215	Spearman

4.3.4 Multiplex cytokine assay performance

Plasma samples from participants were run in two batches and a summary of each assay performance is in Appendix 8 with lower detection and upper limit detection limits. Additionally, the standard curve and curve for parameters are shown in Appendix 9.

4.3.5 Descriptive characteristics for plasma cytokine levels

Descriptive statistics for all cytokines are presented in Table 4.6 and raw data is provided in Appendix 10. Consistent with previous studies, many cytokines measured in plasma were below the lower limit of detection.

Table 4.6 Plasma cytokine concentration confidence intervals in a biomass smoke-exposed non-health-seeking community.
The median plasma cytokine concentrations as well as the upper and lower bounds of the 95% confidence interval were calculated. The normal range is a range previously reported for healthy individuals (189-191). ND: Not detectable. NA: No normative range available.

Cytokine	Median (pg/ml)	95% Confidence Interval (pg/ml)	Normative Range (pg/ml)	Reference
IL-2	14.9	10.3-18.8	0-1.81	(189)
IL-4	18.9	12.2-28.5	0-2.0	(191)
IL-5	15.2	13.3-20.9	0-2.23	(189)
IL-6	6103	1188-15020	0-9.3	(191)
IL-9	8.73	4.44-14.5	0-17	(191)
IL-10	18.9	11.1-28.9	0-1.15	(189)
IL-13	37.0	23.3-42.8	0-11	(191)
IL-17A	3.12	2.56-4.06	0.73-7.98	(190)
IL-17F	7.14	4.44-9.38	NA	
IL-22	22.2	18.9-28.0	0-33.78	(189)
IFN-γ	61.0	49.3-83.5	0-9.88	(189)
TNF-α	121	87.8-180	0-3.00	(189)

4.3.6 Plasma cytokines are increased in biomass smoke-exposed participants

All median cytokine concentrations except for IL-9, IL-17A, and IL-22 were increased compared to the available normative normal ranges (see Figure 4.6). The cytokines included in this panel account for type-1, type-2 and Th17-driven inflammation and show substantial divergence from the immune profiles expected based on the healthy ranges. This was particularly true for IL-6. It is uncertain if these differences were due to genuine differences in immune states compared to the previously reported ranges or if differences in processing methodologies contributed (see Discussion). Ranges were not reported for IL-17F in any of the comparative studies.

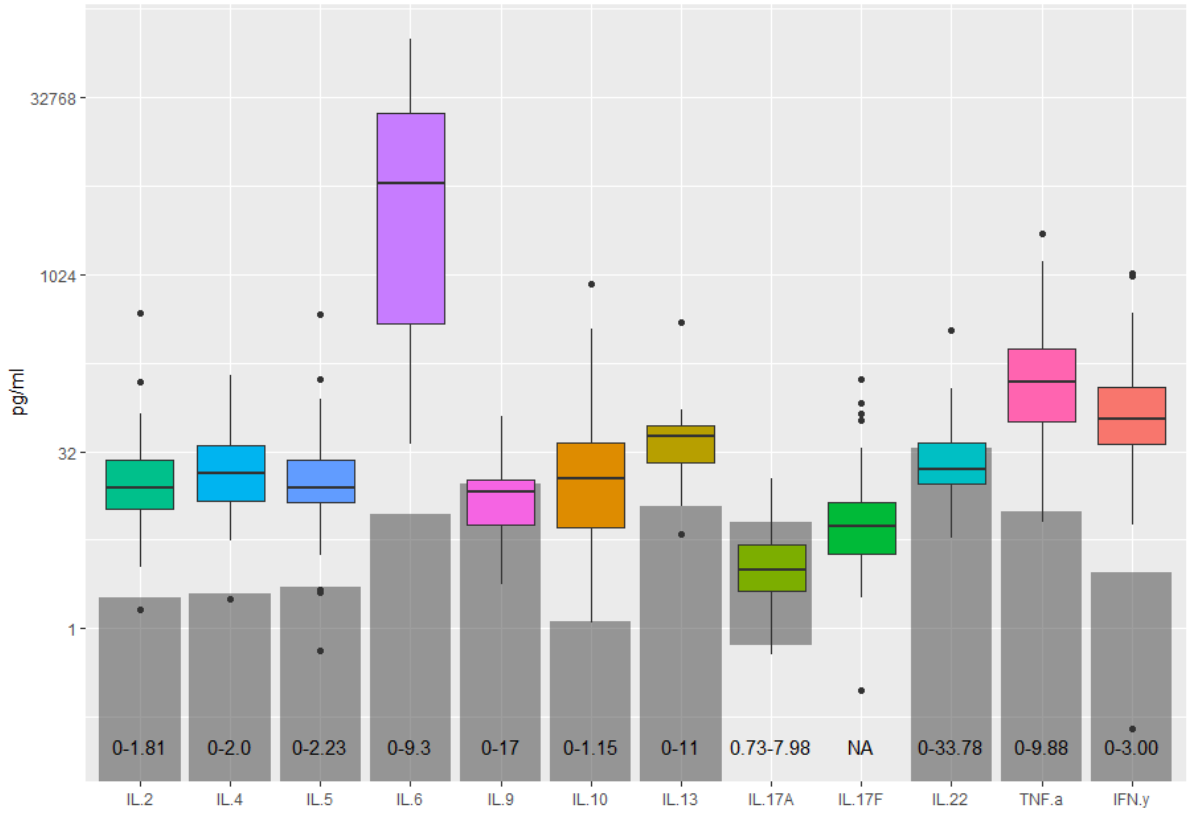

Figure 4.6 Plasma cytokine concentrations in non-health-seeking participants from a remote biomass-smoke exposed community in PNG.
The median and interquartile range of the cytokine concentrations were plotted on top of the range reported in developed. The reported normative ranges are listed on the plot for each cytokine. NA indicates that a normative range was not available.

Similar to the leukocyte data, a heatmap was constructed to inspect and visualize trends in the cytokine data and to visualize their relationships with demographic data (see Figure 4.7). The cytokine data did not show any clear association with age, or sex. Three-way K-means clustering was applied to the results to group participants in an unsupervised fashion according to similarities in relative cytokine expression. The analysis revealed a primary group (Figure 4.7, cluster 1) which consisted of the majority of the participants, generally had low to intermediate relative

concentration of all cytokines. Additionally, cluster 2 showed a higher relative concentration of TNF-α, IL-10, IL-6, and IL-22. Cluster 3 had higher levels of IL-9, IL-4, IL-5, IL-2, IL-13, IFN-γ, IL-17A, IL-17F, and TNF-α and relatively low levels of IL-10, IL-6, and IL-22. There were no correlations between age and plasma concentration of any of the cytokines.

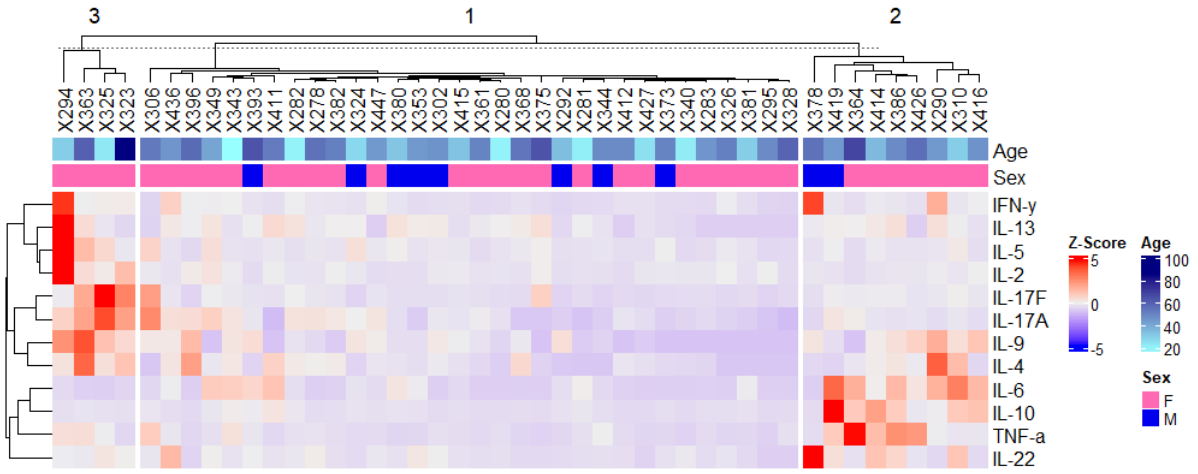

Figure 4.7 Heatmap of relative cytokine concentrations in biomass smoke-exposed non-health seeking participants.
Z-scores of plasma cytokine concentrations were plotted for each participant; one per column. The hierarchical clustering of participants and cytokines shows the relatedness of each variable. K-means clustering grouped the most similar participants into three groups based on cytokine concentration. Additional demographic and clinical data allow for the visualization of associations with cytokine data.

4.4 Discussion

This study evaluated the cytokine, and immune cell concentrations in the peripheral blood of biomass smoke-exposed non-health-seeking participants from a rural area of PNG. The results indicate that the immunological parameters of non-health-seeking people from this study population are substantially different from what is expected in Australia and the USA. Many participants in this study had lower peripheral concentrations of total leukocytes, neutrophils, monocytes, and T-cells. During chronic inflammation, cells traffic out of the bloodstream and into the affected tissue. This can deplete the blood of immune cells if they are being recruited faster than they are being produced. In this population, chronic inhalation of biomass smoke may be initiating inflammatory mechanisms in the lung thereby causing a reduction of cells in the periphery.

Unlike cells, high cytokine concentrations in the blood also indicate that there is a high concentration in the tissue of origin. Cytokines are released from the inflamed tissues and enter the bloodstream where they circulate and can serve as markers of tissue inflammation. The participants in this study exhibited significantly elevated plasma concentrations of most of the measured cytokines compared to normative datasets. This cytokine data accentuates the cellular data in supporting the theory that

chronic biomass smoke exposure causes immune cell migration to the lungs however, direct lung samples were not measured in these participants to confirm this. The participants had particularly high levels of IL-6, which was also found in a previous study on biomass-smoke-exposed participants (162). This is a pleiotropic cytokine that is necessary for the activation and maintenance of Th17 cells (193). Concurrently, IL-17F concentrations appeared to be elevated in this study. While the comparative datasets did not provide ranges for this specific isoforms of IL-17, other studies reported comparatively low or undetectable levels in the serum of healthy controls (194). IL-17 is involved in the recruitment of neutrophils (195). In this study, 40% of the participants had neutrophil counts that were below the Western normative range. Together, this points toward Th17-associated inflammation in these participants, similar to what is seen in response to tobacco smoke exposure (196, 197). The participants also had high plasma concentrations of IL-4, IL-9, and IL-13. These cytokines are associated with type-2 inflammation which is often involved in allergy, asthma, and asthma-COPD overlap syndrome (198). Type-2 inflammatory responses are also associated with helminth infections which are known to be endemic in this population (199). While Th2 cell counts were not measured directly, they contributed to the total T-helper cell count which was reduced in 80% of the participants. There is also strong evidence of type-1 immune activation in the study population. Plasma samples showed increased concentrations of IFN-γ and TNF-α. IFN-γ is produced, in part, by Th1 cells, and NK/NKT (200). This leads to the activation of macrophages. Activated macrophages subsequently release TNF-α (201). The reduction of monocytes in these participants is evidence of macrophage activation and recruitment. In total, the data indicates that these participants have highly active immune systems compared to what is expected in Western countries. The reason for the increased immune activity is unclear as there were no strong associations with other clinical parameters. Previous studies have shown that biomass smoke exposure alters immune markers (159, 162), so it's plausible that the results of the present study are also due, in part, to this exposure.

It is unclear if these dysregulated immune states themselves will eventually lead to disease however, numerous studies have linked biomass smoke exposure to an increased risk of respiratory infections including tuberculosis (170-172, 202). Few functional studies have been conducted to identify the mechanisms involved in this observation. One report found that outdoor air pollution particulate matter inhibited *Mycobacterium tuberculosis*-induced IFN-γ release and phagocytosis *in vitro* (203). Another study demonstrated that cow dung smoke increased NTHi adhesion to human bronchial epithelial cells *in vitro* (177). Further studies revealed that individuals with a higher particulate matter burden in their alveolar macrophages also had greater suppression of responses to tuberculosis challenge and postulated that immune anergy may play a role (204). The increased

type-1 cytokines found in the participants from the present study support the possibility that the type-1 immune response may become anergic or exhausted due to chronic biomass-smoke inhalation as the cells may have 'used up' their ability to respond. However, our findings were not limited to type-1 responses: the role that type-2 and Th17-driven anergy and exhaustion play in the increased susceptibility to respiratory infections among individuals exposed to biomass smoke needs to be investigated.

It is also evident that a portion of the participants are likely to develop COPD since chronic biomass smoke exposure is a major aetiology of the disease. It isn't fully understood how the immune status of healthy biomass smoke-exposed people compares to those with biomass smoke-induced COPD (summarized in Chapter 5). Longitudinal studies and studies involving participants with biomass smoke-induced COPD may reveal immune markers that are associated with the development of the disease and provide insights into the immune state of biomass smoke-induced COPD.

Our results suggest a significant potential for immune dysregulation due to biomass smoke exposure in this and similar remote communities in PNG. Such exposure could alter susceptibility to lung diseases and pathogens, potentially aggravating sub-clinical COPD. Additionally, the study underscores the necessity of establishing baseline immune parameters in individuals not actively seeking healthcare in these communities. This is crucial before exploring the mechanisms through which biomass smoke impacts lung health. Our results provide these baseline immune parameters, which are essential for comparing with the immune profiles of individuals affected by biomass-smoke-induced diseases. This comparison will aid in deciphering the mechanisms of immune dysregulation in people with lung disease from remote rural communities of PNG.

It is important to note that the authors of the normative cytokine data sets al did not report how they accounted for bias in their cytokine data that was introduced by the limits of detection of their assay (189-191). This is a crucial consideration that could have significant effects on the normative ranges they reported. It is also unknown how different handling and laboratory techniques contribute to different cytokine concentration ranges reported in the referenced normative cytokine ranges and this study. Studies comparing the assays used have not been performed. The prolonged transit time from the remote study site in Balimo, Papua New Guinea, to our lab in Townsville, Australia, could have caused higher cytokine levels in our samples. This is supported by a prior study that found that IL-6 levels rose in plasma samples when whole blood was stored for extended periods (205). This may partially explain the highly elevated IL-6 levels in this study. However, it's notable that the samples collected earliest did not necessarily yield the highest plasma IL-6 concentrations indicating that there may be other factors influencing this result.

This study was also constrained by the limited health infrastructure in the study community and its relatively small sample size. The community lacks a resident doctor and facilities that could be used to thoroughly characterize the health status of participants. The definitions of healthy and unhealthy participants used in this study are, therefore, imperfect by Western medical standards and there it is possible that some of the healthy participants had undiagnosed COPD or other diseases that may have influenced their immune profiles and skewed the study results. Despite these limitations, this study is intended as a starting point and has identified issues that should be considered in future research programs in similar communities.

Chapter 5: Immune profiling uncovers evidence of immune dysregulation and functional impairment in biomass-exposed participants with evidence of lung disease in rural, remote PNG

5.1 Introduction

Chapter 4 investigated the immune profiles of biomass-smoke-exposed participants from a rural, remote community in PNG who were not seeking health treatment and lacked evidence of lung disease. This established a baseline in this community where everyone is chronically exposed to biomass smoke due to cultural cooking practices. It was found that individuals from this biomass smoke-exposed community had peripheral blood immune cell counts that tended to be lower than what is expected in healthy individuals from developed countries and plasma cytokine concentrations that trended higher. This provided evidence that biomass smoke exposure may cause an active immune response even in people who don't show symptoms of lung disease. Previously, Chapter 3 of this thesis studied immune dysregulation in a cohort of urban-based, non-biomass-smoke exposed confirmed COPD patients. It found that T-cells in AECOPD patients have unique phenotypes and show signs of early activation and exhaustion indicating that the T-cell response is dysregulated. These two studies demonstrated that the immune profile in biomass-smoke-exposed "healthy" participants from rural PNG and tobacco smoke-induced COPD (TS-COPD) patients show signs of immune dysregulation.

Biomass smoke exposure is common in the developing world and it has been well-established that this chronic exposure can cause chronic bronchitis and COPD (157, 158, 206). Yet, it is less clear why only a portion of those chronically exposed develop lung disease. It is also not fully understood how immune dysregulation underlies the pathology of COPD caused by chronic biomass smoke exposure. In rural PNG biomass exposure and COPD are common (1). This is concerning as COPD increases the risk of pulmonary tuberculosis which is endemic in this area (207, 208).

Research in the context of TS-COPD revealed evidence of a myriad of factors that play a role in the development of the disease including individual effectiveness of lung repair mechanisms, the presence of systemic inflammation, genetic predisposition, as well as racial and gender differences (209-215). However, research on biomass smoke-induced lung disease/COPD (BS-COPD) is more incomplete than TS-COPD and, given its clinical impact, it is a neglected focus of research. Papua New Guinea (PNG) experiences high prevalence and mortality rates from Chronic Obstructive Pulmonary Disease (COPD), with a significant portion likely attributed to the widespread use of

biomass fuels for cooking (1). Despite this, no studies have been performed to investigate the immune response in BS-COPD sufferers in remote communities of PNG.

While BS-COPD shares the hallmark features of restricted and/or obstructed lung function seen in TS-COPD, the distribution of lung inflammation and tissue damage seems different (216). BS-COPD sufferers predominantly develop chronic bronchitis with a low incidence of emphysema. Yet, TS-COPD patients have a high incidence of both conditions (217). BS-COPD is associated with more air trapping, hypoxemia, and dyspnea than TS-COPD (217, 218). Additionally, people with BS-COPD have a higher incidence of cor-pulmonale, a condition of the right ventricle caused by pulmonary hypertension, yet lower rates of ischemic heart disease than those with TS-COPD (219).

While it seems evident that BS-COPD is a distinct clinical phenotype of the disease it is unclear how the immune profiles and mechanisms underlying this unique phenotype differ from what has been found in TS-COPD. Initial studies have described some of the immunological differences between these phenotypes and found evidence that the inflammatory profile in BS-COPD is distinct (219, 220). In one study, individuals with BS-COPD had lower circulating levels of many pro-inflammatory molecules including IL-8, IL-6, and IL-5 compared to those with TS-COPD (219). and higher concentrations of IL-1β, CXCL2, and IFN-γ compared to those with TS-COPD which may indicate a shift toward type-1 inflammation.

Other studies have also found evidence of increased type-2 inflammatory responses in BS-COPD. Examination of the peripheral blood from BS-COPD and TS-COPD patients found lower frequencies of Th17 cells and higher frequencies of Th2 cells along with IL-4 in the BS-COPD group (28). Other studies found a trend towards higher eosinophil numbers in the sputum of BS-COPD subjects compared to those with TS-COPD providing further evidence of type-2 inflammation in BS-COPD (221, 222). Exacerbating BS-COPD patients also had higher ratios of Th2:Th1 in their peripheral blood compared to exacerbating TS-COPD patients (188). Conversely, one study found no evidence of increased type-2 inflammation in BS-COPD patients compared to TS-COPD however, it did not measure the same markers as these other studies (219). Together, these studies hint that there may be an increase in both Th1 and Th2 responses. This is interesting as it is well known that these two types of responses exert regulatory effects on each other. The immunological differences between BS-COPD and TS-COPD remain unclear and BS-COPD itself may be heterogeneous. Furthermore, it is not known how closely the immune response characteristics of BS-COPD in remote communities of PNG resemble those previously reported in other populations.

It is also poorly understood how the immune environment of people with BS-COPD compares to those who are chronically exposed to biomass smoke but do not have COPD. It is evident that the

immune system is altered in response to chronic biomass exposure. However, it is unclear which immune parameters are associated with disease and which are present as part of the healthy response to biomass smoke exposure (as described in Chapter 4).

The Aims of the studies presented in this Chapter are:

- Identify blood immune profiles that are unique to participants with evidence of biomass smoke-induced lung disease compared to healthy biomass smoke-exposed participants.
- Test the functional capacity of peripheral blood T-cells from participants with evidence of biomass smoke-induced lung disease compared to healthy biomass smoke-exposed participants.

This chapter summarises the investigations into the immune profiles of biomass smoke-exposed participants from a rural community in PNG who exhibited respiratory symptoms suggesting the presence of BS-COPD with the aim to identify immune parameters that are dysregulated in lung disease. This includes analysis of immune cell frequencies in the blood and sputum of participants as well as blood T-cell cytokine concentrations. The immune profiles of these participants were analysed in comparison with data from participants who had been chronically exposed to biomass smoke yet had no evidence of COPD. This allowed for the identification of immune states that are associated with biomass smoke-induced disease rather than biomass smoke exposure alone. Additionally, functional studies were performed to compare T-cell function between the healthy participants and those with evidence of lung disease. Together, these examinations expand on our very limited understanding of the immune profiles and mechanisms underlying BS-COPD and thereby may ultimately contribute to improved diagnosis and therapies for this global problem.

5.2 Methods

5.2.1 Participant recruitment and ethics

As previously described in Chapter 4, participants were recruited from the Balimo community. Ethics were approved by the PNG Medical Research Advisory Council (MRAC 19.21) and by James Cook University (H8015). All participants provided consent to be included in the study. Demographic and clinical data including age, sex, height, weight, presence of cough, shortness of breath, and smoke exposure were recorded from each participant. Participants of either sex were included. Participants were excluded if they had confirmed evidence of Tuberculosis infection by Ziehl Neelsen (ZN) stain, Mtb culture of sputum culture and/or a positive qPCR result.

5.2.2 Participant grouping

Participants were grouped as 'healthy' or 'unhealthy' based on evidence of respiratory disease. The participants in this study were not diagnosed with COPD using the Global Initiative for Chronic Obstructive Lung Disease (GOLD) guidelines (223) as is done in Western hospitals as the infrastructure and access to trained personnel in the remote study area is very limited. Instead, an approach that did not rely on face-to-face contact with trained clinicians was used. Using questionnaire self-reported responses, participants were retrospectively assigned into one of two groups for this study: "healthy" or "unhealthy" based on evidence of non-TB respiratory disease and included: (1) cough status and; (2) ability to produce a spontaneous sputum sample subsequently determined to contain leukocytes (see section 5.2.5).

"Healthy" participants were those included in Chapter 4. These healthy participants also had a history of chronic biomass exposure but did not report a cough and were unable to produce spontaneous sputum-containing leukocytes. Participants in the "unhealthy" group were also biomass smoke-exposed individuals who reported the presence of a cough and were able to produce a spontaneous sputum sample that contained leukocytes. Because of this, participants are referred to as having biomass smoke-induced lung disease rather than BS-COPD although, we infer that they are similar.

5.2.3 Sample collection and processing

Blood samples were collected, and the immune cell and cytokine concentrations were determined as described in Chapter 4. Additionally, spontaneous sputum was collected from each participant when possible. Sputum samples were collected into 50ml sterile collection containers. For sputum smear preparation and subsequent Mtb culture, aliquots were taken for sputum decontamination and Mtb Ziehl Neelsen (ZN) staining of fixed microscope slides. Although these samples were not directly used in the current study, the ZN-stained sputum smears do allow us to determine whether leukocytes were present in the spontaneous sputum and any participants with such cells were allocated to the "unhealthy" group. As part of the current study, fresh sputum (0.25-0.3ml) was added to 2ml cryovials with an equal volume of Streck Cell Preservative®. This preservative stabilizes an array of biological samples for subsequent flow cytometric analysis and contains the same preservative as described in Chapter 4 for the delayed analysis of whole blood samples. We previously confirmed that it is suitable for sputum samples (data not shown). Preserved sputum samples were refrigerated until processed for flow cytometry and analysed by flow cytometry in laboratory facilities at James Cook University (see section 5.2.5).

5.2.4 Spirometry

Lung function was measured using a MIR Minispir portable spirometer. Data was acquired on a Windows PC using MIR Spiro software. The participants' age, height, weight, sex, and date of birth were recorded. Ethnicity was set to 'Others' as there are no spirometry reference equations that have been established for this population. The forced expiratory volume in one second (FEV1) and Forced Vital Capacity (FVC) were measured and compared to predicted values using the National Health and Nutrition Examination Survey (NHANES) III reference equations built into the software (224). JCU investigators were trained in the use of the device by a respiratory physician (External Advisor, Dr Jerry Minnei, Townsville University Hospital). Subsequently, local PNG collaborators were trained at the study location. Spirometry reports were evaluated by the respiratory physician (Dr Jerry Minei) at the Townsville University Hospital.

5.2.5 Sputum analysis and flow cytometry for leukocyte presence and type

The presence of leukocytes in sputum samples was required for group assignation and determined by two different methods: (1) microscopy of ZN-stained sputum smears and: (2) flow cytometry. Sputum samples were analysed by flow cytometry to immunophenotype major sputum leukocyte populations. This protocol was based on those described by Freeman et al. 2015 and Lay et al. 2011 (225, 226). Live/dead staining was not possible on Cell-Chex preserved sputum samples as the preservation solution inactivates cells and microorganisms.

Sputum preserved in Streck Cell Preservative® was transferred to the wells of sterile 6-well cell culture plates and disaggregated by extensive syringe plunger homogenisation through 40μM nylon mesh, filtration of the suspension into sterile tubes using 40μM nylon mesh followed by centrifugation at 500xg for 10min. The resulting cell pellet was resuspended in 300μl of PBS and thoroughly vortexed. Sputum samples were stained with an antibody cocktail (see Table 5.1) to determine the relative proportions of $CCR3^+$ eosinophils, neutrophils, $CD14^+$ monocytes, $CD206^+$ alveolar macrophages, $CD3^+$ total T-cells, $CD4^+$ T-helper cells, and $CD8^+$ cytotoxic T-cells (see Table 5.2). Because sputum samples often contain limited numbers of leukocytes, the FMO method for the determination of background fluorescence was not feasible for every individual sputum sample for every cell type. Samples with obvious inflammatory cells (white/yellow/milky appearance) were used as experimental FMO controls and set flow cytometry gates. BD Ms Ig Kpa Comp Bead Sets were used for compensation.

Data was acquired on a BD Fortessa flow cytometer with BD FACS DIVA acquisition software. Analysis was performed using FlowJo V10.7.2 software (BD). Multicolour flow cytometry was

performed using specific gating strategies to determine differential expression of CD45 and cell lineage markers allowing the discrimination of leukocytes from squamous epithelial cells and debris. Data was reported as a frequency of the parent population: neutrophils, eosinophils, and T-cells were reported as a percentage of the total $CD45^+$ leukocytes, T-helper and cytotoxic T-cells were recorded as a percentage of total T-cells.

Table 5.1. Fluorochrome-conjugated antibodies used to enumerate innate and lymphocyte cell populations in sputum samples.

Marker	**Fluorochrome**	**Clone**	**Supplier, Cat No.**
CD45	BD Horizon™ BV510	HI30	BD 563204
CCR3/CD193	PE	5E8	BD 558165
CD16	APC-H7	3G8	BD 560195
CD206	APC	19.2	BD 550889
CD3	Brilliant Violet™ 421	SK7	BD 563798
CD4	BD Horizon™ BUV395	SK3	BD 563550
CD8	PE-Cy7	RPA-T8	BD 557750
CD14	AF488	M5E2	BD 557700

Table 5.2. Maker combinations used to identify leukocytes in sputum samples.

Cell	**Markers**
Neutrophils	$CD45^+CD16^{+/int/lo}CCR3^{lo\#}$
Eosinophils	$CD45^+SSC^{int}/^{hi}CD16^{lo/int}CCR3^+$
Macrophages	$CD45^+CD16^{lo}CCR3^{lo}CD206^+$
Monocytes	$CD45^+CD16^{lo}CCR3^{lo}CD14^+/CD206^{lo}$
T-cells	$FSC^{lo}SSC^{lo}$ $CD45^+CD16^{lo}CCR3^{lo}CD3^+$
CD4 T-cells	$FSC^{lo}SSC^{lo}$ $CD45^+CD16^{lo}CCR3^{lo}CD3^+CD4^+$
CD8 T-cells	$FSC^{lo}SSC^{lo}$ $CD45^+CD16^{lo}CCR3^{lo}CD3^+CD8^+$

[#] in this study many neutrophils expressed lower levels of CD16 than peripheral blood neutrophils which is indicative of apoptosis.

5.2.6 T-cell cytokines and functional responses

Blood T-cell phenotype and function can be measured by evaluation of measurement of cytokines secreted into the plasma with and without stimulation with a polyclonal T-cell activator (i.e. a mitogen) or detection of intracellular T-cell specific cytokines using flow cytometry. We chose to use both these assays to measure circulating T-cell cytokines and functional T-cell responses: (1) Plasma cytokine assays were used to measure total T-cell associated cytokines (with and without T-cell mitogen stimulation), and (2) intracellular cytokine staining and flow cytometry was used to identify the specific T-cell source of any IFN-γ and TNF-α produced following mitogen stimulation. The

Quantiferon TB GOLD Plus blood collection "Mitogen" tube contains the T-cell mitogen phytohemagglutinin (PHA)) and the "Nil" tube has no stimulant. Following 1ml blood collection into QFT heparinised BCTs, tubes were mixed by inversion 10 times to mix with the anticoagulant and allow mitogen precoated on the tube to mix with whole blood. For intracellular cytokine staining (ICS), 120μl of blood was then removed from each participant's IGRA "Mitogen" and "Nil" BCT into screw-capped vials already containing Brefeldin-A (golgi inhibitor) to give a 1X final concentration. The remaining blood in the "Mitogen" and "Nil" BCTs was used for plasma cytokine assays and following removal of the aliquot for ICS, BCTs and ICS vials were incubated at 37°C for 18 hours.

Plasma cytokine concentrations with and without T-cell mitogen stimulation were determined as described previously using a multiplex bead-based assay run on a flow cytometer. The cytokine concentrations that were determined from unstimulated blood were background subtracted from the concentrations determined for the mitogen-stimulated plasma to determine the magnitude of response due to stimulation.

Intracellular cytokine staining was performed on mitogen-stimulated and unstimulated whole blood samples. Following incubation, 120μl Streck Cell Preservative® was added to each vial of blood to allow for transport to James Cook University laboratory facilities for further preparation and flow cytometric analysis. BD Perm/Wash™ buffer was used to permeabilize cells. A four-colour antibody panel was used to identify the presence of TNF and IFN-γ in $CD4^+$ and $CD8^+$ cells (see Table 5.3). Antibody concentrations were previously optimized for prior studies. Antibodies were diluted in BD Horizon™ Brilliant Stain Buffer. FMO controls were used to compensate for background fluorescence. BD Ms Ig Kpa Comp Bead Sets were used for compensation. Data was acquired using a BD FACSCanto II flow cytometer running BD FACS DIVA software. Analysis was performed using FlowJo V10.7.2 software (BD).

Table 5.3. Intracellular four-colour antibody staining panel used to determine T-cell cytokine response to mitogen stimulation.

Marker	**Fluorochrome**	**Clone**	**Supplier, Cat No.**
TNF	BV421	MAb11	BD 562783
IFN-γ	FITC	B27	BD 554700
CD4	BV510	SK3	BD 562970
CD8	APC-H7	SK1	BD 560179

5.2.7 Data analysis

Boxplots displaying median, 25th and 75th percentiles, and outliers were constructed using the ggplot2 package in RStudio (RStudio 2022.12.0) running R version 4.2.2. GraphPad Prism (Version 9.0.0) was used to perform Mann-Whitney U-tests between healthy and unhealthy groups followed by Benjamin, Krieger, and Yekutieli's two-stage set-up method for False discovery rate adjustment (q-values). Spearman correlation analyses between immune parameters and demographic information were also performed in Prism.

5.3 Results

5.3.1 Participant group demographics

Thirty-four participants produced sputum samples that contained immune cells (polymorphonuclear cells) and reported the presence of a cough (see Appendix 11). These participants, therefore, displayed evidence of lung disease and constituted the "unhealthy" group. This was in addition to the 46 participants that were recruited to determine baseline immune parameters (healthy) in Chapter 4 (see Table 5.4). The mean age was identical and the age range was similar between the two groups. There was a lower proportion of females in the unhealthy group (44%) compared to the healthy group (76%). 83% of participants in the healthy group and 85% of participants in the unhealthy group reported that they regularly participated in cooking activities in their households. All participants reported that wood fires were used as the cooking source for their household. Most participants reported that the fires were inside or underneath their houses.

Table 5.4 Healthy and unhealthy participant group characteristics.

	Healthy (n=46)	**Unhealthy** (n=34)
Females	76% (35)	44% (15)
Mean age (years)	45 (range: 17-86)	45 (range: 15-69)
Mean body mass index (BMI)	23.1	22.3
Chronic cooking fire exposure	100%	100%
Location of fire:		
Inside house	61% (28)	68% (23)
Outside/Underneath house	33% (15)	26% (9)
Away from House	7% (3)	6% (2)
Current Tobacco Smoke (smoker)	11% (5)	24% (8)
Participate in Cooking	83% (38)	85% (29)

5.3.2 Peripheral blood immune cell composition similar in healthy compared to unhealthy participants.

Flow cytometric analysis of peripheral blood samples was performed to identify the major immune cell subset concentrations that differed between the healthy and unhealthy groups. This was performed to better understand which immune cell subsets may play a role in the lung disease pathology of biomass-smoke-exposed participants. Analysis of innate and lymphocyte populations did not reveal any significant differences between healthy and unhealthy participants (see Table 5.5 and Figure 5.1). Total leukocytes and neutrophils trended low compared to the reference ranges in both groups and many participants fell below the range. Eosinophil counts were similar in both groups with some participants elevated above the reference range. Monocytes were significantly increased in the unhealthy group before multiple testing correction (Benjamin, Krieger, and Yekutieli's two-stage set-up method) and tended to fall on the lower end of the reference range with many participants below the range. Most patients in the healthy group had NKT cell counts that were above the reference range while the unhealthy group tended to be lower with many patients around the upper fringe of the range. NK cells were similar between groups and tended to fall within the reference range. Additionally, T-lymphocyte populations (total T-cells, T-helper and cytotoxic-T cells) trended towards lower levels in the unhealthy group compared to the healthy group and most participants were near the lower fringe or below the reference range. Cytotoxic ($CD8^+$) T-cells were significantly decreased in the unhealthy group prior to multiple testing correction. B-cell counts were similar between groups and generally fell within the expected range.

Table 5.5 Cell counts summary of healthy and unhealthy participants.

Median peripheral blood cell counts and 95% confidence intervals. The frequency of parent population was calculated as a percentage of the total T-cells ($CD3^+$) for helper T-cells and cytotoxic T-cells. All others were calculated as the percentage of total leukocytes ($CD45^+$). P-values were calculated using Mann-Whitney U-tests on total cell count data. False discovery rate q-values were calculated following Mann-Whitney tests using Benjamin, Krieger, and Yekutieli two-stage set-up method. Reference ranges reported are the values established by the Royal College of Pathologists of Australasia or the American College of Physicians (182, 183). Reference ranges for MAIT cells have not been established.

	Healthy				Unhealthy						
Cell type	**Median (10^9 Cells/L)**	**95% Confidence Interval (10^9 Cells/L)**	**Median Frequency of parent (%)**	**95% Confidence Interval (% of parent)**	**Median (10^9 Cells/L)**	**95% Confidence Interval (10^9 Cells/L)**	**Median Frequency of parent (%)**	**95% Confidence Interval (% of parent)**	**Reference Range (10^9 Cells/L)**	**Healthy vs. Unhealthy p-value**	**Healthy vs. Unhealthy q-value**
Leukocytes	4.2	3.8-4.7	-	-	4.6	3.8-5.6	-	-	4.0-10	0.43	0.55
Neutrophils	2.3	1.9-2.8	55	52-58	2.5	2.0-2.9	58	51-63	2.0-7.5	0.22	0.37
Eosinophils	0.27	0.21-0.40	6.5	5.2-8.4	0.28	0.25-0.40	6.6	4.8-9.5	0.04-0.4	0.61	0.64
Monocytes	0.18	0.14-0.20	4.2	3.7-4.5	0.20	0.16-0.27	4.7	4.0-5.1	0.2-0.8	0.03	0.22
NK cells	0.19	0.16-0.22	4.6	3.4-5.5	0.12	0.098-0.19	2.8	2.2-4.0	0.05-0.35	0.06	0.37
NKT	0.033	0.025-0.040	0.86	0.59-1.1	0.029	0.019-0.037	0.52	0.44-0.84	0-0.03	0.17	0.22
T-cells	0.61	0.53-0.76	-	-	0.53	0.46-0.64	-	-	0.6-2.4	0.13	0.37
B-cells	0.29	0.25-0.34	-	-	0.34	0.22-0.43	-	-	0.04-0.5	0.59	0.64
Helper T-cells	0.31	0.27-0.38	53	51-57	0.30	0.24-0.34	60	53-65	0.5-1.4	0.30	0.44
Cytotoxic T-cells	0.18	0.16-0.23	31	28-36	0.15	0.13-0.19	28	25-35	0.2-0.7	0.04	0.22
MAIT cells	0.05	0.040-0.070	8.4	6.6-9.7	0.044	.035-.051	8.2	6.4-9.4	-	0.21	0.37

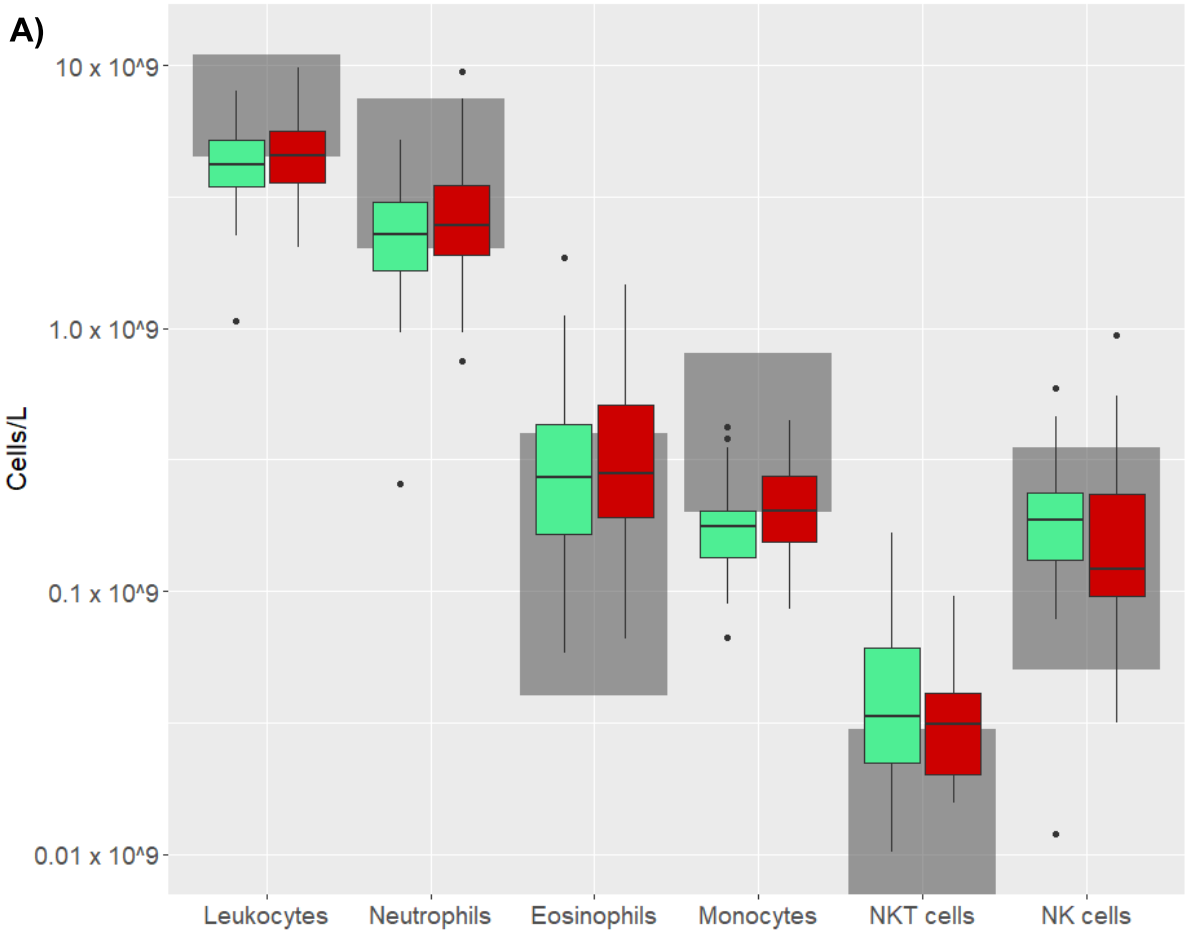
A)
10 x 10^9
1.0 x 10^9
0.1 x 10^9
0.01 x 10^9
Cells/L
Leukocytes
Neutrophils
Eosinophils
Monocytes
NKT cells
NK cells
Healthy
Unhealthy
Western range

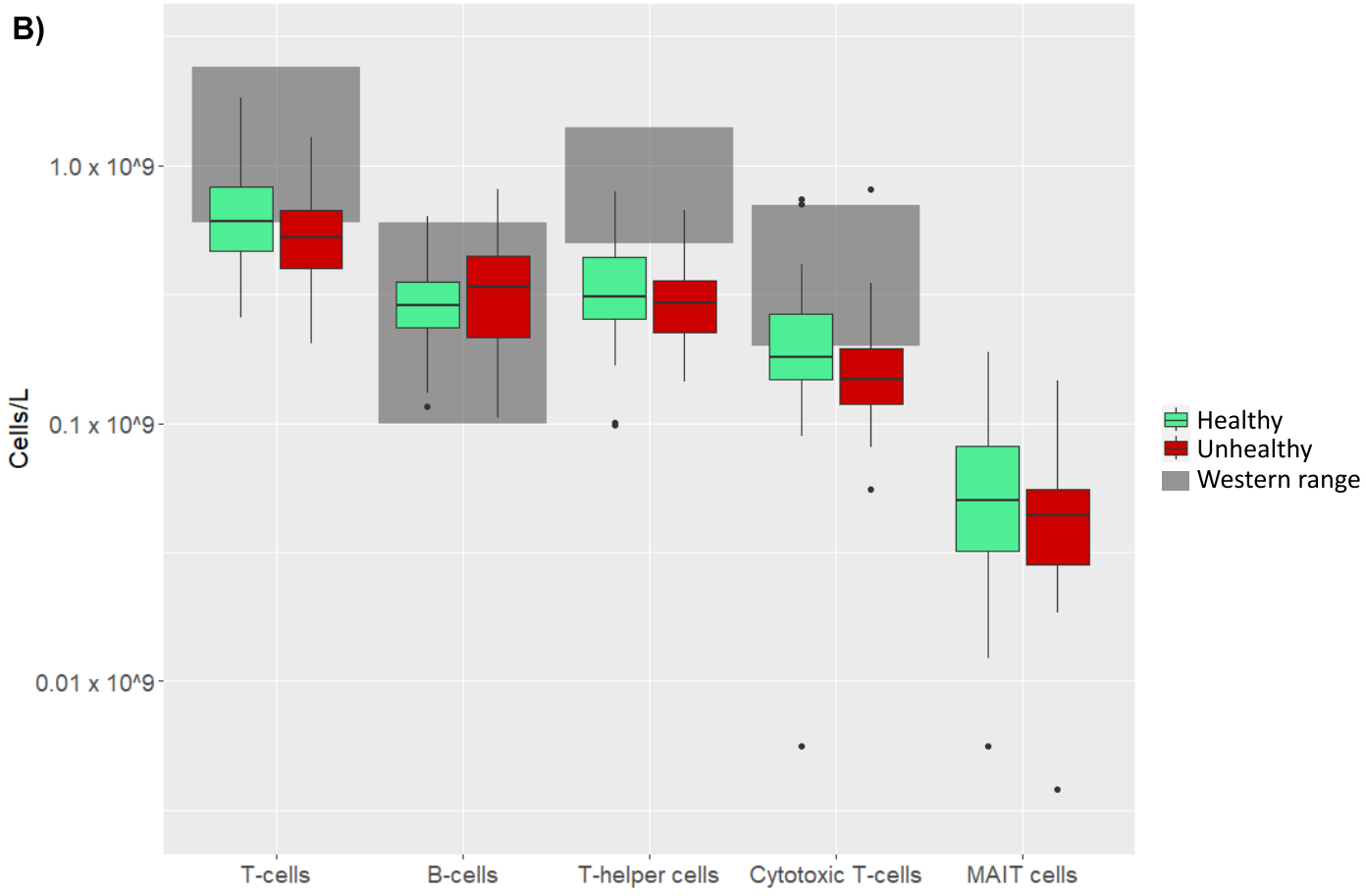
B)
1.0 x 10^9
0.1 x 10^9
0.01 x 10^9
Cells/L
T-cells
B-cells
T-helper cells
Cytotoxic T-cells
MAIT cells
Healthy
Unhealthy
Western range

Figure 5.1 Peripheral blood innate and lymphocyte cell concentrations for participants from healthy and unhealthy groups.

The figure displays the median and interquartile ranges (25th to 75th percentiles) of cell counts per litre, represented by boxes, with Tukey whiskers indicating the spread of the data and outliers marked as dots. Reference ranges from the Royal College of Pathologists of Australasia (182) or American College of Physicians(183) are shown in grey. Total leukocyte, neutrophil, and monocyte concentrations trended low **(A)**; most participants fell on the lower end or below the reference ranges; the unhealthy participants (red) tended to be higher than the healthy participants (green). NKT cells trended higher than the reference ranges for all participants; most participants had higher concentrations than, or were on the high end of the reference ranges; unhealthy participants trended lower than the healthy participants. T-cells, including T-helper (CD4), and cytotoxic (CD8) T-cells trended low in all participants **(B)**; a result that was particularly pronounced in the unhealthy individuals. Total T-cell counts fell on the lower fringe of the reference range. Most participants in both groups were below the reference range for T-helper cells. Cytotoxic T-cell concentrations were on the lower end of or below the reference range in the healthy participants while most of the unhealthy participants fell below the range. B-cell counts were within the reference range for most participants.

5.3.3 Peripheral blood cytokines show evidence of Th17-driven inflammation in participants with evidence of lung disease.

The concentration of 12 plasma cytokines in unstimulated blood was measured and compared between the healthy and unhealthy groups (Table 5.6). The median cytokine concentrations for most cytokines trended higher in the unhealthy group. Unhealthy participants had significantly higher levels of the Th17-related cytokine L-17F (see Figure 5.2). IL-17A was significantly increased in the unhealthy group before multiple testing correction but was not significant post-correction (Benjamin, Krieger, and Yekutieli's two-stage set-up method). Additionally, the type-2 cytokine, IL-4, and the type-1 cytokine TNF-α were both significantly increased in the unhealthy group before multiple testing correction but failed to reach significance afterwards. The median concentrations of each cytokine except IL-9, IL-17A, and IL-22 were above the previously reported range for healthy individuals. However, theses comparative dataset did not report values for IL-17F analysed in our study. Since normative peripheral blood cytokine concentration ranges have not been established, we compared them to the ranges reported for healthy individuals by Li et. al. (189) (described in Chapter 4).

Table 5.6 Median and 95% confidence intervals of plasma cytokines from healthy and unhealthy group participants.

P-values were calculated using Mann-Whitney U-tests. 'ND' indicates that the cytokine was not detected in the normative dataset. 'NA' indicates cytokines for which a normal range has not been established. IL-4, IL-17A, IL-17F, and TNF-α concentrations were significantly higher in the unhealthy group before multiple testing correction. After multiple testing correction, only IL-17F concentration was significantly increased in the unhealthy group.

	Healthy		Unhealthy					
Cytokine	**Median (pg/ml)**	**95% Confidence Interval (pg/ml)**	**Median (pg/ml)**	**95% Confidence Interval (pg/ml)**	**Healthy vs. Unhealthy p-value**	**Healthy vs. Unhealthy q-value**	**Normative Range**	**Reference**
IL-2	14.9	10.3-18.8	21.0	13.3-31.1	0.093673	0.18032	0-1.81	(189)
IL-4	18.9	12.2-28.5	32.3	15.5-48.8	0.044646	0.128914	0-2.0	(191)
IL-5	15.2	13.3-20.9	30.7	14.2-66.3	0.065626	0.151596	0-2.23	(189)
IL-6	6103	1188-15020	13355	4146-19842	0.382978	0.491488	0-9.3	(191)
IL-9	8.73	4.44-14.5	16.4	7.81-21.3	0.126258	0.208326	0-17	(191)
IL-10	18.9	11.1-28.9	25.2	18.9-45.8	0.14831	0.214123	0-1.15	(189)
IL-13	37.0	23.3-42.8	37.0	19.9-53.3	0.662028	0.73656	0-11	(191)
IL-17A	3.12	2.56-4.06	4.55	2.74-12.5	0.027513	0.105924	0.73-7.98	(190)
IL-17F	7.14	4.44-9.38	20.6	8.11-66.9	0.002943	0.033997	NA	
IL-22	22.2	18.9-28.0	26.7	11.0-43.8	0.861285	0.828987	0-33.78	(189)
IFN-γ	61.0	49.3-83.5	66.6	32.9-79.4	0.701486	0.73656	0-9.88	(189)
TNF-α	121	87.8-180	229	147-544	0.012996	0.075052	0-3.00	(189)

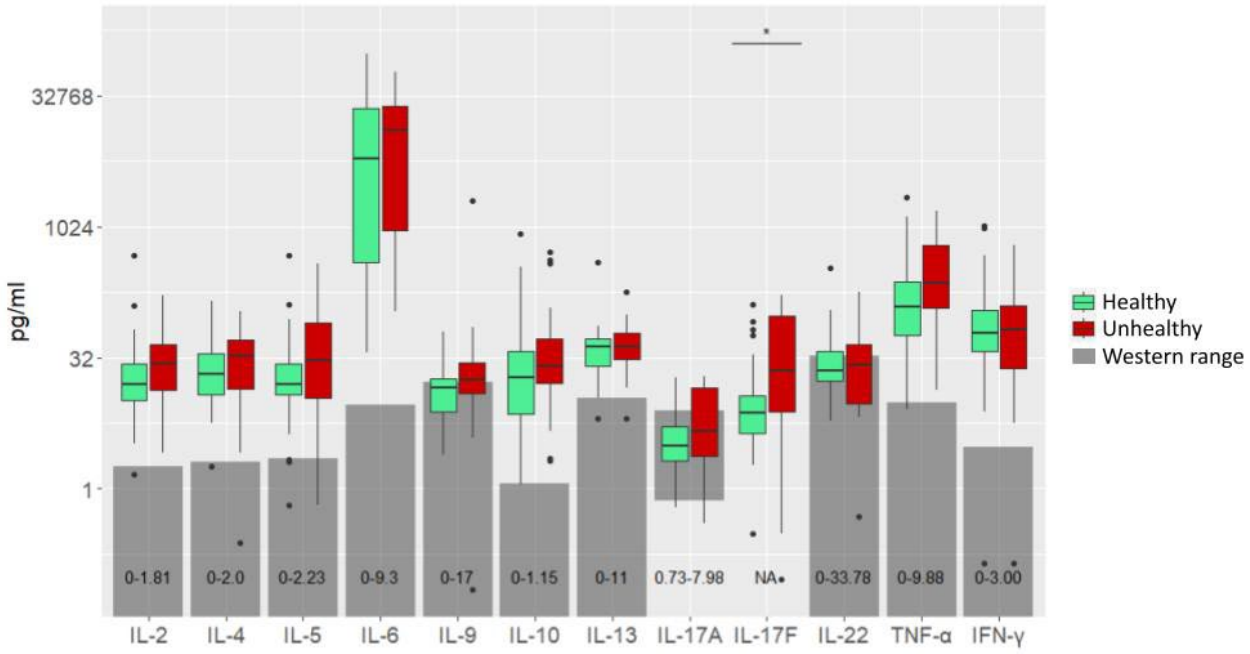

Figure 5.2. Plasma cytokine concentrations from biomass smoke exposed participants with evidence of lung disease or without.

Median and interquartile ranges (25th to 75th percentiles) are shown as boxes and Tukey whiskers indicate the spread of the data with outliers marked as dots. Reference ranges are shaded grey and listed along the bottom of the plot. 'NA' indicates cytokines for which a normal range has not been established. Aside from IL-9, IL-17A, and IL-22, all median cytokine concentrations were elevated compared to normative values. IL-17F was significantly increased in the unhealthy group (red) compared to the healthy group (green). Significance cut offs: * q≤0.05, ** q≤0.01, *** q≤0.001, **** q≤0.0001.

5.3.4 Mitogen stimulation shows evidence of reduced T-cell function in participants with evidence of lung disease.

Mitogen stimulation was performed on peripheral whole blood samples to quantify differences in T-cell functional responses between the unhealthy and healthy participant groups (Table 5.7). For all tested cytokines, the median background-subtracted concentrations trended lower in the unhealthy group indicating reduced functional capabilities (see Figure 5.3). There were significant differences among the Th17-related cytokines IL-17A, IL-17F, and IL-22 which were lower in the unhealthy group indicating a relative degree impaired T-cell function. Additionally, IL-6, IL-9, IL-10, and IFN-γ were also released at significantly lower levels in the blood from the unhealthy group compared to the healthy group.

Table 5.7. Median and 95% confidence intervals in plasma from mitogen stimulated blood in healthy and unhealthy participants.

Mann-Whitney U-test were performed to determine significance between participant groups. IL-6, IL-9, IL-10, IL-13, IL17A, IL-17F, IL-22, and IFN-γ concentrations were significantly lower in the plasma isolated from the blood of unhealthy participants after mitogen stimulation compared to that from healthy participants.

	Healthy		**Unhealthy**			
Cytokine	**Median (pg/ml)**	**95% Confidence Interval (pg/ml)**	**Median (pg/ml)**	**95% Confidence Interval (pg/ml)**	**Healthy vs. Unhealthy p-value**	**Healthy vs. Unhealthy q-value**
IL-2	465	193-849	189	112-616	0.117	0.052
IL-4	188	133-300	134	85.7-247	0.221	0.078
IL-5	6627	5063-10617	4978	2791-8009	0.185	0.071
IL-6	**35245**	**28434-44311**	**17933**	**8361-28807**	**0.001**	**0.001**
IL-9	**1504**	**913-2151**	**705**	**250-1241**	**0.001**	**0.001**
IL-10	**242**	**153-362**	**157**	**82.4-213**	**0.030**	**0.016**
IL-13	**2381**	**1013-2681**	**923**	**495-1776**	**0.005**	**0.003**
IL-17A	**188**	**122-260**	**50.4**	**27.5-103**	**<0.0001**	**<0.0001**
IL-17F	**321**	**210-379**	**87.9**	**56.1-119**	**<0.0001**	**<0.0001**
IL-22	**757**	**489-1289**	**107**	**49.7-222**	**<0.0001**	**<0.0001**
IFN-γ	**32693**	**18966-44250**	**11557**	**5440-20602**	**0.003**	**0.002**
TNF-α	846	476-1630	209	157-1194	0.124	0.052

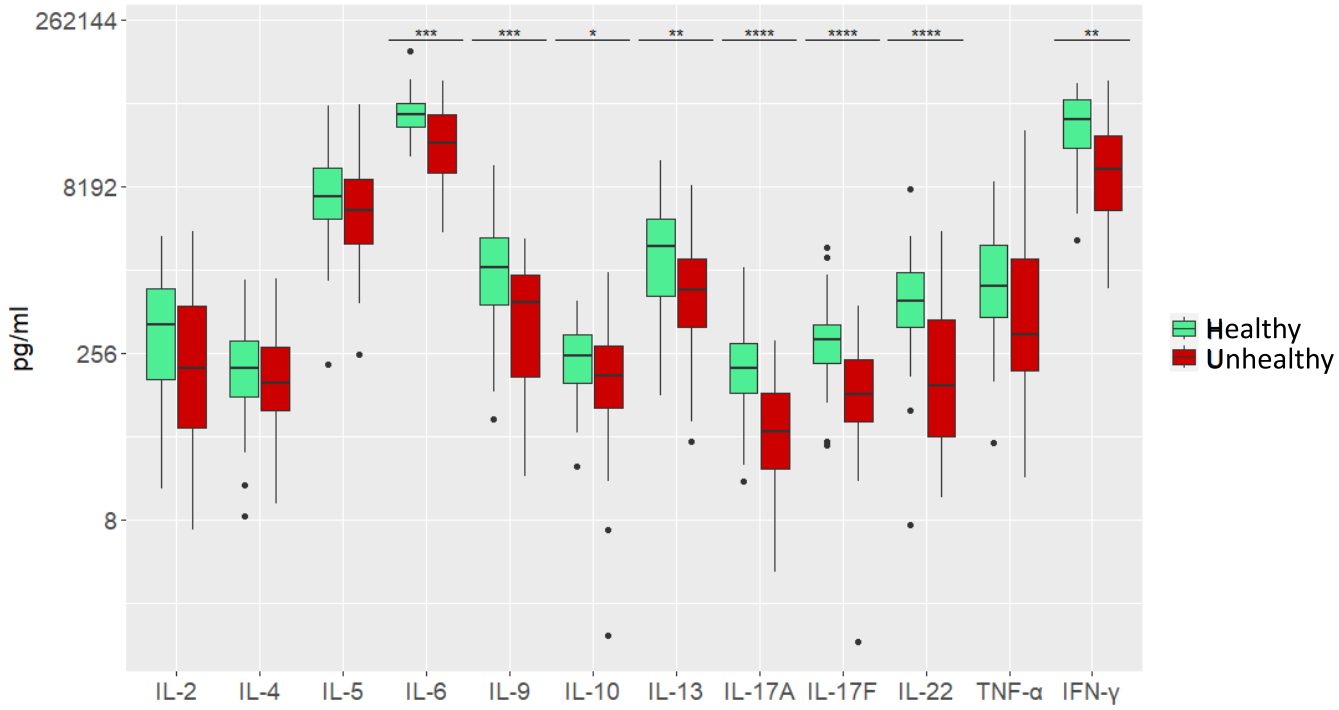

Figure 5.3. Background subtracted plasma cytokine concentrations after mitogen stimulation from biomass smoke-exposed participants with or without evidence of lung disease.
Median and interquartile ranges (25th to 75th percentiles) are shown for unhealthy (red) and healthy (green) participants as boxes and Tukey whiskers indicate the spread of the data with outliers marked as dots. IL-6, IL-9, IL-10, IL-13. IL-17A, IL-17F, IL-22, and IFN-γ were released at significantly lower concentrations in the unhealthy group after mitogen stimulation. Significance cut offs: * q≤0.05, ** q≤0.01, *** q≤0.001, **** q≤0.0001.

5.3.5 Sputum from unhealthy participants shows evidence of neutrophilic and eosinophilic inflammation.

The flow cytometric evaluation of sputum leukocytes was an opportunity to assess the characteristics of cells in the central airways, but it presents challenges due to the properties of sputum including large amounts of contaminating cells and debris and cell autofluorescence.

Relative proportions of Innate and lymphocyte cells in sputum from biomass smoke-exposed participants with evidence of lung disease (unhealthy group) were determined by flow cytometry (Figures 5.5 and 5.6). In the study participants, neutrophils were the predominant fraction of the leukocyte population, accounting for a median proportion of 81.6%. Conversely, eosinophils comprised a smaller portion, with a median presence of 3.93% (Table 5.8). As expected, sputum neutrophil proportions were strongly anticorrelated to sputum eosinophils proportions and positively correlated to neutrophil proportions in the peripheral blood (Table 5.9). Sputum T-cells and T-cell subsets did not correlate to their levels in the peripheral blood.

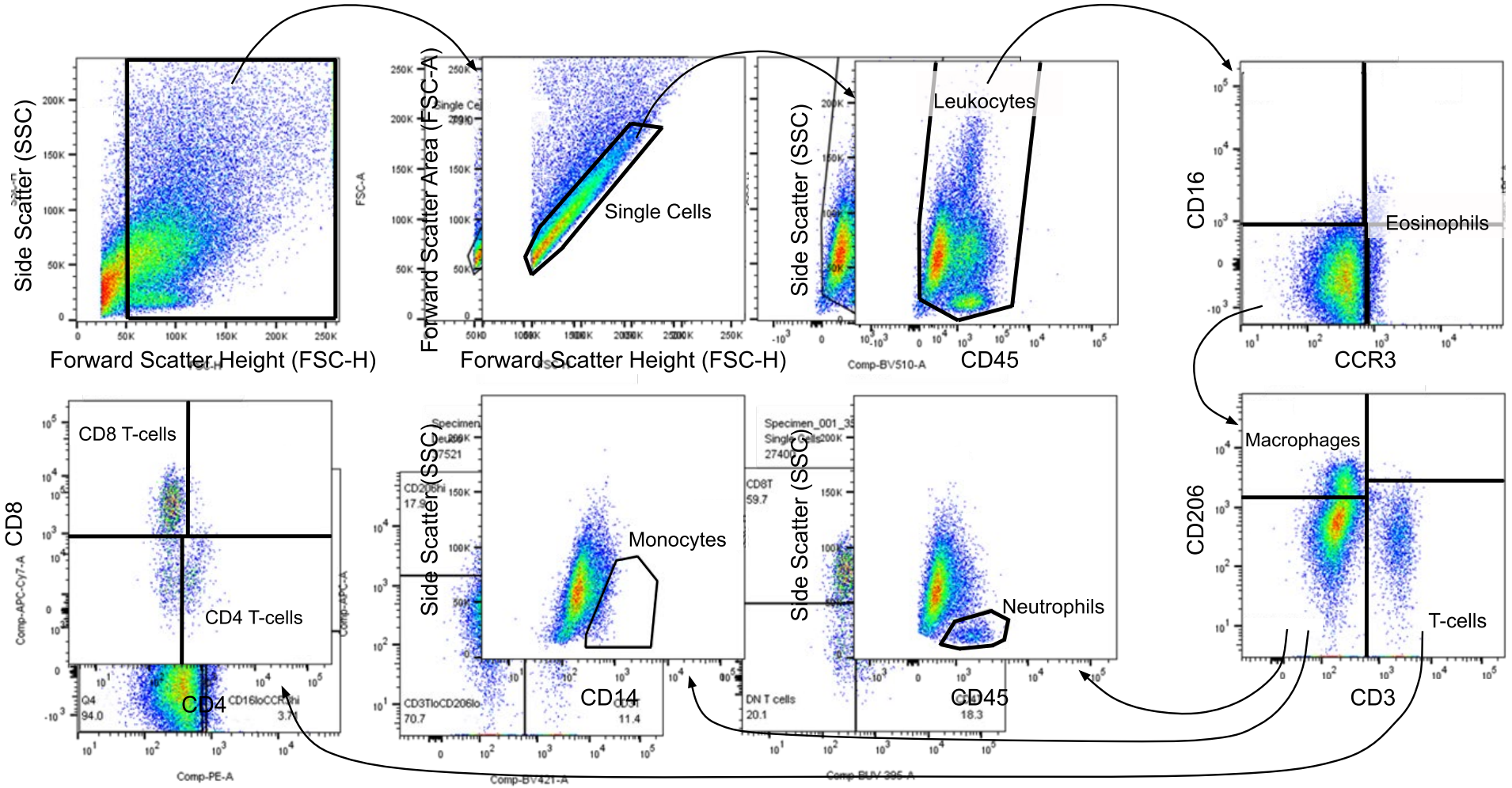

Figure 5.5. Gating strategy used to identify major leukocyte types in sputum samples.

Table 5.8. Median and 95% confidence intervals of immune cell types in sputum samples of biomass smoke exposed participants with evidence of lung disease.
The frequency of parent population was calculated as a percentage of the total T-cells ($CD3^+$) for helper T-cells and cytotoxic T-cells. All others were calculated as the percentage of total leukocytes ($CD45^+$).

Cell type	Median (% of parent)	95% Confidence Interval
Neutrophils	81.6	74.1-87.8
Eosinophils	3.93	3.13-7.05
Monocytes	1.51	0.96-2.48
Macrophages	2.59	1.67-3.26
T-cells	1.01	0.500-1.96
Helper T-Cells	37.9	33.8-58.8
Cytotoxic T-Cells	4.27	1.48-12.7

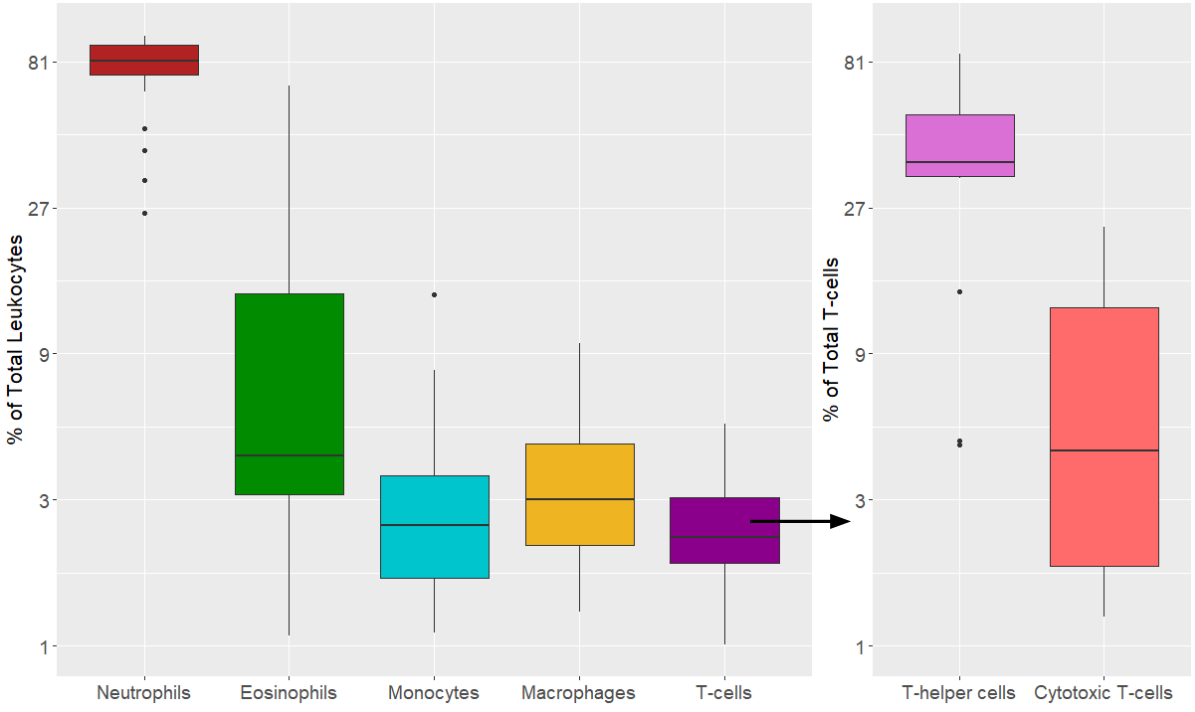

Figure 5.6. Sputum leukocyte relative frequencies.
The frequency of parent population was plotted as a percentage of the total T-cells ($CD3^+$) for helper T-cells and cytotoxic T-cells. All others were plotted as the percentage of total leukocytes ($CD45^+$). Median and interquartile ranges (25th to 75th percentiles) are represented by boxes, with Tukey whiskers indicating the spread within the parent population percentages; outliers are represented as dots.

Table 5.9. Significant Spearman correlations between sputum cell relative frequencies, peripheral blood (PB) immune cell counts, or PB plasma cytokine concentrations.

Independent Variable	Dependent Variable	n	r	p-value
Sputum Neutrophils %	Sputum Eosinophils %	33	-0.910	<0.0001
Sputum Neutrophils %	PB Neutrophils/L	33	0.584	0.00036
Sputum Neutrophils %	Sputum T-Cells %	33	-0.484	0.004
Sputum Eosinophils %	Sputum T-Cells %	33	0.422	0.014
Sputum Eosinophils %	PB Neutrophils/L	33	-0.480	0.005
Sputum T-Helper Cells %	PB NK Cells/L	15	-0.614	0.017
Sputum Cytotoxic T-Cells %	Plasma IL-9	15	-0.666	0.009

5.3.6 Peripheral blood T-cell IFN-γ and TNF-α are not associated with lung disease pathology in biomass smoke-exposed participants from rural PNG.

To further determine if T-cell dysfunction was involved in the pathogenesis of biomass-smoke-induced lung disease in the study population, we analysed intracellular cytokines in peripheral blood T-cell subsets. The proportion of $CD4^+$ and $CD8^+$ T-cells producing IFN-γ and/or TNF-α in unstimulated and mitogen-stimulated blood was determined by flow cytometry. T-tests were performed between healthy and unhealthy groups. There was no significant difference in intracellular IFN-γ or TNF-α from either T-cell subset in the stimulated or unstimulated whole blood samples between healthy or unhealthy participants (see Figure 5.7). Mitogen stimulation increased the expression of all tested cytokines in $CD4^+$ and $CD8^+$ T-cells from both participant groups. TNF-α+ CD8+ cells were increased the least following stimulation. TNF-α^+ IFN-γ^+ $CD8^+$ and IFN-γ^+ $CD8^+$ cells were increased the greatest after stimulation. $CD4^+$ cell frequency was similar between the three cytokine expression profiles both before and after stimulation.

Table 5.10. Intracellular staining of T-cells in unstimulated and mitogen-stimulated blood from healthy and unhealthy participants.

Median and 95% confidence intervals were calculated of the frequency of the parent population; either total $CD4^+$ or total $CD8^+$ cells. Mann-Whitney U-tests were performed to determine the significance between participant groups.

		Healthy		Unhealthy			
	Markers	Median (% of Parent)	95% Confidence Interval	Median (% of Parent)	95% Confidence Interval	Healthy vs. Unhealthy p-value	Healthy vs. Unhealthy q-value
Unstimulated	TNFα+CD4+	0.0895	0.061-0.17	0.0705	0.043-0.14	0.33	0.50
	IFNγ+CD4+	0.145	0.089-0.2	0.086	0.048-0.18	0.21	0.50
	IFNγ+TNFα+CD4+	0.0485	0.027-0.072	0.073	0.025-0.16	0.41	0.50
	TNFα+CD8+	0.185	0.14-0.3	0.17	0.09-0.25	0.39	0.50
	IFNγ+CD8+	0.245	0.14-0.39	0.22	0.12-0.41	0.60	0.60
	IFNγ+TNFα+CD8+	0.0575	0.023-0.16	0.0275	0-0.11	0.16	0.50
Mit. Stimulated	TNFα+CD4+	2.55	1.9-3.8	2.47	1.7-3.6	0.44	0.68
	IFNγ+CD4+	3.23	2.37-3.64	2.34	1.67-3.61	0.24	0.68
	IFNγ+TNFα+CD4+	1.66	1.1-2.58	1.55	1.19-2.88	0.76	0.77
	TNFα+CD8+	0.319	0.18-0.64	0.296	0.133-0.57	0.48	0.68
	IFNγ+CD8+	10.3	7.66-13.2	10.9	8.84-13	0.56	0.68
	IFNγ+TNFα+CD8+	4.26	2.41-7.87	3.21	1.25-8.09	0.34	0.68

A)

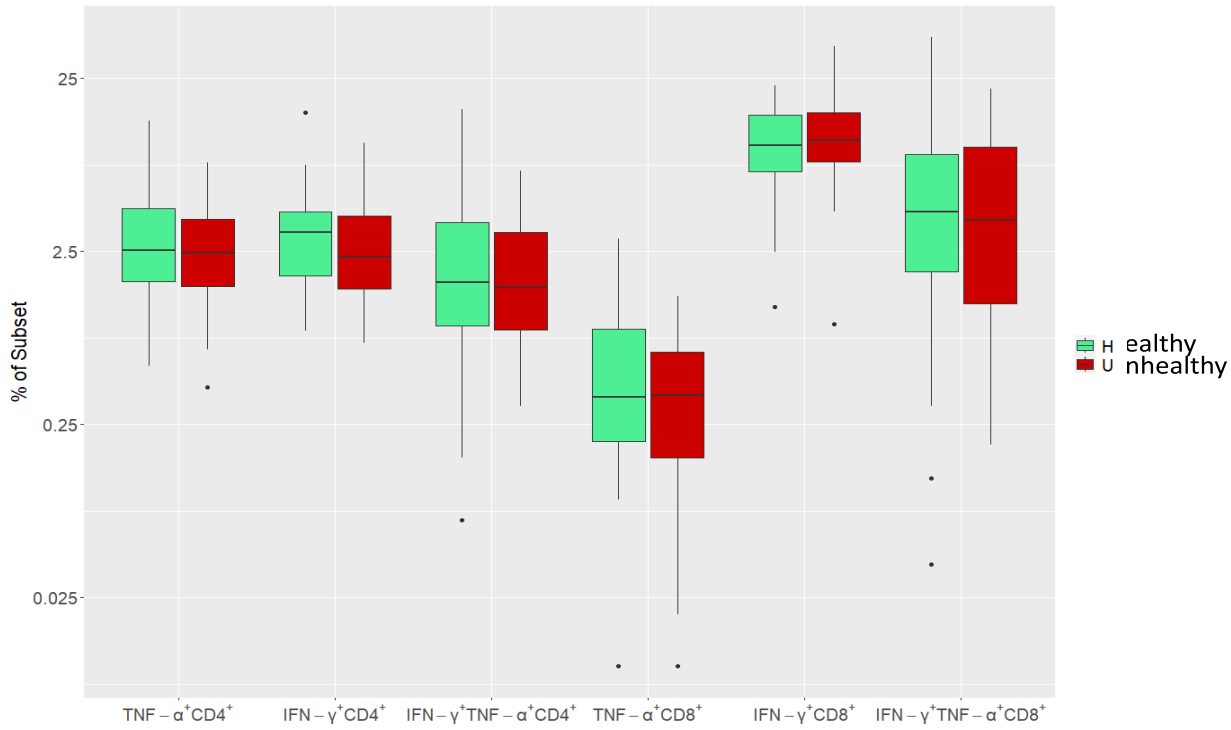

B)

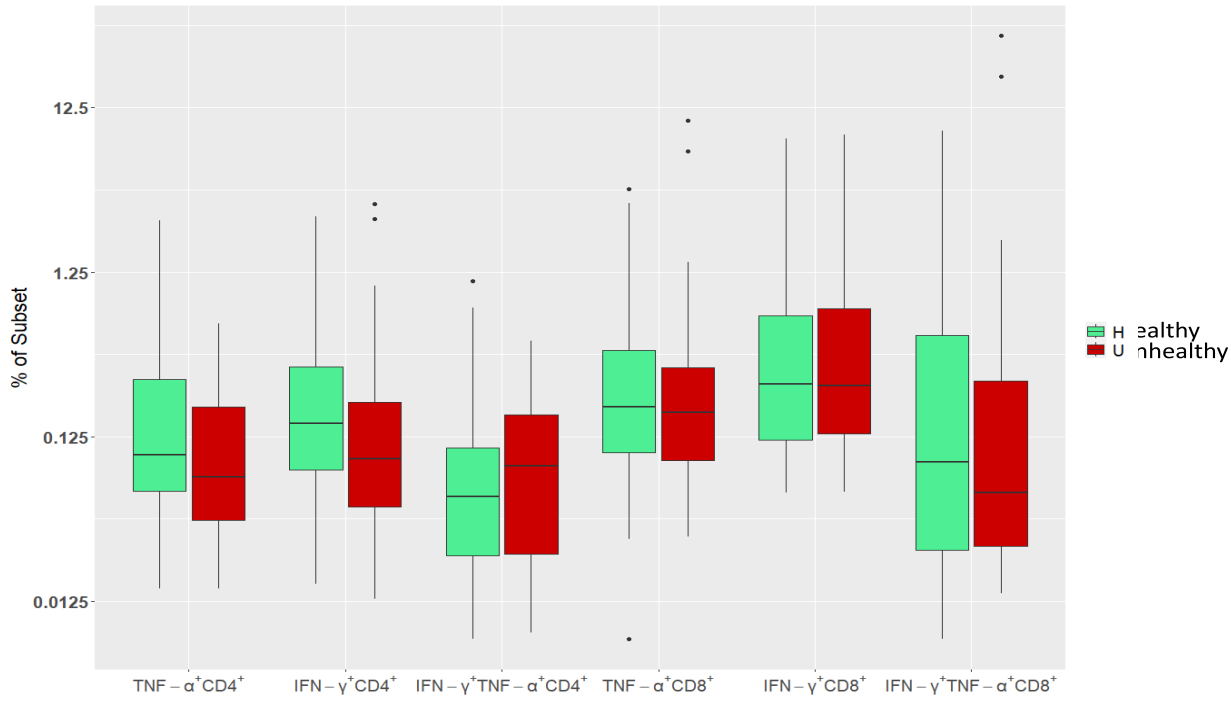

Figure 5.7 Peripheral blood T-cell intracellular cytokine staining from unstimulated and mitogen-stimulated whole blood samples between healthy and unhealthy participants.

Intracellular cytokine staining shows increased frequency of T-cells expressing TNF-α and/or IFN-γ in mitogen-stimulated blood (A) compared to unstimulated blood (B). Similar frequencies were seen in healthy (green) and unhealthy (red) participants. The figure displays the median and interquartile ranges (25th to 75th percentiles) of the frequency of parent cell population ($CD4^+$ or $CD8^+$ cells), represented by boxes, with Tukey whiskers indicating the spread of the data and outliers marked as dots.

5.3.7 Spirometry results highlight the need for alternative diagnostic methods

Spirometry reports were reviewed by a respiratory physician. Test quality was determined by assessing the flow-volume loop to ensure that the participant had produced a consistent, maximal-effort exhale. Spirometry reports that indicated inconsistent/low exhale effort and/or coughing during the test were excluded from the analysis.

After review of the spirometry reports, 10 were deemed to be of acceptable quality. Common challenges in obtaining acceptable spirometry reports include difficulties explaining the manoeuvres to participants due to language barriers, embarrassment felt by participants when performing manoeuvres, and coughing during the tests (Appendix 12). Two showed signs of restriction or obstruction and the remaining eight indicated healthy lung function. Two participants produced spirometry results that disagreed with the initial grouping based on the evidence of respiratory disease. One participant with restricted/obstructed spirometry was categorized as healthy, and one *visa versa*.

The participant in the healthy group with spirometric evidence of lung function impairment was a 59-year-old non-health treatment-seeking female with no history of smoking. Her spirometry revealed a reduced forced expiratory volume in one second (FEV1) and forced vital capacity (FVC) compared to predicted values, but the FEV1/FVC ratio was within the expected percent predicted range (see Figure 5.8). The expiratory curve of this participant showed coving. Together, this is evidence of restriction but not obstruction which suggests that she may have been suffering from lung pathology other than COPD. Her plasma cytokine concentrations trended low; all except TNF-α were in the bottom 30th percentile of the study participants. However, after mitogen stimulation, most plasma cytokine concentrations for this participant were among the top 50%. Exceptions to this were IFN-γ, TNF-α, and IL-22 (7th, 12th and 40th percentile respectively). The leukocyte count for this participant was near the median (55th percentile) but she had comparatively elevated lymphocyte counts with T-cells and B-cells in the 95th and 93rd percentile respectively.

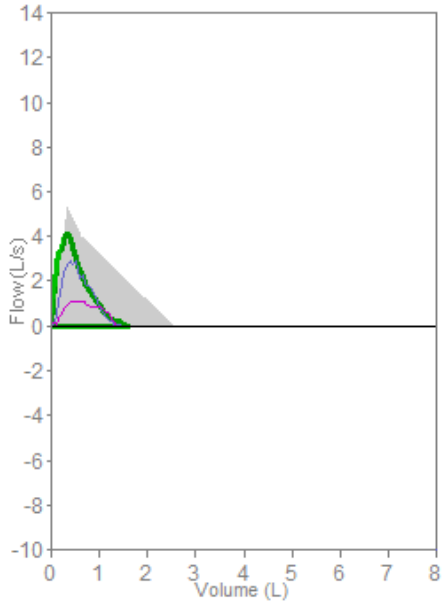

	Best	Predicted	Percent Predicted
FVC (L)	1.63	2.58	63
FEV1 (L)	1.28	2.00	64
FEV1/FVC (%)	78.50	78.30	100
PEF (L/s)	4.14	5.40	77
FEF25-75 (L/s)	1.12	2.04	55

Figure 5.8 Spirometry report from a participant in the healthy group showing signs of restriction.
Forced vital capacity (FVC) and forced expiratory volume in 1-second (FEV1) were greatly reduced from the predicted values however the ratio of FEV1/FVC was not indicative of lung disease. Peak expiratory flow (PEF) and forced expiratory flow 25%-75% (FEF2575) were also greatly reduced compared to predicted values. The expiratory curves displayed caving.

The participant in the unhealthy group with normal spirometry was a 58-year-old male with a history of smoking tobacco. His FEV1 and FVC were only slightly less than predicted values (see Figure 5.9). However, his peak expiratory flow (PEF) and forced expiratory flow 25%-75% were greatly reduced (75% and 76% of predicted values respectively). In addition, there was some coving observed in his expiratory curve. This may indicate sub-clinical lung pathology. He had a leukocyte count that was in the 80th percentile, T-cells at the 49th percentile and B-cells in the 64th percentile. Most of his plasma cytokine concentrations were elevated; all except IL-6 and the regulatory cytokine IL-10 were above the 85th percentile showing evidence of active inflammation.

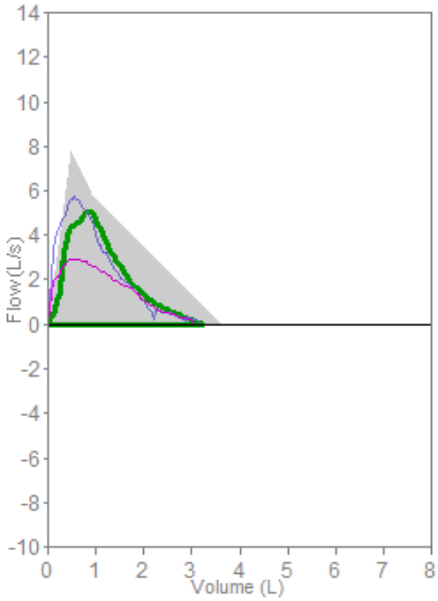

	Best	Predicted	Percent Predicted
FVC (L)	3.24	3.65	89
FEV1 (L)	2.40	2.78	86
FEV1/FVC (%)	74.10	76.10	97
PEF (L/s)	5.81	7.78	75
FEF25-75 (L/s)	1.84	2.42	76

Figure 5.9. Spirometry report for a participant in the unhealthy group showing normal lung function.
The forced vital capacity (FVC) and forced expiratory volume in 1-second (FEV1) were slightly reduced compared to the predicted values and the FEV1/FCV ratio was normal. The participant's peak expiratory flow (PEF) and forced expiratory flow 25%-75% (FEF2575) were reduced from predicted values. The expiratory curve showed caving.

5.4 Discussion

This study evaluated the immune profiles in individuals with evidence of biomass-smoke-induced lung disease from a rural community in PNG to assess the role of immune dysregulation. First, peripheral blood innate and lymphocyte cell populations were enumerated to identify which cell types may be contributing to disease pathology. Next, peripheral plasma cytokine concentrations were determined to elucidate the specific inflammatory responses and signalling pathways involved in the progression of the lung disease associated with biomass smoke exposure. Finally, we performed mitogen stimulation on whole blood samples to test T-cell functional responses. We found that, while peripheral blood cell counts were similar between healthy participants and those with evidence of lung disease (unhealthy participants), there was a significant difference in plasma IL-17F concentration. Additionally, peripheral blood T-cells from unhealthy participants released decreased amounts of type-1, type-2, type-17 and regulatory cytokines in response to mitogen stimulation indicating that they are functionally restrained.

Peripheral blood cell counts were not significantly different in the unhealthy participants compared to those without. Some studies have noted increased peripheral blood neutrophil counts in COPD patients compared to healthy controls (227, 228). However, it was also found that there was no difference in neutrophil counts in COPD patients compared to healthy tobacco smokers (229). This aligns with the results of the present study where we did not find a difference in peripheral blood

neutrophil counts between the two groups, both of which were chronically exposed to biomass smoke. Additionally, in previous studies, blood eosinophil counts were found to be significantly higher in COPD patients compared to healthy tobacco smokers (229). In this study, we did not find a difference in eosinophil counts between the healthy and unhealthy groups. Eosinophil counts were very heterogeneous among participants in both groups with many individuals above the reference range. NKT cells have been reported to be increased in the peripheral blood of tobacco smokers independent of COPD status (89). Accordingly, we found similar levels in both participant groups and many of the participants were above the reference ranges.

It is well established that TS-COPD patients have elevated levels of Type-17 cytokines (see Chapter 2). A rat model has also shown that biomass smoke exposure stimulates pulmonary Th17 differentiation (59). However, BS-COPD patients were shown to have lower serum IL-17 levels than TS-COPD patients (230). Yet, it is unknown how Th17 cytokines differ between healthy biomass-smoke-exposed participants and those with BS-COPD. We found that the Th17 cytokine, IL-17F was elevated in the plasma of the unhealthy compared to the healthy participants. We additionally found that IL-17A was elevated but it failed to reach statistical significance. Further, the Th17-related cytokines, IL-17A, IL-17F, and IL-22 were released at significantly lower levels following mitogen stimulation in the unhealthy group indicating that this inflammatory pathway was chronically activated and had reduced functional capacity upon restimulation. Alternatively, the plasma IL-17A elevation may be a result of spillover from the lungs whereas blood T-cells were functionally compromised. Both isoforms of IL-17 are known to increase neutrophilic inflammation (231, 232). IL-22 on the other hand is a pleiotropic cytokine whose action depends on the greater immune microenvironment (66, 233). However, research in mouse models of COPD has demonstrated that, in the presence of IL-17A, IL-22 increases inflammation (66). The median IL-22 concentration in unstimulated blood was within the range reported for a Western population (189) in both healthy and unhealthy groups, although a portion of participants exceeded the range. It is possible that IL-22 exacerbated inflammatory responses in some of the unhealthy participants given the presence of increased IL-17A however it is unlikely that it is a major contributor to pathology. Analysis of the sputum samples obtained from the unhealthy participants revealed a high proportion of neutrophils compared to all other leukocytes in the lungs. Th17, γδ T-cells, and ILCs in the lungs are likely the primary sources of the increased IL-17 seen in the periphery of these participants thereby inducing neutrophilia in the lungs which may lead to tissue destruction as described in Chapter 2 (234, 235). IL-17 is also involved in mucus secretion and goblet cell metaplasia in the lungs (236, 237).

Previous studies have suggested that biomass-smoke-induced COPD is associated with a type-2 immune response (28, 221, 222). The present study did not find a significant difference in the plasma

concentrations of type-2 cytokines in the unhealthy participants. However, IL-4, IL-5, IL-9, and IL-10 all trended toward higher concentrations in the unhealthy participants. These findings hint that type-2 responses may play a role in the respiratory pathology of these participants but studies with a larger cohort would be needed to investigate this. However, biomass smoke exposure itself does increase type-2 inflammation regardless of disease status (see Chapter 4). Despite this, there were significantly lower levels of the type-2 cytokines IL-9, and IL-13, but not IL-4 or IL-5, elicited by mitogen stimulation in the unhealthy participants. This provides evidence that the type-2 immune pathways may have been chronically activated in the unhealthy participants. A comparison of direct lung samples, such as bronchoalveolar lavage fluid, may confirm the role of type-2 immune responses in biomass smoke-induced lung disease.

This study found variable relative proportions of eosinophils in the sputum of participants who had symptoms of lung disease, but we are unable to compare them to the healthy group, who, by definition, did not produce spontaneous sputum samples containing immune cells. The majority of unhealthy participants had sputum eosinophils that surpassed the 2-3% sputum eosinophil thresholds typically used to classify patients as eosinophilic (26, 238, 239). This may indicate that only a subset of people with biomass smoke-induced lung disease has type-2 inflammation and may indicate that this 'phenotype' of the disease may be heterogeneous itself. However, blood eosinophil counts were similar between healthy and unhealthy participants. In a large cohort of COPD patients from the USA, it was found that high sputum eosinophil proportions were related to increased disease severity, exacerbation frequency, and emphysema (240). Further, sputum eosinophils were a superior marker for these characteristics than blood eosinophils. In the current study, sputum eosinophil proportions did not correlate with blood eosinophil concentrations. It is likely the case that many of the unhealthy participants are experiencing type-2 inflammation in their lungs, as evidenced by high sputum eosinophils and type-2 cytokines, despite not having blood eosinophils counts that reflect this. Overall, while type-2 immune responses are involved with chronic biomass smoke exposure, it is less clear what role they play in lung disease.

This study was the first to evaluate the role of T-cell functional responses in biomass smoke-induced lung disease. In general, peripheral immune cells from participants with evidence of biomass smoke-induced lung disease released fewer cytokines in response to mitogen stimulation than those from healthy biomass smoke-exposed donors indicating functional restraint. However, it is uncertain if the varying levels of cytokines already present in the whole blood samples affected the response to mitogen stimulation as there is potential that the cytokines present dampened or enhanced the cellular response to mitogen stimulation depending on the cytokine milieu. There was also a slightly lower (non-significant) concentration of T-cells in the blood samples of the unhealthy participants

which may have contributed to the reduced response to stimulation. Future studies could investigate mitogen stimulation of isolated T-cells and/or T-cell subsets. This would ensure that the responses were not affected by existing cytokines and could identify the cell types involved in the immune dysfunction. We also performed intracellular staining of peripheral blood T-helper and cytotoxic T-cells pre- and post-mitogen stimulation to identify if these cell types exhibited reduced responses. There was no difference in intracellular staining of either of the two cytokines (IFN-γ and TNF-α) tested between the participant groups demonstrating that T-cells do not have a reduced capacity to produce these cytokines in the unhealthy participants. However, overall, the total peripheral immune cell populations from unhealthy participants were less able to release IFN-γ in response to mitogen challenge as measured in plasma. The cellular source of this reduced functional capacity remains unknown. NKT and γδ T-cells are also known sources of IFN-γ and may play a role in the reduced response in the unhealthy participants (241, 242).

It has been shown that anergic cells do not assume a passive role in immunity but instead may act to suppress immune responses (243-245). This mechanism likely plays a role in the prevention of autoimmune diseases. However, this could have major implications in terms of susceptibility to infectious diseases and cancer progression. Previous studies demonstrated that tuberculosis patients with anergic T-cells were less able to mount an appropriate response to active tuberculosis infections. Isolated T-cells from these patients were unable to produce IFN-γ in response to isolated tuberculin protein (246). It has been established that T-cell responses are reduced in COPD patients and that they are more susceptible to respiratory infections (80, 82, 247). Our studies summarised in Chapter 3 also identified markers of T-cell exhaustion in AECOPD patients. It is likely that BS-COPD in the remote communities of PNG reduces the functional capacities of T-cells leading to increased susceptibility to diseases. This is a critical issue in areas where tuberculosis is endemic such as in rural PNG. Additionally, anergic immune responses impair the suppression of tumour cells (248, 249). This is particularly concerning in biomass smoke-exposed individuals who are chronically exposed to carcinogenic compounds in the smoke.

This study underscores the necessity of developing diagnostic techniques that do not require access to highly trained clinicians and extensive laboratory facilities. We found that there are also potential cultural barriers to obtaining high-quality diagnostic results among people who are not familiar with or comfortable in a Western medical environment. Further, standards for diagnosing patients may be highly variable among different populations and standardized references from Western regions (such as spirometry reference equations) may not be useful in interpreting an individual's lung health status. Yet, in remote communities exposed to biomass smoke, like the one investigated in this study, there is a pressing need to identify individuals with lung diseases, given the high

prevalence. Diagnosis of lung disease in such areas must rely on techniques that are easily reproducible and less subject to cultural hesitation. Analysis of peripheral blood and sputum samples meet these criteria. These samples can be obtained with limited training and can be transported to labs where there are sufficiently trained personnel for analysis and interpretation. Previous research, primarily focused on TS-COPD, has explored the use of various blood, sputum and exhaled breath condensate markers for diagnosing COPD. Fibrinogen, a glycoprotein involved in blood clotting, is one marker that has been investigated in numerous studies It was found to be increased in the plasma of patients with COPD compared to controls and its concentration was related to disease severity (250, 251). Additional research noted that plasma fibrinogen levels were associated with both obstructive and restrictive lung diseases (252) so its ability to distinguish between separate diseases is limited or may require concurrent measurement of additional markers. Serum C-reactive protein (CRP), frequently used as a general inflammatory marker, has also been investigated as a biomarker in TS-COPD patients and was significantly increased compared to healthy smokers and non-smokers. Other, lung-specific markers have also been evaluated as biomarkers in COPD. Serum concentrations of surfactant protein D were increased in COPD patients compared to healthy controls and were related to disease severity and exacerbation status (253-255). Sputum neutrophil gelatinase-associated lipocalin was found to be significantly lower in COPD patients compared to those with COPD/asthma overlap (256-258). These, and many other markers, have not been investigated in remote biomass-smoke-exposed communities including the one studied here. These markers may be useful to stratify participants more precisely in future studies and to help reduce 'noise' in the dataset to better unravel the mechanisms underlying BS-COPD in areas where Western diagnostic techniques are not possible. Further, future studies could assess if these markers were effective in predicting response to therapies and disease trajectories. This preliminary study improves our understanding of the systemic inflammation in people suffering from biomass smoke-induced lung disease in remote communities in PNG. This provides a stepping-stone leading us closer to improved diagnostics and treatments for people suffering from BS-COPD.

Chapter 6. Peripheral blood transcriptomic analysis reveals signatures of immune dysregulation in biomass smoke-induced lung disease

6.1 Introduction

In Chapter 4, the immune profiles of biomass-smoke-exposed participants from a remote community in PNG who did not have evidence of lung disease were analysed to establish baseline healthy immune parameters. Next, biomass-smoke-exposed participants with evidence of lung disease resembling COPD, determined by respiratory symptoms and the presence of leukocytes in their sputum, were recruited and their immune profiles were compared against the baseline to identify immune factors related to lung pathology (Chapter 5). This study identified significant differences in cytokine profiles and mitogen-induced T-cell responses between participants with evidence of lung disease and those without. This approach provided insights into the broad immune states of people experiencing lung disease in this population. However, there are still limited studies on individuals within areas where there are high rates of exposure to biomass smoke. Furthermore, no studies have investigated the peripheral blood transcriptional signatures in individuals from remote PNG who have been chronically exposed to biomass smoke. In Chapter 3, flow cytometry and a transcriptomics approach revealed differences in the activation and exhaustion states of T-cell subsets from exacerbating TS-COPD patients compared to healthy controls. A higher proportion of $CD4^+$ cells expressed activation markers in these patients. Further, MAIT cells were found in lower proportions and had higher expression of exhaustion markers in AECOPD patients than in controls. Further, both $CD4^+$ and $CD8^+$ subsets had transcriptional evidence of dysregulation. Similarly, transcriptomic analysis may provide detailed insights into the immune dysregulation in individuals suffering from biomass smoke-induced lung disease. It is unknown if the transcriptional changes underlying biomass smoke-induced lung disease are similar to those observed in TS-COPD patients. This is key to understanding the immunological nature of the disease.

This research aims:

- To pinpoint transcriptional changes and molecular pathways that are associated with biomass smoke-induced lung disease within a remote community in rural PNG.

By doing so, we will uncover pathways potentially associated with biomass smoke-induced lung disease and shed light on the underlying mechanisms of the disease. This research lays the foundation for future studies that may identify new diagnostics and therapies that could be deployed in remote biomass-smoke-exposed communities.

6.2 Methods

6.2.1 Participant recruitment and sample collection

Participants were recruited from the general population or when they presented to the Balimo District Hospital with respiratory symptoms. Participants were grouped into healthy (no evidence of lung disease; n=36) and unhealthy (evidence of lung disease; n=31) groups as described in Chapters 4 and 5.

Venous blood from each participant was drawn into 2.5 ml PAXgene® blood RNA tubes (Qiagen). These tubes were designed to preserve RNA for downstream analysis. Previous research has demonstrated that they yield more than a sufficient amount of RNA for standard RNA sequencing workflows (259).Tubes were kept refrigerated before transport to James Cook University laboratory facilities (Townsville, Australia). Tubes were then stored at -80°C until further processing.

6.2.2 RNA extraction, preparation, and sequencing

Blood total RNA was extracted using the PAXgene Blood RNA Kit (PreAnalytiX/Qiagen) according to the manufacturer's instructions. Briefly, the blood tubes were centrifuged to pellet nucleic acids. Pellets were rinsed and transferred to microcentrifuge tubes and treated with Proteinase K to remove proteins. Next, on-column DNA digestion was performed, and samples were eluted using nuclease-free water. Purified RNA was stored at -80°C. RNA samples were shipped on dry ice to the Australian Genomics Research Facility (AGRF) for further quality control, library preparation, and sequencing. Library preparation included ribosomal RNA depletion. The Illumina Novaseq 6000 platform was used to sequence 150 base pair paired-end reads with a target of 50 million reads per sample. Samples were extracted and sequenced across two separate batches.

6.2.3 Data Processing

The pipeline for RNA sequence data processing and analysis is summarised in Figure 6.1. Sequencing raw data (FASTQ files) were processed on a Linux computer using command line tools. Data quality was assessed using FastQC (v0.11.9) to generate reports for each sample. The QC reports were subsequently used to establish data-trimming parameters (see Appendix 13). Sequencing reads were trimmed using Trimmomatic (v0.39). Nextera adapter content was removed. The first base of each read was trimmed off. The leading and trailing bases were kept only if they had a phred quality score of at least 20. A sliding window was applied to keep each section of 5 bases only if the average phred quality score was 30 or greater. After trimming, sequences were discarded if the remaining length

was less than 50 basepairs. The trimmed reads were aligned to the hg38 human reference genome using Kallisto (v0.48.0).

6.2.4 Data analysis

Transcriptomic data analysis was based on a previously published workflow but included modifications for the unique parameters and goals of this study (Figure 6.1) (260). Aligned data was imported into RStudio (v2022.12.0+353) running R version 4.2.2. Gene names were annotated using the ensembldb package. Gene count data was converted to log2 counts per million (CPM) using the edgeR package. This dataset contains thousands more genes than the total number of participants in the study. Due to this, there is a large multiple-testing penalty. To reduce this effect, a strict filtering protocol was implemented. Genes that had less than or equal to 50 CPM in all samples combined were filtered out. Normalization was performed using the trimmed mean of M-values (TMM) method using edgeR. This method adjusts for variations in library sizes and compositional differences between RNAseq samples and ensures more accurate comparisons of gene expression levels across different samples. Differential gene expression was performed using the limma package to compare the healthy (no evidence of lung disease) and unhealthy (evidence of lung disease) groups established in Chapter 5. Batch information was included as a factor when performing the analysis to account for any potential batch effects. Violin plots highlighting the effects of filtering and normalization and PCA plots were constructed using the ggplot2 package.

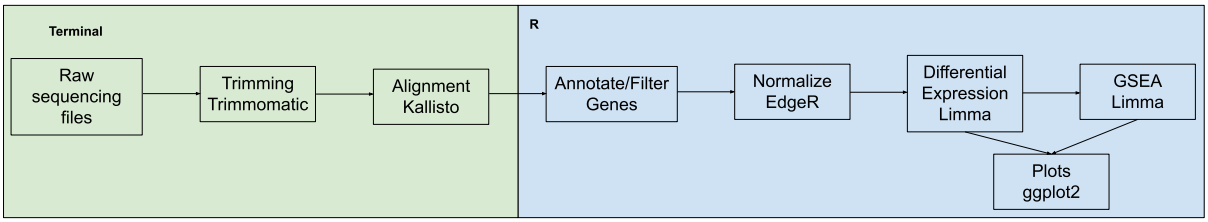

Figure 6.1 Overview of RNAseq data processing and analysis pipeline.

Gene set enrichment analysis (GSEA) was also performed on the data after filtering and normalization. This technique uses pre-defined gene sets that are associated with biological pathways to determine if the pathways are overrepresented in the unhealthy group compared to the healthy group. This technique can reveal pathways that may be associated with lung pathology in the study participants. Additionally, by comparing genes in related sets instead of individually, GSEA reduces the number of comparisons made and increases statistical power. GSEA was performed using the camera function in limma. Gene set collections were obtained from the Molecular Signatures Database (MSigDB) (261, 262). These gene set collections were constructed by

aggregating previously published transcriptomics data from thousands of studies. Three separate gene set collections were used for analysis; the 'hallmark gene sets' collection which contains robust gene signatures produced from aggregating multiple gene sets for well-defined molecular pathways; the 'curated gene sets' (C2) collection which includes an aggregation of gene sets from databases; and the 'cell type signature gene sets' (C8) collection which was derived from single cell transcriptomic sequencing data to identify gene signatures associated with specific cell types. The camera function in the limma package was used to perform the analysis and selected results were plotted using the ggplot2 package. The camera function in limma conducts competitive gene set testing by assessing inter-gene correlation within gene sets, aiming to provide a more precise evaluation of gene sets related to specific conditions or treatments. This function uses Benjamini-Hochberg to adjust for the false discovery rate.

6.3 Results

6.3.1 Filtering and Normalization

The initial combined dataset (unhealthy and healthy) contained expression levels of 35,369 genes across samples from 67 participants and included a large proportion of genes with low expression levels (Figure 6.2 A). After applying a strict filtering protocol to remove the genes with low expression levels, 3451 genes remained (Figure 6.2 B). TMM normalization improved the sample-to-sample mean expression level variance (Figure 6.2 C). Only the filtered and normalized data were used for downstream analysis.

A)

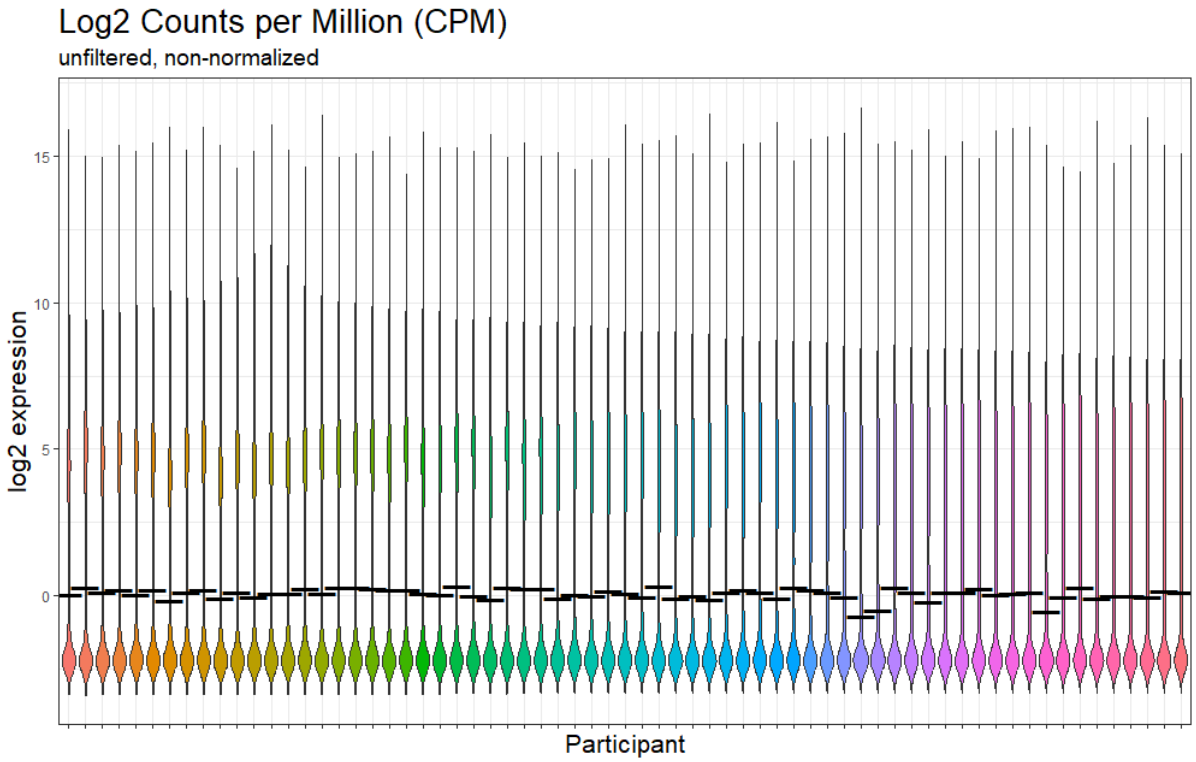
Log2 Counts per Million (CPM)
unfiltered, non-normalized
log2 expression
15
10
5
0
Participant

B)

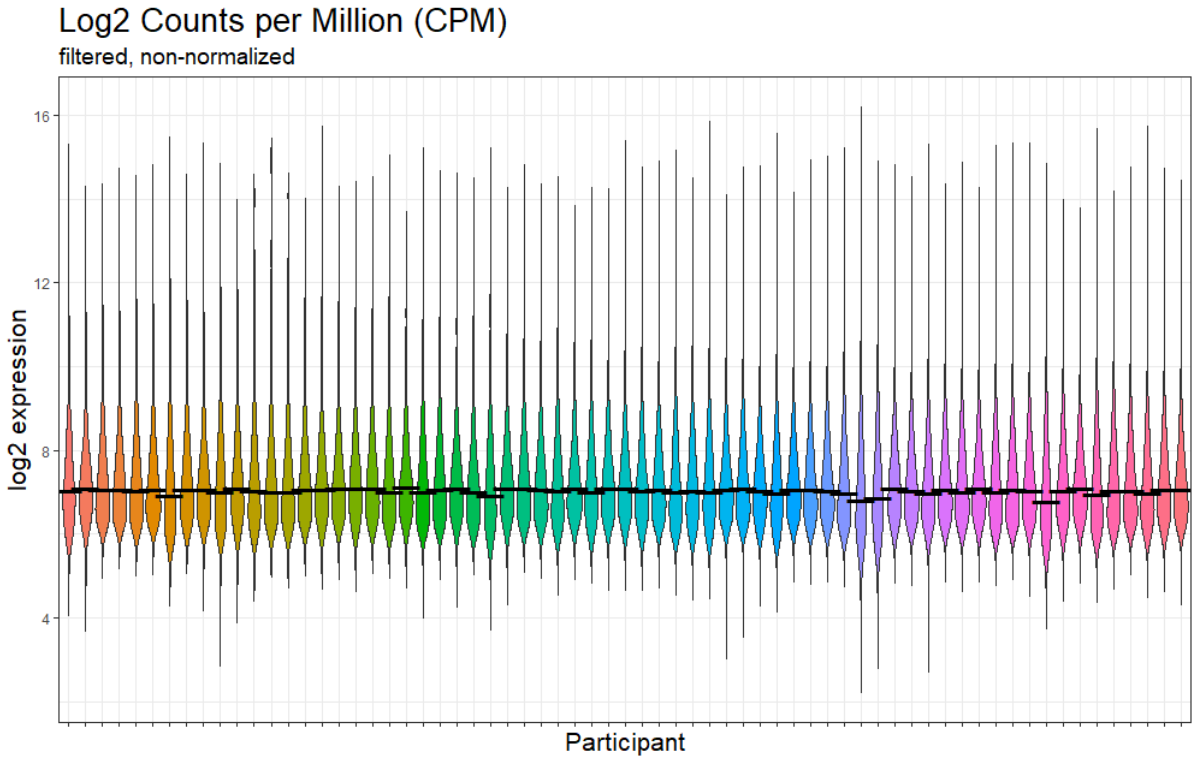
Log2 Counts per Million (CPM)
filtered, non-normalized
log2 expression
16
12
8
4
Participant

C)

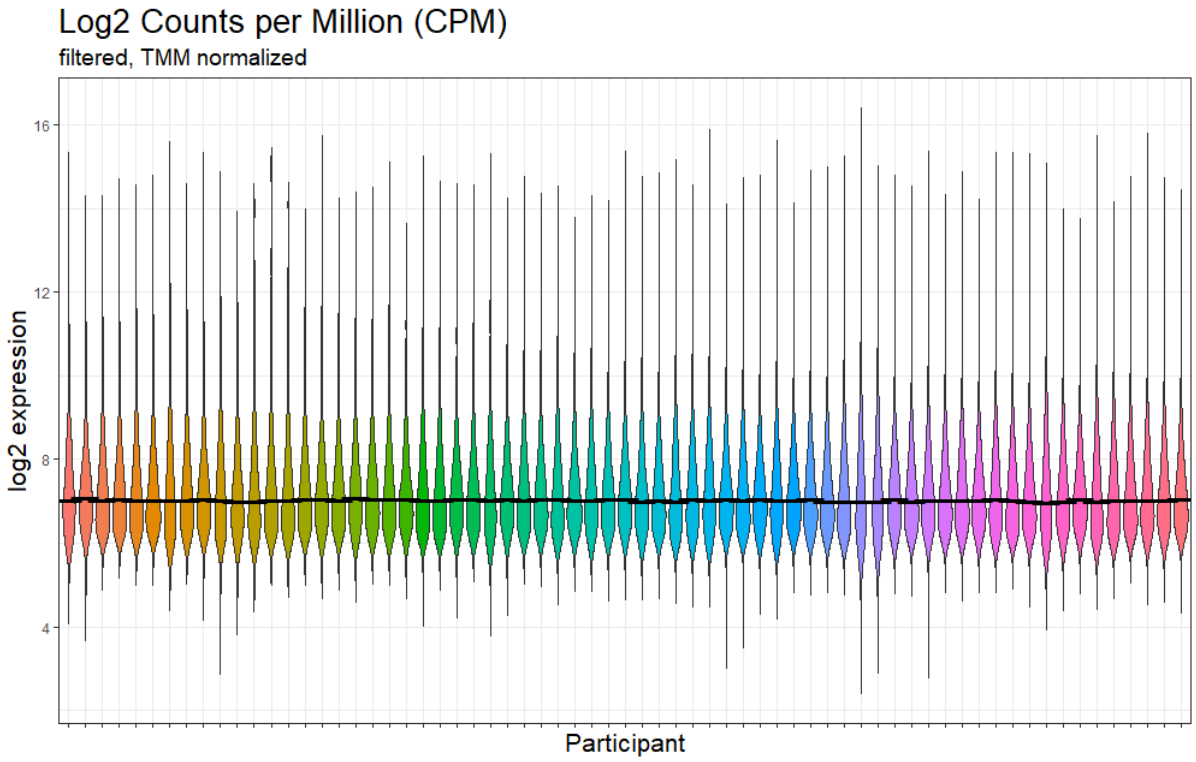

Figure 6.2 Data pre-processing. Violin plots show the distribution of log2 counts per million (CPM) gene expression values plotted for each participant. Participants are represented as different colours. Black bars indicate the median expression levels for each participant. (A) The unprocessed data show an abundance of genes with very low expression and inconsistent median expression levels between participants. (B) After filtering, the median expression level increased yet, the median expression levels remained inconsistent. (C) Trimmed Mean of M-values normalization was applied and the median expression levels between participants improved.

6.3.2 Differential gene expression analysis reveals alternated transcription of immune-related genes

Differential gene expression (DGE) analysis was performed to identify individual genes that were expressed at significantly different levels between the unhealthy (n=31) and healthy (n=36) participant groups using the filtered and normalized read counts. Principal component analysis did not reveal a strong separation between the two groups (see Figure 6.3). However, 15 genes were significantly differentially expressed in unhealthy compared to healthy participant groups; seven increased and eight decreased (see Table 6.1). These results included genes related to T-cell development and signalling, and cellular stress responses. A complete list of DGE analysis results can be viewed at: Gilstrom DGE Results.xlsx.

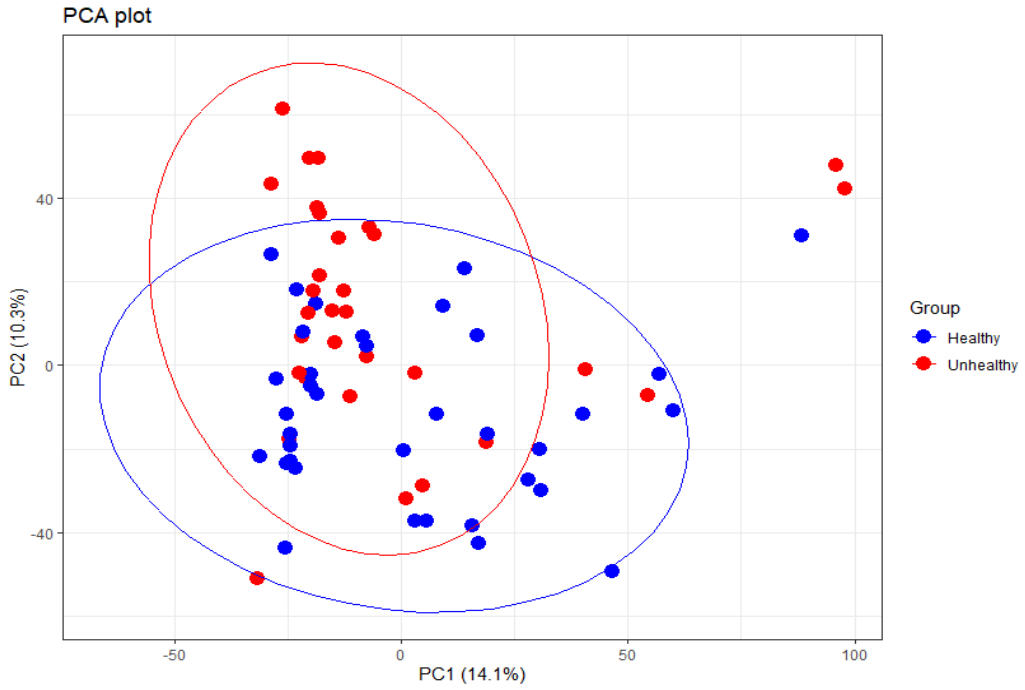

Figure 6.3 Principal component analysis (PCA) of gene expression in PNG cohort. Principal components were computed and healthy and unhealthy participant groups colour coded. Principal components (PC) one and two were plotted and their percent contribution to the total variance across individual samples is listed with the axis labels. PCA analysis did not reveal a well-defined separation between groups.

Table 6.1 Differentially expressed genes between healthy and unhealthy participants. 15 genes were significantly differentially expressed after FDR correction (p-adj.<0.05). Log_2 fold change shows the difference in expression level in unhealthy compared to healthy participants. Negative Log_2FC indicates that the genes have decreased expression in the unhealthy participants. The expression of seven genes was increased while eight genes had decreased expression in unhealthy compared to healthy participants. Uncorrected and FDR-corrected p-values (adj.P.Val) are shown.

Gene	Name	Log_2FC	P.Value	adj.P.Val
HSPA1A	Heat Shock Protein Family A (Hsp70) Member 1A	0.501463	6.35E-05	0.046775
NATD1	N-Acetyltransferase Domain Containing 1	0.427212	0.00021	0.048414
TLN1	Talin 1	0.3104	0.00021	0.048414
UBAP1	Ubiquitin Associated Protein 1	0.276732	0.00017	0.046775
NR1H2	Nuclear Receptor Subfamily 1 Group H Member 2	0.247529	0.000138	0.046775
OS9	Osteosarcoma Amplified 9, Endoplasmic Reticulum Lectin	0.246208	0.000162	0.046775
ILK	Integrin Linked Kinase	0.20625	0.000176	0.046775
STIM2	Stromal Interaction Molecule 2	-0.22258	9.68E-05	0.046775
HNRNPDL	Heterogeneous Nuclear Ribonucleoprotein D-like	-0.26721	4.92E-05	0.046775
GIMAP5	GTPase IMAP Family Member 5	-0.33707	0.000161	0.046775
LY9	Lymphocyte Antigen 9 (CD229)	-0.35633	0.000154	0.046775
ITK	Interleukin-2-inducible T-cell Kinase	-0.40225	0.000112	0.046775
IL7R	Interleukin 7 Receptor	-0.47386	0.000129	0.046775
TC2N	Tandem C2 Domains, Nuclear	-0.48291	8.70E-05	0.046775
CD96	Cluster of Differentiation 96	-0.49583	2.22E-05	0.046775

6.3.4 Gene set enrichment analysis reveals evidence of inflammatory immune response

Finally, the data set was analysed against the Cell Type Signature Gene Sets collection to identify gene sets associated with specific cell types. Complete lists of gene sets included in each collection and genes in each gene set can be viewed on the MSigDB website (https://www.gsea-msigdb.org/gsea/msigdb). The analysis returned 137 total gene sets that were significantly different between the two groups (see Appendix 14C). 89 were enriched and 48 were depleted in the unhealthy group compared to the healthy group. Lymphocyte-associated gene sets, including those related to CD4, CD8, and NKT cells, were depleted in the unhealthy group compared to the healthy group. Conversely, gene sets associated with innate cells, such as monocytes, macrophages, neutrophils, eosinophils, and dendritic cells were enriched in the unhealthy group compared to the healthy group (Figure 6.4).

A)

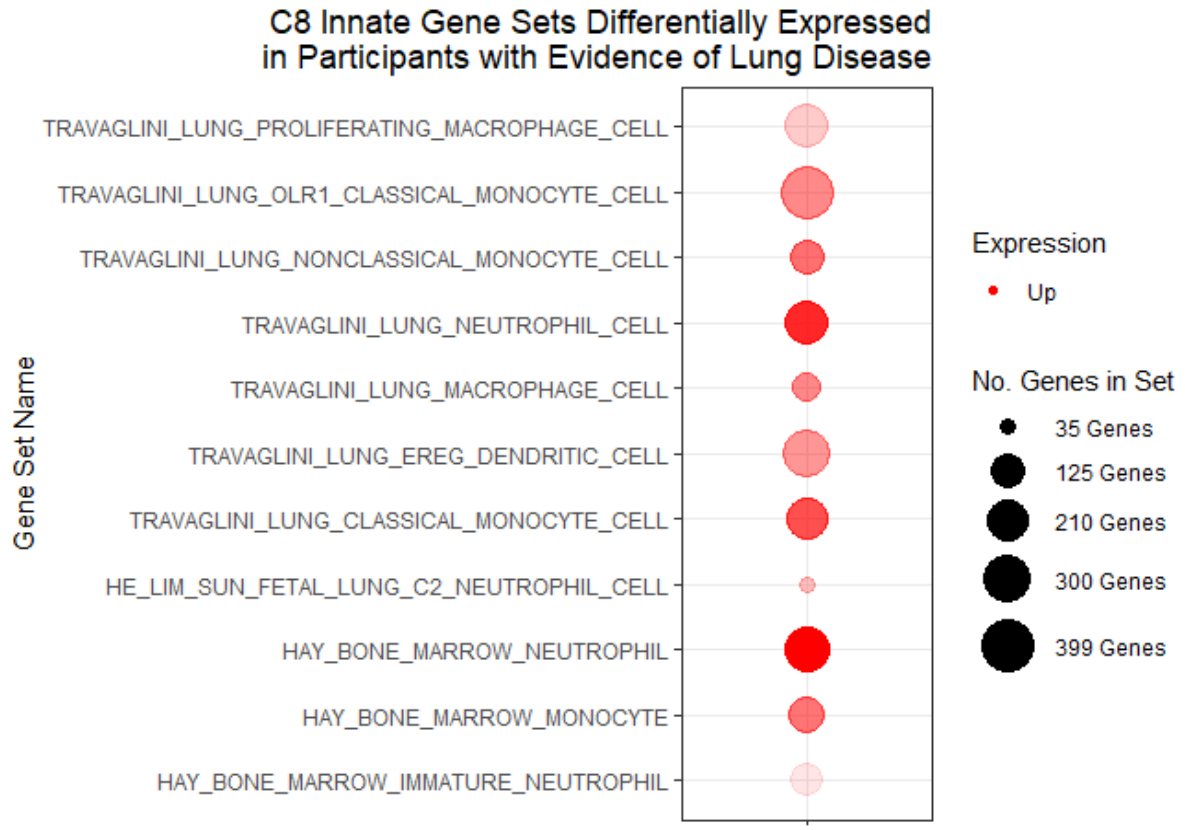

B)

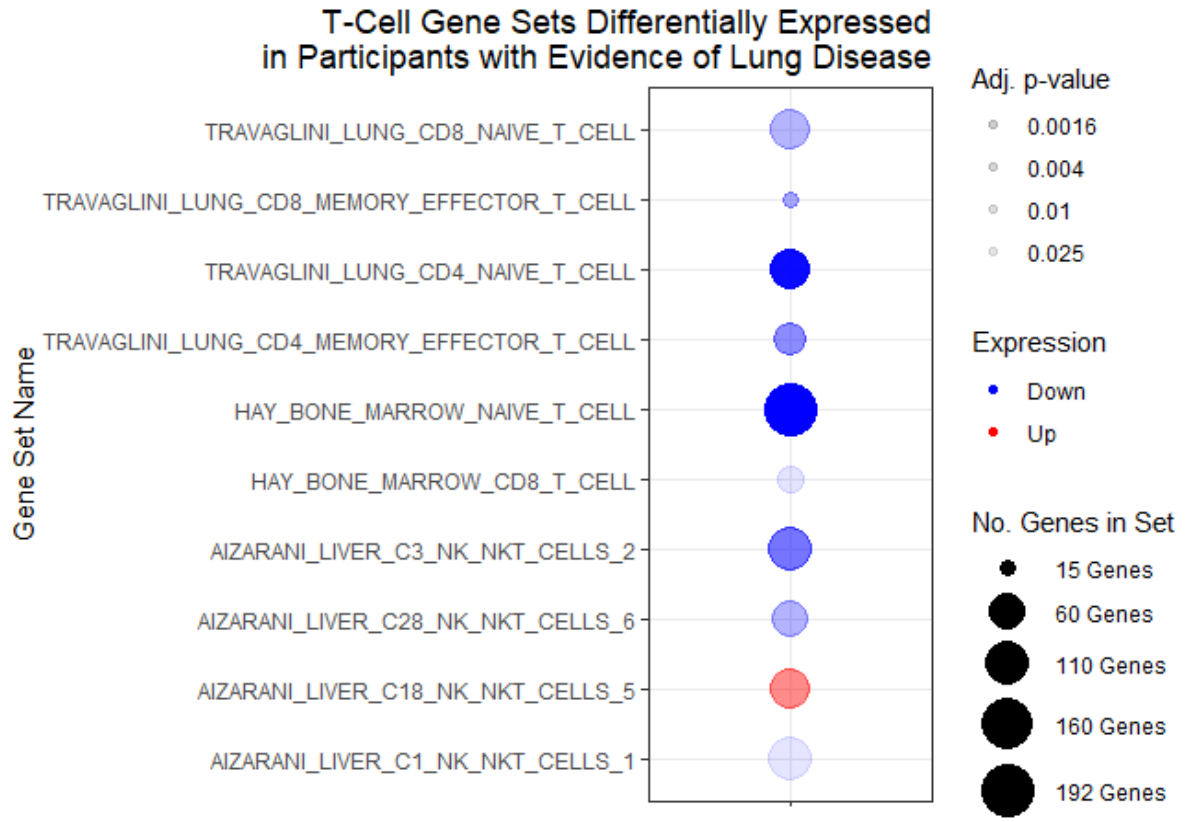

Figure 6.4 Innate and T-cell gene sets differentially expressed in participants with evidence of lung disease. GSEA analysis was performed using the cell type signature gene set collection. Expression of gene sets was compared between the unhealthy and healthy groups. The dot size represents the number of genes included in the gene set. The transparency of the dot represents the significance of the difference; greater transparency indicates lower significance. Red dots indicate that the gene set was enriched in the unhealthy group compared to the healthy group, conversely, blue dots indicate that it was depleted. Results indicate increased expression of gene sets related to innate immune cells (A) and reduced expression of most gene sets associated with T-cells (B).

Next, GSEA was performed using the Hallmark gene set collection to investigate well-defined biological pathways modulated in the unhealthy participants compared to the healthy participants. In total, 13 gene sets were significantly different between the two groups; the expression of 11 was increased and two decreased in the unhealthy group compared to the healthy group (Figure 6.5 and Appendix 14A). The gene sets enriched in the unhealthy group included those related to intracellular signalling, inflammation, and inflammatory response. Specifically, expression of gene sets related to the cytokines TNF-α, IFN-α, IFN-γ, and IL-6 was increased in the unhealthy group. Additionally, expression of gene sets related to reactive oxygen species, complement, NF-kB, JAK/STAT, and PI3K-AKT-mTOR signalling was increased in unhealthy participants. Expression of two gene sets related to cellular proliferation (MYC and E2F) was decreased in the unhealthy group.

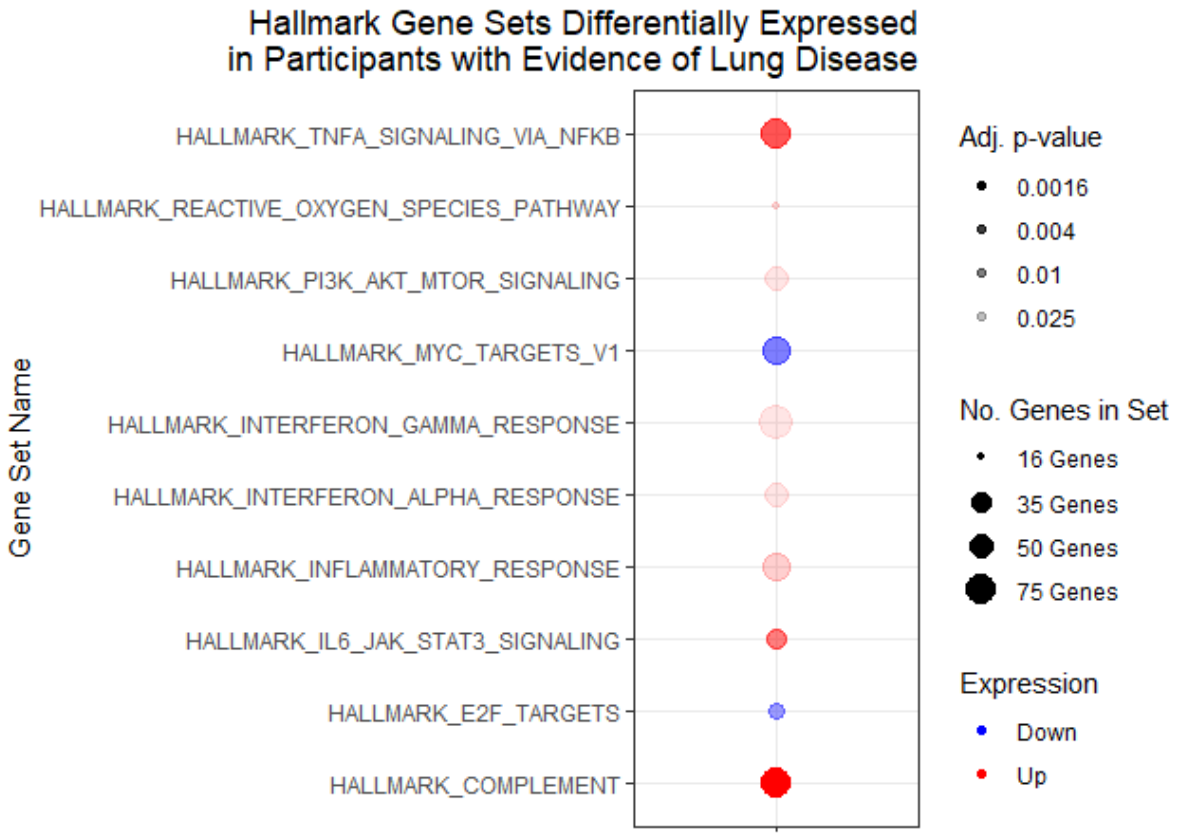

Figure 6.5 Hallmark gene sets differentially expressed in participants with evidence of lung disease. GSEA was performed using Hallmark gene set collection. Expression of gene sets was compared between the unhealthy and healthy groups. The dot size represents the number of genes included in the gene set. The transparency of the dot represents the significance of the difference; greater transparency indicates lower significance. Red dots indicate that the increased gene set expression in the unhealthy group compared to the healthy group, conversely, blue dots indicate that it was depleted. The results indicate enrichment of many gene sets related to cell signalling and inflammatory immune responses.

Finally, GSEA was performed using the Curated (C2) gene sets collection (see Figure 6.6). This analysis yielded 258 gene sets that were significantly different between the two groups. 190 were enriched and 68 were depleted in the unhealthy group compared to the healthy group (see Appendix 14B). The results included gene sets related to the cytokines TGF-β, IL-2, IL-3, IL-4, IL-6, and IL-8. Also, there were gene sets associated with transcription factor pathways including STAT5A, JAK-STAT, S1P, MAPK, and RUNX1. Pathways related to neutrophils and NK cells were also enriched.

Figure 6.6 Curated (C2) gene sets differentially expressed in participants with evidence of lung disease. GSEA analysis was performed using the curated gene sets collection. Selected gene sets related to immune function are displayed. Expression of gene sets was compared between the unhealthy and healthy groups. The dot size represents the number of genes included in the gene set. The transparency of the dot represents the significance of the difference; greater transparency indicates lower significance. Red dots indicate that the gene set was enriched in the unhealthy group compared to the healthy group, conversely, blue dots indicate that it was depleted. Results show many enriched pathways relating to hypoxia, immune signalling, and immune activation.

6.4 Discussion

This study investigated the differences in peripheral blood gene expression profiles between biomass-smoke-exposed participants with evidence of lung disease (unhealthy) and non-health-seeking biomass-smoke-exposed (healthy) participants from a remote community in PNG. The results revealed many transcriptional changes associated with unique immune responses in the

unhealthy participants. This study expanded from Chapter 5 and provided more information about the cellular differences in the peripheral blood of the unhealthy participants compared to the healthy participants. In particular, many transcriptional differences relating to T-cells were identified. A GSEA technique was used in conjunction with a collection of gene sets (MSigDB collection 8) conglomerated from an array of previously published single-cell RNA sequencing studies. This technique was used to identify gene sets that are associated with specific immune cell types (Figure 6.4). Expression of gene sets associated with T-cells was decreased in the unhealthy group. Specifically, gene sets associated with naïve, NKT, CD4, and CD8 T-cells were depleted in the peripheral blood of the unhealthy participants compared to the healthy group suggesting that blood T-cell numbers may be decreased in these individuals. Many of these gene sets were originally characterised by single-cell RNA sequencing studies using lung or liver tissues, yet it remains uncertain whether the specificity of these gene sets to those organs is reflected in the cells studied in the current research.

A key finding related to T-cells was that the expression of *CD96* was decreased in the blood of the unhealthy participants (Table 6.1). CD96 is an inhibitory receptor commonly expressed on activated T-cells and natural killer cells. CD96 on T-cells interacts with CD155 on antigen-presenting cells. The downstream effects of this interaction are not clear. Previous studies on $CD8^+$ cells found a costimulatory effect of CD96 activation leading to enhanced cytotoxic functions (263). However, other studies found that CD96 deletion led to enhanced killing of leukemia cells (264). Further mouse studies revealed that CD96 expression in Th9 cells was associated with a reduced inflammatory profile (265). A study on CD96 expression on NK cells from COPD patients found increased expression of this marker (266). Additionally, the results from Chapter 3 found that CD96 expression was increased in $CD4^+$ T-cells from tobacco-smoke-induced AECOPD patients compared to HCs. It is, therefore, interesting that the present study identified reduced expression of this marker in the unhealthy participants. This may point to different disease mechanisms or may be due to the use of whole blood in this study compared to specific isolated cell types in previous studies. Further research on the role of CD96 in BS-COPD is warranted. Future studies should identify the role of CD96 in isolated T-cell subsets to identify their association with T-cell function.

Other T-cell-associated genes that showed decreased expression in unhealthy compared to healthy participants included *ITK*, *IL7R,* and *LY9* (Table 6.1). IL-7Rα is expressed on lymphoid lineage cells and is required during T-cell development, proliferation and survival. Due to the critical role IL-7 plays in the homeostasis of the immune system, leading to the differentiation, proliferation, and survival of T-cells, B-cells, and NK cells, reduced expression of the IL-7R may compromise T-cell survival in these participants (267, 268). ITK (IL-2 inducible T-cell kinase) is a non-receptor associated tyrosine kinase

highly expressed in T-cells that functions downstream of the T-cell receptor. It plays a role in many aspects of T-cell development and function. ITK deficiency can lead to CD4 T-cell lymphopenia and recurrent pulmonary infections (269, 270). LY9 (CD229) is expressed on B-cells and T-cells and has been shown in mouse studies to negatively regulate the development of NKT cells (271, 272). However, there was no difference in NKT cell concentration in these participants (Figure 5.1A) so the role of this finding is unclear.

Many genes in the targets of RUNX1 gene set were enriched in unhealthy compared to healthy participants (Figure 6.6). RUNX1 is an important transcription factor in memory Th2 cells to induce IL-3 and in Th17 cells, RUNX1 and RORγt cooperate to induce expression of IL-17(273-275). Additionally, RUNX1 is required for transcription of FOXP3 in Treg cells (275). The precise contributions of this large set of RUNX1-related gene targets are unclear but warrant further investigation.

HSPA1A was also significantly increased in the unhealthy participants (Table 6.1). This gene encodes for heat shock protein 70 (HSP70) which has several roles in cellular stress responses and immune function. There are many proteins in the HSP family. Generally, HSPs protect other proteins from damage by binding to and stabilizing them thereby preventing degradation and aggregation. They are also capable of correcting misfolded proteins (276). However, HSPs play additional roles in the immune system exerting inflammatory or anti-inflammatory effects. HSPs, including HSP70, are involved in antigen presentation on both MHC I and MHC II molecules. HSPs bind antigenic peptides and chaperone them to the MHC molecules (277, 278). Presentation of HSP/peptide complexes on MHCs has been shown to increase antigen-specific proliferation of $CD4^+$ T-cells (279). HSPs are also released into the extracellular matrix. Extracellular HSPs act as danger signals, alerting the host immune system to areas of damage. They can be detected through their binding to scavenger receptors on immune cells (280, 281). HSP70 binding to the plasma membrane induces NF-κB activation and is linked to increased production of pro-inflammatory cytokines (282, 283). A gene set associated with NF-κB was also significantly increased in the unhealthy participants and may be associated with increased *HSPA1A* expression (Figure 6.5). Concurrently, a trend towards higher cytokine levels was observed in these participants in Chapter 5. Further, an *in vitro* study found that HSP70 was required for cigarette smoke extract IL-8 release from cultured bronchial epithelial cells (284). The same study found that lung tissue from COPD patients had increased levels of HSP70 which correlated to disease severity. The present study also identified increased expression of gene sets associated with IL-8 signalling through CXCR1 and CXCR2 receptors (Figure 6.6). IL-8 is a cytokine that primarily acts on neutrophils to induce activation and chemotaxis (285, 286). IL-8 levels are also known to be elevated in COPD patients (287). It is likely that HSP70 contributes to IL-8-mediated

neutrophil infiltration in the lungs in TS-COPD patients and a similar mechanism may be at play in people suffering from biomass-smoke-induced lung disease. However, as the present study focused on the peripheral blood instead of lung tissues, it is uncertain if this mechanism is at play in these participants.

HSP70 expression can also lead to anti-inflammatory effects. An *in vitro* study on macrophages found that HSP70 inhibited LPS-induced expression of *TNF-α* and *IL-1* through the inhibition of NF-κB signalling (288). Further anti-inflammatory mechanisms of HSP70 occur through its effects on Tregs. Tregs treated with HSP70 inhibited the proliferation of $CD4^+$ $CD25^-$ cells. These Tregs increased their secretion of the anti-inflammatory cytokines IL-10 and TGF-β (289). In this way, HSP70 may be able to reduce the functional capacity of T-cells. However, the results from Chapter 5 did not find a significant increase in either of these cytokines in the unhealthy participants.

Gene expression of *NR1H2* was increased in the unhealthy group (Table 6.1) and this also has relevance to T-cell function and regulation. This gene encodes the liver X receptor beta (LXRβ). There are two isoforms of LXRs, LXRα and LXRβ, both of which are involved in lipid and cholesterol metabolism and membrane lipid order. However, a mouse study identified that LXRα expression is limited to only a few cell types, including some immune cells, while LXRβ is expressed in most tissues (290). An *in vitro* study demonstrated that treatment of $CD4^+$ T-cells with an LXR agonist reduced the expression of IFN-γ, TNF-α, and IL-2 after PMA/Ionomycin stimulation, indicating a reduced function capacity (291). The previous chapter described the impaired functional responses to mitogen stimulation of T-cells isolated from participants in the unhealthy group. It is plausible that the reduced T-cell functional capacity in the unhealthy group is influenced by the increased *NR1H2* expression observed in these participants. There is also evidence that LXR activation has unique effects on T-reg cells. An LXR agonist was found to increase T-reg differentiation and suppressive capacity *in vitro* (292). Whether or not LXR-mediated T-reg suppression of inflammatory T-cells is partially responsible for the reduced T-cell functional capacity observed in the unhealthy participants is not clear. Cigarette smoke also appears to influence the effects of LXR activation in immune cells. LXR-treated, cigarette-exposed mice had increased neutrophil, IL-1α, CCL2, and G-CSF concentrations in their BAL than untreated cigarette-smoke-exposed mice (293). It is unclear if the increased expression levels of *NR1H2* are leading to increased activation of LXRβ receptors and subsequent immune dysregulation in these participants. Further *ex vivo* studies could help to clarify the role of these receptors in biomass-smoke-exposed individuals. Of note, the gene expression of *NR1H3* (LXRα) was not analysed in this study as it did not meet the filtering criteria.

Another notable finding was the increased expression of an IL-6/JAK/STAT3 gene set in the unhealthy participants (Figure 6.5). IL-6 is a pleiotropic cytokine that can bind to membrane-bound or soluble extracellular receptors. It is produced by many cell types including pulmonary artery smooth muscle cells, pulmonary artery endothelial cells, alveolar and bronchial epithelial cells, macrophages, and dendritic cells (294-296). Expression of membrane-bound IL-6 receptors is primarily limited to naïve T-cells and hepatocytes (297). IL-6 receptor activation in naïve T-cells can activate STAT3 transcription factors via JAK phosphorylation. This leads to the activation of RORγt transcription factors; the master regulator of Th17 cells. In COPD, Th17 are increased and out of balance with Tregs (see Chapter 2). *In vitro* studies noted that both IL-6 and TGF-β induced RORγt and HIF-1α expression in T-cells and the effect was dependent on STAT3 (298). IL-6 and HIF-1α can act in a positive feedback loop whereby IL-6 can aid in the stabilization and transcription of HIF-1α which leads to increased production of IL-6 (299). It has also been demonstrated that in certain conditions, HIF-1α stabilization leads to the degradation of FOXP3, the master regulator of Treg development (298). In accordance with this, multiple gene sets related to FOXP3 were depleted in the unhealthy participants (Figure 6.6). The modulation of these pathways in the peripheral blood could be due to recently activated T-cells transitioning to a Th17 phenotype and trafficking to lung tissues. These results indicate that the unhealthy participants may be experiencing a Th17:Treg imbalance similar to what is experienced by TS-COPD patients. Additional studies on direct lung samples could confirm this and help to better establish how lung disease in these participants compares to COPD patients from Western countries.

There were challenges in obtaining a deeper perspective of the roles of T-cells in lung disease pathology in these participants. This study was undertaken in a remote area of PNG where there are diverse biological and environmental exposures and no medical doctors. For this reason, some participants likely had immune profiles influenced by factors other than biomass-smoke exposure. This introduced variability, or 'noise,' into the data, making it harder to isolate the specific effects of biomass-smoke exposure. A stringent filtering protocol that only kept the most highly expressed genes was used in an attempt to account for this issue. However, this may have largely limited the results to only signals coming from the most abundant cell types in the samples. The most prominent cell type in the blood samples used for sequencing was neutrophils. Other cells such as T-cell subsets and NK cells only represented small fractions and therefore likely contributed a smaller portion of the total RNA transcripts in the sample. Due to the filtering protocol, the signals transcriptomic signals from the T-cells were likely reduced, limiting the potential findings. But regardless of this, the results of this analysis suggested that in participants with lung disease T-cells were reduced in number with changes across multiple signalling pathways and molecules that are

likely to significantly impact T-cell function. Further studies would need to be done to explore these specific defects.

There were also significant findings related to additional immune mechanisms. As mentioned previously, IL-6 also plays important roles in systemic inflammation including activation of the acute phase response and more specifically the complement cascade by interacting with membrane-bound IL-6 receptors on hepatocytes (300, 301). The results of the present study found significantly increased expression of a gene set encoding components of the complement system (Figure 6.5). The genes in the gene set primarily relate to initiating and regulating the complement system, mediating downstream inflammatory and immune responses, and facilitating tissue repair and remodelling following complement activation. However, as hepatocytes are not found in circulation, immune cells including tissue macrophages and circulating monocytes are a more likely source of this signal. It is well-known that complement proteins are produced by an array of different immune cell types yet the link to IL-6 in this context has not been established (302). However, given that IL-6 is also capable of inducing complement proteins in other non-hepatocytes, it may be responsible for the increased expression of the complement gene set in the unhealthy participants from this study (303).

We identified significant enrichment of multiple pathways associated with neutrophils and macrophages in the peripheral blood of the unhealthy participants. The expression of genes involved in neutrophil and macrophage trafficking was increased in the unhealthy participants (Table 6.1). *TLN1* (Talin-1) which is involved in tissue infiltration of both macrophages and neutrophils, was increased in the unhealthy participants (304, 305). Studies have shown that talin-1 plays a crucial role in the slow-rolling and arrest of neutrophils in microvasculature in response to CXCR2 or P-selectin (306). Talin-1. In addition, *ILK* (Integrin Linked Kinase), which is involved in cellular migration and adhesion, was significantly increased in the unhealthy participants (307). Interestingly, this study was able to identify increased expression of gene sets associated with neutrophils and macrophages in the unhealthy participants when our cellular profiling of these patients (Chapter 5) did not detect significant differences. It is likely that the cells present are more active and have increased transcription of genes so these results may be a better reflection of cell activity than concentration in the blood. It is also possible that the unhealthy participants have increased immune cell infiltration into their lungs but that the peripheral blood concentrations do not correlate well with the concentration in the lungs.

Gene sets relating to neutrophils were significantly increased in the unhealthy participants. Specifically, expression of gene sets in the Cell Type Signatures collection relating to immature, bone

marrow, and lung neutrophils was increased in the unhealthy participants (Figure 6.4). Additionally, there was increased expression of a gene set related to neutrophil degranulation (Figure 6.6). These are not surprising results as neutrophils are well established as the primary innate immune cell involved in COPD pathology. These results help to confirm that there are similar mechanisms at play in these participants. This study did not find evidence of eosinophilic inflammation in the unhealthy participants as has been described in BS-COPD patients from other studies (221, 222). Macrophages are also known to play a role in COPD (see Chapter 2). Accordingly, this analysis revealed increased expression of multiple gene sets associated with macrophage and monocyte activity including gene sets associated with lung and proliferating macrophages, as well as classical and non-classical monocytes.

Notably, expression of gene sets relating to hypoxia was increased in the unhealthy participants which is not surprising considering the nature of the disease (Figure 6.6). Previous studies have found that hypoxemia is a common feature of BS-COPD with some studies noting higher severity than in TS-COPD (217, 308). The participants of this study have probably experienced a degree of systemic hypoxia due to the amount of time spent breathing biomass-smoke-polluted air containing carbon monoxide (CO). However, it is not clear what the specific cellular source of these hypoxia signals is (309). Many of the effects of hypoxia are mediated by hypoxia-inducible factor 1α (HIF-1α, encoded by *HIF1A* gene) (310, 311). Hypoxic conditions do not control *HIF1A* transcription directly but HIF-1α is largely regulated post-transcriptionally whereby under normal oxygen conditions, it is degraded yet, under hypoxic conditions, HIF-1α is stabilised and initiates an array of intracellular changes partially through its action as a transcription factor (312, 313). *In vitro* experiments have demonstrated that HIF-1α mRNA does not increase in response to hypoxia (314). In agreement with this, we only saw a small, non-significant increase in *HIF1A* mRNA in the unhealthy group (see online: Gilstrom DGE Results.xlsx). HIF-1α can also be stabilized by many other pathways such as through cellular signalling (315, 316). Hypoxia triggers a cascade of alterations that can be unique to cell types, with neutrophils being particularly susceptible to its effects (317).

Hypoxic mechanisms may have also played a role in the increased expression of neutrophil-related gene sets. Previous research has revealed that hypoxia prolongs neutrophil survival and increases effector functions via the stabilization of HIF-1α (318). *Ex vivo* experiments on isolated human neutrophils have demonstrated that hypoxia increases degranulation through HIF-1α independent mechanisms (319). Furthermore, neutrophils incubated in hypoxic environments secreted increased amounts of elastase, MMP-8, MMP-9, myeloperoxidase, and lactoferrin (319, 320). It was also found that hypoxia-induced degranulation in neutrophils was dependent on activation of the PI3K and AKT signalling pathway (319). In line with this, this study identified the enrichment of a neutrophil

degranulation gene set in addition to a PI3K/AKT/mTOR-associated gene set in the unhealthy participants. It is plausible that hypoxia in these participants induces PI3K/AKT/mTOR signalling in neutrophils leading to increased neutrophil survival and degranulation. Neutrophils are the primary innate effector cells in COPD and contribute to the pathology by the release of proteases in the lungs causing tissue destruction. Inflammation-driven tissue destruction in the lungs can compromise blood vessels and alter the lungs' functional properties. This may result in localized hypoxia within the lungs and, further reduce oxygen levels in the body's systemic circulation. Neutrophils can further contribute to tissue hypoxia by consuming molecular oxygen for the generation of reactive oxygen species (ROS) which may further exacerbate hypoxia within the lungs of these individuals (321). Future studies on the role of hypoxia in the neutrophils of these participants could use proteomics approaches to identify more precisely which proteins and pathways are modulated in response to hypoxia. This method may elucidate how hypoxia affects the neutrophils in these individuals with distinct backgrounds and environmental exposures, and who have lung disease arising from a unique cause.

Overall, the results of this study clearly implicate neutrophils, macrophages, hypoxia, and T cell depletion and dysfunction as key pathways affected in these biomass-exposed communities. As described in Chapter 2, T-cells are crucial players in COPD pathology. This research identified altered expression of multiple genes and gene sets that indicate that dysfunctional T-cell responses in lung disease in these communities. Future studies could further explore the role of T-cells in biomass smoke-induced lung disease and how and why T-cells become dysfunctional in this situation. Additionally, many of the results pointed to increased roles of neutrophils in biomass smoke-induced lung disease in this community. There is transcriptional evidence of increased neutrophil trafficking and degranulation. The results revealed reduced transcription of genes associated with multiple T-cell subsets and phenotypes. It is unclear how these results reflect the immune environment in the lungs of these participants. Chronic recruitment of T-cells to the lungs may have reduced their numbers in the peripheral blood, or this may indicate immune dysfunction in the unhealthy participants. Further studies could compare T-cells in induced sputum or BAL from healthy and unhealthy participants to clarify this. This study also identified the potential role of hypoxia in these participants. Hypoxia is typically considered a symptom of COPD however, there is evidence that hypoxia may contribute to an active immune response and disease progression. Proteomic studies combined with functional studies using *ex vivo* immune cells may clarify the role of hypoxia. Future studies could also endeavour to include healthy, non-biomass smoke-exposed participants to better establish transcriptional and immune changes that occur due to biomass-smoke exposure and to

identify if the changes seen in lung disease sufferers are simply an increase of the response to biomass smoke exposure or if they are unique to lung disease.

This study begins to fill a gap in the knowledge of immune pathology of lung disease in rural biomass smoke-exposed communities. As detailed in Chapter 5, the community where the study was conducted has a significant need for diagnostics that do not require the presence of trained clinicians on site. Additionally, a deeper understanding of lung disease is essential to identify effective therapies for the unique pulmonary conditions prevalent in this under-studied population. Here we have identified mechanisms that may participate in lung disease in this biomass-smoke-exposed community and should be the basis of additional studies that may lead to improved diagnostics and treatment that can work within the infrastructure of remote communities.

Chapter 7: General Discussion

COPD is a serious global health problem with increasing mortality worldwide (322). It is a multifaceted disease caused by frequent exposure to inhaled irritants leading to chronic inflammation, obstructed airways, and progressive tissue damage in the lungs resulting in reduced pulmonary function. Clinical presentation of the disease is very heterogeneous with patients exhibiting different patterns of inflammation, rates of progression, and association with comorbidities. Unique aetiologies of COPD result in different clinical presentations. The two most predominant aetiologies are tobacco smoking and biomass smoke exposure which each have unique patterns of inflammation, and different associations with co-morbidities (10)7. TS-COPD, the most common aetiology in developed countries, is well-characterized and has been the subject of the majority of COPD research. BS-COPD on the other hand, is most common in LMICs due to the use of biomass fuel sources for cooking and heating. PNG has some of the highest rates of COPD in the world. In many of the remote communities, people rely on biomass to fuel their cooking fires as there is no access to efficient cooking technologies such as gas or electric stoves. Lung disease is common in these communities and creates a large unmet health burden. This aetiology and phenotype of COPD is poorly characterised and has been relatively neglected in research.

This thesis describes the immune responses in lung disease by first investigating T-cell phenotypes in TS-COPD patients to gain a deeper understanding of T-cell phenotypes. Next, studies were performed to begin unravelling the immune response to biomass smoke exposure and biomass smoke-induced lung disease in a remote community in PNG by investigating the differences in peripheral blood immune cell and cytokine concentrations. This provided broad insights into the immune status of people in this remote community. Finally, transcriptomics was used to identify more specific changes in the immune cells of these participants, which allowed for greater comparison with the first study on TS-COPD, and with previously published literature.

Underlying COPD is a dysregulated immune response that involves the excess recruitment of neutrophils and other immune cells into lung tissues. These neutrophils release destructive enzymes that degrade their surrounding tissues. Damaged lung tissues are repaired however, the properties and structure of the lung are altered resulting in reduced elasticity, and airway remodelling. T-cells have also been shown to play a major role in COPD pathology. Most notably, there is an imbalance of inflammatory and anti-inflammatory T-cell subsets (18, 44, 50, 67). Th17 cells are particularly increased in proportion to Tregs in COPD sufferers. This contributes to the perpetuation of inflammation in the lungs of COPD patients. However, T-cell subsets, and immune cells in general, are phenotypically diverse. T-cells are very plastic and can modify their expression and behaviours in

response to the immune environment in which they are present. The diverse clinical manifestations of COPD caused by unique aetiologies in different communities are likely matched by a corresponding diversity in immune responses, particularly in unique T-cell phenotypes.

This research characterised the immune characteristics related to these two aetiologies of COPD. The first part of the project investigated T-cell phenotypes in well-characterised COPD patients from an urban area of Australia. While previous studies in areas where TS-COPD is most common found altered ratios of T-cell subsets indicating a role of T-cells in COPD pathology, investigations of the specific T-cell phenotypes are incomplete. This study revealed that T-cell subsets from patients with exacerbating TS-COPD exhibited unique phenotypes when compared to HCs. In particular, there was a notable increase in the percentage of MAIT cells expressing exhaustion markers such as PD1, CTLA4, and TIM3, suggesting a state of immune fatigue in these cells. Furthermore, an array of exhaustion indicators was also detected in isolated $CD4^+$ and $CD8^+$ T-cell populations, further underlining the altered immune response in TS-COPD patients. This study highlighted the diverse phenotypes that T-cells can assume in different disease states and provided a basis for researching other aetiologies of COPD.

The next part of the project investigated the immune profiles that shape the response to biomass smoke and biomass smoke-induced lung disease. A better understanding of the immune response in BS-COPD is urgently needed due to the high mortality of COPD in areas where BS-COPD is prevalent. Biomass fuel burning commonly occurs in remote areas that have limited resources, infrastructure, and access to trained clinicians. It is therefore crucial to develop a better understanding of the disease that may lead to new therapies and diagnostics that can circumvent these limitations. Samples such as blood and sputum are easily obtained and may provide the opportunity to diagnose patients remotely by looking at immune markers without the need for highly trained on-site.

This portion of the project involved participants from a rural community in PNG where wood is burned as a cooking fuel and there was a high prevalence of respiratory illness. The study community is located in a remote area of PNG without access to trained physicians or Western-style medical facilities. The first study of this project performed in this community investigated the immune profiles of participants who were chronically exposed to biomass smoke but had no evidence of lung disease (healthy participants). The results indicated that peripheral blood immune cell composition and cytokine concentrations of healthy individuals were substantially different from what is expected in people from Western countries. The concentration of cytokines in the peripheral blood was consistently elevated. There were also trends toward lower T-cell and monocyte concentrations and higher NKT cells. This provided evidence that biomass smoke exposure alters

immune function even in people who do not have signs of respiratory illness. This study also established baseline parameters of what is normal that could be applied to further research. Next, with these baseline immune parameters established, the immune profiles of participants who had symptoms of lung disease were investigated and compared. Peripheral blood cell counts were not significantly different in the participants with evidence of lung disease (unhealthy participants). However, there was a trend towards lower T-cell counts including cytotoxic, helper, natural killer, and total T-cells. Concurrently, innate cells including neutrophils, eosinophils, and monocytes trended higher in these participants. A comparison of plasma cytokine concentrations indicated that there was a significant increase of Th-17-related cytokines in the unhealthy participants. These results may be due to the trafficking of T-cells out of the bloodstream and into the lung tissues where they mount an immune response and release inflammatory cytokines that return to circulation. Additionally, this study tested the ability of the T-cells to respond to stimuli to identify potential immune dysfunction. It was determined that peripheral blood cells from the unhealthy participants were less able to release cytokines in response to stimulation than the cells from healthy participants. This result was particularly pronounced for the Th17-related cytokines IL-17A, IL-17F, and IL-22 however, IL-6, IL-9, IL-13, IL-10, and IFN-γ responses were also significantly reduced. This reveals that the immune cells in the unhealthy participants have reduced functional capacity which may contribute to the disease pathology and likely increases susceptibility to infections. This is similar to the discovery of exhaustion markers in the Western cohort. However, we were not able to quantify the cell counts or cytokine concentrations in the Western cohort and only looked at the cell phenotypes.

The final study in this project employed transcriptomic techniques to dive deeper into the immune mechanisms at play in the unhealthy participants and to allow for a more detailed comparison with TS-COPD in Western countries. The results identified differential expression of a few genes that are involved in T-cell function including HSPA1A, NR1H2, LY9, ITK, IL7R, and CD96 (Table 6.1). Additionally, GSEA highlighted many pathways that were enriched in the unhealthy participants compared to the healthy participants. These gene sets revealed further evidence of dysregulated T-cell responses. The GSEA results also identified evidence of neutrophil and macrophage involvement in biomass smoke-induced lung disease which is evidence for overlapping mechanisms with TS-COPD. Notably, this study also identified the potential role of hypoxia in the pathology of lung disease in the participants. These results better clarified the findings from previous studies on the PNG cohort.

A notable contrast was observed in the response patterns between the TS-COPD patients from the Australian cohort and the biomass-smoke-exposed individuals from PNG. Specifically, markers such

as *CD96* and *IL7R*, which showed increased levels in T-cells of TS-COPD patients, exhibited decreased expression in the peripheral blood of unhealthy biomass-smoke-exposed participants when compared to their healthy counterparts in PNG. Moreover, while the expression of *NFKB1*, *TGFB1*, *IFNG*, and *STAT3* was reduced in T-cells of TS-COPD patients, the expression of gene sets associated with these markers was increased in unhealthy participants from the PNG cohort. This inverse modulation of responses highlights the complex and diverse effects of different types of smoke exposure on the immune system. This provides evidence that biomass smoke-induced lung disease in this remote community from PNG is underpinned by a unique immune response compared to the patients from the Australian cohort. Interestingly, the results also pointed towards a multifaceted immune response to hypoxia in the unhealthy participants. The roles of hypoxia on the immune response in COPD have not been extensively researched. However, hypoxia has a broad influence on inflammatory pathways many of which there was evidence of in the results. In the context of TS-COPD, hypoxia is viewed as a consequence of COPD due to the lungs' reduced ability to oxygenate the body. Yet, in BS-COPD where long exposure to carbon monoxide-containing smoke is common, hypoxia may act as a co-driver of immune responses that lead to the development of lung disease.

This research project serves as a preliminary study in the quest to better understand immune responses to one of the deadliest diseases the world currently faces. Further research is needed to better understand how these results relate to COPD globally and if the markers and pathways identified could be useful for creating new diagnostics or therapies for people suffering from COPD. Future research in TS-COPD patients should focus on better stratification of phenotypes that may lead to the development of personalized medicine. Studies on BS-COPD should also identify further sub-phenotypes and their relation to different biomass fuel sources, diets, and other cultural practices that may affect disease pathology. Investigation of hypoxic mechanisms in BS-COPD may lead to the development of diagnostic markers or therapeutic targets. These studies would benefit from using proteomic approaches to capture the post-translational changes of hypoxia-related proteins. Future studies should thoroughly investigate samples directly sourced from the lung, such as sputum, to better understand the immune environment in the lungs and how it correlates with the peripheral blood. These studies may produce insights that lead to developments that will alleviate vast amounts of human suffering.

Summary of Experimental Data:

Chapter 3:

- CD4+ and CD8+ T-cells are phenotypically distinct in AECOPD patients displaying an early activation profile and reduced expression of T-cell related transcription factors compared to healthy controls.

- MAIT cell numbers were reduced in AECOPD patients, and a greater proportion expressed a exhausted phenotype compared to healthy controls.

Chapter 4:

- Baseline values of the concentrations of immune cells and cytokines in the blood were established in healthy individuals from a remote biomass-exposed area of Papua New Guinea. Many These values were markedly different from what is expected for healthy people in Western countries. This established a reference for studying disease in this population.

Chapter 5:

- Participants with evidence of lung disease (unhealthy) had signs of increase Th-17 driven inflammation compared healthy biomass smoke exposed participants.
- Peripheral blood immune cells from unhealthy participants had significantly reduced response to mitogen stimulation indicating functional impairment.
- Sputum samples from the unhealthy participants had a high proportion of eosinophils indicating possible involvement of type-2 inflammation in the lungs.

Chapter 6:

- Transcriptomics analysis identified reduced expression of genes related to the development and function of T-cells in the peripheral blood of the unhealthy participants compared to the healthy participants.
- Gene set enrichment analysis found reduction of gene sets related to CD4, CD8, and NKT cells in the blood of the unhealthy group which may indicate a reduction in the frequency or activity of these cells.
- Gene sets relating to specific molecular pathways related to T-cell function were modulated in the unhealthy participants indicating that T-cell activity is altered in these participants.

References

1. Safiri S, Carson-Chahhoud K, Noori M, Nejadghaderi SA, Sullman MJ, Heris JA, et al. Burden of chronic obstructive pulmonary disease and its attributable risk factors in 204 countries and territories, 1990-2019: results from the Global Burden of Disease Study 2019. bmj. 2022;378.
2. Rutgers SR, Postma DS, ten Hacken NH, Kauffman HF, van der Mark TW, Koëter GH, et al. Ongoing airway inflammation in patients with COPD who do not currently smoke. Thorax. 2000;55(1):12-8.
3. Tan W, Sin D, Bourbeau J, Hernandez P, Chapman K, Cowie R, et al. Characteristics of COPD in never-smokers and ever-smokers in the general population: results from the CanCOLD study. Thorax. 2015;70(9):822-9.
4. Chronic obstructive pulmonary disease (COPD): World Health Organization; 2022 [Available from: https://www.who.int/en/news-room/fact-sheets/detail/chronic-obstructive-pulmonary-disease-(copd).
5. Health AIo, Welfare. Chronic obstructive pulmonary disease. Canberra: AIHW; 2024.
6. Global Burden of Disease Study 2019 (GBD 2019) Reference Life Table: Institute for Health Metrics and Evaluation (IHME); 2021 [Available from: https://vizhub.healthdata.org/gbd-compare/.
7. Osei AD, Mirbolouk M, Orimoloye OA, Dzaye O, Uddin SI, Benjamin EJ, et al. Association between e-cigarette use and chronic obstructive pulmonary disease by smoking status: behavioral risk factor surveillance system 2016 and 2017. American journal of preventive medicine. 2020;58(3):336-42.
8. Yang IA, Jenkins CR, Salvi SS. Chronic obstructive pulmonary disease in never-smokers: risk factors, pathogenesis, and implications for prevention and treatment. Lancet Respir Med. 2022.
9. Household air pollution and health: World Health Organization; 2021 [cited 2022 April 1]. Available from: https://www.who.int/news-room/fact-sheets/detail/household-air-pollution-and-health.
10. Jindal S, Jindal A. COPD in Biomass exposed nonsmokers: a different phenotype. Expert review of respiratory medicine. 2021;15(1):51-8.
11. Barnes PJ. Inflammatory endotypes in COPD. Allergy: European Journal of Allergy and Clinical Immunology. 2019.
12. Mittrücker H-W, Visekruna A, Huber M. Heterogeneity in the differentiation and function of CD8+ T cells. Archivum immunologiae et therapiae experimentalis. 2014;62:449-58.
13. Zhu J, Paul WE. CD4 T cells: fates, functions, and faults. Blood, The Journal of the American Society of Hematology. 2008;112(5):1557-69.
14. Shapouri-Moghaddam A, Mohammadian S, Vazini H, Taghadosi M, Esmaeili SA, Mardani F, et al. Macrophage plasticity, polarization, and function in health and disease. J Cell Physiol. 2018;233(9):6425-40.
15. Walker JA, McKenzie AN. TH2 cell development and function. Nat Rev Immunol. 2018;18(2):121-33.
16. Korn T, Bettelli E, Oukka M, Kuchroo VK. IL-17 and Th17 Cells. Annual review of immunology. 2009;27:485-517.
17. Vignali DA, Collison LW, Workman CJ. How regulatory T cells work. Nat Rev Immunol. 2008;8(7):523-32.

18. Chen L, Chen G, Zhang MQ, Xiong XZ, Liu HJ, Xin JB, et al. Imbalance between subsets of CD8(+) peripheral blood T cells in patients with chronic obstructive pulmonary disease. PeerJ. 2016;4(2).
19. Zhang N, Bevan MJ. CD8+ T cells: foot soldiers of the immune system. Immunity. 2011;35(2):161-8.
20. Radicioni G, Ceppe A, Ford AA, Alexis NE, Barr RG, Bleecker ER, et al. Airway mucin MUC5AC and MUC5B concentrations and the initiation and progression of chronic obstructive pulmonary disease: An analysis of the SPIROMICS cohort. Lancet Respir Med. 2021;9(11):1241-54.
21. Higham A, Bostock D, Booth G, Dungwa JV, Singh D. The effect of electronic cigarette and tobacco smoke exposure on COPD bronchial epithelial cell inflammatory responses. International journal of chronic obstructive pulmonary disease. 2018;13:989.
22. Gohy S, Carlier FM, Fregimilicka C, Detry B, Lecocq M, Ladjemi MZ, et al. Altered generation of ciliated cells in chronic obstructive pulmonary disease. Scientific reports. 2019;9(1):1-12.
23. Hao W, Li M, Zhang Y, Zhang C, Xue Y. Expressions of MMP-12, TIMP-4, and neutrophil elastase in PBMCs and exhaled breath condensate in patients with COPD and their relationships with disease severity and acute exacerbations. Journal of Immunology Research. 2019;2019.
24. Shibata S, Miyake K, Tateishi T, Yoshikawa S, Yamanishi Y, Miyazaki Y, et al. Basophils trigger emphysema development in a murine model of COPD through IL-4-mediated generation of MMP-12-producing macrophages. Proceedings of the National Academy of Sciences of the United States of America. 2018;115(51):13057-62.
25. Eurlings IM, Dentener MA, Cleutjens JP, Peutz CJ, Rohde GG, Wouters EF, et al. Similar matrix alterations in alveolar and small airway walls of COPD patients. BMC pulmonary medicine. 2014;14(1):1-11.
26. Singh D, Kolsum U, Brightling CE, Locantore N, Agusti A, Tal-Singer R. Eosinophilic inflammation in COPD: prevalence and clinical characteristics. Eur Respir J. 2014;44(6):1697-700.
27. Cosio BG, Dacal D, Perez de Llano L. Asthma-COPD overlap: identification and optimal treatment. Therapeutic advances in respiratory disease. 2018;12:1753466618805662.
28. Solleiro-Villavicencio H, Quintana-Carrillo R, Falfan-Valencia R, Vargas-Rojas MI. Chronic obstructive pulmonary disease induced by exposure to biomass smoke is associated with a Th2 cytokine production profile. Clinical immunology (Orlando, Fla). 2015;161(2):150-5.
29. Nakamura M, Nakamura H, Minematsu N, Chubachi S, Miyazaki M, Yoshida S, et al. Plasma cytokine profiles related to smoking-sensitivity and phenotypes of chronic obstructive pulmonary disease. Biomarkers. 2014;19(5):368-77.
30. Gao J, Chen B, Wu S, Wu F. Blood cell for the differentiation of airway inflammatory phenotypes in COPD exacerbations. BMC pulmonary medicine. 2020;20(1):1-9.
31. Kandemir Y, Doğan NÖ, Yaka E, Pekdemir M, Yılmaz S. Clinical characteristics of neutrophilic, eosinophilic and mixed-type exacerbation phenotypes of COPD. The American Journal of Emergency Medicine. 2021;45:237-41.
32. Beech AS, Lea S, Kolsum U, Wang Z, Miller BE, Donaldson GC, et al. Bacteria and sputum inflammatory cell counts; a COPD cohort analysis. Respiratory research. 2020;21(1):1-13.

33. Sze MA, Dimitriu PA, Suzuki M, McDonough JE, Campbell JD, Brothers JF, et al. Host Response to the Lung Microbiome in Chronic Obstructive Pulmonary Disease. American journal of respiratory and critical care medicine. 2015;192(4):438-45.
34. Chi X, Jin W, Zhao X, Xie T, Shao J, Bai X, et al. RORγt expression in mature TH17 cells safeguards their lineage specification by inhibiting conversion to TH2 cells. Science Advances. 2022;8(34):eabn7774.
35. Eustace A, Smyth LJ, Mitchell L, Williamson K, Plumb J, Singh D. Identification of cells expressing IL-17A and IL-17F in the lungs of patients with COPD. Chest. 2011;139(5):1089-100.
36. Montalbano AM, Riccobono L, Siena L, Chiappara G, Di Sano C, Anzalone G, et al. Cigarette smoke affects IL-17A, IL-17F and IL-17 receptor expression in the lung tissue: Ex vivo and in vitro studies. Cytokine. 2015;76(2):391-402.
37. Lee K-H, Lee C-H, Woo J, Jeong J, Jang A-H, Yoo C-G. Cigarette smoke extract enhances IL-17A-induced IL-8 production via up-regulation of IL-17R in human bronchial epithelial cells. Molecules and Cells. 2018;41(4):282.
38. Chen K, Pociask DA, McAleer JP, Chan YR, Alcorn JF, Kreindler JL, et al. IL-17RA is required for CCL2 expression, macrophage recruitment, and emphysema in response to cigarette smoke. PloS one. 2011;6(5):e20333.
39. Essilfie A-T, Simpson JL, Horvat JC, Preston JA, Dunkley ML, Foster PS, et al. Haemophilus influenzae infection drives IL-17-mediated neutrophilic allergic airways disease. PLoS pathogens. 2011;7(10):e1002244.
40. Fahy JV, Dickey BF. Airway mucus function and dysfunction. New Engl J Med. 2010;363(23):2233-47.
41. Keatings VM, Barnes PJ. Granulocyte activation markers in induced sputum: comparison between chronic obstructive pulmonary disease, asthma, and normal subjects. American journal of respiratory and critical care medicine. 1997;155(2):449-53.
42. Li XN, Pan X, Qiu D. Imbalances of Th17 and Treg cells and their respective cytokines in COPD patients by disease stage. Int J Clin Exp Med. 2014;7(12):5324-9.
43. Profita M, Albano GD, Riccobono L, Di Sano C, Montalbano AM, Gagliardo R, et al. Increased levels of Th17 cells are associated with non-neuronal acetylcholine in COPD patients. Immunobiology. 2014;219(5):392-401.
44. Li H, Liu Q, Jiang Y, Zhang Y, Zhang Y, Xiao W. Disruption of th17/treg balance in the sputum of patients with chronic obstructive pulmonary disease. Am J Med Sci. 2015;349(5):392-7.
45. Zhang JC, Chen G, Chen L, Meng ZJ, Xiong XZ, Liu HJ, et al. TGF-β/BAMBI pathway dysfunction contributes to peripheral Th17/Treg imbalance in chronic obstructive pulmonary disease. Scientific reports. 2016;6.
46. Duan MC, Zhang JQ, Liang Y, Liu GN, Xiao J, Tang HJ, et al. Infiltration of IL-17-Producing T Cells and Treg Cells in a Mouse Model of Smoke-Induced Emphysema. Inflammation. 2016;39(4):1334-44.
47. Roos AB, Sethi S, Nikota J, Wrona CT, Dorrington MG, Sanden C, et al. IL-17A and the Promotion of Neutrophilia in Acute Exacerbation of Chronic Obstructive Pulmonary Disease. American journal of respiratory and critical care medicine. 2015;192(4):428-37.
48. Lai T, Tian B, Cao C, Hu Y, Zhou J, Wang Y, et al. HDAC2 Suppresses IL17A-Mediated Airway Remodeling in Human and Experimental Modeling of COPD. Chest. 2018;153(4):863-75.

49. Ito JT, Cervilha DAD, Lourenco JD, Goncalves NG, Volpini RA, Caldini EG, et al. Th17/Treg imbalance in COPD progression: A temporal analysis using a CS-induced model. PloS one. 2019;14(1):e0209351.
50. Wang H, Ying H, Wang S, Gu X, Weng Y, Peng W, et al. Imbalance of peripheral blood Th17 and Treg responses in patients with chronic obstructive pulmonary disease. The clinical respiratory journal. 2015;9(3):330-41.
51. Sun SW, Chen L, Zhou M, Wu JH, Meng ZJ, Han HL, et al. BAMBI regulates macrophages inducing the differentiation of Treg through the TGF-β pathway in chronic obstructive pulmonary disease. Respiratory research. 2019;20(1):26.
52. Di Stefano A, Sangiorgi C, Gnemmi I, Casolari P, Brun P, Ricciardolo FL, et al. TGF-β signaling pathways in different compartments of the lower airways of patients with stable COPD. Chest. 2018;153(4):851-62.
53. Schiavinato JLdS, Haddad R, Saldanha-Araujo F, Baiochi J, Araujo AG, Santos Scheucher P, et al. TGF-beta/atRA-induced Tregs express a selected set of microRNAs involved in the repression of transcripts related to Th17 differentiation. Scientific reports. 2017;7(1):1-17.
54. Hasan M, Neumann B, Haupeltshofer S, Stahlke S, Claudio Fantini M, Angstwurm K, et al. Activation of TGF-β-induced non-Smad signaling pathways during Th17 differentiation. Immunology and cell biology. 2015;93(7):662-72.
55. Eapen MS, Hansbro PM, McAlinden K, Kim RY, Ward C, Hackett T-L, et al. Abnormal M1/M2 macrophage phenotype profiles in the small airway wall and lumen in smokers and chronic obstructive pulmonary disease (COPD). Scientific reports. 2017;7(1):13392-12.
56. He S, Sun S, Lu J, Chen L, Mei X, Li L, et al. The effects of the miR-21/SMAD7/TGF-β pathway on Th17 cell differentiation in COPD. Scientific reports. 2021;11(1):1-11.
57. Peñaloza HF, van der Geest R, Ybe JA, Standiford TJ, Lee JS. Interleukin-36 Cytokines in Infectious and Non-Infectious Lung Diseases. Frontiers in immunology. 2021;12:754702-.
58. Li W, Meng X, Hao Y, Chen M, Jia Y, Gao P. Elevated sputum IL-36 levels are associated with neutrophil-related inflammation in COPD patients. The clinical respiratory journal. 2021;15(6):648-56.
59. Pu J, Xu J, Chen L, Zhou H, Cao W, Hao B, et al. Exposure to biomass smoke induces pulmonary Th17 cell differentiation by activating TLR2 on dendritic cells in a COPD rat model. Toxicology Letters. 2021;348:28-39.
60. Vigne S, Palmer G, Lamacchia C, Martin P, Talabot-Ayer D, Rodriguez E, et al. IL-36R ligands are potent regulators of dendritic and T cells. Blood, The Journal of the American Society of Hematology. 2011;118(22):5813-23.
61. Chi H-H, Hua K-F, Lin Y-C, Chu C-L, Hsieh C-Y, Hsu Y-J, et al. IL-36 signaling facilitates activation of the NLRP3 inflammasome and IL-23/IL-17 axis in renal inflammation and fibrosis. Journal of the American Society of Nephrology. 2017;28(7):2022-37.
62. Wu JH, Zhou M, Jin Y, Meng ZJ, Xiong XZ, Sun SW, et al. Generation and Immune Regulation of CD4(+)CD25(-)Foxp3(+) T Cells in Chronic Obstructive Pulmonary Disease. Frontiers in immunology. 2019;10:220.
63. Meng Z-J, Wu J-H, Zhou M, Sun S-W, Miao S-Y, Han H-L, et al. Peripheral blood CD4+ T cell populations by CD25 and Foxp3 expression as a potential biomarker: reflecting inflammatory activity in chronic obstructive pulmonary disease. International journal of chronic obstructive pulmonary disease. 2019;14:1669.

64. Eriksson Ström J, Pourazar J, Linder R, Blomberg A, Lindberg A, Bucht A, et al. Airway regulatory T cells are decreased in COPD with a rapid decline in lung function. Respiratory research. 2020;21(1):1-9.
65. Zielinski CE, Mele F, Aschenbrenner D, Jarrossay D, Ronchi F, Gattorno M, et al. Pathogen-induced human TH17 cells produce IFN-γ or IL-10 and are regulated by IL-1β. Nature. 2012;484:514.
66. Sonnenberg GF, Nair MG, Kirn TJ, Zaph C, Fouser LA, Artis D. Pathological versus protective functions of IL-22 in airway inflammation are regulated by IL-17A. Journal of Experimental Medicine. 2010;207(6):1293-305.
67. Wei B, Sheng Li C. Changes in Th1/Th2-producing cytokines during acute exacerbation chronic obstructive pulmonary disease. The Journal of international medical research. 2018;46(9):3890-902.
68. Schild K, Knobloch J, Yakin Y, Jungck D, Urban K, Müller K, et al. IL-5 release of CD4+ non-effector lymphocytes is increased in COPD—modulating effects of moxifloxacin and dexamethasone. International immunopharmacology. 2011;11(4):444-8.
69. Sun J, Liu T, Yan Y, Huo K, Zhang W, Liu H, et al. The role of Th1/Th2 cytokines played in regulation of specific CD4 (+) Th1 cell conversion and activation during inflammatory reaction of chronic obstructive pulmonary disease. Scandinavian journal of immunology. 2018;88(1):e12674.
70. Zhou J-S, Li Z-Y, Xu X-C, Zhao Y, Wang Y, Chen H-P, et al. Cigarette smoke-initiated autoimmunity facilitates sensitisation to elastin-induced COPD-like pathologies in mice. Eur Respir J. 2020;56(3).
71. Tang S, Ma T, Zhang H, Zhang J, Zhong X, Tan C, et al. Erythromycin Prevents Elastin Peptide-Induced Emphysema and Modulates CD4+ T Cell Responses in Mice. International journal of chronic obstructive pulmonary disease. 2019;14:2697.
72. Lemaire F, Audonnet S, Perotin J-M, Gaudry P, Dury S, Ancel J, et al. The elastin peptide VGVAPG increases CD4+ T-cell IL-4 production in patients with chronic obstructive pulmonary disease. Respiratory research. 2021;22(1):1-11.
73. Jiang M, Liu H, Li Z, Wang J, Zhang F, Cao K, et al. ILC2s Induce Adaptive Th2-Type Immunity in Acute Exacerbation of Chronic Obstructive Pulmonary Disease. Mediators of inflammation. 2019;2019:1-12.
74. Pelly V, Kannan Y, Coomes S, Entwistle L, Rückerl D, Seddon B, et al. IL-4-producing ILC2s are required for the differentiation of TH2 cells following Heligmosomoides polygyrus infection. Mucosal immunology. 2016;9(6):1407-17.
75. Hodge G, Jersmann H, Tran HB, Asare PF, Jayapal M, Reynolds PN, et al. COPD is associated with increased pro-inflammatory CD28null CD8 T and NKT-like cells in the small airways. Clin Exp Immunol. 2022;207(3):351-9.
76. Sales DS, Ito JT, Zanchetta IA, Annoni R, Aun MV, Ferraz LFS, et al. Regulatory T-Cell Distribution within Lung Compartments in COPD. Copd. 2017;14(5):533-42.
77. Chen G, Zhou M, Chen L, Meng ZJ, Xiong XZ, Liu HJ, et al. Cigarette Smoke Disturbs the Survival of CD8(+) Tc/Tregs Partially through Muscarinic Receptors-Dependent Mechanisms in Chronic Obstructive Pulmonary Disease. PloS one. 2016;11(1):e0147232.
78. Kubysheva N, Postnikova L, Soodaeva S, Novikov V, Eliseeva T, Batyrshin I, et al. Relationship of the Content of Systemic and Endobronchial Soluble Molecules of CD25, CD38, CD8, and HLA-I-CD8 and Lung Function Parameters in COPD Patients. Disease markers. 2017;2017:8216723.

79. Hodge G, Mukaro V, Reynolds P, Hodge S. Role of increased CD8/CD28null T cells and alternative co-stimulatory molecules in chronic obstructive pulmonary disease. Clinical & Experimental Immunology. 2011;166(1):94-102.
80. Kalathil SG, Lugade AA, Pradhan V, Miller A, Parameswaran GI, Sethi S, et al. T-regulatory cells and programmed death 1+ T cells contribute to effector T-cell dysfunction in patients with chronic obstructive pulmonary disease. American journal of respiratory and critical care medicine. 2014;190(1):40-50.
81. Biton J, Ouakrim H, Dechartres A, Alifano M, Mansuet-Lupo A, Si H, et al. Impaired Tumor-Infiltrating T Cells in Patients with Chronic Obstructive Pulmonary Disease Impact Lung Cancer Response to PD-1 Blockade. American journal of respiratory and critical care medicine. 2018;198(7):928-40.
82. McKendry RT, Spalluto CM, Burke H, Nicholas B, Cellura D, Al-Shamkhani A, et al. Dysregulation of Antiviral Function of CD8(+) T Cells in the Chronic Obstructive Pulmonary Disease Lung. Role of the PD-1-PD-L1 Axis. American journal of respiratory and critical care medicine. 2016;193(6):642-51.
83. Ritzmann F, Borchardt K, Vella G, Chitirala P, Angenendt A, Herr C, et al. Blockade of PD-1 decreases neutrophilic inflammation and lung damage in experimental COPD. American Journal of Physiology-Lung Cellular and Molecular Physiology. 2021;320(5):L958-L68.
84. Kamphorst AO, Wieland A, Nasti T, Yang S, Zhang R, Barber DL, et al. Rescue of exhausted CD8 T cells by PD-1–targeted therapies is CD28-dependent. Science. 2017;355(6332):1423-7.
85. Qiu SL, Kuang LJ, Tang QY, Duan MC, Bai J, He ZY, et al. Enhanced activation of circulating plasmacytoid dendritic cells in patients with Chronic Obstructive Pulmonary Disease and experimental smoking-induced emphysema. Clinical immunology (Orlando, Fla). 2018;195:107-18.
86. Gianello V, Salvi V, Parola C, Moretto N, Facchinetti F, Civelli M, et al. The PDE4 inhibitor CHF6001 modulates pro-inflammatory cytokines, chemokines and Th1-and Th17-polarizing cytokines in human dendritic cells. Biochem Pharmacol. 2019;163:371-80.
87. Gupta V, Banyard A, Mullan A, Sriskantharajah S, Southworth T, Singh D. Characterization of the inflammatory response to inhaled lipopolysaccharide in mild to moderate chronic obstructive pulmonary disease. Br J Clin Pharmacol. 2015;79(5):767-76.
88. Tang Y, Li X, Wang M, Zou Q, Zhao S, Sun B, et al. Increased numbers of NK cells, NKT-like cells, and NK inhibitory receptors in peripheral blood of patients with chronic obstructive pulmonary disease. Clinical and Developmental Immunology. 2013;2013.
89. Wang J, Urbanowicz RA, Tighe PJ, Todd I, Corne JM, Fairclough LC. Differential activation of killer cells in the circulation and the lung: a study of current smoking status and chronic obstructive pulmonary disease (COPD). PloS one. 2013;8(3):e58556.
90. Eriksson Ström J, Pourazar J, Linder R, Blomberg A, Lindberg A, Bucht A, et al. Cytotoxic lymphocytes in COPD airways: Increased NK cells associated with disease, iNKT and NKT-like cells with current smoking. Respiratory research. 2018;19(1).
91. Szabó M, Sárosi V, Balikó Z, Bodó K, Farkas N, Berki T, et al. Deficiency of innate-like T lymphocytes in chronic obstructive pulmonary disease. Respiratory research. 2017;18(1):197.
92. Tsao CC, Tsao PN, Chen YG, Chuang YH. Repeated Activation of Lung Invariant NKT Cells Results in Chronic Obstructive Pulmonary Disease-Like Symptoms. PloS one. 2016;11(1):e0147710.

93. Kim EY, Battaile JT, Patel AC, You Y, Agapov E, Grayson MH, et al. Persistent activation of an innate immune response translates respiratory viral infection into chronic lung disease. Nature Medicine. 2008;14:633.
94. Crosby CM, Kronenberg M. Tissue-specific functions of invariant natural killer T cells. Nat Rev Immunol. 2018;18(9):559-74.
95. Kwon YS, Jin HM, Cho YN, Kim MJ, Kang JH, Jung HJ, et al. Mucosal-Associated Invariant T Cell Deficiency in Chronic Obstructive Pulmonary Disease. Copd. 2016;13(2):196-202.
96. Qiu W, Kang N, Wu Y, Cai Y, Xiao L, Ge H, et al. Mucosal Associated Invariant T Cells Were Activated and Polarized Toward Th17 in Chronic Obstructive Pulmonary Disease. Frontiers in immunology. 2021;12:640455.
97. Hinks TS, Wallington JC, Williams AP, Djukanovic R, Staples KJ, Wilkinson TM. Steroid-induced Deficiency of Mucosal-associated Invariant T Cells in the Chronic Obstructive Pulmonary Disease Lung. Implications for Nontypeable Haemophilus influenzae Infection. American journal of respiratory and critical care medicine. 2016;194(10):1208-18.
98. Beckett EL, Stevens RL, Jarnicki AG, Kim RY, Hanish I, Hansbro NG, et al. A new short-term mouse model of chronic obstructive pulmonary disease identifies a role for mast cell tryptase in pathogenesis. J Allergy Clin Immunol. 2013;131(3):752-62. e7.
99. Metzger RJ, Klein OD, Martin GR, Krasnow MA. The branching programme of mouse lung development. Nature. 2008;453(7196):745-50.
100. Basil MC, Cardenas-Diaz FL, Kathiriya JJ, Morley MP, Carl J, Brumwell AN, et al. Human distal airways contain a multipotent secretory cell that can regenerate alveoli. Nature. 2022;604(7904):120-6.
101. Rahman I, De Cunto G, Sundar IK, Lungarella G. Vulnerability and genetic susceptibility to cigarette smoke–induced emphysema in mice. American Thoracic Society; 2017. p. 270-1.
102. Lokke A, Lange P, Scharling H, Fabricius P, Vestbo J. Developing COPD: a 25 year follow up study of the general population. Thorax. 2006;61(11):935-9.
103. Polverino F, Doyle-Eisele M, McDonald J, Wilder JA, Royer C, Laucho-Contreras M, et al. A novel nonhuman primate model of cigarette smoke–induced airway disease. The American Journal of Pathology. 2015;185(3):741-55.
104. Lange P, Celli B, Agustí A, Boje Jensen G, Divo M, Faner R, et al. Lung-function trajectories leading to chronic obstructive pulmonary disease. New Engl J Med. 2015;373(2):111-22.
105. Celli BR, Anderson JA, Brook RD, Calverley PM, Cowans NJ, Crim C, et al. Regional differences in rate of FEV1 decline in COPD: lessons from SUMMIT. Eur Respir J. 2019;53(6):1900278.
106. Barnes PJFRSF. Inflammatory mechanisms in patients with chronic obstructive pulmonary disease. Journal of Allergy and Clinical Immunology, The. 2016;138(1):16-27.
107. Jemal A, Ward E, Hao Y, Thun M. Trends in the leading causes of death in the United States, 1970-2002. Jama. 2005;294(10):1255-9.
108. Salvi SS, Barnes PJ. Chronic obstructive pulmonary disease in non-smokers. Lancet. 2009;374(9691):733-43.
109. Mittal R, Chhabra SK. GOLD classification of COPD: discordance in criteria for symptoms and exacerbation risk assessment. COPD J Chronic Obstructive Pulm Dis. 2017;14(1):1-6.

110. Cervilha DAB, Ito JT, Lourenco JD, Olivo CR, Saraiva-Romanholo BM, Volpini RA, et al. The Th17/Treg Cytokine Imbalance in Chronic Obstructive Pulmonary Disease Exacerbation in an Animal Model of Cigarette Smoke Exposure and Lipopolysaccharide Challenge Association. Scientific reports. 2019;9(1):1921.
111. Freeman CM, McCubbrey AL, Crudgington S, Nelson J, Martinez FJ, Han MK, et al. Basal gene expression by lung CD4+ T cells in chronic obstructive pulmonary disease identifies independent molecular correlates of airflow obstruction and emphysema extent. PloS one. 2014;9(5):e96421.
112. Klonowski KD, Williams KJ, Marzo AL, Blair DA, Lingenheld EG, Lefrançois L. Dynamics of blood-borne CD8 memory T cell migration in vivo. Immunity. 2004;20(5):551-62.
113. Obeidat M, Nie Y, Chen V, Shannon CP, Andiappan AK, Lee B, et al. Network-based analysis reveals novel gene signatures in peripheral blood of patients with chronic obstructive pulmonary disease. Respiratory research. 2017;18(1):72.
114. Pincikova T, Parrot T, Hjelte L, Högman M, Lisspers K, Ställberg B, et al. MAIT cell counts are associated with the risk of hospitalization in COPD. Respiratory research. 2022;23(1):127.
115. Huber ME, Larson E, Lust TN, Heisler CM, Harriff MJ. Chronic obstructive pulmonary disease and cigarette smoke exposure lead to dysregulated MAIT cell activation by bronchial epithelial cells. bioRxiv. 2022:2022.02. 28.482383.
116. Tsoumakidou M, Tzanakis N, Chrysofakis G, Kyriakou D, Siafakas NM. Changes in sputum T-lymphocyte subpopulations at the onset of severe exacerbations of chronic obstructive pulmonary disease. Respir Med. 2005;99(5):572-9.
117. Tan DBA, Teo TH, Setiawan AM, Ong NE, Zimmermann M, Price P, et al. Increased CTLA-4+ T cells may contribute to impaired T helper type 1 immune responses in patients with chronic obstructive pulmonary disease. Immunology. 2017;151(2):219-26.
118. Wu X, Sun X, Chen C, Bai C, Wang X. Dynamic gene expressions of peripheral blood mononuclear cells in patients with acute exacerbation of chronic obstructive pulmonary disease: a preliminary study. Critical care. 2014;18:1-27.
119. Singh D, Fox SM, Tal-Singer R, Bates S, Riley JH, Celli B. Altered gene expression in blood and sputum in COPD frequent exacerbators in the ECLIPSE cohort. PloS one. 2014;9(9):e107381.
120. Bruggner RV, Bodenmiller B, Dill DL, Tibshirani RJ, Nolan GP. Automated identification of stratifying signatures in cellular subpopulations. Proceedings of the National Academy of Sciences. 2014;111(26):E2770-E7.
121. Cibrián D, Sánchez-Madrid F. CD69: from activation marker to metabolic gatekeeper. European journal of immunology. 2017;47(6):946-53.
122. Ju JK, Cho Y-N, Park K-J, Kwak HD, Jin H-M, Park S-Y, et al. Activation, deficiency, and reduced IFN-γ production of mucosal-associated invariant T cells in patients with inflammatory bowel disease. J Innate Immun. 2020;12(5):422-34.
123. Durant L, Watford WT, Ramos HL, Laurence A, Vahedi G, Wei L, et al. Diverse targets of the transcription factor STAT3 contribute to T cell pathogenicity and homeostasis. Immunity. 2010;32(5):605-15.
124. Canaria DA, Yan B, Clare MG, Zhang Z, Taylor GA, Boone DL, et al. STAT5 represses a STAT3-independent Th17-like program during Th9 cell differentiation. The Journal of Immunology. 2021;207(5):1265-74.

125. Roychoudhuri R, Hirahara K, Mousavi K, Clever D, Klebanoff CA, Bonelli M, et al. BACH2 represses effector programs to stabilize Treg-mediated immune homeostasis. Nature. 2013;498(7455):506-10.
126. Zhu J, Yamane H, Paul WE. Differentiation of effector CD4 T cell populations. Annual review of immunology. 2009;28(1):445-89.
127. Choi J, Crotty S. Bcl6-mediated transcriptional regulation of follicular helper T cells (TFH). Trends in immunology. 2021;42(4):336-49.
128. Gerondakis S, Fulford TS, Messina NL, Grumont RJ. NF-κB control of T cell development. Nature immunology. 2014;15(1):15-25.
129. Djuretic IM, Levanon D, Negreanu V, Groner Y, Rao A, Ansel KM. Transcription factors T-bet and Runx3 cooperate to activate Ifng and silence Il4 in T helper type 1 cells. Nature immunology. 2007;8(2):145-53.
130. Hayes MD, Ovcinnikovs V, Smith AG, Kimber I, Dearman RJ. The aryl hydrocarbon receptor: differential contribution to T helper 17 and T cytotoxic 17 cell development. PloS one. 2014;9(9):e106955.
131. Weinreich MA, Odumade OA, Jameson SC, Hogquist KA. T cells expressing the transcription factor PLZF regulate the development of memory-like CD8+ T cells. Nature immunology. 2010;11(8):709-16.
132. Hsu F-C, Shapiro MJ, Dash B, Chen C-C, Constans MM, Chung JY, et al. An essential role for the transcription factor Runx1 in T cell maturation. Scientific reports. 2016;6(1):1-15.
133. Wong WF, Kohu K, Nagashima T, Funayama R, Matsumoto M, Movahed E, et al. The artificial loss of Runx1 reduces the expression of quiescence-associated transcription factors in CD4+ T lymphocytes. Molecular immunology. 2015;68(2):223-33.
134. Sreeramkumar V, Hons M, Punzón C, Stein JV, Sancho D, Fresno M, et al. Efficient T-cell priming and activation requires signaling through prostaglandin E2 (EP) receptors. Immunology and cell biology. 2016;94(1):39-51.
135. Lee J, Aoki T, Thumkeo D, Siriwach R, Yao C, Narumiya S. T cell–intrinsic prostaglandin E2-EP2/EP4 signaling is critical in pathogenic TH17 cell–driven inflammation. J Allergy Clin Immunol. 2019;143(2):631-43.
136. Barnawi J, Tran H, Jersmann H, Pitson S, Roscioli E, Hodge G, et al. Potential link between the sphingosine-1-phosphate (S1P) system and defective alveolar macrophage phagocytic function in chronic obstructive pulmonary disease (COPD). PloS one. 2015;10(10):e0122771.
137. Mackay LK, Braun A, Macleod BL, Collins N, Tebartz C, Bedoui S, et al. Cutting edge: CD69 interference with sphingosine-1-phosphate receptor function regulates peripheral T cell retention. The Journal of Immunology. 2015;194(5):2059-63.
138. Rong Y, Xiang Xd, Li Ym, Peng Zy, Li Jx. IL-32 was involved in cigarette smoke-induced pulmonary inflammation in COPD. The clinical respiratory journal. 2015;9(4):430-5.
139. Khawar B, Abbasi MH, Sheikh N. A panoramic spectrum of complex interplay between the immune system and IL-32 during pathogenesis of various systemic infections and inflammation. Eur J Med Res. 2015;20(1).
140. Calabrese F, Baraldo S, Bazzan E, Lunardi F, Rea F, Maestrelli P, et al. IL-32, a novel proinflammatory cytokine in chronic obstructive pulmonary disease. American journal of respiratory and critical care medicine. 2008;178(9):894-901.

141. Rong B, Fu T, Rong C, Liu W, Li K, Liu H. Correlation between serum IL-32 concentration and clinical parameters of stable COPD: a retrospective clinical analysis. Scientific reports. 2020;10(1):1-11.
142. Staples KJ, McKendry RT, Spalluto CM, Wilkinson TM. Evidence for cell mediated immune dysfunction in the COPD lung: The role of cytotoxic CD4+ T cells. Eur Respiratory Soc; 2015.
143. Takahashi R, Nakatsukasa H, Shiozawa S, Yoshimura A. SOCS1 is a key molecule that prevents regulatory T cell plasticity under inflammatory conditions. The Journal of Immunology. 2017;199(1):149-58.
144. Guan Y, Ma Y, Tang Y, Liu X, Zhao Y, An L. MiRNA-221-5p suppressed the Th17/Treg ratio in asthma via RORγt/Foxp3 by targeting SOCS1. Allergy, Asthma & Clinical Immunology. 2021;17(1):1-14.
145. Bhandari N, Upadhyay RP, Chowdhury R, Taneja S. Challenges of adopting new trial designs in LMICs. Lancet Global Health. 2021;9(5):e575-e6.
146. Stoner O, Lewis J, Martínez IL, Gumy S, Economou T, Adair-Rohani H. Household cooking fuel estimates at global and country level for 1990 to 2030. Nature communications. 2021;12(1):5793.
147. How tobacco smoke causes disease: The biology and behavioral basis for smoking-attributable disease: A report of the surgeon general. In: Promotion NCfCDPaH, editor. USA: Centers for Disease Control and Prevention; 2010.
148. Fine PM, Cass GR, Simoneit BR. Organic compounds in biomass smoke from residential wood combustion: Emissions characterization at a continental scale. Journal of Geophysical Research: Atmospheres. 2002;107(D21):ICC 11-1-ICC -9.
149. Sussan TE, Ingole V, Kim J-H, McCormick S, Negherbon J, Fallica J, et al. Source of biomass cooking fuel determines pulmonary response to household air pollution. American journal of respiratory cell and molecular biology. 2014;50(3):538-48.
150. Li F, Wang Y, Zhang J, Lu Y, Zhu X, Chen X, et al. Toxic metals in top selling cigarettes sold in China: pulmonary bioaccessibility using simulated lung fluids and fuzzy health risk assessment. Journal of Cleaner Production. 2020;275:124131.
151. Nicolaou L, Checkley W. Differences between cigarette smoking and biomass smoke exposure: An in silico comparative assessment of particulate deposition in the lungs. Environmental research. 2021;197:111116.
152. Jebet A, Kibet JK, Kinyanjui T, Nyamori VO. Environmental inhalants from tobacco burning: tar and particulate emissions. Scientific African. 2018;1:e00004.
153. Xu F, Xu A, Guo Y, Bai Q, Wu X, Ji S-P, et al. PM2.5 exposure induces alveolar epithelial cell apoptosis and causes emphysema through p53/Siva-1. European Review for Medical & Pharmacological Sciences. 2020;24(7).
154. Deng Q, Deng L, Miao Y, Guo X, Li Y. Particle deposition in the human lung: Health implications of particulate matter from different sources. Environmental research. 2019;169:237-45.
155. Muala A, Nicklasson H, Boman C, Swietlicki E, Nyström R, Pettersson E, et al. Respiratory tract deposition of inhaled wood smoke particles in healthy volunteers. Journal of aerosol medicine and pulmonary drug delivery. 2015;28(4):237-46.
156. Memon TA, Nguyen ND, Burrell KL, Scott AF, Almestica-Roberts M, Rapp E, et al. Wood smoke particles stimulate MUC5AC overproduction by human bronchial epithelial cells through TRPA1 and EGFR signaling. Toxicological Sciences. 2020;174(2):278-90.

157. Ramírez-Venegas A, Velázquez-Uncal M, Pérez-Hernández R, Guzmán-Bouilloud NE, Falfán-Valencia R, Mayar-Maya ME, et al. Prevalence of COPD and respiratory symptoms associated with biomass smoke exposure in a suburban area. International journal of chronic obstructive pulmonary disease. 2018:1727-34.
158. Olloquequi J, Jaime S, Parra V, Cornejo-Córdova E, Valdivia G, Agustí, et al. Comparative analysis of COPD associated with tobacco smoking, biomass smoke exposure or both. Respiratory research. 2018;19(1):13.
159. Dutta A, Roychoudhury S, Chowdhury S, Ray MR. Changes in sputum cytology, airway inflammation and oxidative stress due to chronic inhalation of biomass smoke during cooking in premenopausal rural Indian women. International journal of hygiene and environmental health. 2013;216(3):301-8.
160. McCarthy CE, Duffney PF, Gelein R, Thatcher TH, Elder A, Phipps RP, et al. Dung biomass smoke activates inflammatory signaling pathways in human small airway epithelial cells. American Journal of Physiology-Lung Cellular and Molecular Physiology. 2016;311(6):L1222-L33.
161. Mehra D, Geraghty PM, Hardigan AA, Foronjy R. A comparison of the inflammatory and proteolytic effects of dung biomass and cigarette smoke exposure in the lung. PloS one. 2012;7(12):e52889.
162. Falfán-Valencia R, Ramírez-Venegas A, Lara-Albisua JLP, Ramírez-Rodriguez SL, Márquez-García JE, Buendía-Roldan I, et al. Smoke exposure from chronic biomass burning induces distinct accumulative systemic inflammatory cytokine alterations compared to tobacco smoking in healthy women. Cytokine. 2020;131:155089.
163. Grip O, Janciauskiene S. Atorvastatin reduces plasma levels of chemokine (CXCL10) in patients with Crohn's disease. PloS one. 2009;4(5):e5263.
164. Sallusto F, Lenig D, Mackay CR, Lanzavecchia A. Flexible programs of chemokine receptor expression on human polarized T helper 1 and 2 lymphocytes. The Journal of experimental medicine. 1998;187(6):875-83.
165. Gimenes Jr JA, Srivastava V, ReddyVari H, Kotnala S, Mishra R, Farazuddin M, et al. Rhinovirus-induces progression of lung disease in a mouse model of COPD via IL-33/ST2 signaling axis. Clin Sci. 2019;133(8):983-96.
166. Menten P, Wuyts A, Van Damme J. Macrophage inflammatory protein-1. Cytokine & growth factor reviews. 2002;13(6):455-81.
167. Ma A, Koka R, Burkett P. Diverse functions of IL-2, IL-15, and IL-7 in lymphoid homeostasis. Annu Rev Immunol. 2006;24:657-79.
168. O'Leary SM, Coleman MM, Chew WM, Morrow C, McLaughlin AM, Gleeson LE, et al. Cigarette smoking impairs human pulmonary immunity to Mycobacterium tuberculosis. American journal of respiratory and critical care medicine. 2014;190(12):1430-6.
169. Bagaitkar J, Demuth DR, Scott DA. Tobacco use increases susceptibility to bacterial infection. Tobacco induced diseases. 2008;4:1-10.
170. Rabbani U, Sahito A, Nafees AA, Kazi A, Fatmi Z. Pulmonary tuberculosis is associated with biomass fuel use among rural women in Pakistan: an age-and residence-matched case-control study. Asia Pacific Journal of Public Health. 2017;29(3):211-8.
171. Haque M, Barman N, Islam M, Mannan M, Khan M, Karim M, et al. Biomass Fuel Smoke and Tuberculosis: A Case-Control Study. Mymensingh Medical Journal: MMJ. 2016;25(1):31-8.

172. Obore N, Kawuki J, Guan J, Papabathini S, Wang L. Association between indoor air pollution, tobacco smoke and tuberculosis: an updated systematic review and meta-analysis. Public health. 2020;187:24-35.
173. Thakur M, Boudewijns EA, Babu GR, van Schayck OC. Biomass use and COVID-19: a novel concern. Environmental Research. 2020;186:109586.
174. Hollada J, Williams KN, Miele CH, Danz D, Harvey SA, Checkley W. Perceptions of improved biomass and liquefied petroleum gas stoves in Puno, Peru: implications for promoting sustained and exclusive adoption of clean cooking technologies. International journal of environmental research and public health. 2017;14(2):182.
175. Bakhsh K, Sadiqa A, Yasin MA, Haider S, Ali R. Exploring the nexus between households' choice of cooking fuels, sanitation facilities and access to information in Pakistan. Journal of Cleaner Production. 2020;257:120621.
176. Loebel Roson M, Duruisseau-Kuntz R, Wang M, Klimchuk K, Abel RJ, Harynuk JJ, et al. Chemical characterization of emissions arising from solid fuel combustion—contrasting wood and cow dung burning. ACS Earth and Space Chemistry. 2021;5(10):2925-37.
177. KC R, Hyland IK, Smith JA, Shukla SD, Hansbro PM, Zosky GR, et al. Cow dung biomass smoke exposure increases adherence of respiratory pathogen nontypeable Haemophilus influenzae to human bronchial epithelial cells. Exposure and Health. 2020;12:883-95.
178. Wang H, Ye X, Zhang Y, Ling S. Global, regional, and national burden of chronic obstructive pulmonary disease from 1990 to 2019. Front Physiol. 2022;13:925132.
179. Warrino DE, DeGennaro LJ, Hanson M, Swindells S, Pirruccello SJ, Ryan WL. Stabilization of white blood cells and immunologic markers for extended analysis using flow cytometry. Journal of immunological methods. 2005;305(2):107-19.
180. Faucher JL, Lacronique-Gazaille C, Frébet E, Trimoreau F, Donnard M, Bordessoule D, et al. "6 markers/5 colors" extended white blood cell differential by flow cytometry. Cytometry Part A: the journal of the International Society for Analytical Cytology. 2007;71(11):934-44.
181. Roussel M, Benard C, Ly-Sunnaram B, Fest T. Refining the white blood cell differential: the first flow cytometry routine application. Cytometry Part A. 2010;77(6):552-63.
182. RCPA MANUAL - MANUAL OF USE AND INTERPRETATION OF PATHOLOGY TESTS Surry Hills, NSW Australia: The Royal College of Pathologists of Australasia; 2015 [Available from: https://www.rcpa.edu.au/Manuals/RCPA-Manual.
183. Reference Ranges Philadelphia, PA USA: American College of Physicians; [Available from: https://annualmeeting.acponline.org/educational-program/reference-ranges.
184. Suzukawa M, Takeda K, Akashi S, Asari I, Kawashima M, Ohshima N, et al. Evaluation of cytokine levels using QuantiFERON-TB Gold Plus in patients with active tuberculosis. J Infect. 2020;80(5):547-53.
185. Wergeland I, Assmus J, Dyrhol-Riise AM. Cytokine patterns in tuberculosis infection; IL-1ra, IL-2 and IP-10 differentiate borderline QuantiFERON-TB samples from uninfected controls. PloS one. 2016;11(9):e0163848.
186. Lighter-Fisher J, Peng C, Tse D. Cytokine responses to QuantiFERON® peptides, purified proteinderivative and recombinant ESAT-6 in children with tuberculosis. The International journal of tuberculosis and lung disease. 2010;14(12):1548-55.
187. Ruhwald M, Bjerregaard-Andersen M, Rabna P, Kofoed K, Eugen-Olsen J, Ravn P. CXCL10/IP-10 release is induced by incubation of whole blood from tuberculosis patients with ESAT-6, CFP10 and TB7. 7. Microbes and infection. 2007;9(7):806-12.

188. Sansores RH, Paulin-Prado P, Robles-Hernández R, Montiel-Lopez F, Bautista-Félix NE, Guzmán-Bouilloud NE, et al. Clinical and microbiological characteristics and inflammatory profile during an exacerbation of COPD due to biomass exposure. A comparison with COPD due to tobacco exposure. Respir Med. 2022;204:107010.
189. Li Y, John SY, Russo MA, Rosa-Bray M, Weinhold KJ, Guptill JT. Normative dataset for plasma cytokines in healthy human adults. Data in brief. 2021;35:106857.
190. Liu Q, Xia Z, Huang T, Yang F, Wang X, Yang F. Establishment of reference intervals for plasma IL-2, IL-4, IL-5, and IL-17A in healthy adults from the Jiangsu region of eastern China using flow cytometry: A single-center study. Cytokine. 2024;179:156594.
191. Hennø LT, Storjord E, Christiansen D, Bergseth G, Ludviksen JK, Fure H, et al. Effect of the anticoagulant, storage time and temperature of blood samples on the concentrations of 27 multiplex assayed cytokines–consequences for defining reference values in healthy humans. Cytokine. 2017;97:86-95.
192. Population of Balimo 2023: all-populations.com; 2023 [Available from: https://all-populations.com/en/pg/population-of-balimo.html.
193. Harbour SN, DiToro DF, Witte SJ, Zindl CL, Gao M, Schoeb TR, et al. TH17 cells require ongoing classic IL-6 receptor signaling to retain transcriptional and functional identity. Science immunology. 2020;5(49):eaaw2262.
194. Robak E, Gerlicz-Kowalczuk Z, Dziankowska-Bartkowiak B, Wozniacka A, Bogaczewicz J. Serum concentrations of IL-17A, IL-17B, IL-17E and IL-17F in patients with systemic sclerosis. Archives of Medical Science. 2019;15(3):706-12.
195. Griffin GK, Newton G, Tarrio ML, Bu D-x, Maganto-Garcia E, Azcutia V, et al. IL-17 and TNF-α sustain neutrophil recruitment during inflammation through synergistic effects on endothelial activation. The Journal of Immunology. 2012;188(12):6287-99.
196. Duan M, Zhong X, Huang Y, He Z, Tang H. Mechanisms and dynamics of Th17 cells in mice with cigarette smoke-induced emphysema. Zhonghua Yi Xue Za Zhi. 2011;91(28):1996-2000.
197. Torii K, Saito C, Furuhashi T, Nishioka A, Shintani Y, Kawashima K, et al. Tobacco smoke is related to Th17 generation with clinical implications for psoriasis patients. Experimental dermatology. 2011;20(4):371-3.
198. Akdis CA, Arkwright PD, Brüggen M-C, Busse W, Gadina M, Guttman-Yassky E, et al. Type 2 immunity in the skin and lungs. Allergy. 2020;75(7):1582-605.
199. Scott J, Emeto T, Melrose W, Warner J, Rush C. Seroepidemiology of Strongyloides spp. Infection in Balimo, Western Province, Papua New Guinea. The American Journal of Tropical Medicine and Hygiene. 2022:tpmd220408-tpmd.
200. Luetke-Eversloh M, Cicek BB, Siracusa F, Thom JT, Hamann A, Frischbutter S, et al. NK cells gain higher IFN-γ competence during terminal differentiation. European journal of immunology. 2014;44(7):2074-84.
201. Martí-Lliteras P, Regueiro V, Morey P, Hood DW, Saus C, Sauleda J, et al. Nontypeable Haemophilus influenzae clearance by alveolar macrophages is impaired by exposure to cigarette smoke. Infection and immunity. 2009;77(10):4232-42.
202. Kurmi OP, Sadhra CS, Ayres JG, Sadhra SS. Tuberculosis risk from exposure to solid fuel smoke: a systematic review and meta-analysis. J Epidemiol Community Health. 2014;68(12):1112-8.
203. Sarkar S, Rivas-Santiago CE, Ibironke OA, Carranza C, Meng Q, Osornio-Vargas Á, et al. Season and size of urban particulate matter differentially affect cytotoxicity and human immune responses to Mycobacterium tuberculosis. PloS one. 2019;14(7):e0219122.

204. Torres M, Carranza C, Sarkar S, Gonzalez Y, Vargas AO, Black K, et al. Urban airborne particle exposure impairs human lung and blood Mycobacterium tuberculosis immunity. Thorax. 2019;74(7):675-83.
205. Gong Y, Liang S, Zeng L, Ni Y, Zhou S, Yuan X. Effects of blood sample handling procedures on measurable interleukin 6 in plasma and serum. Journal of Clinical Laboratory Analysis. 2019;33(7):e22924.
206. Hu G, Zhou Y, Tian J, Yao W, Li J, Li B, et al. Risk of COPD from exposure to biomass smoke: a metaanalysis. Chest. 2010;138(1):20-31.
207. Inghammar M, Ekbom A, Engström G, Ljungberg B, Romanus V, Löfdahl C-G, et al. COPD and the risk of tuberculosis-a population-based cohort study. PloS one. 2010;5(4):e10138.
208. Lee C-H, Lee M-C, Shu C-C, Lim C-S, Wang J-Y, Lee L-N, et al. Risk factors for pulmonary tuberculosis in patients with chronic obstructive airway disease in Taiwan: a nationwide cohort study. BMC Infect Dis. 2013;13:1-11.
209. Silverman EK. Genetics of COPD. Annual review of physiology. 2020;82:413-31.
210. Chatila WM, Wynkoop WA, Vance G, Criner GJ. Smoking patterns in African Americans and whites with advanced COPD. Chest. 2004;125(1):15-21.
211. Dransfield MT, Davis JJ, Gerald LB, Bailey WC. Racial and gender differences in susceptibility to tobacco smoke among patients with chronic obstructive pulmonary disease. Respir Med. 2006;100(6):1110-6.
212. Hersh CP, Hokanson JE, Lynch DA, Washko GR, Make BJ, Crapo JD, et al. Family history is a risk factor for COPD. Chest. 2011;140(2):343-50.
213. Tetley TD. Macrophages and the pathogenesis of COPD. Chest. 2002;121(5):156S-9S.
214. Beghé B, Verduri A, Bottazzi B, Stendardo M, Fucili A, Balduzzi S, et al. Echocardiography, spirometry, and systemic acute-phase inflammatory proteins in smokers with COPD or CHF: an observational study. PloS one. 2013;8(11):e80166.
215. Siafakas NM, Tzortzaki EG, Sourvinos G, Bouros D, Tzanakis N, Kafatos A, et al. Microsatellite DNA instability in COPD. Chest. 1999;116(1):47-51.
216. Rivera R, Cosio M, Ghezzo H, Salazar M, Pérez-Padilla R. Comparison of lung morphology in COPD secondary to cigarette and biomass smoke. The International Journal of Tuberculosis and Lung Disease. 2008;12(8):972-7.
217. Meneghini AC, Koenigkam-Santos M, Pereira MC, Tonidandel PR, Terra-Filho J, Cunha FdQ, et al. Biomass smoke COPD has less tomographic abnormalities but worse hypoxemia compared with tobacco COPD. Brazilian Journal of Medical and Biological Research. 2019;52.
218. Camp PG, Ramirez-Venegas A, Sansores RH, Alva LF, McDougall JE, Sin DD, et al. COPD phenotypes in biomass smoke-versus tobacco smoke-exposed Mexican women. Eur Respir J. 2014;43(3):725-34.
219. Golpe R, Martín-Robles I, Sanjuán-López P, Pérez-de-Llano L, González-Juanatey C, López-Campos JL, et al. Differences in systemic inflammation between cigarette and biomass smoke-induced COPD. International journal of chronic obstructive pulmonary disease. 2017:2639-46.
220. Vishweswaraiah S, Thimraj TA, George L, Krishnarao CS, Lokesh KS, Siddaiah JB, et al. Putative systemic biomarkers of biomass smoke-induced chronic obstructive pulmonary disease among women in a rural south Indian population. Disease markers. 2018;2018.

221. Salvi SS, Brashier BB, Londhe J, Pyasi K, Vincent V, Kajale SS, et al. Phenotypic comparison between smoking and non-smoking chronic obstructive pulmonary disease. Respiratory research. 2020;21(1):1-12.
222. Fernandes L, Rane S, Mandrekar S, Mesquita AM. Eosinophilic airway inflammation in patients with stable biomass smoke-versus tobacco smoke-associated chronic obstructive pulmonary disease. Journal of Health and Pollution. 2019;9(24):191209.
223. Agustí A, Celli BR, Criner GJ, Halpin D, Anzueto A, Barnes P, et al. Global initiative for chronic obstructive lung disease 2023 report: GOLD executive summary. American journal of respiratory and critical care medicine. 2023;207(7):819-37.
224. Hankinson JL, Odencrantz JR, Fedan KB. Spirometric reference values from a sample of the general US population. American journal of respiratory and critical care medicine. 1999;159(1):179-87.
225. Freeman CM, Crudgington S, Stolberg VR, Brown JP, Sonstein J, Alexis NE, et al. Design of a multi-center immunophenotyping analysis of peripheral blood, sputum and bronchoalveolar lavage fluid in the Subpopulations and Intermediate Outcome Measures in COPD Study (SPIROMICS). Journal of translational medicine. 2015;13(1):19.
226. Lay JC, Peden DB, Alexis NE. Flow cytometry of sputum: assessing inflammation and immune response elements in the bronchial airways. Inhalation toxicology. 2011;23(7):392-406.
227. Wang D, Rao L, Lei H, Li W, Yu Q, Li W, et al. Clinical significance of serum levels of 14-3-3β protein in patients with stable chronic obstructive pulmonary disease. Scientific reports. 2023;13(1):4861.
228. Günay E, Sarınç Ulaşlı S, Akar O, Ahsen A, Günay S, Koyuncu T, et al. Neutrophil-to-lymphocyte ratio in chronic obstructive pulmonary disease: a retrospective study. Inflammation. 2014;37:374-80.
229. Kolsum U, Southworth T, Jackson N, Singh D. Blood eosinophil counts in COPD patients compared to controls. Eur Respir J. 2019;54(4).
230. Ponce-Gallegos MA, Pérez-Rubio G, Ambrocio-Ortiz E, Partida-Zavala N, Hernández-Zenteno R, Flores-Trujillo F, et al. Genetic variants in IL17A and serum levels of IL-17A are associated with COPD related to tobacco smoking and biomass burning. Scientific reports. 2020;10(1):784.
231. Nadeem A, Al-Harbi NO, Alfardan AS, Ahmad SF, AlAsmari AF, Al-Harbi MM. IL-17A-induced neutrophilic airway inflammation is mediated by oxidant-antioxidant imbalance and inflammatory cytokines in mice. Biomedicine & Pharmacotherapy. 2018;107:1196-204.
232. Oda N, Canelos PB, Essayan DM, Plunkett BA, Myers AC, Huang S-K. Interleukin-17F induces pulmonary neutrophilia and amplifies antigen-induced allergic response. American journal of respiratory and critical care medicine. 2005;171(1):12-8.
233. Yang G, Sun Y, Tsuneyama K, Zhang W, Leung P, He X, et al. Endogenous interleukin-22 protects against inflammatory bowel disease but not autoimmune cholangitis in dominant negative form of transforming growth factor beta receptor type II mice. Clinical & Experimental Immunology. 2016;185(2):154-64.
234. Lockhart E, Green AM, Flynn JL. IL-17 production is dominated by γδ T cells rather than CD4 T cells during Mycobacterium tuberculosis infection. The Journal of Immunology. 2006;177(7):4662-9.
235. Sutton CE, Mielke LA, Mills KH. IL-17-producing γδ T cells and innate lymphoid cells. European journal of immunology. 2012;42(9):2221-31.

236. Xia W, Bai J, Wu X, Wei Y, Feng S, Li L, et al. Interleukin-17A promotes MUC5AC expression and goblet cell hyperplasia in nasal polyps via the Act1-mediated pathway. PloS one. 2014;9(6):e98915.
237. Danahay H, Pessotti AD, Coote J, Montgomery BE, Xia D, Wilson A, et al. Notch2 is required for inflammatory cytokine-driven goblet cell metaplasia in the lung. Cell Rep. 2015;10(2):239-52.
238. Yi F, Fang Z, Liang H, Huang L, Jiang M, Feng Z, et al. Diagnostic accuracy of blood eosinophils in comparison to other common biomarkers for identifying sputum eosinophilia in patients with chronic cough. World Allergy Organ J. 2023;16(9):100819.
239. Tashkin DP, Wechsler ME. Role of eosinophils in airway inflammation of chronic obstructive pulmonary disease. International journal of chronic obstructive pulmonary disease. 2018:335-49.
240. Hastie AT, Martinez FJ, Curtis JL, Doerschuk CM, Hansel NN, Christenson S, et al. Association of sputum and blood eosinophil concentrations with clinical measures of COPD severity: an analysis of the SPIROMICS cohort. Lancet Respir Med. 2017;5(12):956-67.
241. Schoenborn JR, Wilson CB. Regulation of interferon-γ during innate and adaptive immune responses. Advances in immunology. 2007;96:41-101.
242. Paget C, Chow MT, Duret H, Mattarollo SR, Smyth MJ. Role of γδ T Cells in α-Galactosylceramide–Mediated Immunity. The Journal of Immunology. 2012;188(8):3928-39.
243. Zheng Y, Zha Y, Spaapen RM, Mathew R, Barr K, Bendelac A, et al. Egr2-dependent gene expression profiling and ChIP-Seq reveal novel biologic targets in T cell anergy. Molecular immunology. 2013;55(3-4):283-91.
244. Taams LS, van Rensen AJ, Poelen MC, van Els CA, Besseling AC, Wagenaar JP, et al. Anergic T cells actively suppress T cell responses via the antigen-presenting cell. European journal of immunology. 1998;28(9):2902-12.
245. Steinbrink K, Graulich E, Kubsch S, Knop J, Enk AH. CD4+ and CD8+ anergic T cells induced by interleukin-10–treated human dendritic cells display antigen-specific suppressor activity. Blood, The Journal of the American Society of Hematology. 2002;99(7):2468-76.
246. Boussiotis VA, Tsai EY, Yunis EJ, Thim S, Delgado JC, Dascher CC, et al. IL-10–producing T cells suppress immune responses in anergic tuberculosis patients. The Journal of clinical investigation. 2000;105(9):1317-25.
247. Chen J, Wang X, Schmalen A, Haines S, Wolff M, Ma H, et al. Antiviral CD8+ T-cell immune responses are impaired by cigarette smoke and in COPD. Eur Respir J. 2023;62(2).
248. Niccolai E, Ricci F, Russo E, Nannini G, Emmi G, Taddei A, et al. The different functional distribution of “Not Effector” T cells (Treg/Tnull) in colorectal cancer. Frontiers in immunology. 2017;8:1900.
249. Ihara F, Sakurai D, Takami M, Kamata T, Kunii N, Yamasaki K, et al. Regulatory T cells induce CD4− NKT cell anergy and suppress NKT cell cytotoxic function. Cancer Immunol Immunother. 2019;68:1935-47.
250. Zhou B, Liu S, He D, Wang K, Wang Y, Yang T, et al. Fibrinogen is a promising biomarker for chronic obstructive pulmonary disease: evidence from a meta-analysis. Bioscience reports. 2020;40(7):BSR20193542.
251. Valvi D, Mannino DM, Müllerova H, Tal-Singer R. Fibrinogen, chronic obstructive pulmonary disease (COPD) and outcomes in two United States cohorts. International journal of chronic obstructive pulmonary disease. 2012:173-82.

252. Mannino DM, Ford ES, Redd SC. Obstructive and restrictive lung disease and markers of inflammation: data from the Third National Health and Nutrition Examination. The American journal of medicine. 2003;114(9):758-62.
253. Sin DD, Leung R, Gan WQ, Man SP. Circulating surfactant protein D as a potential lung-specific biomarker of health outcomes in COPD: a pilot study. BMC pulmonary medicine. 2007;7:1-7.
254. Ju C-R, Liu W, Chen R-C. Serum surfactant protein D: biomarker of chronic obstructive pulmonary disease. Disease markers. 2012;32(5):281-7.
255. Lv M-Y, Qiang L-X, Wang B-C, Zhang Y-P, Li Z-H, Li X-S, et al. Complex Evaluation of Surfactant Protein A and D as Biomarkers for the Severity of COPD. International journal of chronic obstructive pulmonary disease. 2022:1537-52.
256. Iwamoto H, Gao J, Koskela J, Kinnula V, Kobayashi H, Laitinen T, et al. Differences in plasma and sputum biomarkers between COPD and COPD–asthma overlap. Eur Respir J. 2014;43(2):421-9.
257. Kawagoe J, Kono Y, Togashi Y, Ishiwari M, Toriyama K, Yajima C, et al. Serum neutrophil gelatinase-associated lipocalin (NGAL) is elevated in patients with asthma and airway obstruction. Current Medical Science. 2021;41:323-8.
258. Jo YS, Kwon SO, Kim J, Kim WJ. Neutrophil gelatinase-associated lipocalin as a complementary biomarker for the asthma-chronic obstructive pulmonary disease overlap. Journal of thoracic disease. 2018;10(8):5047.
259. Häntzsch M, Tolios A, Beutner F, Nagel D, Thiery J, Teupser D, et al. Comparison of whole blood RNA preservation tubes and novel generation RNA extraction kits for analysis of mRNA and MiRNA profiles. PloS one. 2014;9(12):e113298.
260. Berry ASF, Amorim CF, Berry CL, Syrett CM, English ED, Beiting DP. An Open-Source Toolkit To Expand Bioinformatics Training in Infectious Diseases. mBio. 2021;12(4):10.1128/mbio.01214-21.
261. Liberzon A, Subramanian A, Pinchback R, Thorvaldsdóttir H, Tamayo P, Mesirov JP. Molecular signatures database (MSigDB) 3.0. Bioinformatics. 2011;27(12):1739-40.
262. Liberzon A, Birger C, Thorvaldsdóttir H, Ghandi M, Mesirov JP, Tamayo P. The molecular signatures database hallmark gene set collection. Cell systems. 2015;1(6):417-25.
263. Chiang EY, de Almeida PE, de Almeida Nagata DE, Bowles KH, Du X, Chitre AS, et al. CD96 functions as a co-stimulatory receptor to enhance CD8+ T cell activation and effector responses. European Journal of Immunology. 2020;50(6):891-902.
264. Wang CQ, Choy FC, Sanny A, Murakami T, Tan AH-M, Lam K-P. An Inhibitory Role for Human CD96 Endodomain in T Cell Anti-Tumor Responses. Cells. 2023;12(2):309.
265. Stanko K, Iwert C, Appelt C, Vogt K, Schumann J, Strunk FJ, et al. CD96 expression determines the inflammatory potential of IL-9–producing Th9 cells. Proceedings of the National Academy of Sciences. 2018;115(13):E2940-E9.
266. Zhao X, Feng X, Liu P, Ye J, Tao R, Li R, et al. Abnormal expression of CD96 on natural killer cell in peripheral blood of patients with chronic obstructive pulmonary disease. The clinical respiratory journal. 2022;16(8):546-54.
267. Niu N, Qin X. New insights into IL-7 signaling pathways during early and late T cell development. Cellular & molecular immunology. 2013;10(3):187-9.
268. Carrette F, Surh CD, editors. IL-7 signaling and CD127 receptor regulation in the control of T cell homeostasis. Seminars in immunology; 2012: Elsevier.

269. Huang L, Ye K, McGee MC, Nidetz NF, Elmore JP, Limper CB, et al. Interleukin-2-Inducible T-cell kinase deficiency impairs early pulmonary protection against Mycobacterium tuberculosis infection. Frontiers in immunology. 2020;10:508432.
270. Kannan AK, Kim D-G, August A, Bynoe MS. Itk signals promote neuroinflammation by regulating CD4+ T-cell activation and trafficking. Journal of Neuroscience. 2015;35(1):221-33.
271. Sintes J, Cuenca M, Romero X, Bastos R, Terhorst C, Angulo A, et al. Cutting edge: Ly9 (CD229), a SLAM family receptor, negatively regulates the development of thymic innate memory-like CD8+ T and invariant NKT cells. The Journal of Immunology. 2013;190(1):21-6.
272. Cuenca M, Puñet-Ortiz J, Ruart M, Terhorst C, Engel P. Ly9 (SLAMF3) receptor differentially regulates iNKT cell development and activation in mice. European journal of immunology. 2018;48(1):99-105.
273. Bevington SL, Cauchy P, Piper J, Bertrand E, Lalli N, Jarvis RC, et al. Inducible chromatin priming is associated with the establishment of immunological memory in T cells. The EMBO journal. 2016;35(5):515-35.
274. Nakajima T, Kanno T, Yokoyama S, Sasamoto S, Asou HK, Tumes DJ, et al. ACC1-expressing pathogenic T helper 2 cell populations facilitate lung and skin inflammation in mice. Journal of Experimental Medicine. 2021;218(12):e20210639.
275. Korinfskaya S, Parameswaran S, Barski A. Runx transcription factors in t cells—what is beyond thymic development? Frontiers in immunology. 2021;12:701924.
276. Hu C, Yang J, Qi Z, Wu H, Wang B, Zou F, et al. Heat shock proteins: Biological functions, pathological roles, and therapeutic opportunities. MedComm, 3 (3), e161. 2022.
277. van Eden W, Broere F, van der Zee R. HSP70 Is a Major Contributor to the MHCII Ligandome and Inducer of Regulatory T Cells. HSP70 in Human Diseases and Disorders. 2018:163-71.
278. Li Z, Menoret A, Srivastava P. Roles of heat-shock proteins in antigen presentation and cross-presentation. Current opinion in immunology. 2002;14(1):45-51.
279. Haug M, Dannecker L, Schepp CP, Kwok WW, Wernet D, Buckner JH, et al. The heat shock protein Hsp70 enhances antigen-specific proliferation of human CD4+ memory T cells. European journal of immunology. 2005;35(11):3163-72.
280. Fischer N, Haug M, Kwok WW, Kalbacher H, Wernet D, Dannecker GE, et al. Involvement of CD91 and scavenger receptors in Hsp70-facilitated activation of human antigen-specific CD4+ memory T cells. European journal of immunology. 2010;40(4):986-97.
281. Thériault JR, Adachi H, Calderwood SK. Role of scavenger receptors in the binding and internalization of heat shock protein 70. The Journal of Immunology. 2006;177(12):8604-11.
282. Somensi N, Brum PO, de Miranda Ramos V, Gasparotto J, Zanotto-Filho A, Rostirolla DC, et al. Extracellular HSP70 activates ERK1/2, NF-kB and pro-inflammatory gene transcription through binding with RAGE in A549 human lung cancer cells. Cellular Physiology and Biochemistry. 2017;42(6):2507-22.
283. Asea A, Rehli M, Kabingu E, Boch JA, Baré O, Auron PE, et al. Novel signal transduction pathway utilized by extracellular HSP70: role of toll-like receptor (TLR) 2 and TLR4. Journal of Biological Chemistry. 2002;277(17):15028-34.
284. Dong J, Guo L, Liao Z, Zhang M, Zhang M, Wang T, et al. Increased expression of heat shock protein 70 in chronic obstructive pulmonary disease. International immunopharmacology. 2013;17(3):885-93.

285. Stillie R, Farooq SM, Gordon JR, Stadnyk AW. The functional significance behind expressing two IL–8 receptor types on PMN. J Leukocyte Biol. 2009;86(3):529-43.
286. Shu Q, Zhang N, Liu Y, Wang X, Chen J, Xie H, et al. IL-8 Triggers Neutrophil Extracellular Trap Formation Through an Nicotinamide Adenine Dinucleotide Phosphate Oxidase-and Mitogen-Activated Protein Kinase Pathway-Dependent Mechanism in Uveitis. Investigative Ophthalmology & Visual Science. 2023;64(13):19-.
287. Rybka J, Korte SM, Czajkowska-Malinowska M, Wiese M, Kedziora-Kornatowska K, Kedziora J. The links between chronic obstructive pulmonary disease and comorbid depressive symptoms: role of IL-2 and IFN-gamma. Clinical and experimental medicine. 2016;16(4):493-502.
288. Shi Y, Tu Z, Tang D, Zhang H, Liu M, Wang K, et al. The inhibition of LPS-induced production of inflammatory cytokines by HSP70 involves inactivation of the NF-κB pathway but not the MAPK pathways. Shock. 2006;26(3):277-84.
289. Wachstein J, Tischer S, Figueiredo C, Limbourg A, Falk C, Immenschuh S, et al. HSP70 enhances immunosuppressive function of CD4+ CD25+ FoxP3+ T regulatory cells and cytotoxicity in CD4+ CD25− T cells. PloS one. 2012;7(12):e51747.
290. Bookout AL, Jeong Y, Downes M, Ruth TY, Evans RM, Mangelsdorf DJ. Anatomical profiling of nuclear receptor expression reveals a hierarchical transcriptional network. Cell. 2006;126(4):789-99.
291. Walcher D, Kümmel A, Kehrle B, Bach H, Grüb M, Durst R, et al. LXR activation reduces proinflammatory cytokine expression in human CD4-positive lymphocytes. Arteriosclerosis, thrombosis, and vascular biology. 2006;26(5):1022-8.
292. Herold M, Breuer J, Hucke S, Knolle P, Schwab N, Wiendl H, et al. Liver X receptor activation promotes differentiation of regulatory T cells. PloS one. 2017;12(9):e0184985.
293. Jubinville É, Routhier J, Maranda-Robitaille M, Pineault M, Milad N, Talbot M, et al. Pharmacological activation of liver X receptor during cigarette smoke exposure adversely affects alveolar macrophages and pulmonary surfactant homeostasis. American Journal of Physiology-Lung Cellular and Molecular Physiology. 2019;316(4):L669-L78.
294. Gubernatorova EO, Gorshkova EA, Namakanova OA, Zvartsev RV, Hidalgo J, Drutskaya MS, et al. Non-redundant functions of IL-6 produced by macrophages and dendritic cells in allergic airway inflammation. Frontiers in immunology. 2018;9:2718.
295. Abe T, Oka M, Tangoku A, Hayashi H, Yamamoto K, Yahara N, et al. Interleukin-6 production in lung tissue after transthoracic esophagectomy. Journal of the American College of Surgeons. 2001;192(3):322-9.
296. Simpson CE, Chen JY, Damico RL, Hassoun PM, Martin LJ, Yang J, et al. Cellular sources of interleukin-6 and associations with clinical phenotypes and outcomes in pulmonary arterial hypertension. Eur Respir J. 2020;55(4).
297. Jones GW, McLoughlin RM, Hammond VJ, Parker CR, Williams JD, Malhotra R, et al. Loss of CD4+ T cell IL-6R expression during inflammation underlines a role for IL-6 trans signaling in the local maintenance of Th17 cells. The journal of immunology. 2010;184(4):2130-9.
298. Dang EV, Barbi J, Yang H-Y, Jinasena D, Yu H, Zheng Y, et al. Control of TH17/Treg balance by hypoxia-inducible factor 1. Cell. 2011;146(5):772-84.
299. Xu S, Yu C, Ma X, Li Y, Shen Y, Chen Y, et al. IL-6 promotes nuclear translocation of HIF-1α to aggravate chemoresistance of ovarian cancer cells. European journal of pharmacology. 2021;894:173817.

300. Heinrich PC, Castell JV, Andus T. Interleukin-6 and the acute phase response. Biochemical journal. 1990;265(3):621.
301. Andrews E, Feldhoff P, Feldhoff R, Lassiter H. Comparative effects of cytokines and cytokine combinations on complement component C3 secretion by HepG2 cells. Cytokine. 2003;23(6):164-9.
302. Lubbers R, Van Essen M, Van Kooten C, Trouw L. Production of complement components by cells of the immune system. Clinical & Experimental Immunology. 2017;188(2):183-94.
303. Katz Y, Revel M, Strunk RC. Interleukin 6 stimulates synthesis of complement proteins factor B and C3 in human skin fibroblasts. European journal of immunology. 1989;19(6):983-8.
304. Lim TJF, Su I. Talin1 methylation is required for neutrophil infiltration and lipopolysaccharide-induced lethality. The Journal of Immunology. 2018;201(12):3651-61.
305. Latour YL, McNamara KM, Allaman MM, Barry DP, Smith TM, Asim M, et al. Myeloid deletion of talin-1 reduces mucosal macrophages and protects mice from colonic inflammation. Scientific reports. 2023;13(1):22368.
306. Lefort CT, Rossaint J, Moser M, Petrich BG, Zarbock A, Monkley SJ, et al. Distinct roles for talin-1 and kindlin-3 in LFA-1 extension and affinity regulation. Blood, The Journal of the American Society of Hematology. 2012;119(18):4275-82.
307. Górska A, Mazur AJ. Integrin-linked kinase (ILK): the known vs. the unknown and perspectives. Cellular and Molecular Life Sciences. 2022;79(2):100.
308. Pérez-Padilla R, Ramirez-Venegas A, Sansores-Martinez R. Clinical characteristics of patients with biomass smoke-associated COPD and chronic bronchitis, 2004-2014. Chronic Obstructive Pulmonary Diseases: Journal of the COPD Foundation. 2014;1(1):23.
309. Fricker M, Goggins BJ, Mateer S, Jones B, Kim RY, Gellatly SL, et al. Chronic cigarette smoke exposure induces systemic hypoxia that drives intestinal dysfunction. JCI insight. 2018;3(3).
310. Ueno M, Maeno T, Nomura M, Aoyagi-Ikeda K, Matsui H, Hara K, et al. Hypoxia-inducible factor-1α mediates TGF-β-induced PAI-1 production in alveolar macrophages in pulmonary fibrosis. American Journal of Physiology-Lung Cellular and Molecular Physiology. 2011;300(5):L740-L52.
311. Cimmino F, Avitabile M, Lasorsa VA, Montella A, Pezone L, Cantalupo S, et al. HIF-1 transcription activity: HIF1A driven response in normoxia and in hypoxia. BMC medical genetics. 2019;20:1-15.
312. Epstein AC, Gleadle JM, McNeill LA, Hewitson KS, O'Rourke J, Mole DR, et al. C. elegans EGL-9 and mammalian homologs define a family of dioxygenases that regulate HIF by prolyl hydroxylation. Cell. 2001;107(1):43-54.
313. Slemc L, Kunej T. Transcription factor HIF1A: downstream targets, associated pathways, polymorphic hypoxia response element (HRE) sites, and initiative for standardization of reporting in scientific literature. Tumor Biology. 2016;37:14851-61.
314. van Uden P, Kenneth NS, Rocha S. Regulation of hypoxia-inducible factor-1α by NF-κB. Biochemical Journal. 2008;412(3):477-84.
315. Albina JE, Mastrofrancesco B, Vessella JA, Louis CA, Henry Jr WL, Reichner JS. HIF-1 expression in healing wounds: HIF-1α induction in primary inflammatory cells by TNF-α. American Journal of Physiology-Cell Physiology. 2001;281(6):C1971-C7.

316. Jung YJ, Isaacs JS, Lee S, Trepel J, Neckers L. IL-1beta-mediated up-regulation of HIF-1alpha via an NFkappaB/COX-2 pathway identifies HIF-1 as a critical link between inflammation and oncogenesis. Faseb j. 2003;17(14):2115-7.
317. Lodge KM, Cowburn AS, Li W, Condliffe AM. The impact of hypoxia on neutrophil degranulation and consequences for the host. International journal of molecular sciences. 2020;21(4):1183.
318. Walmsley SR, Print C, Farahi N, Peyssonnaux C, Johnson RS, Cramer T, et al. Hypoxia-induced neutrophil survival is mediated by HIF-1α–dependent NF-κB activity. The Journal of experimental medicine. 2005;201(1):105-15.
319. Hoenderdos K, Lodge KM, Hirst RA, Chen C, Palazzo SG, Emerenciana A, et al. Hypoxia upregulates neutrophil degranulation and potential for tissue injury. Thorax. 2016;71(11):1030-8.
320. Ong CW, Fox K, Ettorre A, Elkington PT, Friedland JS. Hypoxia increases neutrophil-driven matrix destruction after exposure to Mycobacterium tuberculosis. Scientific reports. 2018;8(1):11475.
321. Campbell EL, Bruyninckx WJ, Kelly CJ, Glover LE, McNamee EN, Bowers BE, et al. Transmigrating neutrophils shape the mucosal microenvironment through localized oxygen depletion to influence resolution of inflammation. Immunity. 2014;40(1):66-77.
322. Khakban A, Sin DD, FitzGerald JM, McManus BM, Ng R, Hollander Z, et al. The projected epidemic of chronic obstructive pulmonary disease hospitalizations over the next 15 years. A population-based perspective. American journal of respiratory and critical care medicine. 2017;195(3):287-91.

Appendixes

A)

Cell Sorting Panel

Marker	Fluorochrome	Supplier
αCD4	BV711	BD Biosciences
αCD8	PercpCy5.5	Biolegend
αCD3	APCe780	eBioscience
αCD14	PB	BD Biosciences
αCD19	PB	BD Biosciences
αCD56	PB	BD Biosciences
Live/Dead Aqua		Invitrogen

B)

Panel 1

Marker	Fluorochrome	Supplier
αCD4	FITC	BD Biosciences
αCD8	PercpCy5.5	BioLegend
αCD16	PECy7	BD Biosciences
αCD19	BV421	BD Biosciences
αCD14	APC	BD Biosciences
αTIM3	PE	R&D Systems

C)

Panel 2

Marker	Fluorochrome	Supplier
αCD4	FITC	BD Biosciences
αCD8	PercpCy5.5	BioLegned
αCD25	PE	BD Biosciences
PD1	BV605	BD Biosciences
αFOXP3	APC	eBioscience
αCTLA4	BV421	BD Biosciences

D)

Panel 3

Marker	Fluorochrome	Supplier
αCD3	AF700	BioLegend
αVα7.2	FITC	BioLegend
αCD161	PercpCy5.5	BioLegend
αCD69	PECy7	BD Biosciences
αPD1	BV605	BD Biosciences
αTIM3	PE	R&D Systems

αCTLA4	BV421	BD Biosciences

Appendix 1. Flow cytometry and sorting panels (Chapter 3).

Cell Sorting (A): panel to isolate $CD4^+$ and $CD8^+$ T-cells. **Panel 1 (B):** Staining for T-cell lineage markers. **Panel 2 (C):** Staining panel for intracellular and surface markers. **Panel 3 (D):** Staining for activation and exhaustion markers in MAITs.

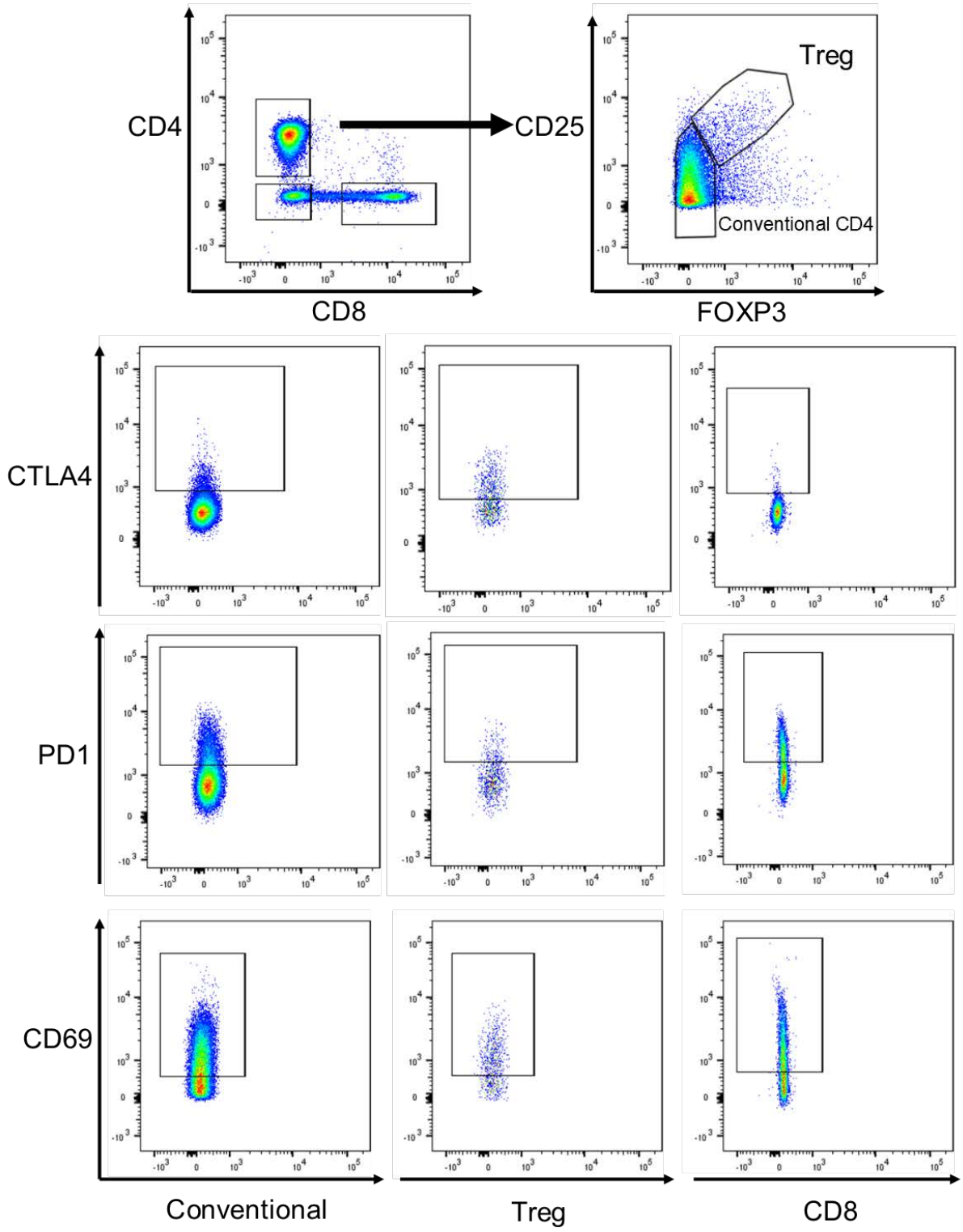

Appendix 2. Flow cytometry CD8 and CD4 gating strategy (Chapter 3).

Gating strategy showing gating of CD4 and CD8 T cells. CD4 T cells were then gated based on CD25 and FOXP3 expression as conventional CD4 T cells and T regulatory cells (Tregs). Expression of CTLA4, PD1 and CD69 on conventional CD4, CD8 and Treg cells are shown. Gating based on Fluorescence minus one controls (FMOs).

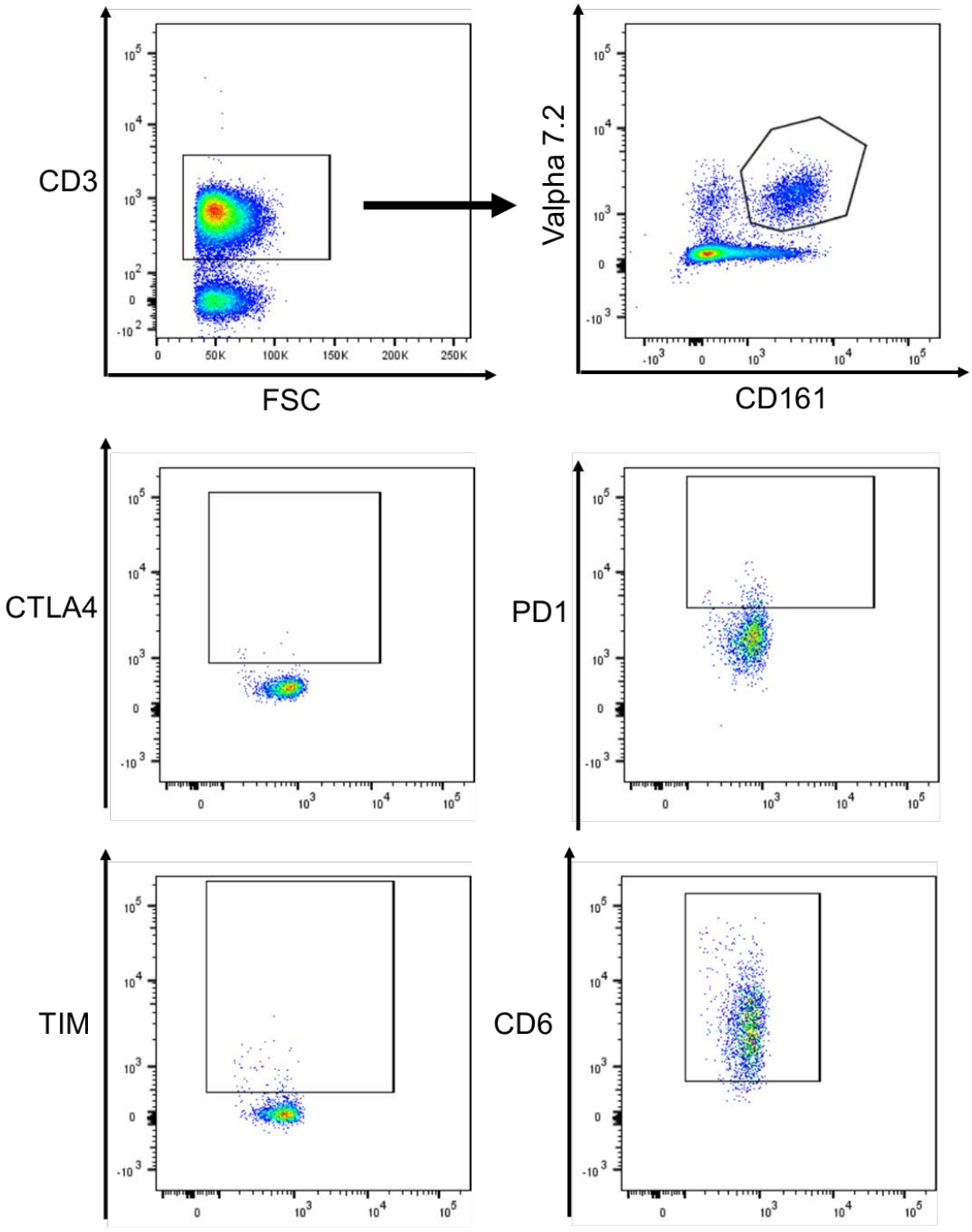

Appendix 3. Gating Strategy for MAIT cells (Chapter 3)

Gating strategy showing gating of MAIT (mucosal invariant T) cells. $CD3^{+}$ lymphocytes were gated against forward scatter. These cells were then plotted on CD161 and V alpha 7.2 and double-positive cells were gated on as MAIT cells. CLTA4, PD1, TIM3 and CD69 expression in MAIT cells were gated based on FMO controls.

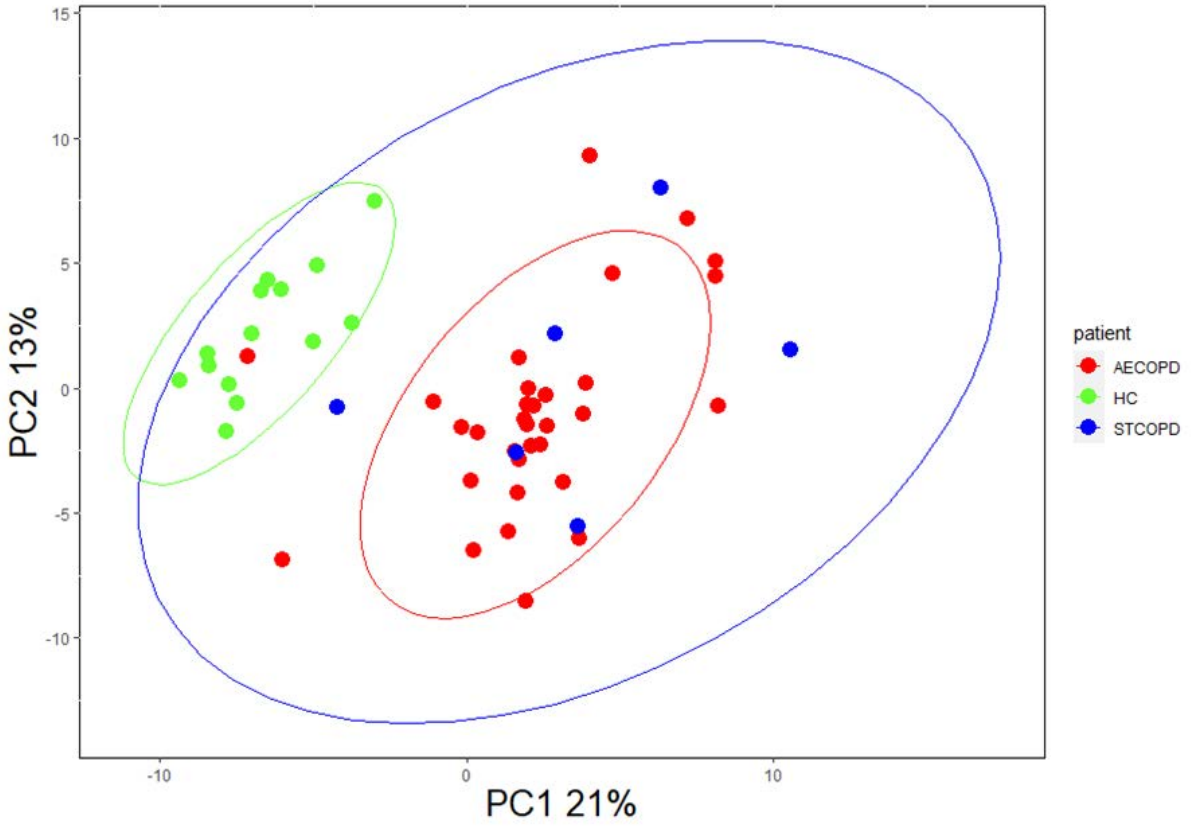

Appendix 4. PCA analysis on gene expression data from CD4+ cells of Australian Cohort (Chapter3). PCA analysis revealed separation of both patient groups (AECOPD and STCOPD) from HCs but not separation between patient groups (AECOPD vs STCOPD).

(A) CD4+ AECOPD vs HC Gene Expression

Gene	q-value	log2FC
CD4	9.909E-12	1.984243
IL32	3.29968E-09	2.062525
PTGER2	3.11292E-08	3.465133
SELL	1.67562E-07	1.966023
STAT5B	2.95536E-06	0.810182
JAK2	9.73921E-06	0.877947
CD96	3.29722E-05	0.786508
CD226	3.45024E-05	1.352417
CD27	7.29738E-05	1.337364
ITGA4	0.000129098	1.133975
GZMA	0.001422256	3.001539
PRDM1	0.002432974	1.194929
ZBTB16	0.004809153	2.094556
GZMK	0.007636741	1.46461
RUNX1	0.007862342	0.516559
SOCS1	0.009198877	0.826941
EOMES	0.011357994	0.676855
KLRG1	0.011497503	1.816267
GZMM	0.017370932	0.46719
PRF1	0.024510908	2.127411
CD300A	0.032109108	1.289668
CCR5	0.034318607	0.813401
CD244	0.034318607	1.200648
FOXP3	0.034725452	0.633468
IL7R	0.043001749	0.438929
GZMH	0.045106672	1.994936
IL2RA	0.045106672	0.53962

Gene	q-value	log2FC
BCL6	1E-15	-2.282888
STAT5A	1.6908E-11	-1.360318
AHR	1.76426E-08	-1.272214
CD45RA	1.76426E-08	-1.32147
IFNGR1	1.76426E-08	-1.268052
ICOS	2.36889E-08	-1.093122
IL2RB	6.57346E-08	-0.925975
IL21R	7.82663E-08	-1.414172
BACH2	1.90063E-07	-1.382563
CCR4	5.06049E-07	-1.305126
CTLA4	5.38488E-07	-0.938701
STAT3	8.43165E-06	-0.779996
NFKB1	1.11069E-05	-0.87267
TGFB1	6.11751E-05	-0.903554
CXCR5	8.46225E-05	-1.059579
CD28	0.000130791	-0.643312
GATA3	0.000208645	-0.873142
CD69	0.000994522	-0.571233
IL23A	0.000994522	-1.119807
CCR7	0.002409982	-0.891058
CXCR6	0.002561129	-0.774737
IL2	0.00517849	-1.223266
EGR2	0.006141005	-0.818598
SOCS5	0.007809462	-0.378255
CXCR3	0.008401491	-0.764772
IFNG	0.008990665	-0.968589
IL12RB2	0.008990665	-0.68445
ITK	0.011668604	-0.411677
CCR6	0.013387885	-0.786957
ITGAE	0.014585849	-0.401527
IRF4	0.02042169	-0.656941
RUNX3	0.024550328	-0.323752
FAS	0.024929197	-0.442602
KLRB1	0.032109108	-0.572001
S1PR1	0.034318607	-1.02209
CCR9	0.036504075	-0.80818
GFI1	0.043001749	-0.835556
IL4R	0.048702919	-0.325628

(B) CD8$^+$ AECOPD vs HC Gene Expression

Gene	q-value	log2FC
PTGER2	0.000193317	2.512653
GZMA	0.00045554	3.507763
KLRG1	0.000908589	2.248179
IL32	0.000933636	2.344122
GZMK	0.001263426	2.261696
CD244	0.001405529	2.248585
GZMH	0.001502979	2.002353
RUNX1	0.002950529	0.587144
JAK2	0.004445853	1.30186
GZMM	0.010276258	1.037539
IL18R1	0.012631718	1.092617
CD226	0.027434392	1.784502
PRF1	0.028513632	1.719395
CCL5	0.034288357	0.750575
SELL	0.034288357	1.952713
SOCS1	0.040164989	0.80155
GZMB	0.040292321	1.727437

Gene	q-value	log2FC
BCL6	1.75204E-07	-1.868253
ICOS	2.00668E-07	-1.778617
STAT5A	2.51153E-06	-1.699668
TGFB1	3.40765E-06	-1.544135
AHR	1.43348E-05	-1.514853
STAT3	2.31779E-05	-0.894815
BACH2	0.000212022	-1.717734
RUNX3	0.000212022	-0.777506
CCR7	0.000310241	-1.735487
GATA3	0.000408403	-1.548869
CD28	0.00046494	-1.372599
IL21R	0.00046494	-1.379522
RORC	0.00046494	-1.189673
CD8A	0.000554131	-0.97122
NFKB1	0.000579768	-1.229228
CD45RA	0.000776667	-0.89013
IL23A	0.000908589	-1.36019
S1PR1	0.001148333	-1.803866
IFNGR1	0.001317943	-0.939667
KLRB1	0.003032505	-1.077625
CCR6	0.00418544	-0.952464
STAT4	0.00418544	-0.491596
FOS	0.011809719	-0.825579
JAK1	0.011809719	-0.382934
CXCR3	0.014761312	-1.393787
CXCR6	0.019004306	-0.94042
ITK	0.019172332	-0.605584
IL4R	0.022802631	-0.706606

(C) $CD4^+$ STCOPD vs HC Gene Expression

Gene	q value	Log2 FC
CD226	0.000576	1.929271
CD4	0.000576	2.054442
IL32	0.000576	2.787544
PTGER2	0.000576	2.91878
CD96	0.001535	0.919369
PRDM1	0.001535	1.059483
ITGA4	0.001594	1.42601
IL1RL1	0.001996	0.993417
GZMA	0.002942	3.546719
JAK2	0.004145	0.774081
LGALS1	0.005406	0.97324
GZMM	0.007004	0.661016
SELL	0.010115	1.451382
KLRG1	0.010163	2.474293
JAK3	0.016478	0.9387
STAT5B	0.023487	0.630997
LAG3	0.026992	0.871897
CD45R0	0.037251	0.723839
IL22	0.037251	0.86019
CD160	0.044661	0.860925
PRF1	0.044661	2.295149
GZMK	0.046711	2.421535

Gene	q value	Log2 FC
EGR2	0.000576	-2.41326
BACH2	0.000576	-1.82597
IL21R	0.000576	-1.66723
STAT5A	0.000576	-1.24996
BCL6	0.001023	-1.76602
CCR7	0.001535	-1.72518
TGFB1	0.001645	-0.8842
IL2RB	0.002878	-0.81433
IL23A	0.002942	-1.76963
CTLA4	0.004145	-0.86544
ICOS	0.004167	-0.99424
ITK	0.005406	-1.02237
STAT3	0.007737	-1.13495
CD45RA	0.008768	-0.99864
STAT4	0.009722	-0.73385
AHR	0.014814	-1.0946
CCR4	0.016478	-1.11281
IRF4	0.022259	-1.43185
NFKB1	0.023487	-1.18659
TNF	0.034415	-0.78912
CCR9	0.037251	-1.22906
IFNGR1	0.037251	-0.96983
FOS	0.037251	-0.96703
SOCS1	0.037251	-0.7549
CD28	0.037251	-0.59775
IL4R	0.037251	-0.58473
FAS	0.044661	-0.59986
IL2	0.048171	-1.34306

(D) $CD4^+$ AECOPD vs STCOPD Gene Expression

Gene	q-value	log2FC
FOXP3	0.047629	1.326985
SOCS1	0.047629	1.533926
IL1RL1	0.047629	-0.85957

Appendix 5. Differentially expressed genes between AECOPD patients, STCOPD patients, and HCs (Chapter 3). Tables (A-D): Unpaired t-tests were performed on NanoString gene expression datasets. The analysis compared the expression of $CD4^+$ T-cell genes between AECOPD (n=32) and HCs (n=14) (A), and $CD8^+$ T-cell genes between AECOPD (n=25) and HCs (n=14) (B). $CD4^+$ T-cell gene expression data was also compared between stable COPD patients (n=6) and HCs (n=14) (C), and stable COPD patients and AECOPD patients (D). FDR-adjusted p-values are reported as q-values (FDR $p<0.05$).

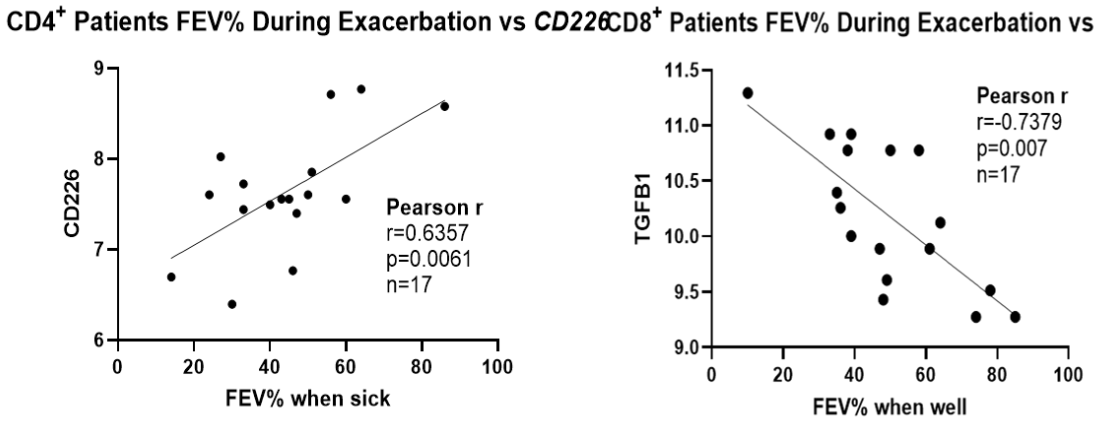

Appendix 6. Pearson's correlations using clinical data and gene expression datasets. (A) CD226 (DNAM-1) gene expression in $CD4^+$ cells from AECOPD patients was positively correlated with forced expiratory volume in 1-second percent predicted (FEV1%). (B) Gene expression of TGFB1 in CD8+ cells from AECOPD patients was anti-correlated with the patients' FEV1% after recovery to COPD stability.

CONFIDENTIAL

Date: Interviewers Name: **Sample Number:**

Patient Information:			
Name:		TB Register number:	
Sex: M/F	Height:	Weight:	
Year of birth:		If year unknown:	Adult / Child
Home village:		Current residence:	
Father's clan:		Mother's clan:	
Religion:			
Employment:			
Education:			

1. Presence and # of BCG scar/s:	Yes&# / No
2. Do you have TB?	Yes/No- go to Q6
3. What kind of TB do you have ?	Pulmonary/ Extrapulmonary
4. Are you currently on treatment for TB ?	Yes / No
5. Are you currently well?	Yes / No
6. Does anyone in your household have TB?	Yes / No
7. Do you have a cough?	Yes/ No
8. How long have you had the cough?	
9.Do you have asthma/SOB?	Yes/No

10 . Have you ever worked In a logging camp?	Yes/No	Which camps? When(Relevant years and length of employment)?
11. Do you currently smoke?	Yes/No	How many cigarettes/day? Homemade/Purchased cigarettes? How long have you been smoking for?
12. Do you currently chew buai/betel nut?	Yes/No	
13. Are you the main cook for your family? Modify for child – Are you with Mum when she does the cooking? Then ask Mum details about cooking.	Yes/No	How do you cook your meals? Fire/Gas Stove If fire: What fuel do you use? Wood/Petrol/Leaves/Kerosene/Other: Are the kids with you when you are cooking? Always/Mostly/Sometimes/Occasionally/Never Where do you cook the meals? Inside/Outside/ Under the house/Away from the house

Clinical information to be obtained from TB register	TB Register Number:
Reason for participation: Current health status: If TB patient or suspect: - If pulmonary: - If extrapulmonary:	TB patient (on treatment) / TB suspect (not on treatment) / Past patient / General population / Other (give details below): Well / Unwell Pulmonary / Extrapulmonary Smear positive / Smear negative Site of Infection: Site of infection:

TB history (current patients)	
Date of diagnosis:	Date treatment started:
Treatment type:	DOTS / Loose
Treatment category:	Category 1 / Category 2
Duration of treatment so far:	
Has there been any improvement? - If Yes or Some, how much? - If Yes or Some, how soon after starting treatment?	Yes/ No / Some

TB history (for people with previous diagnosis and treatment of TB)	
Date of previous TB diagnosis:	
Type of previous TB diagnosis: - If Pulmonary: - If EP, site of infection:	Pulmonary / Extrapulmonary Smear positive / Smear negative
Type of previous treatment:	DOTS / Loose
Category of previous treatment:	Category 1 / Category 2
Were there any treatment interruptions: If yes, how often? - If yes, how long?	Yes / No
Was treatment completed?	Yes / No
Was treatment successful?	Yes / No

Appendix 7. Recruitment Questionnaire used to screen the cohort from PNG.

	Batch 1				Batch 2			
Cytokine	**R^2**	**Lower LOD**	**LOQ**	**Upper LOD**	**R^2**	**Lower LOD**	**LOQ**	**Upper LOD**
IL-2	0.99	14.63	68.27	10000	0.99	16.66	70.02	10000
IL-4	1.00	5.30	21.44	10000	0.99	23.50	135.10	7000
IL-5	0.99	18.32	178.26	10000	0.99	9.85	80.61	9000
IL-6	1.00	11.90	49.30	10000	1.00	31.23	175.96	18000
IL-9	0.99	17.25	99.39	10000	1.00	14.93	69.64	16000
IL-10	0.99	6.94	49.32	10000	0.99	1.23	5.55	14000
IL-13	0.99	21.13	69.78	10000	1.00	30.39	57.68	14000
IL-17A	1.00	1.95	14.04	5000	1.00	1.11	7.15	6000
IL-17F	0.99	0.62	1.59	10000	1.00	0.54	1.11	11000
IL-22	1.00	4.72	31.72	10000	1.00	6.81	26.96	9000
IFN-γ	0.99	14.71	290.44	10000	0.95	38.03	8335.19	17000
TNF-α	0.98	91.25	1154.15	10000	0.99	8.85	147.45	20000

Appendix 8. Multiplex cytokine assay batch performance. Cytokine concentrations in Chapters 4 and 5 were determined across two batches. Cytokine standards were run in duplicate using eight concentrations (16 total wells) for each batch. Standards were used to construct five-parameter logistics curves to fit the participant data to. R^2 values indicate how closely the regression line fits the standard data points. Lower LOD is the lower limit of detection. LOQ is the lower limit of quantitation. Upper LOD represents the value of the top standard concentration.

Batch 1 **Batch 2**

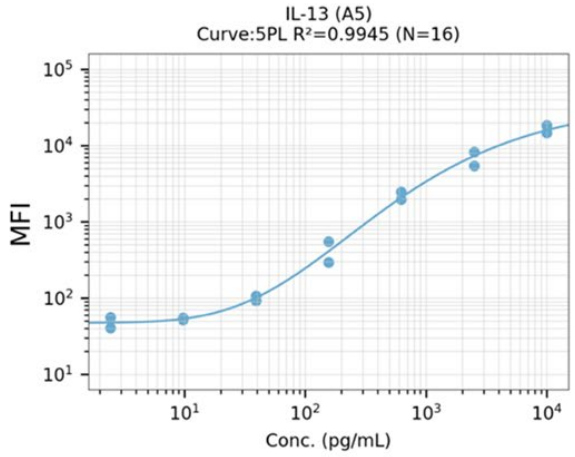

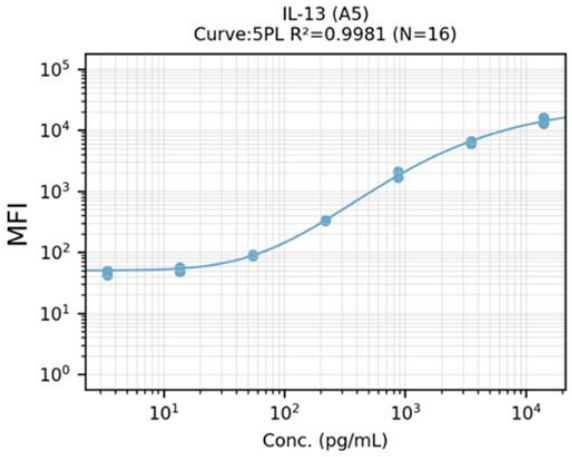

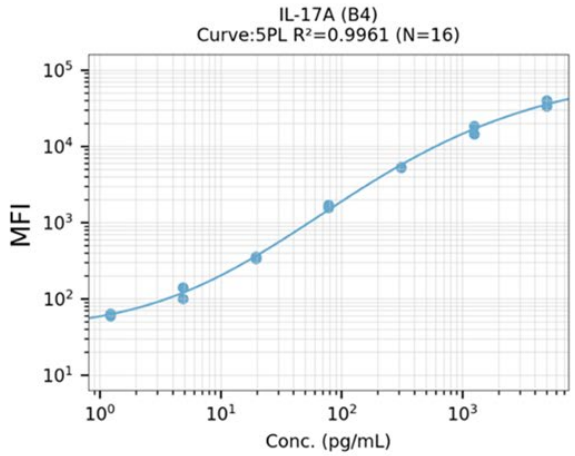

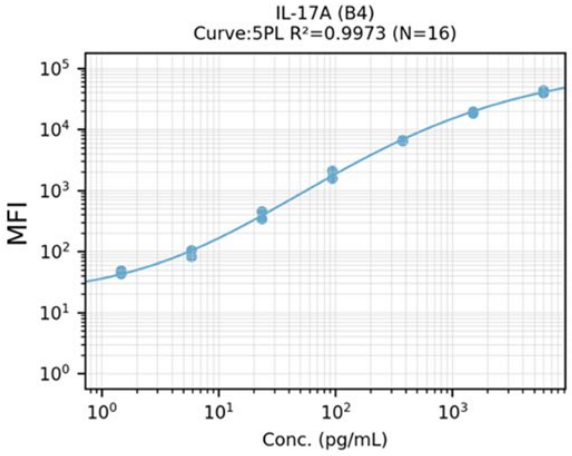

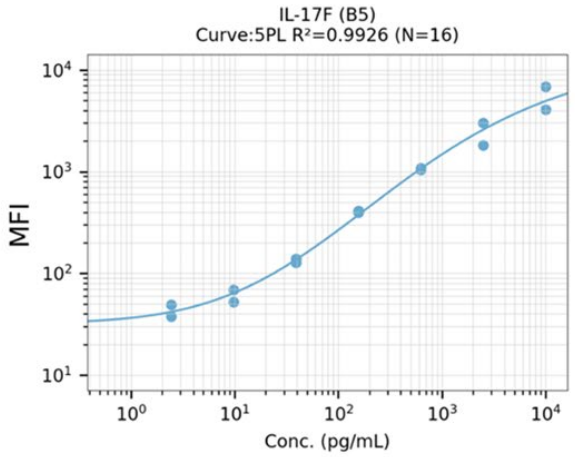

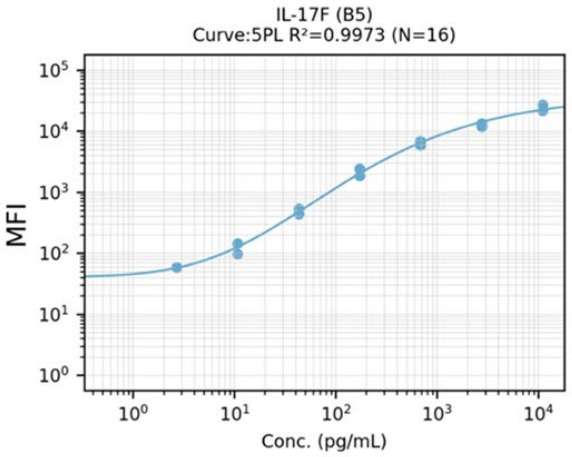

Batch 1

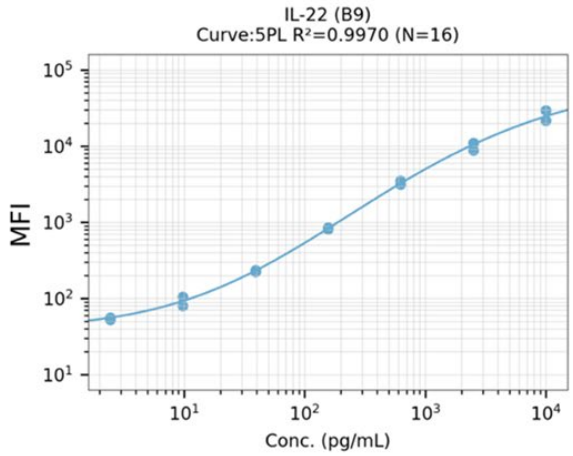

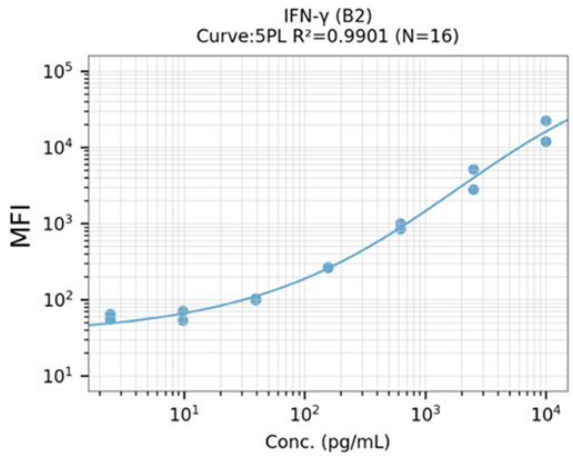

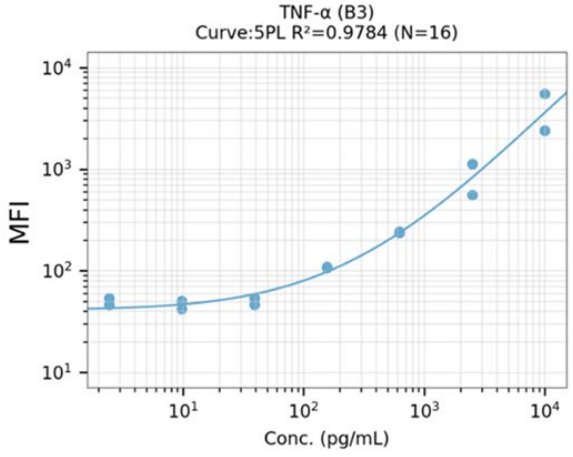

Batch 2

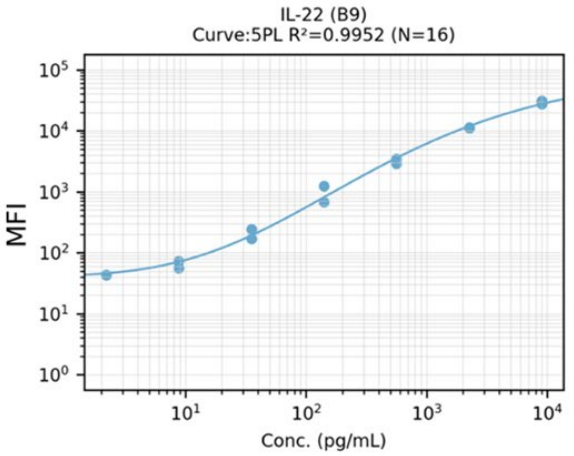

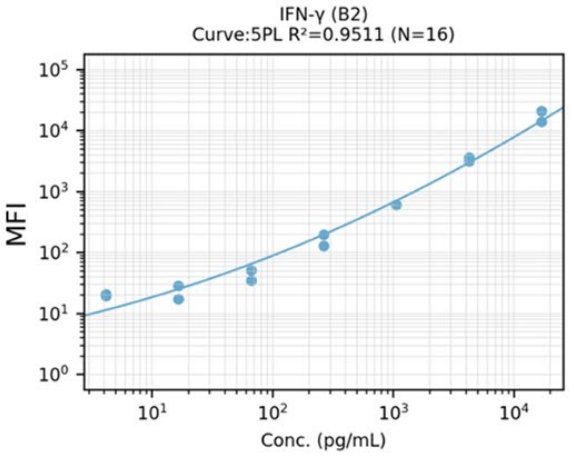

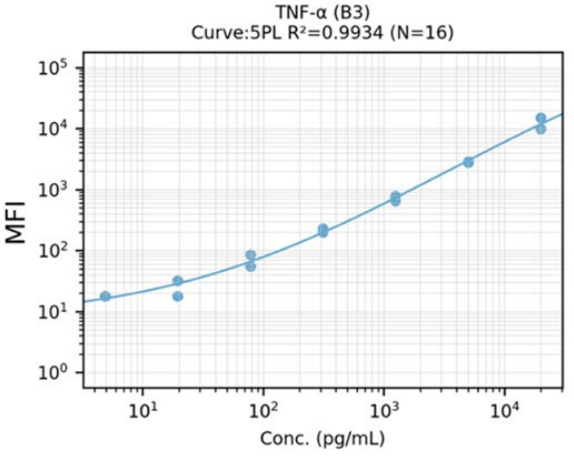

Batch 1 **Batch 2**

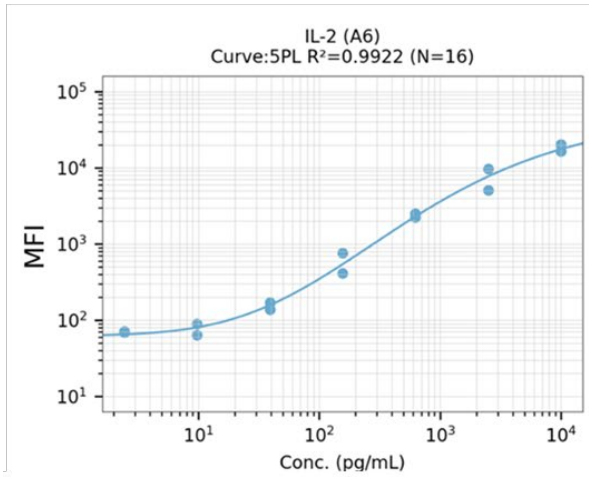

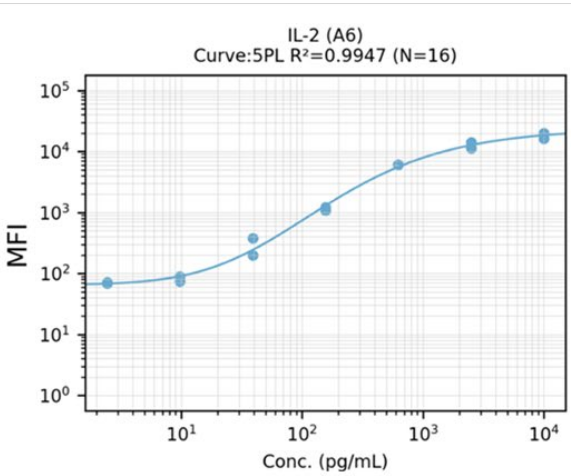

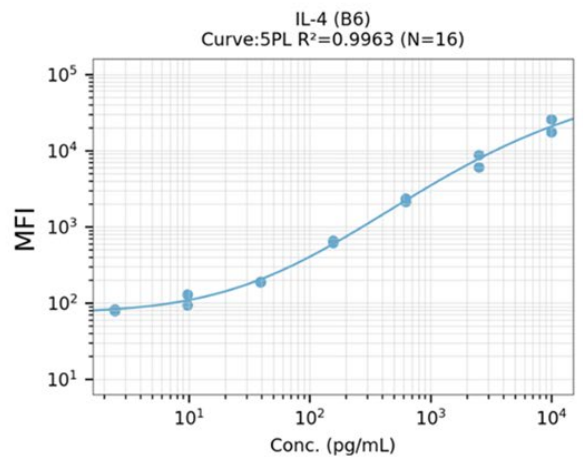

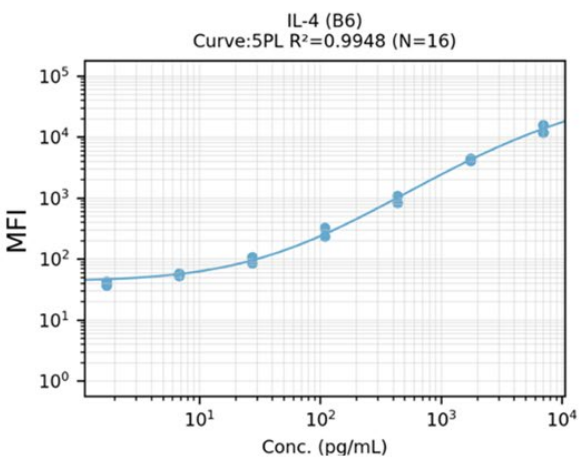

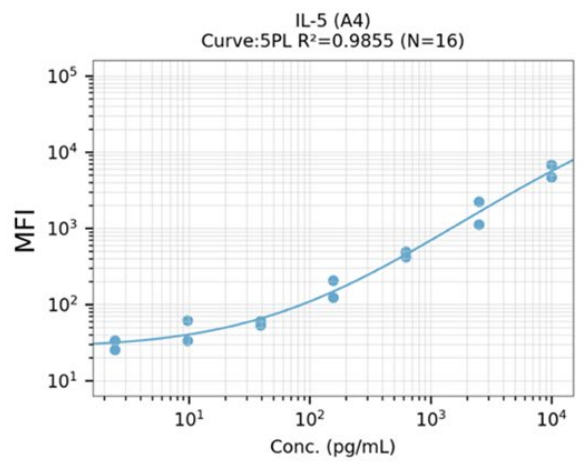

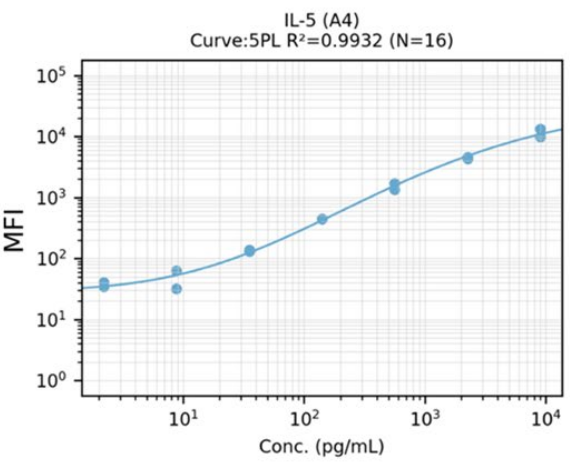

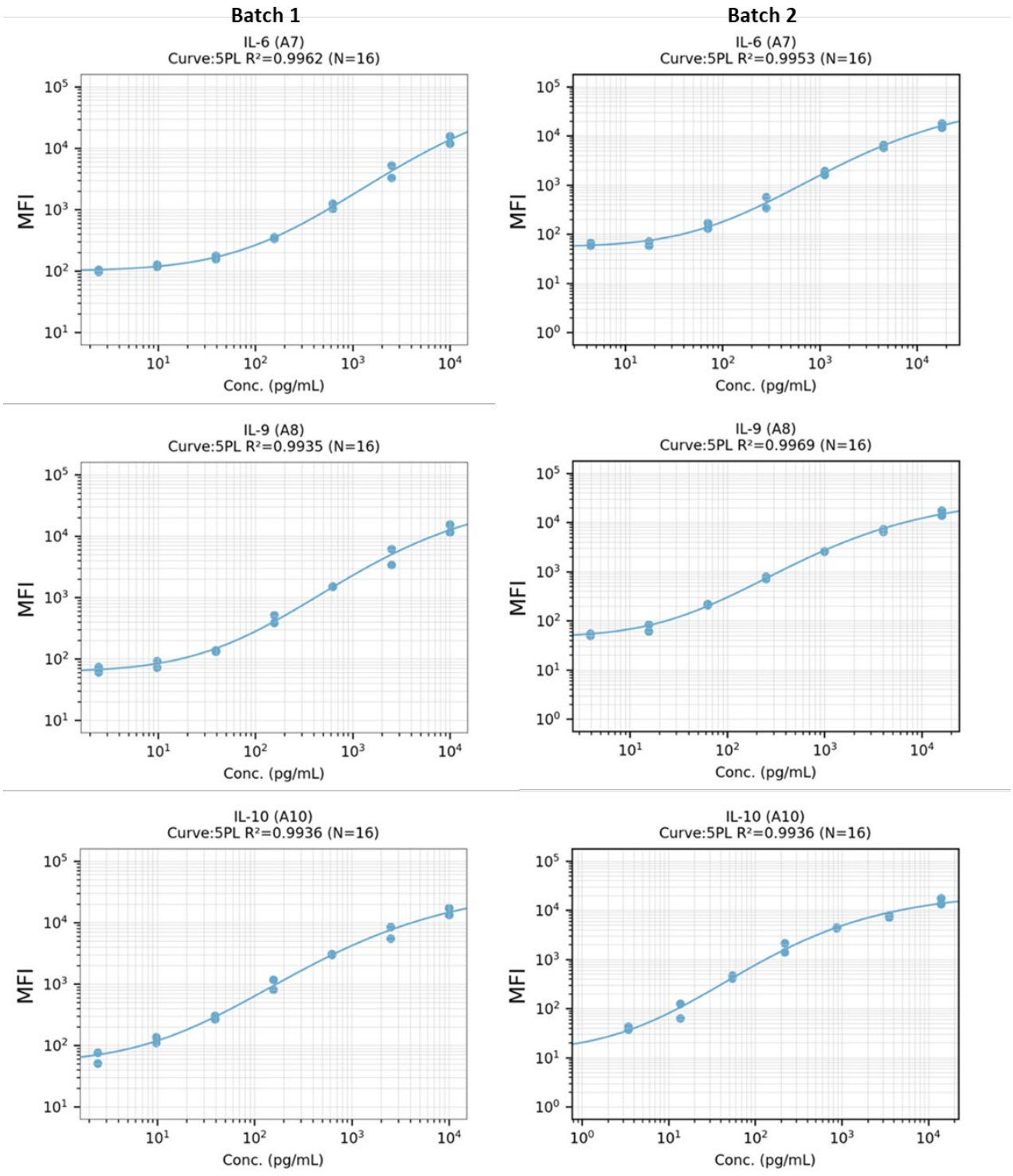

Appendix 9. Cytokine standard curves. Cytokine standard curves were created for each cytokine for each batch. 5 parameter logistics curves were created and plotted with the raw MFI (mean fluorescence intensity) values from each standard replicate.

A)

Batch 1														
Sample	**Treatment**	**Replicate**	**IL-5**	**IL-13**	**IL-2**	**IL-6**	**IL-9**	**IL-10**	**IFN-γ**	**TNF-α**	**IL-17A**	**IL-17F**	**IL-4**	**IL-22**
C0	Standard	1	2.97	0.00	0.00	3.47	0.00	0.00	0.00	0.00	0.00	0.19	0.00	0.00
C0	Standard	2	0.00	7.92	3.46	0.00	4.51	1.87	1.20	6.70	1.02	0.35	1.69	2.26
C1	Standard	1	4.06	12.32	4.54	0.00	5.11	0.00	9.22	25.53	1.06	4.73	1.31	1.89
C1	Standard	2	0.00	0.00	5.91	2.73	0.00	3.29	4.62	9.52	1.32	1.38	2.46	2.52
C2	Standard	1	34.90	11.16	13.83	14.46	13.56	12.81	13.08	18.80	6.21	11.61	16.15	12.57
C2	Standard	2	4.06	8.62	1.80	9.24	4.81	8.67	4.07	1.59	3.59	5.65	5.64	7.24
C3	Standard	1	24.50	42.41	43.16	45.79	35.07	41.81	33.53	25.53	19.39	40.44	34.01	39.73
C3	Standard	2	33.13	34.76	32.16	32.64	32.11	35.21	30.51	9.52	18.04	35.55	35.32	37.37
C4	Standard	1	244.06	200.34	215.30	161.12	204.09	203.56	163.56	196.40	90.98	177.76	162.79	152.92
C4	Standard	2	119.32	118.05	120.40	145.00	148.35	132.05	161.29	187.10	83.52	167.66	174.73	162.21
C5	Standard	1	681.86	734.99	685.33	699.44	648.35	652.12	701.80	626.65	285.45	639.90	666.66	679.19
C5	Standard	2	575.48	597.89	609.16	576.97	631.19	637.45	604.74	650.53	290.42	606.44	596.63	603.32
C6	Standard	1	1690.93	1720.42	1482.23	1941.76	1573.56	1491.33	1833.60	1664.76	990.16	1387.10	1842.46	1968.61
C6	Standard	2	3532.54	2988.27	3475.57	3176.92	3325.70	3112.77	3203.03	3396.81	1449.93	3306.13	2921.79	2664.10
C7	Standard	1	12547.87	15088.52	14217.03	12145.10	15189.85	16254.77	14594.01	14809.21	6867.52	26635.40	14739.62	14719.87
C7	Standard	2	8138.18	8273.72	8808.77	8347.80	8497.90	7975.31	7214.01	6909.21	4352.84	6250.05	7566.46	7964.11
276	Mit		1597.01	437.48	317.34	33929.16	102.26	141.21	11685.34	524.57	51.58	216.72	85.51	414.20
279	Mit		6288.67	486.38	171.98	28339.34	922.56	124.68	2143.62	677.27	18.43	99.60	44.44	107.67
284	Mit		2888.83	19.88	3322.87	39174.98	443.41	410.52	11650.16	706.04	104.77	219.56	99.90	230.42
285	Mit		3350.06	1019.69	894.48	20282.54	814.98	272.08	16384.48	2009.02	117.53	203.30	286.26	131.42
286	Mit		3368.22	854.26	3560.87	20176.58	1365.68	466.73	6067.94	2213.36	342.33	463.72	338.35	623.09
289	Mit		4432.54	483.51	108.37	11547.58	283.52	43.36	1870.37	246.65	19.12	121.41	53.16	49.18
293	Mit		6243.07	1389.41	1326.75	43447.86	1716.43	366.47	7978.25	453.67	63.74	195.60	236.59	263.11
295	Mit		12082.24	953.37	1186.71	45144.58	1787.46	747.12	41451.21	696.45	236.56	544.55	503.94	1025.05
299	Mit		22101.49	2539.19	612.58	36034.77	1310.09	170.04	4132.77	300.66	32.87	17.59	696.87	50.98

300	Mit		2534.17	534.80	430.60	24523.23	594.20	196.41	9777.41	1042.43	54.72	131.86	75.90	66.77
303	Mit		292.71	93.12	288.29	28953.57	15.76	61.67	6821.91	653.32	48.89	158.52	69.77	99.87
304	Mit		20311.48	3339.73	1520.29	37499.51	4434.97	685.10	47269.61	869.39	315.22	342.29	364.65	286.94
306	Mit		4173.67	832.57	867.49	32945.17	281.63	234.58	16479.83	955.94	263.99	438.90	176.15	474.61
307	Mit		15312.34	2393.66	669.67	46494.70	944.90	239.56	43191.79	3714.64	234.79	545.42	345.34	359.05
308	Mit		7456.35	827.15	193.08	29154.35	750.91	292.68	32736.64	907.86	36.08	79.65	128.09	77.11
311	Mit		6061.08	1153.40	224.25	35488.68	989.03	185.36	18879.58	486.68	84.43	240.36	274.62	230.97
313	Mit		3856.45	898.39	208.34	21488.93	325.49	71.15	7714.51	562.59	19.12	50.93	162.91	41.97
314	Mit		23304.25	3190.83	1159.04	21000.56	1709.16	103.31	4747.40	691.65	134.82	137.80	1239.26	101.03
316	Mit		7113.82	1506.91	750.19	36607.37	1068.90	527.60	33201.52	515.08	81.19	212.46	232.82	404.57
317	Mit		7771.46	1179.67	255.55	32194.85	525.98	77.25	5230.42	715.63	43.30	118.81	149.20	76.52
318	Mit		44597.58	8481.05	1959.26	35762.99	2755.51	170.55	20080.02	773.25	74.61	161.22	1268.08	139.36
319	Mit		23858.94	4925.12	908.36	17139.87	1142.93	225.43	4800.09	224.52	99.51	101.50	800.05	58.15
320	Mit		4921.39	756.53	130.60	19505.29	168.47	46.48	2468.24	486.68	22.16	126.62	130.25	89.99
321	Mit		25585.53	4341.31	751.68	20709.07	1266.18	425.30	18760.98	496.14	332.00	295.69	921.65	96.39
322	Mit		1544.11	374.86	65.35	4726.31	183.89	32.90	620.68	291.58	16.50	114.94	49.66	51.58
323	Mit		15517.53	3252.74	1996.77	38753.74	1718.42	225.43	19017.76	420.81	118.56	297.20	461.76	196.62
325	Mit		5019.72	453.34	55.01	15255.26	688.18	114.47	5327.93	181.12	43.38	108.51	84.64	57.55
327	Mit		2798.84	591.28	189.66	27111.98	102.92	82.88	5322.19	806.89	51.42	112.36	91.62	100.74
328	Mit		14931.82	2800.35	898.98	24102.50	1221.80	368.70	2671.92	95.17	158.01	242.54	299.53	237.52
329	Mit		10963.18	2524.54	178.05	16624.18	2502.12	273.68	17870.08	667.69	43.30	181.72	292.07	84.15
330	Mit		5019.72	1126.80	516.25	33851.56	831.64	325.18	9141.09	975.16	314.84	350.84	277.95	130.85
331	Mit		7128.46	1557.92	759.89	17640.26	516.13	317.28	15130.50	309.77	88.63	196.30	280.44	142.47
332	Mit		242.76	14.35	9.09	448.50	6.62	37.17	1152.99	44.23	9.90	25.31	58.40	13.33
333	Mit		3010.55	644.71	79.43	41785.71	501.36	171.82	7871.38	215.75	87.28	220.98	86.38	328.45
334	Mit		7768.99	1674.69	447.37	22935.80	922.56	268.89	20971.61	667.69	69.50	133.18	254.18	151.77
336	Mit		12159.56	7164.19	1100.89	22827.59	2304.60	408.54	19269.86	420.81	130.72	147.77	574.29	279.91
338	Mit		4134.49	1465.13	310.61	40042.67	65.54	384.04	3921.09	185.40	23.44	333.78	171.03	162.99
339	Mit		6082.60	1246.20	860.00	23011.56	1090.82	322.45	28691.57	667.69	154.80	157.17	260.45	100.45

342	Mit		12547.64	2444.76	2943.01	24483.28	710.93	207.25	22796.78	477.23	272.08	277.75	533.89	521.67
345	Mit		8748.05	982.05	1402.58	30874.94	1623.57	549.75	35563.80	864.58	454.34	778.79	420.25	586.00
350	Mit		34749.25	6109.50	18370.42	52384.76	9688.71	3577.57	82857.04	3982.03	3674.87	2500.70	2109.54	2409.26
351	Mit		7677.72	1002.61	335.46	27331.54	753.37	381.25	8103.31	927.09	62.97	62.10	224.41	104.21
355	Mit		4026.32	868.20	1250.05	35736.26	1210.41	482.46	38509.52	246.65	105.37	255.64	257.11	173.88
356	Mit		11517.41	1923.15	647.67	32527.25	1097.09	72.37	43459.50	1329.70	42.98	126.62	472.72	88.24
360	Mit		3516.05	786.44	429.45	26625.94	450.21	278.48	6658.48	346.45	72.17	204.70	166.33	300.98
363	Mit		2292.98	468.68	81.41	20002.88	425.50	149.26	4753.99	207.02	47.38	99.60	153.06	207.93
365	Mit		1574.96	229.64	124.19	12089.20	70.79	79.45	13311.61	1756.15	29.87	137.14	54.03	192.20
366	Mit		6147.21	332.59	1397.84	57358.62	1191.46	593.13	35984.34	6432.50	552.67	1702.93	279.61	1403.56
377	Mit		5832.09	1547.28	515.87	45329.12	591.13	212.43	19935.36	840.54	60.65	153.13	207.54	186.94
379	Mit		10091.41	1776.47	185.38	21047.45	1298.62	106.77	2664.06	264.52	47.14	127.28	95.11	110.84
390	Mit		9624.71	2206.17	269.36	28346.00	3082.58	513.05	22024.60	1004.00	173.80	225.27	310.29	189.71
392	Mit		2805.58	575.74	207.50	44492.75	977.21	215.54	23732.20	2009.02	111.05	238.20	132.41	590.83
396	Mit		6705.68	867.81	196.49	27948.29	529.67	151.79	10309.76	198.33	73.09	159.87	102.08	262.02
397	Mit		6778.34	222.11	1145.24	22071.57	1356.08	391.05	5589.02	706.04	96.39	217.43	205.01	195.79
399	Mit		15043.50	2182.83	392.62	24606.29	2562.35	236.67	37025.50	1934.34	59.48	188.64	321.03	121.16
401	Mit		2375.50	868.20	2453.34	53911.33	483.50	612.18	31621.97	624.62	166.82	437.26	142.75	1884.86
406	Mit		7004.19	1747.84	3229.77	43447.86	2053.32	752.98	40758.74	1056.83	384.86	573.44	259.61	749.71
407	Mit		764.76	165.02	93.60	39205.33	106.18	167.50	5479.39	850.16	25.32	83.34	67.15	37.76
410	Mit		3691.69	672.22	235.03	42457.78	233.01	292.41	13936.58	581.65	196.17	300.21	100.34	210.68
411	Mit		6065.86	1086.21	316.55	43236.12	1140.41	154.06	40423.29	1281.97	111.64	255.64	229.45	453.76
417	Mit		8841.14	707.44	65.35	45899.30	505.06	252.98	8162.59	420.81	207.77	187.95	247.07	2830.73
422	Mit		1462.66	345.94	55.53	20932.47	62.92	47.92	1038.68	383.49	25.57	104.68	57.96	71.21
424	Mit		1797.93	416.42	131.51	58007.44	80.64	377.33	9547.54	1732.62	122.37	169.38	124.64	229.33
430	Mit		5184.00	592.48	194.79	5640.10	1572.55	187.16	30277.24	1429.74	37.23	150.45	214.30	90.28
431	Mit		4930.75	975.85	710.67	55262.05	440.33	252.98	20602.60	2361.03	155.02	478.77	117.71	633.05
434	Mit		1625.67	248.87	29.96	45688.56	159.45	604.79	10292.92	3079.11	21.72	49.19	170.60	96.39
439	Mit		3168.73	712.12	65.86	51562.48	416.22	1694.75	60105.02	5244.12	109.13	310.81	112.07	1196.84

444	Mit		734.35	40.73	41.11	55767.40	90.47	1784.56	66965.38	7746.44	158.88	291.94	26.74	1698.25
448	Mit		660.64	195.33	112.13	54367.33	112.72	93.19	42560.75	237.77	68.51	114.94	34.90	905.62
357	Nil		93.56	59.44	56.58	15321.67	0.00	72.37	106.12	792.47	15.79	108.51	40.96	41.07
360	Nil		106.74	62.60	53.43	307.92	66.85	3.75	71.15	337.24	9.53	38.38	54.90	24.84
363	Nil		131.78	71.78	66.37	1187.71	62.92	28.90	126.99	467.80	11.52	58.54	136.72	28.74
365	Nil		95.43	39.81	60.21	225.26	93.10	36.45	51.23	802.08	35.10	245.44	44.44	107.10
366	Nil		48.99	81.98	37.81	25167.01	0.00	17.56	212.88	102.95	3.59	17.09	12.91	15.07
370	Nil		39.13	35.07	43.83	18466.36	16.38	18.93	11.03	176.85	4.48	21.14	48.79	9.35
371	Nil		389.84	180.39	60.21	1054.11	43.29	21.69	623.93	754.04	18.43	95.82	60.15	43.78
376	Nil		20.94	63.38	19.39	427.27	0.00	10.21	38.17	58.05	3.59	38.94	0.00	8.79
377	Nil		59.24	58.64	31.10	31523.74	0.00	55.62	5.59	135.03	12.50	97.08	52.28	30.54
379	Nil		80.64	0.00	2.59	13043.85	0.00	28.20	69.10	898.24	10.26	66.88	36.62	27.54
390	Nil		366.48	93.12	66.37	30367.12	80.64	85.57	418.75	1868.82	14.20	95.82	153.92	50.68
392	Nil		14.18	51.25	18.17	13666.19	43.94	21.69	60.03	159.92	2.12	14.14	0.00	11.04
396	Nil		0.65	38.88	38.92	96.00	30.33	1.11	111.57	58.05	5.92	0.00	93.36	6.61
397	Nil		248.97	94.48	13.13	13710.89	25.85	79.69	149.32	610.28	3.42	1.69	36.62	0.47
399	Nil		54.07	22.33	4.50	7378.00	11.44	26.56	75.27	309.77	11.34	87.68	16.20	32.35
401	Nil		45.66	6.36	10.47	7223.23	55.05	17.11	81.52	110.84	6.82	62.69	14.55	30.54
406	Nil		15.48	0.00	25.34	20384.57	0.00	69.93	27.80	102.95	3.42	30.67	20.38	19.18
407	Nil		91.70	70.28	55.53	900.17	55.05	16.20	176.43	282.53	18.25	97.08	38.36	47.38
410	Nil		55.78	0.00	0.00	51796.48	4.84	177.18	36.39	305.21	4.84	21.14	5.70	7.15
411	Nil		20.94	73.26	24.17	44951.68	0.00	105.04	49.31	65.20	0.00	6.80	51.41	22.15
417	Nil		15.48	86.22	0.00	48342.78	20.14	240.35	27.80	355.68	9.17	74.14	36.19	22.15
422	Nil		66.25	6.36	31.10	107.55	19.51	8.27	58.05	237.77	3.59	42.89	31.45	21.56
424	Nil		3.94	43.44	14.42	61051.71	9.01	523.43	69.10	1538.94	6.46	56.77	50.54	28.74
430	Nil		205.79	97.85	61.24	242.37	55.05	25.86	32.88	1272.41	16.76	114.94	79.83	49.48
431	Nil		0.65	0.00	0.00	36959.10	0.00	50.56	0.14	13.39	7.91	24.79	12.50	9.35
434	Nil		2.15	14.35	0.00	4145.80	70.79	6.80	227.74	543.57	1.06	20.12	108.16	7.15
439	Nil		32.81	31.08	13.13	42138.88	0.00	283.56	10.42	562.59	6.46	55.60	17.87	28.44

444	Nil		19.54	0.00	13.13	55976.14	16.38	423.87	22.97	439.57	0.40	0.00	8.86	12.75
448	Nil		5.94	36.04	13.78	6337.90	44.59	14.40	53.16	176.85	2.38	19.10	23.76	8.79
307	Nil		42.37	42.55	28.81	42417.31	0.00	119.69	21.43	99.05	1.79	2.77	38.36	8.79
316	Nil		14.18	21.12	0.00	4054.96	3.09	14.85	11.03	37.59	12.14	82.11	61.46	35.96
317	Nil		52.37	79.11	51.85	961.54	46.55	9.56	113.76	273.51	2.04	16.10	17.87	22.15
318	Nil		42.37	31.08	28.81	20418.17	25.85	28.43	142.59	754.04	8.99	53.25	67.15	32.35
319	Nil		52.37	14.35	31.10	8641.93	5.43	36.22	9.25	21.97	4.84	17.09	19.96	17.41
320	Nil		181.44	89.70	45.45	16348.68	35.49	45.76	79.43	496.14	19.47	165.29	39.22	56.96
321	Nil		22.35	46.10	4.50	388.23	25.21	2.21	7.59	220.13	3.16	19.10	2.61	7.70
322	Nil		118.22	59.44	77.44	345.48	52.43	33.85	377.05	821.31	31.71	260.03	94.67	95.23
323	Nil		20.94	10.99	125.11	4214.09	19.51	18.47	147.07	54.53	11.69	83.34	63.65	38.67
325	Nil		77.00	29.01	38.92	177.51	27.77	22.15	142.59	237.77	18.78	130.55	40.09	50.38
327	Nil		127.89	19.88	77.44	735.48	0.07	24.00	184.38	634.18	14.91	111.72	22.91	50.68
328	Nil		2.15	0.00	0.00	656.78	0.00	4.74	0.14	126.88	0.00	3.53	0.00	0.00
329	Nil		80.64	0.00	48.13	140.63	0.00	20.08	65.04	411.46	15.79	114.94	0.24	45.88
330	Nil		0.65	0.00	35.59	433.46	6.62	7.43	22.19	0.00	1.87	18.09	0.00	7.70
331	Nil		18.16	19.88	33.36	209.05	12.05	18.93	39.98	147.39	16.50	125.32	33.60	45.28
332	Nil		106.74	14.35	24.76	46.42	58.98	13.07	100.70	185.40	11.07	46.31	90.75	26.94
333	Nil		0.00	19.88	20.60	6773.08	0.00	14.40	99.62	237.77	5.92	40.63	58.40	29.64
334	Nil		59.24	0.00	25.34	3297.03	17.63	16.20	39.07	126.88	11.16	83.34	8.86	33.55
336	Nil		290.62	38.88	57.10	5517.56	41.99	39.55	200.32	543.57	20.69	121.41	11.28	54.87
338	Nil		34.37	17.25	31.10	26104.98	0.00	70.90	85.73	151.55	14.55	79.03	82.02	30.24
339	Nil		11.66	0.00	0.00	1391.33	0.00	13.07	8.68	562.59	6.73	54.42	6.49	18.00
342	Nil		32.81	0.00	0.00	17134.70	3.09	28.67	3.85	151.55	0.00	0.00	12.09	4.53
345	Nil		0.00	18.59	0.00	701.81	23.94	11.74	34.62	176.85	0.61	8.55	7.67	6.61
350	Nil		712.66	137.43	102.70	33128.91	21.40	83.61	103.95	3.19	3.59	5.95	22.91	6.08
351	Nil		95.43	14.35	0.00	548.75	29.05	10.86	1.78	406.78	9.35	46.31	6.49	47.08
355	Nil		203.75	82.69	82.89	38876.38	28.41	159.88	208.31	515.08	9.26	65.68	27.16	147.27
356	Nil		122.07	64.16	65.86	27071.42	2034.87	54.41	68.08	811.70	19.47	150.45	48.79	51.58

276	Nil		48.99	0.00	45.45	1985.72	70.79	15.75	57.07	1195.88	20.69	141.11	13.73	64.10
279	Nil		181.44	65.71	165.43	10406.69	30.33	35.74	410.88	467.80	14.55	102.14	33.17	181.39
284	Nil		10.45	31.08	128.32	110.22	7.81	4.54	93.17	159.92	1.62	0.09	9.67	8.24
285	Nil		213.96	107.72	112.13	499.62	43.29	39.55	244.90	927.09	24.13	232.43	63.65	81.80
286	Nil		129.83	33.10	27.09	128.08	0.00	19.39	83.62	402.12	17.99	135.82	4.15	49.78
289	Nil		55.78	22.33	18.17	172.11	0.00	29.61	17.71	486.68	24.13	195.60	22.07	71.80
293	Nil		133.73	38.88	16.93	52026.33	23.94	389.09	162.84	1186.31	13.31	85.82	72.40	58.75
295	Nil		0.00	0.00	28.24	37.17	0.00	1.29	8.13	0.00	0.68	0.00	0.00	0.00
299	Nil		8.12	56.21	0.00	7228.05	16.38	29.37	7.59	420.81	0.00	0.00	53.16	6.61
300	Nil		26.73	0.00	32.23	185.62	12.67	18.02	61.03	524.57	15.88	126.62	19.54	55.16
303	Nil		0.00	0.00	15.68	543.49	25.21	7.85	21.43	31.17	4.30	0.00	46.18	1.24
304	Nil		29.73	53.75	72.44	2512.30	11.44	17.11	84.68	287.05	4.22	40.63	74.15	14.49
306	Nil		87.99	6.36	18.78	4511.62	14.52	31.96	7.59	648.54	13.84	66.88	0.00	26.34
308	Nil		0.65	68.01	36.71	7902.22	9.62	30.08	70.12	68.84	4.48	5.95	16.20	18.59
311	Nil		69.80	61.03	58.14	12102.69	0.73	19.85	153.82	220.13	7.91	55.60	68.02	42.58
313	Nil		3.02	33.10	0.00	112.00	12.67	13.96	11.64	936.71	14.20	66.88	11.28	29.34
314	Nil		0.00	0.00	0.00	979.41	0.00	5.76	49.31	5.58	0.00	11.29	0.00	0.00

B)

Batch 2

Sample	Treatment	Replicate	IL-5	IL-13	IL-2	IL-6	IL-9	IL-10	IFN-γ	TNF-α	IL-17A	IL-17F	IL-4	IL-22
C0	Standard	1	0.00	21.38	0.00	0.00	0.00	0.13	12.02	2.01	0.55	0.15	0.00	0.00
C0	Standard	2	2.53	15.30	5.82	7.46	6.41	0.47	0.00	0.00	0.00	0.32	9.45	2.61
C1	Standard	1	2.09	0.00	2.94	11.91	4.37	4.58	10.79	6.48	1.56	2.91	0.00	1.24
C1	Standard	2	4.10	0.00	3.99	4.00	1.89	3.69	12.02	6.48	1.94	2.91	0.00	1.45
C2	Standard	1	12.31	16.40	9.64	15.19	16.71	16.34	20.07	24.37	5.95	12.73	4.75	9.28
C2	Standard	2	1.22	0.00	4.94	4.00	7.27	7.57	9.01	6.48	4.41	7.42	7.08	4.89
C3	Standard	1	36.98	57.50	31.81	62.43	65.58	53.43	27.44	60.64	20.92	40.04	22.57	30.85

C3	Standard	2	40.26	53.25	58.41	93.39	71.36	62.35	48.44	112.41	27.39	48.45	33.63	45.49
C4	Standard	1	149.96	218.85	134.52	218.13	244.31	190.86	161.16	318.39	86.44	159.58	98.62	119.30
C4	Standard	2	149.07	215.01	148.73	371.96	277.14	313.50	265.88	371.51	112.80	207.86	140.33	206.73
C5	Standard	1	620.05	992.71	692.11	1233.35	958.34	842.84	915.43	1333.06	354.09	754.93	468.01	543.78
C5	Standard	2	474.53	817.75	691.55	1021.14	934.57	900.19	916.43	1121.27	371.90	594.45	362.79	459.22
C6	Standard	1	1924.68	3505.52	3306.59	4721.99	3805.39	2575.40	5075.49	4815.02	1373.25	2437.27	1819.95	2048.72
C6	Standard	2	2089.83	3046.17	1957.29	3982.96	3115.73	2068.86	4509.09	4660.84	1483.28	1920.87	1692.12	2094.46
C7	Standard	1	14297.27	20457.72	17894.03	22111.19	26932.52	58810.60	23101.23	25731.00	7168.56	26150.23	8541.80	11495.56
C7	Standard	2	7293.93	11297.93	5495.24	15536.40	13921.78	12581.95	16558.77	16638.57	5688.17	9625.86	5732.93	9101.47
272	Mit		6314.76	3989.08	4727.62	72148.77	6890.17	707.05	60034.41	963.85	552.66	1105.73	316.99	2157.87
274	Mit		3604.74	1667.07	91.64	99903.49	688.11	101.09	25756.49	2082.75	27.95	234.35	97.20	510.61
278	Mit		3478.94	2345.51	434.56	44612.34	707.87	126.68	11362.18	297.51	23.10	47.11	133.74	258.38
280	Mit		2627.55	776.80	132.71	39770.19	462.90	180.92	31877.45	747.64	168.20	508.65	78.22	1371.22
281	Mit		5708.28	403.81	517.57	35817.73	2174.73	267.31	32217.88	1498.34	158.32	566.70	218.45	1364.04
282	Mit		1155.12	722.53	84.12	38066.20	121.92	147.95	7639.38	655.27	135.15	184.82	64.51	532.50
283	Mit		5562.03	2448.07	2489.13	52857.40	1160.42	454.87	65564.34	4565.88	348.44	373.47	143.54	1570.90
288	Mit		5250.94	1580.03	161.04	40949.91	1342.02	180.41	30253.11	263.31	57.86	162.71	80.26	770.26
290	Mit		8295.54	172.86	2259.68	91657.35	716.86	710.96	55220.07	7319.36	1501.68	1322.76	469.22	7659.85
291	Mit		20803.79	11131.68	5546.20	87019.73	11425.49	856.84	64048.37	4561.59	316.30	913.21	1060.87	2307.66
292	Mit		5502.62	2926.65	814.63	49688.47	1643.17	203.99	26787.42	945.50	309.43	354.54	177.00	786.98
294	Mit		12776.34	5524.42	652.42	35011.54	6406.16	300.81	18665.56	222.57	141.10	221.87	463.61	521.94
296	Mit		5878.56	2512.74	3903.14	62203.74	3332.50	179.39	71534.83	3913.52	203.41	378.63	162.94	1111.86
297	Mit		37.99	62.91	18.58	11259.00	0.00	28.41	204.92	169.04	6.13	7.14	18.90	12.77
301	Mit		16442.81	5349.82	249.71	83928.96	3036.53	467.73	23431.71	329.58	190.61	455.32	374.80	657.00
302	Mit		5752.29	865.79	254.12	32149.46	1260.27	145.45	6117.64	169.04	124.97	141.85	174.45	115.24
309	Mit		30501.39	4249.74	2754.79	66509.30	11796.64	518.19	19054.78	743.02	266.90	277.58	1320.91	1195.52
310	Mit		8153.34	1253.10	535.95	63416.39	769.20	289.43	69218.79	5037.30	550.39	429.05	174.45	893.60
312	Mit		4464.13	2407.27	123.07	43376.96	279.48	37.95	2647.26	322.70	8.36	33.80	80.94	74.08
315	Mit		14810.19	4207.85	361.73	65075.52	564.94	180.58	67589.74	6486.01	150.57	101.66	331.72	521.75

324	Mit		44179.17	14237.37	680.46	58506.69	12005.57	621.67	40869.07	479.49	761.48	574.57	1181.34	1302.78
326	Mit		14476.75	11456.96	2911.18	45087.89	4757.83	362.86	49604.25	927.14	566.48	685.49	482.10	2056.40
335	Mit		15811.38	6537.07	243.72	50552.55	5192.65	210.55	18588.10	733.79	123.59	277.37	395.52	340.92
340	Mit		11771.07	3092.44	1181.03	137985.25	1486.16	564.23	58969.98	6146.05	386.09	1880.03	180.81	1385.59
343	Mit		6562.23	4103.99	626.25	62728.74	1941.67	201.93	20496.27	308.95	182.11	218.68	166.79	764.05
344	Mit		14748.27	4968.41	1967.33	73632.82	8083.30	563.78	65155.39	3047.25	360.48	352.73	532.65	2072.22
346	Mit		9515.63	5177.67	2013.83	32807.94	3770.97	475.25	24759.70	2333.28	160.66	451.95	437.11	364.05
347	Mit		15626.17	7917.69	2821.74	81452.58	10577.52	1082.49	69305.71	6065.23	344.53	1190.70	235.74	1896.05
348	Mit		33806.72	5571.22	371.74	54099.60	10340.75	151.12	27048.38	1014.26	123.66	107.24	555.78	826.74
349	Mit		4318.17	2355.78	1761.38	83228.37	3616.05	747.88	64918.63	3223.91	266.70	313.39	300.39	1127.09
353	Mit		2824.52	1998.73	509.92	89042.72	2158.91	701.19	33236.43	1768.11	213.30	345.94	117.26	1437.42
354	Mit		11558.00	5185.42	1011.28	72148.77	9815.25	749.88	46626.63	1371.74	402.71	1349.68	439.94	2113.00
358	Mit		7967.06	2978.75	349.85	91900.97	5182.44	478.60	28627.08	2209.29	231.54	552.73	183.35	1076.67
359	Mit		940.17	149.99	136.02	54014.02	93.75	120.89	34.55	2951.09	52.53	90.17	48.61	1666.02
361	Mit		13957.96	6447.21	993.31	46934.07	3407.62	259.06	49995.10	3664.79	296.21	265.42	816.32	1662.92
362	Mit		8539.57	4108.12	184.20	70602.66	4808.95	307.65	49781.38	885.80	144.37	1003.50	235.74	1427.19
364	Mit		8177.74	4557.26	298.72	76365.52	2612.56	517.32	61292.11	4282.17	579.49	2318.76	236.97	2880.72
367	Mit		530.53	53.29	22.35	53584.17	37.76	125.03	8647.75	1312.81	48.52	64.15	46.53	294.19
369	Mit		267.65	205.95	29.56	15391.34	37.76	21.88	2806.99	341.07	10.19	27.05	38.21	39.67
372	Mit		12444.24	3920.04	400.86	63399.21	8381.59	648.51	24267.46	733.79	537.32	694.90	499.39	445.94
373	Mit		8291.85	6543.33	1016.43	29952.09	7207.73	393.90	38192.71	1260.59	552.00	679.97	380.57	970.94
374	Mit		1657.33	1729.79	336.33	37994.19	1017.52	216.44	10223.30	1328.69	197.82	231.03	169.35	1470.36
375	Mit		15736.30	3748.41	115.14	75376.96	2080.44	373.33	19000.95	572.02	101.91	301.02	207.25	418.11
378	Mit		2454.48	2024.27	268.27	35817.73	652.29	333.46	56449.65	9123.12	64.73	207.01	327.02	828.11
380	Mit		21811.97	10000.08	198.25	60471.41	12674.08	388.78	27951.78	858.21	114.41	384.05	352.18	911.73
381	Mit		10631.02	4857.68	88.10	72148.77	1521.09	290.90	33398.62	2167.15	200.68	347.41	244.93	2469.56
382	Mit		9690.02	4108.12	153.62	49716.14	3403.54	162.85	44320.85	1153.62	103.11	97.77	249.20	620.06
384	Mit		21138.68	5445.09	177.26	70830.46	9154.28	437.64	26668.85	414.79	161.31	691.29	291.45	1448.53
385	Mit		12212.42	6253.40	1422.91	84432.87	4932.76	429.92	37238.54	511.87	157.34	315.17	363.23	1237.14

389	Mit		3159.20	2259.72	608.86	46331.27	3466.37	540.59	61811.10	497.99	661.77	750.90	192.20	1497.01
391	Mit		4676.99	2944.80	250.88	73608.17	2560.67	393.90	53818.58	1498.34	606.33	1596.98	169.35	2259.29
394	Mit		6765.72	3764.30	2088.27	85205.54	7186.82	403.81	68864.51	844.40	112.96	585.21	178.27	696.32
398	Mit		3604.74	1779.54	639.83	51354.81	705.17	94.82	23147.90	1283.30	129.71	98.64	134.40	755.90
400	Mit		21058.29	7259.43	730.50	121233.35	12793.97	602.12	47068.44	9009.04	245.45	1152.55	186.52	6755.18
402	Mit		6112.60	3049.49	520.46	45129.30	1565.94	222.70	51105.62	853.61	251.93	543.06	259.55	1474.65
403	Mit		8884.87	4682.69	263.40	71791.79	2082.11	107.03	11518.34	236.11	238.59	94.09	358.00	823.23
404	Mit		7981.47	3358.24	313.52	74774.63	2052.10	393.11	50484.78	894.99	244.21	509.89	213.48	2015.28
405	Mit		3014.77	184.82	181.52	73357.31	943.04	310.06	46401.79	191.21	394.73	1000.71	131.77	2737.89
408	Mit		8022.40	120.91	194.11	47726.98	2191.71	230.04	3751.73	1233.31	43.64	122.18	290.25	190.01
413	Mit		11449.45	3761.65	348.86	63253.47	4063.87	304.69	14689.63	1432.84	207.51	147.23	173.18	3356.12
415	Mit		223.23	287.99	86.78	43198.44	75.53	232.14	46521.27	1734.50	93.46	201.50	64.51	602.39
416	Mit		3175.75	1364.57	244.38	74515.03	940.27	288.70	18610.03	982.19	223.32	178.92	96.53	741.95
418	Mit		4456.47	2792.29	437.04	81133.14	1353.86	339.90	42424.88	1478.02	314.30	304.55	176.36	963.98
420	Mit		6653.86	4865.17	695.15	94422.38	2380.52	204.68	45899.51	599.78	182.95	514.12	150.04	1524.43
421	Mit		1067.46	541.47	71.63	57622.66	64.20	152.12	15401.56	1344.56	44.09	61.86	34.05	174.17
423	Mit		2652.85	3055.00	473.60	37994.19	1637.99	191.98	28813.84	142.79	141.76	345.60	95.18	633.52
426	Mit		5076.80	2721.07	125.67	40932.27	1335.62	61.98	31175.69	1721.04	226.06	433.20	105.26	676.26
428	Mit		2388.86	2921.82	1650.99	63652.86	1004.42	248.02	40364.05	669.14	295.81	635.95	204.75	853.93
432	Mit		1453.35	848.04	260.96	39486.75	625.94	136.63	18170.33	299.80	255.73	146.49	113.27	151.03
433	Mit		3194.51	2549.88	296.58	14845.40	643.35	343.51	48296.82	4917.46	69.50	240.87	225.88	1103.75
435	Mit		1439.23	453.60	49.96	83594.64	388.76	711.20	45887.76	12931.29	139.60	291.35	73.43	1496.58
437	Mit		1899.73	639.10	57.19	81073.73	228.92	317.69	64845.00	5912.04	74.22	413.13	87.74	2013.41
438	Mit		933.76	498.86	234.15	55291.40	235.34	116.27	51546.83	565.08	294.49	315.39	42.37	953.07
440	Mit		2341.05	1311.33	41.73	73367.13	766.48	782.57	73489.67	26408.87	89.81	376.34	147.44	3246.92
441	Mit		934.75	989.44	36.40	91347.68	106.69	208.65	50045.62	5903.52	118.58	689.91	101.24	1374.81
442	Mit		1224.46	594.98	59.21	60045.20	253.61	441.11	54279.38	1797.22	26.67	131.08	90.45	1009.20
446	Mit		119.44	80.42	1.44	61607.43	23.53	60.64	10889.70	2753.95	47.79	177.66	4.32	1383.47
272	Nil		2.44	25.86	3.29	44.43	0.00	0.59	6.84	24.59	0.00	0.00	16.19	0.29

274	Nil		8.66	8.26	0.00	229.45	3.78	12.66	43.01	37.94	1.82	0.00	0.00	30.12
275	Nil		10.03	20.43	8.96	60282.56	0.00	218.87	54.88	551.20	2.74	7.30	3.04	55.88
278	Nil		19.88	30.59	10.78	301.16	6.32	7.19	76.96	158.05	5.38	9.38	28.52	42.21
280	Nil		15.15	42.76	11.64	113.64	5.08	5.20	37.32	108.57	2.93	4.27	5.60	18.87
281	Nil		12.35	38.94	7.48	18438.37	2.40	36.38	31.84	134.13	0.60	3.91	0.00	16.65
282	Nil		10.49	61.35	11.64	8004.74	8.73	37.43	115.79	140.62	5.28	14.25	32.66	27.15
283	Nil		6.84	0.00	15.64	1241.51	0.00	12.28	31.84	91.93	2.37	4.44	10.83	15.37
288	Nil		27.49	58.19	18.58	288.12	9.91	7.19	112.32	93.99	4.06	7.47	25.76	17.29
290	Nil		17.98	65.96	23.99	56808.85	34.51	55.59	483.42	238.37	2.56	9.70	140.93	11.78
291	Nil		7.75	42.76	1.44	692.00	0.00	11.11	45.91	79.72	5.10	5.14	13.50	19.81
292	Nil		10.49	13.51	4.01	7828.52	17.94	21.14	12.52	54.33	1.46	0.30	1.78	14.72
294	Nil		471.19	397.34	475.96	6307.38	44.20	17.60	1036.39	451.75	6.88	11.86	37.52	32.47
296	Nil		46.57	234.30	93.29	67411.59	69.37	147.78	455.32	1060.02	6.22	51.27	55.54	1332.50
297	Nil		13.28	83.17	24.63	5538.17	8.73	25.35	300.81	195.67	6.88	12.16	47.92	26.55
301	Nil		118.52	71.90	5.87	61515.53	17.94	71.00	51.85	222.57	6.50	13.66	25.76	35.38
302	Nil		20.82	49.90	18.58	693.68	14.53	6.79	43.01	129.83	3.40	4.79	23.69	37.39
309	Nil		273.03	71.90	98.90	82764.44	44.20	152.46	310.57	380.19	7.99	21.65	63.13	120.11
310	Nil		45.61	36.96	14.49	87344.09	17.94	201.93	80.22	180.10	3.31	14.99	70.00	92.92
312	Nil		17.04	25.86	10.78	20402.44	14.53	26.25	112.32	138.45	5.47	9.70	34.05	33.93
315	Nil		57.48	44.60	34.74	172.00	0.00	6.79	73.72	31.09	2.19	0.00	0.00	27.75
324	Nil		64.09	42.76	17.14	10329.30	15.67	24.26	57.94	87.83	4.06	0.30	9.51	14.08
326	Nil		25.58	0.00	28.96	262.76	0.00	14.20	107.13	48.73	1.82	2.43	0.00	24.12
335	Nil		17.98	0.00	7.99	1006.35	3.78	9.16	61.04	45.07	3.68	1.83	21.64	29.23
340	Nil		2.01	13.51	14.88	178.91	0.00	2.83	37.32	12.96	2.00	4.27	12.16	28.04
341	Nil		17.98	34.91	10.78	18359.18	2.40	14.20	107.13	263.31	2.00	9.54	25.76	28.04
343	Nil		14.22	23.26	22.68	38110.56	15.67	74.32	124.55	433.26	5.19	10.32	34.05	22.59
344	Nil		16.57	25.86	5.87	6102.58	4.44	10.33	33.19	254.22	1.37	0.00	0.00	19.81
346	Nil		28.92	56.58	59.66	8652.78	43.13	37.43	580.29	108.57	7.06	16.15	125.19	115.24
347	Nil		16.10	34.91	5.87	5204.67	8.13	14.96	78.59	93.99	2.74	1.62	34.05	27.75

348	Nil		22.73	38.94	14.10	35762.30	9.32	20.21	67.32	188.98	3.40	9.38	29.90	18.24
349	Nil		66.92	59.78	52.10	39615.39	0.00	35.68	110.58	125.54	7.06	12.76	21.64	37.96
353	Nil		13.75	48.17	3.29	14903.57	7.54	20.58	37.32	52.45	1.28	4.79	16.19	49.95
354	Nil		23.20	13.51	21.01	72323.03	24.64	119.90	48.86	968.44	4.25	13.36	27.83	38.53
358	Nil		28.44	20.43	11.64	66160.43	15.67	138.46	47.38	304.37	3.12	12.16	5.60	21.05
361	Nil		4.17	32.80	8.96	124.87	8.73	6.40	27.87	71.73	3.68	5.81	12.16	17.60
362	Nil		741.30	545.99	331.48	14100.84	43.67	29.84	1264.25	125.54	9.09	77.75	8.19	582.99
364	Nil		4.17	42.76	0.00	57634.48	0.00	200.21	51.85	2246.97	4.44	11.24	20.27	21.05
368	Nil		23.68	49.90	6.96	695.36	9.91	9.55	57.94	45.07	0.93	3.73	45.84	13.10
369	Nil		17.04	53.29	18.58	19841.91	17.94	15.34	142.34	151.49	4.62	8.11	61.75	21.05
372	Nil		8.20	0.00	14.88	2083.36	6.32	12.66	34.55	67.79	2.56	2.23	32.66	16.01
373	Nil		32.26	17.26	17.14	394.29	0.00	11.11	34.55	54.33	1.55	3.55	13.50	20.12
374	Nil		9.57	0.00	9.42	29.29	5.08	2.83	24.04	63.89	0.93	0.65	5.60	82.11
375	Nil		38.94	67.47	33.62	60.45	0.00	4.81	34.55	8.06	0.93	34.43	8.85	13.42
378	Nil		12.35	34.91	14.88	176.94	15.67	5.60	987.47	100.20	2.19	5.48	12.16	339.74
380	Nil		36.56	62.91	5.29	23671.64	7.54	27.15	73.72	45.07	2.74	4.79	18.90	20.74
381	Nil		14.22	0.00	7.99	15020.29	0.00	21.32	48.86	56.22	1.37	3.91	0.00	13.42
382	Nil		13.28	42.76	27.14	1291.32	2.40	10.33	70.50	121.27	4.81	7.14	31.28	18.87
383	Nil		34.65	93.84	16.40	52435.61	12.24	264.97	48.86	872.00	2.93	14.40	27.14	138.10
384	Nil		18.93	0.00	15.64	35904.96	0.00	60.64	31.84	87.83	3.68	7.79	16.19	14.08
385	Nil		351.96	182.85	154.37	22171.91	54.27	51.02	2431.78	398.63	9.64	18.58	43.07	42.21
386	Nil		15.15	65.96	13.30	52077.98	17.37	190.11	81.86	1319.62	2.93	11.70	36.13	71.28
387	Nil		15.15	0.00	13.30	44909.86	5.70	79.30	24.04	373.28	2.19	5.81	8.19	12.11
389	Nil		34.17	0.00	4.67	11101.38	0.00	29.84	61.04	52.45	3.31	4.79	1.78	28.34
391	Nil		31.31	49.90	12.48	90592.99	21.30	420.02	72.11	1563.71	4.62	10.94	13.50	60.13
393	Nil		12.35	38.94	0.00	33037.98	18.50	51.53	62.59	182.32	3.31	7.47	9.51	34.22
394	Nil		16.57	42.76	12.48	66419.69	16.24	1137.58	80.22	789.14	2.46	11.09	17.55	37.68
398	Nil		10.49	0.00	23.34	7028.49	0.00	11.11	73.72	65.84	1.64	5.48	25.76	7.37
400	Nil		109.31	287.99	72.24	3451.78	75.53	31.80	928.34	609.03	2.00	5.65	6.24	428.17

402	Nil		48.47	83.17	49.72	1060.75	0.00	6.79	131.63	87.83	3.68	5.14	13.50	24.73
403	Nil		20.82	0.00	11.64	14194.16	16.81	24.62	37.32	91.93	2.37	6.15	25.76	16.01
404	Nil		17.51	20.43	21.35	31587.28	32.33	65.33	90.16	160.24	7.25	17.73	36.82	153.46
405	Nil		8.66	0.00	19.29	7986.40	0.74	27.15	227.59	18.52	2.65	6.48	20.27	19.18
408	Nil		13.28	59.78	18.58	8481.94	21.30	16.85	142.34	39.70	2.74	3.00	13.50	25.94
412	Nil		8.66	0.00	0.00	1486.05	0.00	1.86	61.04	91.93	3.12	3.37	20.27	18.55
413	Nil		6.84	42.76	0.00	2571.31	5.08	7.19	80.22	63.89	1.55	10.63	14.84	21.05
414	Nil		25.58	53.29	10.33	18117.96	13.39	354.78	96.89	821.39	3.12	12.16	29.90	96.54
415	Nil		19.40	20.43	21.35	5782.13	11.08	12.66	54.88	104.37	3.12	7.47	17.55	21.05
416	Nil		9.11	23.26	28.36	52128.42	26.85	229.69	114.05	182.32	2.56	9.38	11.49	12.44
418	Nil		9.11	34.91	27.14	26662.76	29.05	139.79	37.32	138.45	3.40	5.48	0.00	19.81
419	Nil		31.31	44.60	10.33	100801.56	7.54	845.12	83.51	678.38	5.00	12.61	9.51	58.01
420	Nil		27.97	20.43	23.66	21109.77	12.24	30.38	40.14	77.71	1.82	5.48	0.48	14.08
421	Nil		10.03	53.29	9.88	53757.97	3.78	263.72	67.32	218.07	1.82	8.75	16.19	21.36
423	Nil		8.20	13.51	10.78	89.88	0.74	3.62	64.16	87.83	2.93	5.48	25.76	14.72
425	Nil		8.66	32.80	13.30	50812.88	8.73	83.93	26.58	195.67	2.37	10.01	14.17	10.11
426	Nil		14.22	0.00	15.64	24193.14	22.42	37.95	54.88	1244.68	3.12	7.95	23.01	24.12
427	Nil		9.11	23.26	15.64	171.01	2.40	2.83	61.04	45.07	2.56	1.83	16.87	5.95
428	Nil		3.30	0.00	0.00	96.12	30.15	31.44	29.18	32.78	2.37	2.03	4.32	60.66
432	Nil		8.66	0.00	17.86	643.06	5.08	7.39	25.30	12.96	0.85	0.30	6.89	2.05
433	Nil		5.05	0.00	10.33	7075.81	0.74	25.35	27.87	31.09	1.02	0.00	0.00	17.29
435	Nil		5.94	62.91	1.44	27101.06	7.54	52.88	98.58	112.78	3.68	13.66	29.90	57.75
436	Nil		14.22	53.29	7.99	15225.79	14.53	14.96	293.02	182.32	5.57	8.75	35.44	110.56
437	Nil		17.98	20.43	8.96	7817.82	8.73	17.60	124.55	104.37	4.15	4.62	0.00	48.85
438	Nil		0.72	36.96	21.35	9137.37	0.74	24.62	169.60	41.47	1.46	4.27	12.16	29.53
440	Nil		18.93	20.43	10.78	874.74	0.00	2.06	76.96	39.70	1.11	0.30	9.51	47.76
441	Nil		56.06	65.96	13.30	19176.00	16.81	16.10	70.50	112.78	3.68	4.09	15.51	31.89
442	Nil		6.84	42.76	25.27	26777.16	3.78	84.92	48.86	108.57	3.87	11.86	25.76	44.44
443	Nil		18.46	53.29	7.99	15467.07	11.08	31.44	86.82	79.72	3.12	7.47	20.27	18.55

445	Nil		30.35	53.29	10.78	71974.89	11.08	111.64	98.58	288.37	4.25	15.72	16.19	25.34
446	Nil		17.04	53.29	15.26	1547.66	0.74	9.16	48.86	56.22	2.74	7.47	12.16	41.92
447	Nil		21.77	0.00	1.44	7078.91	13.39	18.91	131.63	96.05	5.10	8.27	20.27	27.75
450	Nil		23.68	0.00	4.67	227.53	7.54	11.11	29.18	39.70	7.25	5.14	1.78	201.64
451	Nil		19.88	25.86	6.96	38888.12	0.00	80.62	48.86	327.29	1.82	10.63	18.90	28.34

Appendix 10. Participant and standard cytokine concentrations. Cytokine concentrations were calculated from standard curves for standards, mitogen-stimulated plasma (Mit), and unstimulated (Nil) plasma samples. Samples were run across two batches; batch 1 **(A)** and batch 2 **(B)**.

						Sputum		
Participant	**Group**	**Age**	**Smoking Status**	**Fire Location**	**Participation in Cooking**	**AFB**	**Polys****	**SEC****
278	Healthy	55	Yes	Under	Yes	no sample		
280	Healthy	20	No	Under	Shared	no sample		
281	Healthy	21	No	Under	Shared	no sample		
282	Healthy	20	No	Under	Shared	no sample		
283	Healthy	45	No	Inside	Yes	no sample		
290	Healthy	44	No	Away	Yes	no sample		
292	Healthy	34	Yes	Inside	Yes	no sample		
294	Healthy	30	No	Outside	Yes	no sample		
295	Healthy	48	No	Outside	Yes	neg	0	3+
302	Healthy	46	No	Inside	No	no sample		
306	Healthy	53	No	Inside	Yes	neg	0	3+
310	Healthy	30	No	Inside	Yes	no sample		
323	Healthy	86	No	Inside	Yes	neg	0	0
324	Healthy	27	Past	Under	No	no sample		
325	Healthy	23	Past	Inside	Yes	neg	0	0
326	Healthy	51	No	Inside	Yes	no sample		
328	Healthy	59	No	Inside	Shared	neg	0	1+
340	Healthy	22	No	Inside	Shared	no sample		
343	Healthy	17	No	Inside	Shared	no sample		
344	Healthy	48	Past	Inside	No	no sample		
349	Healthy	41	No	Outside	Yes	No sample		
353	Healthy	44	Yes	Inside	Yes	no sample		
361	Healthy	50	No	Away	Yes	no sample		
363	Healthy	60	No	Inside	Yes	neg	0	0
364	Healthy	68	No	Under	Yes	no sample		
367	Healthy	55	No	Inside	No	no sample		
368	Healthy	54	No	Inside	Yes	no sample		

373	Healthy	50	Yes	Inside	No	no sample		
375	Healthy	64	No	Under	Yes	no sample		
378	Healthy	55	No	Inside	No	no sample		
380	Healthy	32	Yes	Under	No	no sample		
381	Healthy	30	Past	Under	Yes	no sample		
382	Healthy	51	No	Inside	Yes	no sample		
386	Healthy	48	No	Inside	Yes	no sample		
393	Healthy	64	Past	Inside	Yes	no sample		
396	Healthy	57	No	Away	Shared	neg	0	0
411	Healthy	52	No	Inside	Yes	neg	0	0
412	Healthy	48	No	Inside	Yes	no sample		
414	Healthy	35	No	Inside	Yes	no sample		
415	Healthy	33	No	Inside	Yes	no sample		
416	Healthy	46	No	Outside	Shared	no sample		
419	Healthy	44	No	Inside	Yes	no sample		
426	Healthy	56	No	Inside	Yes	no sample		
427	Healthy	25	No	Under	No	no sample		
436	Healthy	45	No	Inside	Yes	no sample		
447	Healthy	44	No	Outside	Yes	no sample		
279	Unhealthy	62	No	Inside	Shared	neg	2+	1+
284	Unhealthy	58	No	Outside	No	neg	1+	3+
293	Unhealthy	48	Yes	Inside	Yes	neg	1+	2+
299	Unhealthy	49	No	Inside	Yes	neg	3+	0
307	Unhealthy	31	Yes	Inside	Yes	neg	3+	0
313	Unhealthy	68	No	Inside	Yes	neg	3+	0
318	Unhealthy	48	Yes	Away	Yes	neg	3+	0
319	Unhealthy	27	Yes	Inside	No	neg	3+	0
320	Unhealthy	15	No	Under	Yes	neg	3+	0
321	Unhealthy	46	No	Outside	Yes	neg	1+	2+

327	Unhealthy	20	No	Inside	Shared	neg	3+	0
329	Unhealthy	60	No	Inside	Yes	neg	3+	0
331	Unhealthy	38	No	Inside	Yes	neg	3+	0
356	Unhealthy	36	No	Inside	Shared	neg	3+	0
369	Unhealthy	19	No	Inside	Shared	neg	2+	0
370	Unhealthy	23	No	Inside	Yes	neg	1+	0
371	Unhealthy	58	Yes	Inside	Shared	neg	3+	0
377	Unhealthy	48	Past	Away	Shared	neg	2+	0
379	Unhealthy	50	No	Under	Yes	neg	3+	0
392	Unhealthy	50	Past	Inside	Shared	neg	1+	0
397	Unhealthy	59	No	Inside	Shared	neg	3+	0
398	Unhealthy	58	No	Inside	Yes	neg	3+	0
403	Unhealthy	34	No	Inside	Yes	neg	3+	0
408	Unhealthy	50	Yes	Inside	Shared	neg	3+	0
422	Unhealthy	38	No	Outside	Shared	neg	3+	0
424	Unhealthy	63	Past	Inside	No	neg	3+	0
425	Unhealthy	58	No	Under	Shared	neg	3+	1+
430	Unhealthy	30	Yes	Inside	Shared	neg	3+	0
431	Unhealthy	68	No	Inside	No	neg	1+	0
434	Unhealthy	48	No	Inside	Yes	neg	3+	1+
440	Unhealthy	51	Past	Outside	Shared	neg	3+	0
441	Unhealthy	42	Yes	Outside	Yes	neg	3+	0
442	Unhealthy	48	No	Outside	No	neg	3+	0
444	Unhealthy	30	No	Inside	Shared	neg	3+	0

Appendix 11. Participant demographic and sputum smear information. Participant demographics were recorded, and participants were sorted into healthy and unhealthy groups based on the presence of a cough and sputum smear results. Sputum polymorphonuclear cell (polys) and squamous epithelial cell counts were ranked from 0 – 3+ where 0 represents no cells and 3+ represents numerous cells. The presence of polys in the sputum was used as evidence of an immune response in the lungs. Participants who had a cough and produced sputum-containing polys were sorted into the unhealthy group. A positive sputum acid fast bacilli (AFB) test was evidence of a pulmonary tuberculosis infection and was used as exclusion criteria.

A)

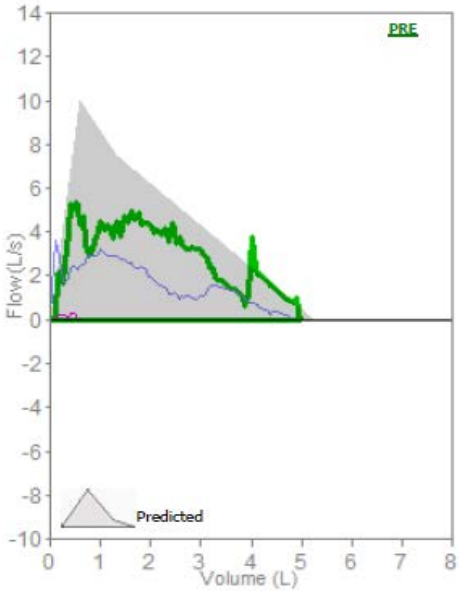

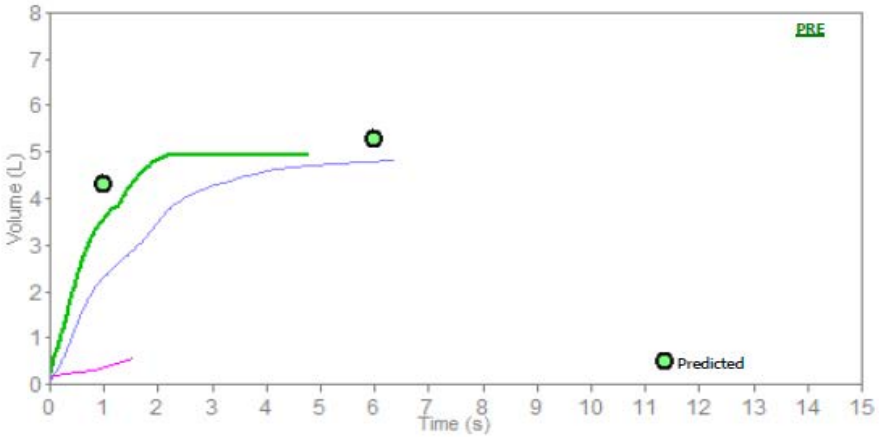

Quality Control Grade: F Variability: FEV1=1.21L (51.05%), FVC=0.16L (3.31%)

0 Acceptable trials

Interpretation

Normal Spirometry

PRE Trial date 19/01/2020 1:44:05 PM

Parameters		LLN	Pred	Best	%Pred	Z-score	PRE # 1	PRE # 2	PRE # 3	POST	%Pred	%Chg
FVC	L	4.37	5.28	4.99*	95	-0.52	0.57	4.83	4.99	*		
FEV1	L	3.54	4.30	3.58*	83	-1.94	0.37	**2.37**	3.58	*		
FEV1/FVC	%	72.0	81.7	71.7*	88	-1.69	64.9	**49.1**	**71.7**	*		
PEF	L/s	7.77	10.01	5.88*	59	-3.03	0.37	**3.69**	**5.88**	*		
ELA	Years		31	57	184		128	89	57			
FEF2575	L/s	2.77	4.32	2.96	69	-1.46	0.19	**1.55**	2.96			
FET	s		6.00	4.75	79		1.53	6.37	4.75			
FIVC	L	4.37	5.28				2.26					
FEV1/VC	%	72.0	81.7									

*Best values from all loops - BTPS 1.048 34 °C (93.2 °F) - Predicted NHANES III

B)

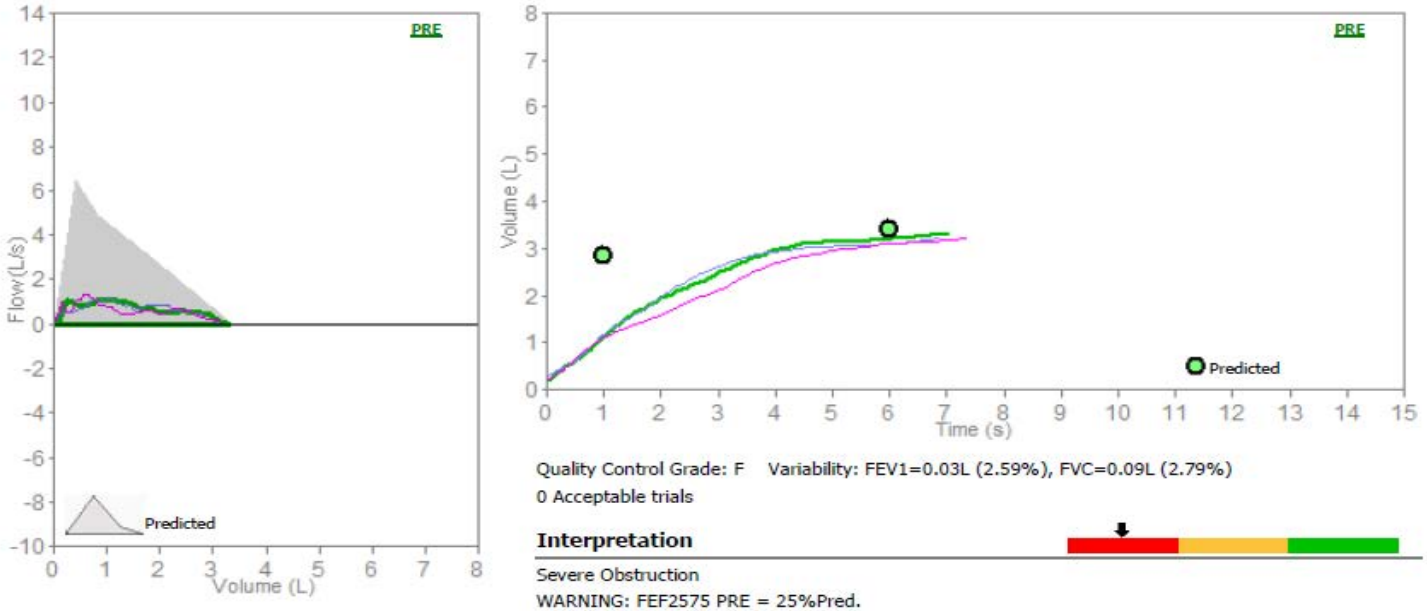

PRE Trial date 19/01/2020 6:24:29 PM

Parameters		LLN	Pred	Best	%Pred	Z-score	PRE # 1	PRE # 2	PRE # 3	POST	%Pred	%Chg
FVC	L	2.76	3.39	3.32*	98	-0.18	3.23	3.22	3.32	*		
FEV1	L	2.30	2.83	1.19*	42	-5.08	1.13	**1.19**	**1.16**	*		
FEV1/FVC	%	73.6	83.4	35.8*	43	-7.99	35.0	**37.0**	**34.9**	*		
PEF	L/s	5.01	6.56	1.37*	21	-5.49	1.37	**1.20**	**1.17**	*		
ELA	Years		35	94	269		94	93	94			
FEF2575	L/s	2.01	3.13	0.77	25	-3.46	0.60	**0.86**	**0.77**			
FET	s		6.00	7.02	117		7.37	6.90	7.02			
FIVC	L	2.76	3.39									
FEV1/VC	%	73.6	83.4									

*Best values from all loops - BTPS 1.043 35 °C (95 °F) - Predicted NHANES III

Appendix 12. Poor quality spirometry report examples. Spirometry reports from participants in Papua New Guinea were recorded using a portable spirometer. Many of the reports were not of acceptable quality due to language and cultural barriers and were discarded from analysis. One common problem was participants did not maintain a consistent exhale force **(A)**. Additionally, some participants did not exhale with maximal effort which led to incorrect FEV1 results **(B)**.

A)

Per base sequence quality

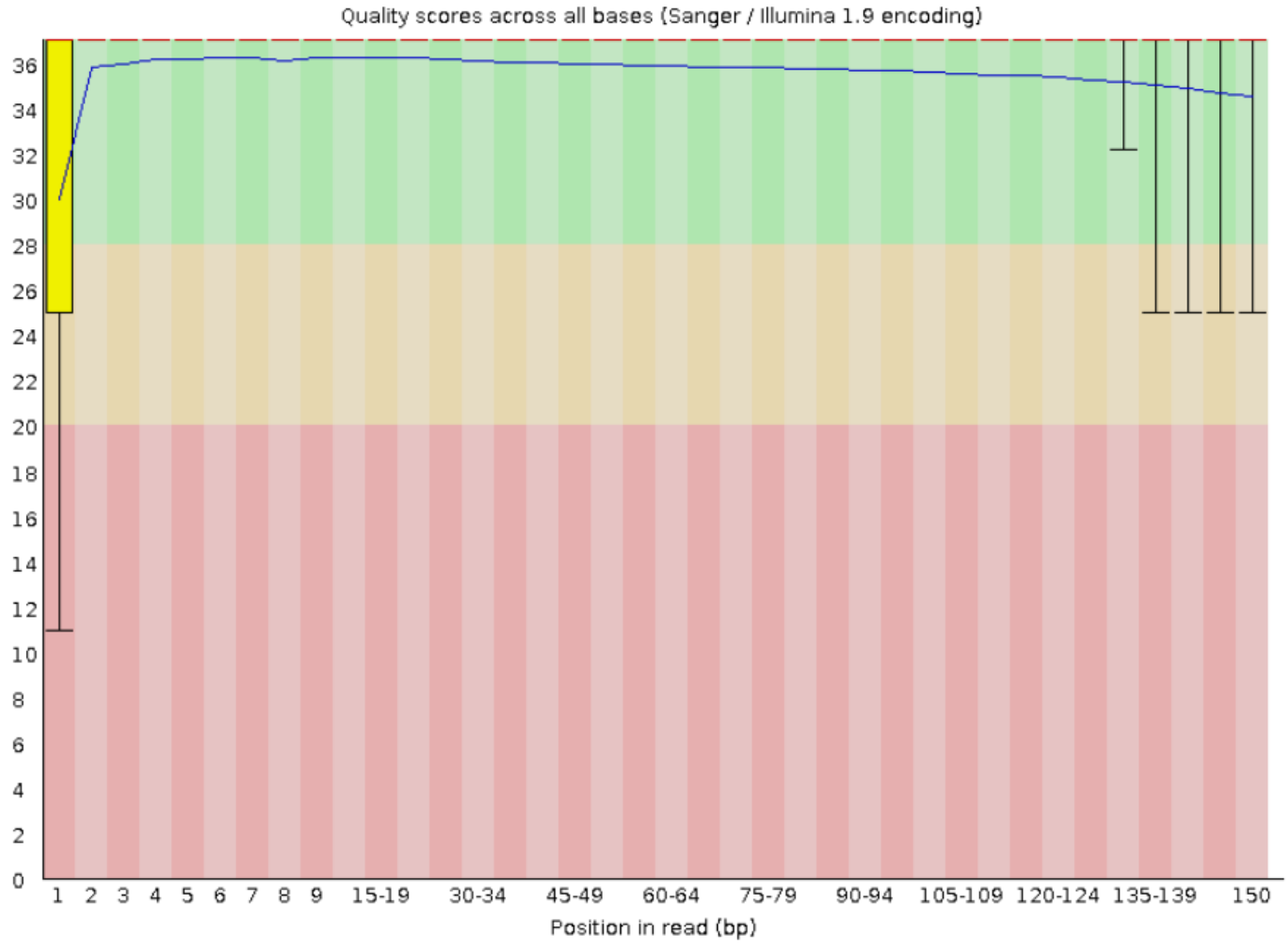

B)

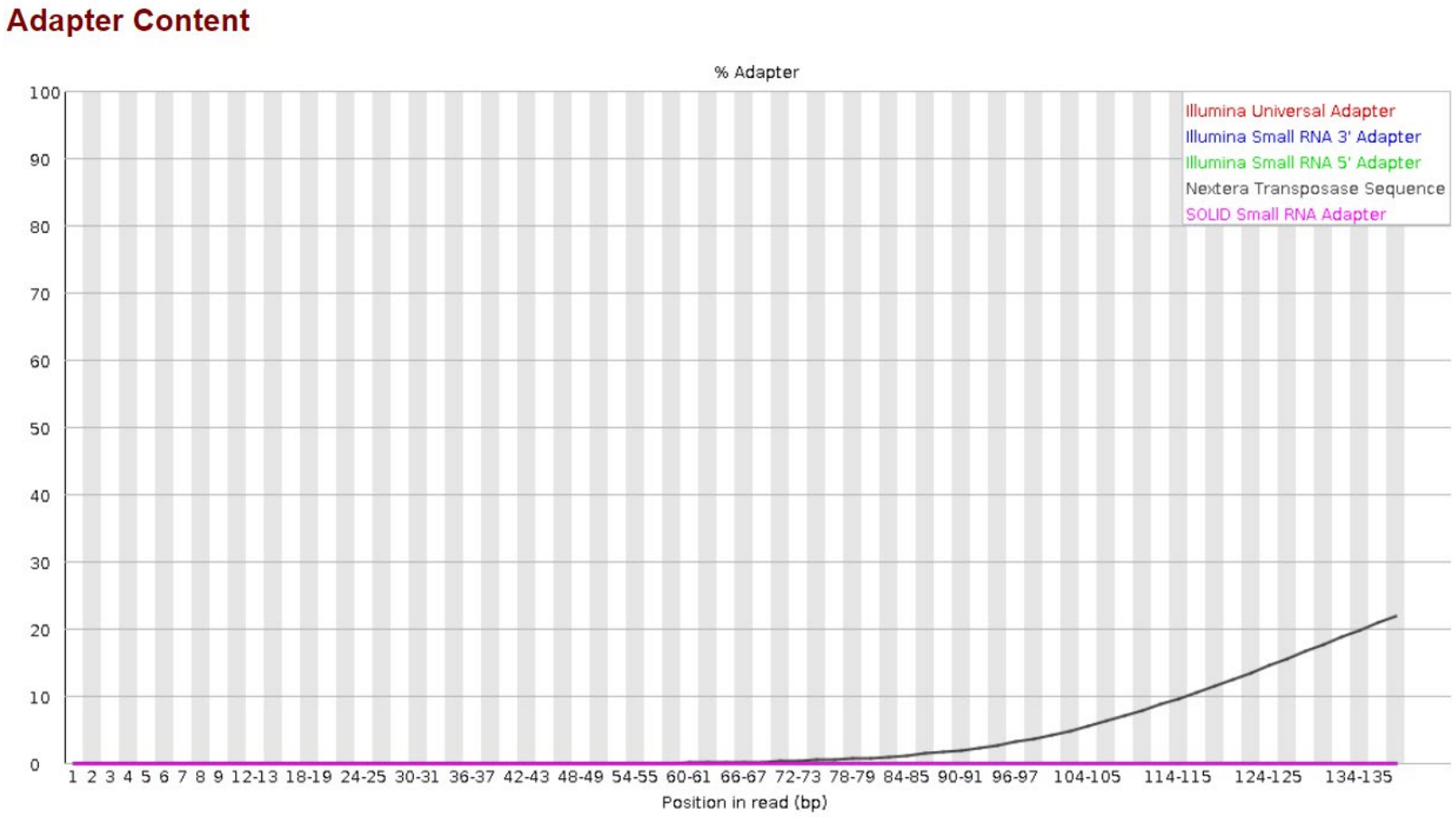

Appendix 13. Example FastQC results. FastQC results showed that the first base pair reads tended to be of low quality but the while the quality of the reminder of the sequences were acceptable on average (A). There results also revealed that there was some adapter content in the reads (B). These results were used to inform the trimming protocol.

A)

	Gene Set	NGenes	Direction	PValue	FDR
1	HALLMARK_COMPLEMENT	73	Up	<0.01	<0.01
2	HALLMARK_TNFA_SIGNALING_VIA_NFKB	74	Up	<0.01	0.01
3	HALLMARK_IL6_JAK_STAT3_SIGNALING	35	Up	<0.01	0.01
4	HALLMARK_APICAL_JUNCTION	47	Up	<0.01	0.01
5	HALLMARK_MYC_TARGETS_V1	61	Down	<0.01	0.01
6	HALLMARK_E2F_TARGETS	27	Down	<0.01	0.02
7	HALLMARK_INFLAMMATORY_RESPONSE	64	Up	<0.01	0.03
8	HALLMARK_REACTIVE_OXYGEN_SPECIES_PATHWAY	16	Up	0.01	0.04
9	HALLMARK_UV_RESPONSE_UP	44	Up	0.01	0.04
10	HALLMARK_INTERFERON_ALPHA_RESPONSE	49	Up	0.01	0.04
11	HALLMARK_PI3K_AKT_MTOR_SIGNALING	47	Up	0.01	0.04
12	HALLMARK_COAGULATION	23	Up	0.01	0.04
13	HALLMARK_INTERFERON_GAMMA_RESPONSE	94	Up	0.01	0.04

B)

	Gene Set	NGenes	Direction	PValue	FDR
1	REACTOME_EUKARYOTIC_TRANSLATION_ELONGATION	54	Down	<0.01	<0.01
2	REACTOME_SELENOAMINO_ACID_METABOLISM	52	Down	<0.01	<0.01
3	REACTOME_EUKARYOTIC_TRANSLATION_INITIATION	66	Down	<0.01	<0.01
4	REACTOME_RESPONSE_OF_EIF2AK4_GCN2_TO_AMINO_ACID_DEFICIENCY	54	Down	<0.01	<0.01
5	KEGG_RIBOSOME	49	Down	<0.01	<0.01
6	JISON_SICKLE_CELL_DISEASE_DN	99	Down	<0.01	<0.01
7	REACTOME_TRANSLATION	85	Down	<0.01	<0.01
8	REACTOME_NEUTROPHIL_DEGRANULATION	241	Up	<0.01	<0.01

9	REACTOME_SRP_DEPENDENT_COTRANSLATIONAL_PROTEIN_TARGETING_TO_MEMBRANE	58	Down	<0.01	<0.01
10	SMIRNOV_CIRCULATING_ENDOTHELIOCYTES_IN_CANCER_UP	51	Up	<0.01	<0.01
11	WP_CYTOPLASMIC_RIBOSOMAL_PROTEINS	54	Down	<0.01	<0.01
12	REACTOME_RRNA_PROCESSING	60	Down	<0.01	<0.01
13	VERHAAK_AML_WITH_NPM1_MUTATED_UP	69	Up	<0.01	<0.01
14	MULLIGHAN_MLL_SIGNATURE_2_UP	206	Up	<0.01	<0.01
15	MARTENS_BOUND_BY_PML_RARA_FUSION	221	Up	<0.01	<0.01
16	REACTOME_NONSENSE_MEDIATED_DECAY_NMD	62	Down	<0.01	<0.01
17	MULLIGHAN_MLL_SIGNATURE_1_UP	182	Up	<0.01	<0.01
18	ZHANG_BREAST_CANCER_PROGENITORS_UP	98	Down	<0.01	<0.01
19	VERHAAK_GLIOBLASTOMA_MESENCHYMAL	114	Up	<0.01	<0.01
20	REACTOME_INFLUENZA_INFECTION	75	Down	<0.01	<0.01
21	REACTOME_ACTIVATION_OF_THE_MRNA_UPON_BINDING_OF_THE_CAP_BINDING_COMPLEX_AND_EIFS_AND_SUBSEQUENT_BINDING_TO_43S	35	Down	<0.01	<0.01
22	BROWN_MYELOID_CELL_DEVELOPMENT_UP	75	Up	<0.01	<0.01
23	REACTOME_SARS_COV_2_MODULATES_HOST_TRANSLATION_MACHINERY	20	Down	<0.01	<0.01
24	REACTOME_SARS_COV_1_MODULATES_HOST_TRANSLATION_MACHINERY	22	Down	<0.01	<0.01
25	NADLER_OBESITY_UP	27	Up	<0.01	<0.01
26	RICKMAN_METASTASIS_DN	115	Up	<0.01	<0.01
27	BILANGES_SERUM_AND_RAPAMYCIN_SENSITIVE_GENES	42	Down	<0.01	<0.01
28	REACTOME_CELLULAR_RESPONSE_TO_STARVATION	68	Down	<0.01	<0.01
29	REACTOME_REGULATION_OF_EXPRESSION_OF_SLITS_AND_ROBOS	72	Down	<0.01	<0.01

30	CHNG_MULTIPLE_MYELOMA_HYPERPLOID_UP	33	Down	<0.01	<0.01
31	REACTOME_INNATE_IMMUNE_SYSTEM	432	Up	<0.01	<0.01
32	VALK_AML_CLUSTER_5	18	Up	<0.01	<0.01
33	CHEN_METABOLIC_SYNDROM_NETWORK	355	Up	<0.01	<0.01
34	REACTOME_METABOLISM_OF_RNA	212	Down	<0.01	<0.01
35	MARKEY_RB1_ACUTE_LOF_DN	102	Up	<0.01	<0.01
36	BLANCO_MELO_COVID19_SARS_COV_2_POS_PATIENT_LUNG_TISSUE_UP	66	Up	<0.01	<0.01
37	REN_ALVEOLAR_RHABDOMYOSARCOMA_DN	145	Up	<0.01	<0.01
38	ACOSTA_PROLIFERATION_INDEPENDENT_MYC_TARGETS_DN	48	Up	<0.01	<0.01
39	WP_MICROGLIA_PATHOGEN_PHAGOCYTOSIS_PATHWAY	25	Up	<0.01	<0.01
40	REACTOME_MRNA_SPLICING	66	Down	<0.01	<0.01
41	HAMAI_APOPTOSIS_VIA_TRAIL_UP	166	Down	<0.01	<0.01
42	PUJANA_XPRSS_INT_NETWORK	36	Down	<0.01	<0.01
43	WP_COMPLEMENT_SYSTEM	24	Up	<0.01	<0.01
44	REACTOME_PROCESSING_OF_CAPPED_INTRON_CONTAINING_PRE_MRNA	92	Down	<0.01	<0.01
45	PID_IL8_CXCR2_PATHWAY	22	Up	<0.01	<0.01
46	PUJANA_CHEK2_PCC_NETWORK	156	Down	<0.01	<0.01
47	REACTOME_METABOLISM_OF_AMINO_ACIDS_AND_DERIVATIVES	84	Down	<0.01	<0.01
48	PARK_TRETINOIN_RESPONSE_AND_PML_RARA_FUSION	19	Up	<0.01	<0.01
49	MARKEY_RB1_ACUTE_LOF_UP	46	Down	<0.01	<0.01
50	KEGG_REGULATION_OF_ACTIN_CYTOSKELETON	78	Up	<0.01	<0.01
51	APPEL_IMATINIB_RESPONSE	12	Up	<0.01	<0.01

52	PID_IL8_CXCR1_PATHWAY	16	Up	<0.01	<0.01
53	HAHTOLA_MYCOSIS_FUNGOIDES_CD4_DN	48	Down	<0.01	<0.01
54	KEGG_FC_GAMMA_R_MEDIATED_PHAGOCYTOSIS	52	Up	<0.01	<0.01
55	WP_REGULATION_OF_ACTIN_CYTOSKELETON	51	Up	<0.01	<0.01
56	LENAOUR_DENDRITIC_CELL_MATURATION_DN	67	Up	<0.01	<0.01
57	HESS_TARGETS_OF_HOXA9_AND_MEIS1_DN	43	Up	<0.01	<0.01
58	HUTTMANN_B_CLL_POOR_SURVIVAL_UP	100	Up	<0.01	<0.01
59	DELYS_THYROID_CANCER_UP	101	Up	<0.01	<0.01
60	MODY_HIPPOCAMPUS_PRENATAL	17	Down	<0.01	<0.01
61	JISON_SICKLE_CELL_DISEASE_UP	51	Up	<0.01	<0.01
62	MARTENS_TRETINOIN_RESPONSE_UP	62	Up	<0.01	<0.01
63	MILI_PSEUDOPODIA_HAPTOTAXIS_UP	163	Down	<0.01	<0.01
64	WP_COMPLEMENT_SYSTEM_IN_NEURONAL_DEVELOPMENT_AND_PLASTICITY	22	Up	<0.01	<0.01
65	SCHLOSSER_SERUM_RESPONSE_UP	70	Up	<0.01	<0.01
66	JOHNSTONE_PARVB_TARGETS_3_DN	204	Down	<0.01	<0.01
67	THEILGAARD_NEUTROPHIL_AT_SKIN_WOUND_DN	168	Up	<0.01	<0.01
68	KEGG_CHEMOKINE_SIGNALING_PATHWAY	70	Up	<0.01	<0.01
69	ALTEMEIER_RESPONSE_TO_LPS_WITH_MECHANICAL_VENTILATION	49	Up	<0.01	<0.01
70	WP_MRNA_PROCESSING	67	Down	<0.01	<0.01
71	REACTOME_PLATELET_ACTIVATION_SIGNALING_AND_AGGREGATION	93	Up	<0.01	<0.01
72	RICKMAN_TUMOR_DIFFERENTIATED_WELL_VS_POORLY_UP	69	Down	<0.01	<0.01
73	PUJANA_BRCA2_PCC_NETWORK	97	Down	<0.01	<0.01

74	MEISSNER_NPC_HCP_WITH_H3_UNMETHYLATED	59	Up	<0.01	<0.01
75	FEVR_CTNNB1_TARGETS_DN	115	Down	<0.01	<0.01
76	PARK_APL_PATHOGENESIS_DN	24	Up	<0.01	<0.01
77	WP_CHEMOKINE_SIGNALING_PATHWAY	67	Up	<0.01	<0.01
78	QI_PLASMACYTOMA_UP	118	Up	<0.01	<0.01
79	SENGUPTA_NASOPHARYNGEAL_CARCINOMA_WITH_LMP1_UP	80	Down	<0.01	<0.01
80	HOSHIDA_LIVER_CANCER_SUBCLASS_S1	101	Up	<0.01	0.01
81	REACTOME_MAP2K_AND_MAPK_ACTIVATION	18	Up	<0.01	0.01
82	OSMAN_BLADDER_CANCER_DN	215	Down	<0.01	0.01
83	WP_NEURAL_CREST_CELL_MIGRATION_IN_CANCER	13	Up	<0.01	0.01
84	REACTOME_SIGNALING_BY_MODERATE_KINASE_ACTIVITY_BRAF_MUTANTS	22	Up	<0.01	0.01
85	AMIT_EGF_RESPONSE_480_HELA	53	Up	<0.01	0.01
86	WP_NEURAL_CREST_CELL_MIGRATION_DURING_DEVELOPMENT	12	Up	<0.01	0.01
87	RODRIGUES_THYROID_CARCINOMA_POORLY_DIFFERENTIATED_UP	131	Down	<0.01	0.01
88	BENPORATH_ES_1	64	Down	<0.01	0.01
89	REACTOME_HEMOSTASIS	177	Up	<0.01	0.01
90	DAVIES_MULTIPLE_MYELOMA_VS_MGUS_DN	15	Up	<0.01	0.01
91	RICKMAN_METASTASIS_UP	63	Down	<0.01	0.01
92	BIOCARTA_BARRESTIN_SRC_PATHWAY	9	Up	<0.01	0.01
93	KEGG_LEUKOCYTE_TRANSENDOTHELIAL_MIGRATION	51	Up	<0.01	0.01
94	GNATENKO_PLATELET_SIGNATURE	27	Up	<0.01	0.01
95	NEMETH_INFLAMMATORY_RESPONSE_LPS_UP	41	Up	<0.01	0.01

96	HAHTOLA_MYCOSIS_FUNGOIDES_CD4_UP	20	Up	<0.01	0.01
97	MIKKELSEN_IPS_LCP_WITH_H3K4ME3	40	Up	<0.01	0.01
98	REACTOME_RHO_GTPASES_ACTIVATE_NADPH_OXIDASES	14	Up	<0.01	0.01
99	PID_S1P_S1P2_PATHWAY	11	Up	<0.01	0.01
100	REACTOME_PARASITE_INFECTION	35	Up	<0.01	0.01
101	GABRIELY_MIR21_TARGETS	114	Down	<0.01	0.01
102	KEGG_SPLICEOSOME	45	Down	<0.01	0.01
103	BILANGES_SERUM_RESPONSE_TRANSLATION	20	Down	<0.01	0.01
104	SANSOM_APC_TARGETS_DN	95	Up	<0.01	0.01
105	REACTOME_SIGNALING_BY_ROBO_RECEPTORS	89	Down	<0.01	0.01
106	GALINDO_IMMUNE_RESPONSE_TO_ENTEROTOXIN	37	Up	<0.01	0.01
107	EPPERT_HSC_R	31	Down	<0.01	0.01
108	MCLACHLAN_DENTAL_CARIES_UP	110	Up	<0.01	0.01
109	MACLACHLAN_BRCA1_TARGETS_UP	7	Up	<0.01	0.01
110	REACTOME_ROS_AND_RNS_PRODUCTION_IN_PHAGOCYTES	16	Up	<0.01	0.01
111	WP_INTEGRINMEDIATED_CELL_ADHESION	45	Up	<0.01	0.01
112	DACOSTA_UV_RESPONSE_VIA_ERCC3_UP	85	Up	<0.01	0.01
113	REACTOME_LEISHMANIA_INFECTION	69	Up	<0.01	0.01
114	PID_RAC1_PATHWAY	36	Up	<0.01	0.01
115	PID_UPA_UPAR_PATHWAY	11	Up	<0.01	0.01
116	CHIBA_RESPONSE_TO_TSA_UP	10	Up	<0.01	0.01
117	OISHI_CHOLANGIOMA_STEM_CELL_LIKE_DN	64	Up	<0.01	0.01
118	HOLLEMAN_ASPARAGINASE_RESISTANCE_B_ALL_UP	17	Down	<0.01	0.01
119	PID_INTEGRIN2_PATHWAY	9	Up	<0.01	0.01

120	WP_SPINAL_CORD_INJURY	27	Up	<0.01	0.01
121	SHIPP_DLBCL_VS_FOLLICULAR_LYMPHOMA_DN	17	Down	<0.01	0.02
122	VILIMAS_NOTCH1_TARGETS_DN	11	Up	<0.01	0.02
123	ICHIBA_GRAFT_VERSUS_HOST_DISEASE_35D_UP	69	Up	<0.01	0.02
124	REACTOME_RECYCLING_PATHWAY_OF_L1	19	Up	<0.01	0.02
125	DACOSTA_UV_RESPONSE_VIA_ERCC3_COMMON_DN	186	Down	<0.01	0.02
126	VERRECCHIA_EARLY_RESPONSE_TO_TGFB1	17	Up	<0.01	0.02
127	ZHENG_BOUND_BY_FOXP3	210	Down	<0.01	0.02
128	PARK_TRETINOIN_RESPONSE_AND_RARA_PLZF_FUSION	15	Up	<0.01	0.02
129	WP_TYROBP_CAUSAL_NETWORK_IN_MICROGLIA	35	Up	<0.01	0.02
130	TAKEDA_TARGETS_OF_NUP98_HOXA9_FUSION_8D_DN	61	Up	<0.01	0.02
131	PYEON_HPV_POSITIVE_TUMORS_UP	14	Down	<0.01	0.02
132	WP_GLYCOLYSIS_AND_GLUCONEOGENESIS	12	Up	<0.01	0.02
133	REACTOME_RHO_GTPASES_ACTIVATE_WASPS_AND_WAVES	21	Up	<0.01	0.02
134	BANDRES_RESPONSE_TO_CARMUSTIN_MGMT_48HR_DN	31	Up	<0.01	0.02
135	LINDSTEDT_DENDRITIC_CELL_MATURATION_D	25	Up	<0.01	0.02
136	KEGG_FC_EPSILON_RI_SIGNALING_PATHWAY	35	Up	<0.01	0.02
137	JOHNSTONE_PARVB_TARGETS_3_UP	188	Up	<0.01	0.02
138	JOHNSTONE_PARVB_TARGETS_2_UP	72	Up	<0.01	0.02
139	MARKEY_RB1_CHRONIC_LOF_DN	34	Up	<0.01	0.02

140	TONKS_TARGETS_OF_RUNX1_RUNX1T1_FUSION_HSC_DN	87	Up	<0.01	0.02
141	RUTELLA_RESPONSE_TO_HGF_VS_CSF2RB_AND_IL4_UP	141	Up	<0.01	0.02
142	PID_TXA2PATHWAY	27	Up	<0.01	0.02
143	MOREAUX_MULTIPLE_MYELOMA_BY_TACI_DN	34	Down	<0.01	0.02
144	CAIRO_HEPATOBLASTOMA_CLASSES_UP	142	Down	<0.01	0.02
145	PUJANA_BRCA1_PCC_NETWORK	428	Down	<0.01	0.02
146	SHIPP_DLBCL_VS_FOLLICULAR_LYMPHOMA_UP	10	Up	<0.01	0.02
147	WP_CORI_CYCLE	8	Up	<0.01	0.02
148	PID_IL4_2PATHWAY	26	Up	<0.01	0.02
149	WP_IL4_SIGNALING_PATHWAY	35	Up	<0.01	0.02
150	BIOCARTA_GRANULOCYTES_PATHWAY	6	Up	<0.01	0.02
151	PUJANA_BRCA_CENTERED_NETWORK	25	Down	<0.01	0.02
152	DODD_NASOPHARYNGEAL_CARCINOMA_DN	252	Down	<0.01	0.02
153	GARY_CD5_TARGETS_DN	110	Down	<0.01	0.02
154	REACTOME_EXTRACELLULAR_MATRIX_ORGANIZATION	43	Up	<0.01	0.03
155	REACTOME_GAP_JUNCTION_TRAFFICKING_AND_REGULATION	9	Up	<0.01	0.03
156	PID_PDGFRB_PATHWAY	68	Up	<0.01	0.03
157	FLECHNER_BIOPSY_KIDNEY_TRANSPLANT_REJECTED_VS_OK_UP	58	Up	<0.01	0.03
158	BROCKE_APOPTOSIS_REVERSED_BY_IL6	55	Up	<0.01	0.03
159	SHEN_SMARCA2_TARGETS_DN	35	Up	<0.01	0.03
160	WP_IL3_SIGNALING_PATHWAY	31	Up	<0.01	0.03
161	REACTOME_INTERLEUKIN_3_INTERLEUKIN_5_AND_GM_CSF_SIGNALING	29	Up	<0.01	0.03

162	DACOSTA_UV_RESPONSE_VIA_ERCC3_DN	336	Down	<0.01	0.03
163	REACTOME_RESPONSE_TO_ELEVATED_PLATELET_CYTOSOLIC_CA2	39	Up	<0.01	0.03
164	GRAESSMANN_APOPTOSIS_BY_DOXORUBICIN_UP	263	Up	<0.01	0.03
165	GOLUB_ALL_VS_AML_DN	14	Up	<0.01	0.03
166	KEGG_GLYCOLYSIS_GLUCONEOGENESIS	14	Up	<0.01	0.03
167	DASU_IL6_SIGNALING_UP	21	Up	<0.01	0.03
168	STEARMAN_LUNG_CANCER_EARLY_VS_LATE_DN	24	Up	<0.01	0.03
169	REACTOME_DISEASES_OF_METABOLISM	20	Up	<0.01	0.03
170	PID_ENDOTHELIN_PATHWAY	20	Up	<0.01	0.03
171	WP_CORTICOTROPINRELEASING_HORMONE_SIGNALING_PATHWAY	36	Up	<0.01	0.03
172	WONG_EMBRYONIC_STEM_CELL_CORE	56	Down	<0.01	0.03
173	FLOTHO_PEDIATRIC_ALL_THERAPY_RESPONSE_UP	27	Down	<0.01	0.03
174	LIN_APC_TARGETS	24	Up	<0.01	0.03
175	KEGG_LEISHMANIA_INFECTION	39	Up	<0.01	0.03
176	RUTELLA_RESPONSE_TO_CSF2RB_AND_IL4_DN	145	Up	<0.01	0.03
177	DEURIG_T_CELL_PROLYMPHOCYTIC_LEUKEMIA_DN	144	Down	<0.01	0.03
178	PID_PTP1B_PATHWAY	20	Up	<0.01	0.03
179	WINTER_HYPOXIA_UP	18	Up	<0.01	0.03
180	WP_METABOLIC_REPROGRAMMING_IN_COLON_CANCER	16	Up	<0.01	0.03
181	BIOCARTA_INTEGRIN_PATHWAY	24	Up	<0.01	0.03
182	WP_NETRINUNC5B_SIGNALING_PATHWAY	15	Up	<0.01	0.03
183	BIOCARTA_MAPK_PATHWAY	44	Up	<0.01	0.03

184	MARTINELLI_IMMATURE_NEUTROPHIL_DN	9	Up	<0.01	0.03
185	REACTOME_FCGAMMA_RECEPTOR_FCGR_DEPENDENT_PHAGOCYTOSIS	45	Up	<0.01	0.03
186	PID_CXCR4_PATHWAY	56	Up	<0.01	0.03
187	DUNNE_TARGETS_OF_AML1_MTG8_FUSION_UP	35	Up	<0.01	0.03
188	KEGG_CYTOKINE_CYTOKINE_RECEPTOR_INTERACTION	37	Up	<0.01	0.03
189	DANG_MYC_TARGETS_UP	38	Down	<0.01	0.03
190	REACTOME_PENTOSE_PHOSPHATE_PATHWAY	5	Up	<0.01	0.03
191	WP_PENTOSE_PHOSPHATE_METABOLISM	5	Up	<0.01	0.03
192	REACTOME_SIGNAL_REGULATORY_PROTEIN_FAMILY_INTERACTIONS	8	Up	<0.01	0.03
193	BLANCO_MELO_BETA_INTERFERON_TREATED_BRONCHIAL_EPITHELIAL_CELLS_DN	18	Up	<0.01	0.03
194	DEURIG_T_CELL_PROLYMPHOCYTIC_LEUKEMIA_UP	68	Up	<0.01	0.03
195	ZHENG_FOXP3_TARGETS_IN_THYMUS_UP	92	Down	<0.01	0.04
196	KEGG_TOLL_LIKE_RECEPTOR_SIGNALING_PATHWAY	37	Up	<0.01	0.04
197	ONDER_CDH1_TARGETS_1_DN	46	Down	<0.01	0.04
198	NUTT_GBM_VS_AO_GLIOMA_UP	21	Up	<0.01	0.04
199	WP_PROLACTIN_SIGNALING_PATHWAY	42	Up	<0.01	0.04
200	WP_EGFEGFR_SIGNALING_PATHWAY	77	Up	<0.01	0.04
201	HUMMERICH_SKIN_CANCER_PROGRESSION_UP	31	Up	<0.01	0.04
202	NABA_MATRISOME	69	Up	<0.01	0.04
203	WIERENGA_STAT5A_TARGETS_DN	47	Up	<0.01	0.04
204	SHEN_SMARCA2_TARGETS_UP	179	Down	<0.01	0.04

205	NABA_MATRISOME_ASSOCIATED	59	Up	<0.01	0.04
206	PID_IL6_7_PATHWAY	29	Up	<0.01	0.04
207	KAMIKUBO_MYELOID_CEBPA_NETWORK	16	Up	<0.01	0.04
208	ZHAN_V1_LATE_DIFFERENTIATION_GENES_UP	18	Up	<0.01	0.04
209	REACTOME_SIGNALING_BY_CSF3_G_CSF	19	Up	<0.01	0.04
210	ENK_UV_RESPONSE_KERATINOCYTE_UP	169	Up	<0.01	0.04
211	WP_FIBRIN_COMPLEMENT_RECEPTOR_3_SIGNALING_PATHWAY	14	Up	<0.01	0.04
212	PID_ARF6_DOWNSTREAM_PATHWAY	9	Up	<0.01	0.04
213	WU_ALZHEIMER_DISEASE_UP	4	Up	<0.01	0.04
214	EPPERT_CE_HSC_LSC	8	Down	<0.01	0.04
215	PID_LYSOPHOSPHOLIPID_PATHWAY	21	Up	<0.01	0.04
216	HELLER_HDAC_TARGETS_SILENCED_BY_METHYLATION_UP	84	Up	<0.01	0.04
217	WP_TOLLLIKE_RECEPTOR_SIGNALING_PATHWAY	38	Up	<0.01	0.04
218	JIANG_TIP30_TARGETS_DN	9	Up	<0.01	0.04
219	LAMB_CCND1_TARGETS	7	Up	<0.01	0.04
220	ALONSO_METASTASIS_EMT_UP	8	Up	<0.01	0.04
221	KEGG_EPITHELIAL_CELL_SIGNALING_IN_HELICOBACTER_PYLORI_INFECTION	26	Up	<0.01	0.04
222	REACTOME_SIGNALING_BY_INTERLEUKINS	166	Up	<0.01	0.04
223	DELPUECH_FOXO3_TARGETS_UP	27	Up	<0.01	0.04
224	HUANG_GATA2_TARGETS_UP	87	Up	<0.01	0.04
225	FOROUTAN_INTEGRATED_TGFB_EMT_UP	18	Up	<0.01	0.04
226	GRUETZMANN_PANCREATIC_CANCER_UP	127	Up	<0.01	0.04
227	REACTOME_GPVI_MEDIATED_ACTIVATION_CASCADE	19	Up	<0.01	0.04
228	LI_INDUCED_T_TO_NATURAL_KILLER_UP	123	Up	<0.01	0.04

229	NABA_ECM_REGULATORS	23	Up	<0.01	0.04
230	KEGG_JAK_STAT_SIGNALING_PATHWAY	44	Up	<0.01	0.04
231	REACTOME_SEMAPHORIN_INTERACTIONS	26	Up	<0.01	0.04
232	BIOCARTA_RHO_PATHWAY	14	Up	<0.01	0.04
233	REACTOME_RAB_GERANYLGERANYLATION	24	Up	<0.01	0.04
234	MULLIGHAN_MLL_SIGNATURE_2_DN	68	Down	<0.01	0.04
235	CHUNG_BLISTER_CYTOTOXICITY_DN	36	Up	<0.01	0.04
236	RODWELL_AGING_KIDNEY_UP	210	Up	<0.01	0.05
237	REACTOME_COMPLEMENT_CASCADE	8	Up	<0.01	0.05
238	REACTOME_CLASS_B_2_SECRETIN_FAMILY_RECEPTORS	11	Up	<0.01	0.05
239	KEGG_B_CELL_RECEPTOR_SIGNALING_PATHWAY	42	Up	<0.01	0.05
240	BILD_CTNNB1_ONCOGENIC_SIGNATURE	34	Down	<0.01	0.05
241	REACTOME_COOPERATION_OF_PREFOLDIN_AND_TRIC_CCT_IN_ACTIN_AND_TUBULIN_FOLDING	5	Up	<0.01	0.05
242	WP_INTRACELLULAR_TRAFFICKING_PROTEINS_INVOLVED_IN_CMT_NEUROPATHY	7	Up	<0.01	0.05
243	WP_GENETIC_CAUSES_OF_PORTOSINUSOIDAL_VASCULAR_DISEASE	14	Up	<0.01	0.05
244	BURTON_ADIPOGENESIS_9	19	Up	<0.01	0.05
245	WP_NANOPARTICLEMEDIATED_ACTIVATION_OF_RECEPTOR_SIGNALING	11	Up	<0.01	0.05
246	KEGG_NATURAL_KILLER_CELL_MEDIATED_CYTOTOXICITY	57	Up	<0.01	0.05
247	CHEN_LUNG_CANCER_SURVIVAL	10	Up	<0.01	0.05
248	TSUDA_ALVEOLAR_SOFT_PART_SARCOMA	6	Up	<0.01	0.05

249	MOREAUX_B_LYMPHOCYTE_MATURATION_BY_TACI_UP	22	Up	<0.01	0.05
250	BIOCARTA_MTA3_PATHWAY	6	Up	<0.01	0.05
251	REACTOME_INTERLEUKIN_2_FAMILY_SIGNALING	23	Up	<0.01	0.05
252	REACTOME_GROWTH_HORMONE_RECEPTOR_SIGNALING	11	Up	<0.01	0.05
253	BUFFA_HYPOXIA_METAGENE	12	Up	<0.01	0.05
254	BURTON_ADIPOGENESIS_PEAK_AT_2HR	15	Up	<0.01	0.05
255	REACTOME_EPHB_MEDIATED_FORWARD_SIGNALING	19	Up	<0.01	0.05
256	VERRECCHIA_RESPONSE_TO_TGFB1_C2	4	Up	<0.01	0.05
257	REACTOME_THROMBIN_SIGNALLING_THROUGH_PROTEINASE_ACTIVATED_RECEPTORS_PARS	11	Up	<0.01	0.05
258	COULOUARN_TEMPORAL_TGFB1_SIGNATURE_DN	33	Up	<0.01	0.05

C)

	Gene Set	**NGenes**	**Direction**	**PValue**	**FDR**
1	HAY_BONE_MARROW_NEUTROPHIL	264	Up	<0.01	<0.01
2	HAY_BONE_MARROW_NAIVE_T_CELL	192	Down	<0.01	<0.01
3	TRAVAGLINI_LUNG_CD4_NAIVE_T_CELL	83	Down	<0.01	<0.01
4	TRAVAGLINI_LUNG_NEUTROPHIL_CELL	241	Up	<0.01	<0.01
5	AIZARANI_LIVER_C23_KUPFFER_CELLS_3	171	Up	<0.01	<0.01
6	CUI_DEVELOPING_HEART_C8_MACROPHAGE	200	Up	<0.01	<0.01

7	TRAVAGLINI_LUNG_CLASSICAL_MONOCYTE_CELL	210	Up	<0.01	<0.01
8	TRAVAGLINI_LUNG_NONCLASSICAL_MONOCYTE_CELL	125	Up	<0.01	<0.01
9	AIZARANI_LIVER_C6_KUPFFER_CELLS_2	132	Up	<0.01	<0.01
10	HAY_BONE_MARROW_MONOCYTE	128	Up	<0.01	<0.01
11	TRAVAGLINI_LUNG_TREM2_DENDRITIC_CELL	206	Up	<0.01	<0.01
12	DESCARTES_FETAL_PANCREAS_MYELOID_CELLS	81	Up	<0.01	<0.01
13	TRAVAGLINI_LUNG_MACROPHAGE_CELL	78	Up	<0.01	<0.01
14	TRAVAGLINI_LUNG_OLR1_CLASSICAL_MONOCYTE_CELL	399	Up	<0.01	<0.01
15	DURANTE_ADULT_OLFACTORY_NEUROEPITHELIUM_DENDRITIC_CELLS	84	Up	<0.01	<0.01
16	ZHONG_PFC_MAJOR_TYPES_MICROGLIA	234	Up	<0.01	<0.01
17	HU_FETAL_RETINA_MICROGLIA	260	Up	<0.01	<0.01
18	FAN_EMBRYONIC_CTX_BIG_GROUPS_MICROGLIA	197	Up	<0.01	<0.01
19	FAN_OVARY_CL13_MONOCYTE_MACROPHAGE	282	Up	<0.01	<0.01
20	DESCARTES_FETAL_PANCREAS_LYMPHOID_CELLS	34	Down	<0.01	<0.01
21	TRAVAGLINI_LUNG_EREG_DENDRITIC_CELL	296	Up	<0.01	<0.01
22	AIZARANI_LIVER_C3_NK_NKT_CELLS_2	113	Down	<0.01	<0.01
23	BUSSLINGER_DUODENAL_STEM_CELLS	131	Down	<0.01	<0.01
24	BUSSLINGER_GASTRIC_PPP1R1B_POSITIVE_CELLS	60	Down	<0.01	<0.01
25	DESCARTES_FETAL_KIDNEY_LYMPHOID_CELLS	55	Down	<0.01	<0.01
26	DESCARTES_FETAL_CEREBELLUM_MICROGLIA	225	Up	<0.01	<0.01
27	AIZARANI_LIVER_C18_NK_NKT_CELLS_5	80	Up	<0.01	<0.01
28	TRAVAGLINI_LUNG_CD4_MEMORY_EFFECTOR_T_CELL	44	Down	<0.01	<0.01
29	DESCARTES_FETAL_INTESTINE_LYMPHOID_CELLS	42	Down	<0.01	<0.01
30	DESCARTES_FETAL_LIVER_MYELOID_CELLS	59	Up	<0.01	<0.01
31	HE_LIM_SUN_FETAL_LUNG_C2_NEUTROPHIL_CELL	35	Up	<0.01	<0.01
32	DESCARTES_FETAL_INTESTINE_MYELOID_CELLS	94	Up	<0.01	<0.01
33	DESCARTES_FETAL_ADRENAL_MYELOID_CELLS	63	Up	<0.01	<0.01
34	TRAVAGLINI_LUNG_PLATELET_MEGAKARYOCYTE_CELL	176	Up	<0.01	<0.01
35	DESCARTES_FETAL_LUNG_LYMPHOID_CELLS	39	Down	<0.01	<0.01

36	DESCARTES_FETAL_LIVER_LYMPHOID_CELLS	32	Down	<0.01	<0.01
37	TRAVAGLINI_LUNG_PROLIFERATING_MACROPHAGE_CELL	236	Up	<0.01	<0.01
38	DESCARTES_MAIN_FETAL_THYMOCYTES	23	Down	<0.01	<0.01
39	DESCARTES_FETAL_CEREBRUM_MICROGLIA	146	Up	<0.01	<0.01
40	DESCARTES_FETAL_KIDNEY_MYELOID_CELLS	58	Up	<0.01	<0.01
41	AIZARANI_LIVER_C25_KUPFFER_CELLS_4	109	Up	<0.01	<0.01
42	GAO_LARGE_INTESTINE_24W_C11_PANETH_LIKE_CELL	161	Up	<0.01	<0.01
43	DESCARTES_FETAL_LUNG_MYELOID_CELLS	62	Up	<0.01	<0.01
44	DESCARTES_FETAL_HEART_LYMPHOID_CELLS	30	Down	<0.01	<0.01
45	DESCARTES_FETAL_ADRENAL_LYMPHOID_CELLS	57	Down	<0.01	<0.01
46	BUSSLINGER_ESOPHAGEAL_DENDRITIC_CELLS	134	Up	<0.01	<0.01
47	DESCARTES_MAIN_FETAL_MYELOID_CELLS	39	Up	<0.01	<0.01
48	FAN_OVARY_CL0_XBP1_SELK_HIGH_STROMAL_CELL	71	Down	<0.01	<0.01
49	FAN_EMBRYONIC_CTX_BRAIN_MYELOID	103	Up	<0.01	<0.01
50	TRAVAGLINI_LUNG_BRONCHIAL_VESSEL_1_CELL	82	Down	<0.01	<0.01
51	BUSSLINGER_DUODENAL_TRANSIT_AMPLIFYING_CELLS	81	Down	<0.01	<0.01
52	TRAVAGLINI_LUNG_CD8_MEMORY_EFFECTOR_T_CELL	15	Down	<0.01	<0.01
53	BUSSLINGER_DUODENAL_DIFFERENTIATING_STEM_CELLS	122	Down	<0.01	<0.01
54	RUBENSTEIN_SKELETAL_MUSCLE_T_CELLS	118	Down	<0.01	<0.01
55	BUSSLINGER_GASTRIC_LYZ_POSITIVE_CELLS	51	Down	<0.01	<0.01
56	AIZARANI_LIVER_C2_KUPFFER_CELLS_1	122	Up	<0.01	<0.01
57	DESCARTES_FETAL_PLACENTA_LYMPHOID_CELLS	52	Down	<0.01	<0.01
58	MANNO_MIDBRAIN_NEUROTYPES_HMGL	277	Up	<0.01	<0.01
59	HE_LIM_SUN_FETAL_LUNG_C2_HSC_CELL	232	Down	<0.01	<0.01
60	HAY_BONE_MARROW_IMMATURE_NEUTROPHIL	107	Up	<0.01	<0.01
61	RUBENSTEIN_SKELETAL_MUSCLE_MYELOID_CELLS	220	Up	<0.01	<0.01
62	DESCARTES_FETAL_HEART_MYELOID_CELLS	49	Up	<0.01	<0.01
63	AIZARANI_LIVER_C28_NK_NKT_CELLS_6	64	Down	<0.01	<0.01
64	TRAVAGLINI_LUNG_CD8_NAIVE_T_CELL	88	Down	<0.01	<0.01

65	DURANTE_ADULT_OLFACTORY_NEUROEPITHELIUM_MACROPHAGES	44	Up	<0.01	<0.01
66	DESCARTES_FETAL_ADRENAL_MEGAKARYOCYTES	16	Up	<0.01	<0.01
67	DESCARTES_FETAL_SPLEEN_MYELOID_CELLS	33	Up	<0.01	<0.01
68	TRAVAGLINI_LUNG_CLUB_CELL	50	Down	<0.01	<0.01
69	HE_LIM_SUN_FETAL_LUNG_C2_S100A12_HI_CLASSICAL_MONOCYTE	16	Up	<0.01	<0.01
70	FAN_EMBRYONIC_CTX_BRAIN_NAIVE_LIKE_T_CELL	107	Down	<0.01	<0.01
71	CUI_DEVELOPING_HEART_C7_MAST_CELL	88	Up	<0.01	<0.01
72	DESCARTES_FETAL_EYE_CORNEAL_AND_CONJUNCTIVAL_EPITHELIAL_CELLS	31	Up	<0.01	<0.01
73	HAY_BONE_MARROW_PLATELET	43	Up	<0.01	<0.01
74	DESCARTES_FETAL_MUSCLE_LYMPHOID_CELLS	45	Down	<0.01	<0.01
75	DESCARTES_FETAL_PLACENTA_MYELOID_CELLS	50	Up	<0.01	<0.01
76	DESCARTES_FETAL_THYMUS_ANTIGEN_PRESENTING_CELLS	71	Up	<0.01	<0.01
77	HE_LIM_SUN_FETAL_LUNG_C3_EARLY_CAP_CELL	73	Up	<0.01	<0.01
78	HE_LIM_SUN_FETAL_LUNG_C2_HSC_ELP_CELL	72	Down	<0.01	<0.01
79	DESCARTES_FETAL_LUNG_MEGAKARYOCYTES	31	Up	<0.01	<0.01
80	MURARO_PANCREAS_DUCTAL_CELL	449	Up	<0.01	<0.01
81	AIZARANI_LIVER_C10_MVECS_1	52	Up	<0.01	<0.01
82	BUSSLINGER_DUODENAL_MATURE_ENTEROCYTES	56	Up	<0.01	<0.01
83	DESCARTES_FETAL_STOMACH_MYELOID_CELLS	44	Up	<0.01	<0.01
84	MENON_FETAL_KIDNEY_10_IMMUNE_CELLS	66	Up	<0.01	<0.01
85	AIZARANI_LIVER_C31_KUPFFER_CELLS_5	63	Up	<0.01	<0.01
86	HE_LIM_SUN_FETAL_LUNG_C2_CYCLING_DC_CELL	95	Down	<0.01	<0.01
87	DESCARTES_FETAL_SPLEEN_LYMPHOID_CELLS	42	Down	<0.01	<0.01
88	DESCARTES_FETAL_EYE_MICROGLIA	77	Up	<0.01	<0.01
89	DESCARTES_MAIN_FETAL_CORNEAL_AND_CONJUNCTIVAL_EPITHELIAL_CELLS	31	Up	<0.01	<0.01
90	DESCARTES_FETAL_HEART_MEGAKARYOCYTES	17	Up	<0.01	<0.01
91	LAKE_ADULT_KIDNEY_C7_PROXIMAL_TUBULE_EPITHELIAL_CELLS_S3	62	Down	<0.01	<0.01
92	BUSSLINGER_GASTRIC_MATURE_PIT_CELLS	58	Up	<0.01	<0.01
93	RUBENSTEIN_SKELETAL_MUSCLE_SATELLITE_CELLS	128	Down	<0.01	<0.01

94	HU_FETAL_RETINA_BLOOD	93	Up	<0.01	<0.01
95	AIZARANI_LIVER_C21_STELLATE_CELLS_1	36	Up	<0.01	<0.01
96	DESCARTES_FETAL_MUSCLE_MEGAKARYOCYTES	57	Up	<0.01	<0.01
97	FAN_OVARY_CL16_LYMPHATIC_ENDOTHELIAL_CELL	92	Up	<0.01	<0.01
98	MENON_FETAL_KIDNEY_0_CAP_MESENCHYME_CELLS	29	Down	<0.01	<0.01
99	CUI_DEVELOPING_HEART_VASCULAR_ENDOTHELIAL_CELL	33	Up	<0.01	<0.01
100	RUBENSTEIN_SKELETAL_MUSCLE_B_CELLS	109	Down	<0.01	<0.01
101	FAN_EMBRYONIC_CTX_MICROGLIA_3	8	Up	<0.01	<0.01
102	DESCARTES_FETAL_LIVER_MEGAKARYOCYTES	21	Up	<0.01	<0.01
103	DESCARTES_FETAL_MUSCLE_MYELOID_CELLS	50	Up	<0.01	<0.01
104	BUSSLINGER_ESOPHAGEAL_LATE_SUPRABASAL_CELLS	30	Up	<0.01	<0.01
105	TRAVAGLINI_LUNG_ALVEOLAR_EPITHELIAL_TYPE_2_CELL	26	Up	<0.01	<0.01
106	BUSSLINGER_ESOPHAGEAL_EARLY_SUPRABASAL_CELLS	38	Down	<0.01	0.01
107	BUSSLINGER_GASTRIC_IMMATURE_PIT_CELLS	36	Up	<0.01	0.01
108	BUSSLINGER_GASTRIC_IMMUNE_CELLS	1,024.00	Down	<0.01	0.01
109	HE_LIM_SUN_FETAL_LUNG_C4_ILCP_CELL	48	Up	<0.01	0.01
110	DESCARTES_FETAL_STOMACH_LYMPHOID_CELLS	41	Down	<0.01	0.01
111	DESCARTES_MAIN_FETAL_MEGAKARYOCYTES	58	Up	<0.01	0.01
112	FAN_OVARY_CL14_MATURE_SMOOTH_MUSCLE_CELL	104	Up	<0.01	0.01
113	CUI_DEVELOPING_HEART_C4_ENDOTHELIAL_CELL	30	Up	<0.01	0.01
114	LAKE_ADULT_KIDNEY_C12_THICK_ASCENDING_LIMB	127	Down	<0.01	0.01
115	MANNO_MIDBRAIN_NEUROTYPES_BASAL	44	Down	<0.01	0.02
116	DURANTE_ADULT_OLFACTORY_NEUROEPITHELIUM_CD4_T_CELLS	22	Down	<0.01	0.02
117	LAKE_ADULT_KIDNEY_C14_DISTAL_CONVOLUTED_TUBULE	48	Down	<0.01	0.02
118	HAY_BONE_MARROW_CD8_T_CELL	29	Down	<0.01	0.02
119	DESCARTES_FETAL_LUNG_SQUAMOUS_EPITHELIAL_CELLS	15	Up	<0.01	0.02
120	RUBENSTEIN_SKELETAL_MUSCLE_FBN1_FAP_CELLS	90	Up	<0.01	0.02
121	MANNO_MIDBRAIN_NEUROTYPES_HENDO	265	Up	<0.01	0.02
122	ZHENG_CORD_BLOOD_C2_PUTATIVE_BASOPHIL_EOSINOPHIL_MAST_CELL_PROGENITOR	42	Up	<0.01	0.02

123	FAN_OVARY_CL6_PUTATIVE_EARLY_ATRETIC_FOLLICLE_THECAL_CELL_2	81	Up	<0.01	0.03
124	MANNO_MIDBRAIN_NEUROTYPES_HPERIC	201	Up	<0.01	0.03
125	AIZARANI_LIVER_C1_NK_NKT_CELLS_1	114	Down	<0.01	0.03
126	HE_LIM_SUN_FETAL_LUNG_C0_MID_MESOTHELIAL_CELL	162	Up	<0.01	0.03
127	TRAVAGLINI_LUNG_CAPILLARY_INTERMEDIATE_1_CELL	49	Up	0.01	0.03
128	GAO_LARGE_INTESTINE_ADULT_CE_OLFM4HIGH_STEM_CELL	41	Up	0.01	0.03
129	DESCARTES_MAIN_FETAL_MICROGLIA	57	Up	0.01	0.03
130	DESCARTES_FETAL_THYMUS_THYMOCYTES	2	Down	0.01	0.04
131	BUSSLINGER_ESOPHAGEAL_PROLIFERATING_BASAL_CELLS	30	Down	0.01	0.04
132	DESCARTES_FETAL_PLACENTA_MEGAKARYOCYTES	40	Up	0.01	0.04
133	MENON_FETAL_KIDNEY_2_NEPHRON_PROGENITOR_CELLS	10	Down	0.01	0.04
134	TRAVAGLINI_LUNG_PROXIMAL_BASAL_CELL	192	Down	0.01	0.04
135	BUSSLINGER_DUODENAL_TUFT_CELLS	26	Up	0.01	0.04
136	AIZARANI_LIVER_C29_MVECS_2	80	Up	0.01	0.05
137	ZHONG_PFC_MAJOR_TYPES_ASTROCYTES	54	Up	0.01	0.05

Appendix 14. Gene set enrichment analysis results. MSigDB gene set collections were utilized to identify sets of genes related to specific molecular mechanisms or cell types in unhealthy compare to healthy participants. The Hallmark (A), Curated (B), and Cell Type Signature (C) were used for analysis. Gene Set is the name of the set in the MSigDB collection. NGenes is the number of gene inside of the gene set. Direction indicates whether the expression of the gene set is increased (Up) or decreased (Down) in the unhealthy participants compared to the healthy participants. PValue is the uncorrected p-value. FDR is the false discovery rate corrected p-value. Gene set expression was considered significant if the FDR-corrected p-value was ≤0.05.